

**IMPACT RESISTANCE OF ULTRA HIGH PERFORMANCE FIBRE
REINFORCED CONCRETE PANELS AND STEEL FIBRE REINFORCED
CONCRETE PANELS STRENGTHENED WITH FIBRE REINFORCED
POLYMER STRAPS AT LOW TEMPERATURES**

**RÉSISTANCE AU CHOC DE PANNEAUX EN BÉTON FIBRÉ À ULTRA-
HAUTE PERFORMANCE ET EN BÉTON FIBRÉ ENVELOPPÉ DE
POLYMÈRE RENFORCÉ DE FIBRE À TEMPÉRATURE ARCTIQUE**

A Thesis Submitted to the Division of Graduate Studies
of the Royal Military College of Canada
by

Matthew Beirnes, rmc
Captain

In Partial Fulfillment of the Requirements for the Degree of
Master of Applied Science in Civil Engineering

June 2017

©This thesis may be used within the Department of National Defence but copyright for
open publication remains the property of the author.

ACKNOWLEDGEMENT

First, I would like to thank my supervisors, Dr. Gordon Wight and Dr. Marc-André Dagenais for all the support they have provided to me over the past two years. Without their expertise and supervision, I would not have been able to complete this research within the required timeframe.

I would especially like to thank Mr. Dexter Gaskin for all his hard work in the laboratory, first helping to construct the testing frame and then with all the instrumentation set-up and the conduct of the testing. His expertise was essential in getting everything constructed and instrumented and his patience when providing construction advice was greatly appreciated. I would also like to thank Mr. Steve VanVolkingburgh for his help during the testing phase. His experience with running the testing machines was extremely helpful and made the testing process run smoothly.

The help of OCdt Philippe Bolduc and OCdt Jordan Larocque was greatly appreciated and without their hard work the testing frame would have taken much longer to construct. Their dedication to ensuring there was a place to sit near each machine in the lab was an insight into the priorities of a modern day RMCC cadet.

I am extremely grateful to King Industries for their donation of all the materials required for the mixing and casting of the UHPFRC panels. My sincerest thanks goes to Mr. Julian Pena Cruz from King Industries for his support during the planning process and his willingness to travel to RMCC to help us mix the UHPFRC properly. His expertise with the mixing process allowed us to quickly mix the required amount and achieve consistent results.

Finally, I would like to extend a special thanks to my wife, Liz, for her constant support and motivation over the past two years. Without her motivating me to focus on my writing despite the other distractions like the arrival of our new child, Brayden, I would still be writing my Literature Review.

ABSTRACT

In an age of global terrorism, structures designed with the inherent ability to protect critical persons and assets within them are of key importance to both the private and public sectors. There is an ever-present threat of accidental explosions in some industrial and resource sectors and deployed military forces are living under the constant threat of enemy offensive action. In Canada, oil and gas facilities are located in northern climates, where extreme cold temperatures are the norm during the winter months. Cities in the Athabasca oil patch in northern Alberta, like Fort McMurray and Peace River, have outside air temperatures of -40°C while the coldest design air temperature in Canada is Snag, Yukon with a temperature of -53°C . The northernmost base occupied by the Canadian Armed Forces (CAF), CFS Alert, has a January outside air temperature of -44°C . With the Canadian government's focus on sovereignty of the Arctic, the CAF is focused on achieving this mandate by increasing the military footprint in the Arctic and ensuring there are quick reaction forces in place in the event of an emergency. Being an extremely cold climate during the winter months, building materials and equipment slated to be used in the Arctic or in northern regions must be tested under those cold weather conditions to ensure they are effective in these environments.

This project focuses on the design and testing of two types of armoured panels which could be used in a spaceframe structure to provide a lightweight, modular force or infrastructure protection system. This protection system could be constructed with basic tools, without the requirement for heavy equipment. It would be adaptable to any austere environment, including the Arctic, and could be adapted for use as a variety of infrastructure elements, such as a perimeter wall or to fortify existing structures. The primary focus of this project is on the armoured panels. Two types of panels were cast and tested, a steel fibre reinforced concrete (SFRC) panel strengthened with fibre reinforced polymer (FRP) straps, and an ultra high performance fibre reinforced concrete (UHPFRC) panel. The two types of panels were designed to have similar flexural strengths to compare their behaviour under dynamic loading conditions.

A pendulum-type impact hammer was used to investigate the extreme dynamic loading effects on the panels to determine if they were suitable for use in Arctic conditions. Panels were tested at two different temperatures, the ambient laboratory temperature of 20°C and a cold temperature of -55°C to simulate an Arctic environment. The panels were cooled to the cold temperature using an industrial-sized freezer of sufficient size to accommodate the specimens. Both types of panels had the same dimensions, being 1040 mm long, 535 mm wide and 38 mm thick. The SFRC panels had two FRP straps which were each 100 mm wide and 0.33 mm thick and wrapped around the entire panel. Quasi-static three-point flexural bending tests were conducted on both types of panels to obtain their threshold failure energy level. A total of eight quasi-static tests were completed, two of each type of panel at ambient temperatures and two of each type of panel at cold temperatures. Dynamic tests were conducted using the impact hammer with the impact energy being varied by altering the hammer drop height. Drop heights were varied from 350 mm up to 1500 mm which corresponded to input energies ranging from 470 J to 2016 J. A total of sixteen impact tests were conducted and following each ambient temperature impact test, the panel was tested for residual strength using the same three-point flexural bending test as the baseline quasi-static testing. For the residual strength tests of the cold temperature panels, the panels were returned to the freezer after impact testing and then transferred to the three-point flexural bending test setup once they returned to the required temperature.

The testing program demonstrated that both types of panels could resist impact loads with energies up to 1900 J without complete failure. Both types of panels were not adversely affected by the extreme cold temperatures and in fact displayed increased effectiveness. The residual strength of UHPFRC panels was easily predicted based on the permanent midspan deflection caused by the impact

test. The ambient temperature FRP strengthened SFRC panels had decreasing residual strengths as the amount of permanent deflection increased, while the cold temperature panels had the same residual strength despite having different amounts of permanent deflection. Both types of panels exhibited ductile behaviour, with the UHPFRC panels reaching maximum deflections of 100 mm and the FRP strengthened SFRC panels reaching maximum deflections of 120 mm.

A single-degree-of-freedom (SDOF) model was designed and validated with laboratory results to predict panel behaviour based on various impact energies. Resistance functions were determined based on the load-deflection curves produced using quasi-static flexural bending test results. The model is an iterative numerical approach which uses constant acceleration throughout the time-steps to determine midspan displacement throughout the time-history. The model provided accurate results which could be used to predict peak displacement of panels based on forcing function data.

RÉSUMÉ

À une époque où le terrorisme prend de plus en plus d'ampleur, les structures ayant la capacité de protéger le personnel et le matériel prennent une importance capitale dans les secteurs privé et public. Il existe également une menace omniprésente d'explosions accidentelles dans certains secteurs industriels et de plus, les forces militaires déployées vivent sous la menace constante d'une action offensive de l'ennemi. Au Canada, les installations pétrolières et gazières sont situées dans des secteurs nordiques où la température est extrêmement froide pendant l'hiver. Les villes situées dans le secteur d'exploitation pétrolière d'Athabasca dans le nord de l'Alberta, comme Fort McMurray et Peace River, doivent intégrer dans la conception une température de $-40\text{ }^{\circ}\text{C}$. La base des Forces armées canadienne (FAC) positionnée le plus au nord à Alert doit gérer une température de $-44\text{ }^{\circ}\text{C}$ alors que la plus basse température utilisée pour la conception au Canada est de $-53\text{ }^{\circ}\text{C}$ à Snag au Yukon. Afin d'assurer la souveraineté du territoire canadien dans l'Arctique, une des priorités du gouvernement canadien, les FAC jouent un rôle primordial dans ce mandat en augmentant l'empreinte militaire dans l'Arctique et en assurant des forces de réaction rapide en cas d'urgence. Compte tenu du climat extrêmement froid, les matériaux de construction qui pourraient être utilisés dans l'Arctique ou dans les régions du nord doivent être mis à l'essai pour vérifier leur efficacité dans de telles conditions.

Ce projet se concentre sur la conception et la mise à l'essai de deux types de panneaux blindés qui pourraient être utilisés dans une structure en treillis formant ainsi un système de protection léger et modulaire. Ce système de protection pourrait être construit avec des outils de base, sans machinerie lourde. Il serait adaptable à tout environnement austère, y compris l'Arctique, et pourrait être adapté à des fins d'utilisation sur une variété d'éléments d'infrastructure, comme un mur périmétrique ou pour fortifier une structure existante. Ce projet vise principalement les panneaux blindés. Deux types de panneaux ont été fabriqués et testés, des panneaux en béton fibré enveloppé de bandes de polymère renforcé de fibres et des panneaux de béton fibré à ultra haute performance. Les deux types de panneaux ont été conçus afin d'avoir des résistances à la flexion similaires pour comparer leur comportement dans des conditions de charge dynamiques.

Un montage expérimental de type pendule a été utilisé pour étudier les effets de chargement dynamique extrêmes sur les panneaux et ainsi déterminer leur efficacité en conditions arctique. Les panneaux ont été testés à deux températures différentes, à la température ambiante du laboratoire de $20\text{ }^{\circ}\text{C}$ et une température froide de $-55\text{ }^{\circ}\text{C}$ pour simuler un environnement arctique. Les panneaux devant être testés à $-55\text{ }^{\circ}\text{C}$ ont été placés dans un congélateur industriel de grande taille. Les deux types de panneaux avaient les mêmes dimensions, une longueur de 1040 mm, une largeur de 535 mm et une épaisseur de 38 mm. Les panneaux en béton renforcé de fibre étaient enveloppés de deux bandes de polymère renforcé de fibres de 100 mm de largeur et de 0,33 mm d'épaisseur. Des essais de résistance à la flexion trois-points quasi statiques ont été réalisés sur les deux types de panneaux afin de déterminer leur comportement charge déflexion ainsi que leur capacité à dissiper l'énergie. Un total de huit essais quasi statiques ont été réalisés, deux pour chaque types de panneaux à température ambiante et deux pour chaque types de panneaux à des températures arctique. Des essais dynamiques ont été effectués à l'aide du système de type pendule, l'énergie d'impact étant modifiée en variant la hauteur de chute du marteau. Les hauteurs de chute varient de 350 mm à 1500 mm, ce qui correspond à des énergies initiales allant de 450 J à 1900 J. Un total de seize essais d'impact a été effectué. Suite aux essais d'impact à température ambiante, les panneaux ont été testés en flexion trois-points afin de déterminer leur capacité résiduelle de la même façon que pour les essais quasi statiques. Pour les essais de résistance résiduelle des panneaux à température arctique, les panneaux ont été replacés au congélateur après l'essai d'impact afin d'atteindre à nouveau une température de $-55\text{ }^{\circ}\text{C}$ et ensuite testés en flexion trois-points.

Le programme expérimental a démontré que les deux types de panneaux pouvaient résister à des charges d'impact correspondant à des niveaux d'énergies de près de 1900 J sans rupture. La température arctique n'a pas affecté la performance des deux types de panneaux, apportant même une légère amélioration de la résistance de certains panneaux. La résistance résiduelle des panneaux de béton fibré à ultra haute performance a été facilement prédite en fonction de la déflexion permanente à mi-portée causée par l'essai d'impact. Les panneaux en béton de fibré enveloppés de bandes de polymère renforcé de fibres à température ambiante ont vu leurs résistances résiduelles diminuer et leur déflexion permanente augmenter, tandis que les panneaux testés à température arctique ont gardé la même résistance résiduelle malgré des quantités différentes de déflexion permanente. Les deux types de panneaux ont présenté un comportement ductile, les panneaux en béton fibré à ultra haute performance ont atteint des déflexions maximales de 100 mm et les panneaux en béton de fibres enveloppé de bandes de polymère renforcé de fibre on atteint des déflexions maximales de 120 mm.

Un modèle à un degré de liberté a été conçu et validé afin de prédire le comportement des panneaux en fonction de différents niveaux d'énergie d'impact. Des fonctions de résistances ont également été déterminées en utilisant les courbes charge-déflexion des essais quasi statiques. Le modèle est basé sur une approche numérique itérative qui utilise une accélération constante pour chaque incrément de temps pour déterminer le déplacement de la mi-portée dans le temps. Le modèle fournit des résultats précis pouvant être utilisés pour prédire le déplacement maximal des panneaux selon les données de fonction de forces.

CO-AUTHORSHIP STATEMENT

This thesis has been written in the article-based format as laid out in the Royal Military College of Canada Thesis Preparation Guidelines. The author of this thesis, Captain Matthew Beirnes, was the main contributor to both articles, with the co-authors providing guidance, advice and feedback. As the author plans to submit both articles for publication in peer-reviewed journals, the individual articles will include both supervisors as co-authors.

TABLE OF CONTENTS

ACKNOWLEDGEMENT	i
ABSTRACT.....	ii
RÉSUMÉ	iv
CO-AUTHORSHIP STATEMENT.....	vi
TABLE OF CONTENTS.....	vii
LIST OF FIGURES	xi
LIST OF TABLES.....	xiii
LIST OF ABBREVIATIONS.....	xiv
LIST OF SYMBOLS	xv
1. INTRODUCTION	1
1.1 Project Background.....	1
1.2 Aim	2
1.3 Scope.....	2
1.4 Thesis Organization	4
1.5 Description of Appendices.....	5
2. LITERATURE REVIEW	7
2.1 General.....	7
2.2 Steel Fibre Reinforced Concrete	7
2.3 Ultra High Performance Fibre Reinforced Concrete	9
2.3.1 Definition	9
2.3.2 Mix Design.....	9
2.3.3 Material Properties	10
2.4 FRP Strengthening	13
2.5 Blast and Impact Loads.....	15

2.5.1	Blast Phases and Parameters	16
2.5.2	Laboratory Impact Tests	17
2.5.2.1	Effects of Testing Apparatus.....	18
2.5.2.2	Transfer of Energy	18
2.5.3	Instrumentation of Impact Testing.....	19
2.5.4	Previous Experimental Impact Research	19
2.6	Cold Temperature Effects	20
2.7	Single Degree of Freedom Modeling.....	21
2.8	Summary	23
3.	MANUSCRIPT #1: “COLD TEMPERATURE EFFECTS ON THE IMPACT RESISTANCE OF SFRC PANELS STRENGTHENED WITH FRP STRAPS”	24
3.1	Abstract.....	24
3.2	Introduction.....	24
3.2.1	Protective Structures in Austere Environments	24
3.2.2	Impact Resistant Properties of SFRC.....	25
3.2.3	FRP Strengthening	25
3.2.4	Pendulum-Type Impact Hammer Testing.....	25
3.3	Research Objectives and Scope	26
3.4	Experimental Program	26
3.4.1	Specimens	26
3.4.2	Materials	28
3.4.3	Test Setup, Instrumentation, Procedures.....	28
3.5	Test Results.....	31
3.5.1	General Behaviour	32
3.5.2	Load-deflection behaviour and ductility	33
3.5.3	Residual Strength of Dynamic Panels.....	37

3.5.4	Failure Modes	38
3.5.5	Conservation of Energy	40
3.6	SDOF Modelling.....	42
3.7	Conclusions.....	45
3.8	Acknowledgments.....	46
3.9	References.....	46
4.	MANUSCRIPT #2: “COLD TEMPERATURE EFFECTS ON THE IMPACT RESISTANCE OF THIN, LIGHTWEIGHT UHPFRC PANELS.”	48
4.1	Abstract.....	48
4.2	Introduction.....	48
4.2.1	Protective Works for Civilian and Military Applications	48
4.2.2	Impact Resistant Properties of UHPFRC.....	49
4.2.3	Pendulum-Type Impact Hammer Testing.....	49
4.2.4	Background Test Series	49
4.3	Research Objectives and Scope	49
4.4	Experimental Program	50
4.4.1	Specimens	50
4.4.2	Materials	51
4.4.3	Test Setup, Instrumentation, Procedures.....	51
4.5	Test Results.....	55
4.5.1	General Behaviour	55
4.5.2	Load-deflection behaviour and ductility	57
4.5.3	Residual Strength of Dynamic Panels.....	61
4.5.4	Failure Modes	62
4.5.5	Conservation of Energy	63
4.6	SDOF Modelling.....	65

4.7	Comparison to FRP Strengthened SFRC Panels.....	68
4.8	Conclusions.....	70
4.9	Acknowledgments.....	71
4.10	References.....	71
5.	CONCLUSIONS AND RECOMMENDATIONS	73
5.1	General.....	73
5.2	Summary of Research Program	73
5.3	Conclusions.....	74
5.4	Recommendations.....	75
	References.....	76
	APPENDICES	81
	Curriculum Vita	157

LIST OF FIGURES

Figure 1-1 - Modular Protective System designed by U.S. Army ERDC [2]	1
Figure 1-2 – Panel Dimensions	2
Figure 1-3 - Three-point flexural bending test set-up	3
Figure 1-4 - Impact Hammer Drop Heights.....	3
Figure 2-1 - Random fibre orientation in SFRC [7].....	7
Figure 2-2 - Typical profiles of commonly used steel fibres in concrete [9].....	8
Figure 2-3 - Superplasticizer effect on concrete matrix [23]	10
Figure 2-4 - Behaviour of UHPFRC under uniaxial compression [22]	11
Figure 2-5 – Characteristic stress-strain behaviour of UHPFRC materials in tension [24]	11
Figure 2-6 - Typical stress elongation response of fibre reinforced cement composites [9]	12
Figure 2-7 – Direct tension test for UHPFRC using dog bone specimens.....	13
Figure 2-8 – FRP wet lay-up on concrete beam [38]	14
Figure 2-9 - FRP strips added to bottom of flexural beams [39]	14
Figure 2-10 - Variations of blast effects associated with positive and negative phase pressures with time [42].....	15
Figure 2-11 - Typical pressure-time history [43].....	16
Figure 2-12 - Idealized pressure-time history	17
Figure 2-13 - Drop height of pendulum-type hammer.....	18
Figure 2-14 - Idealized inertial load, after [45].....	19
Figure 2-15 - Structures idealized as spring-mass systems [63]	21
Figure 2-16 - Dynamic single degree of freedom model, adapted from [63]	22
Figure 2-17 - Typical resistance function, adapted from [43]	22
Figure 3-1 - Panel dimensions	27
Figure 3-2 – Quasi-static three-point bending testing apparatus	28
Figure 3-3 - Bolted connection of specimen to testing frame.....	29
Figure 3-4 - Impact hammer instrumentation	30
Figure 3-5 - Impact hammer test set-up	30
Figure 3-6 - Typical impact event captured by highspeed camera	33
Figure 3-7 – Load-deflection behaviour of quasi-static panels.....	34
Figure 3-8 - Load-deflection behaviour of ambient temperature dynamic panels.....	35
Figure 3-9 - Load-deflection behaviour of cold temperature dynamic panels.....	36
Figure 3-10 - Load-deflection behaviour of residual strength of FRP/SFRC panels.....	37
Figure 3-11 – Panel SCI4 post-impact. Complete debonding of FRP straps and cracking and spalling of concrete. No residual strength.....	38
Figure 3-12 - Panel SCI2 pre- and post-impact	39
Figure 3-13 – Panel SCI4 pre- and post-impact.....	39
Figure 3-14 – Panel SAI2 post-residual strength testing. Fracture and debonding of one FRP strap, large cracks and spalling of concrete.....	40
Figure 3-15 – Energy Conservation of Panel SAI1	41
Figure 3-16 – Energy Conservation of Panel SAI4	42
Figure 3-17 - Resistance Function for FRP/SFRC Panels	43
Figure 3-18 - Forcing Function (from hammer force transducer data of panel SAI1).....	43
Figure 3-19 – SDOF Model for panel SAI1	44
Figure 4-1 - Panel dimensions	50
Figure 4-2 - Quasi-static three-point bending testing apparatus	52
Figure 4-3 - Bolted connection of specimen to testing frame.....	53
Figure 4-4 - Impact hammer instrumentation	54
Figure 4-5 - Impact hammer test set-up	54

Figure 4-6 - Post-impact cracking of panel UAI4.....	56
Figure 4-7 - Typical impact event captured by high-speed camera	57
Figure 4-8 - Load-deflection behaviour of quasi-static panels	58
Figure 4-9 - Load-deflection behaviour of ambient temperature dynamic panels	59
Figure 4-10 - Load-deflection behaviour of cold temperature dynamic panels	60
Figure 4-11 - Load-deflection behaviour of residual strength panels	61
Figure 4-12 – Photos of panel UAI1 from high-speed camera	62
Figure 4-13 - Photos of panel UAI3 from high-speed camera.....	63
Figure 4-14 - Energy Conservation of Panel UAI3	64
Figure 4-15 - Energy Conservation of Panel UAI4	65
Figure 4-16 - Resistance Function for UHPFRC Panels.....	66
Figure 4-17 - Forcing Function (from hammer force transducer data of panel UCI2)	66
Figure 4-18 - SDOF Model for panel UCI3.....	67
Figure 4-19 - Load-deflection behaviour of FRP/SFRC Panels and UHPFRC Panels.....	69
Figure 4-20 – Comparison of Residual Strength Behaviour of Panels	70
Figure A-1 - Panel Dimensions.....	A-1
Figure A-2 - Forms used to cast specimens	A-3
Figure A-3 - Form dimensions.....	A-3
Figure A-4 - Cumflow RP100XD HD Rotating Pan Mixer.....	A-4
Figure A-5 - Adding steel fibres to the UHPFRC mix.....	A-5
Figure A-6 - Modulus of Elasticity Testing Setup	A-6
Figure A-7 - Exposed Aggregate of SFRC Panels.....	A-7
Figure A-8 - Quasi-static three-point bending testing apparatus	A-8
Figure A-9 - Three-point flexural bending quasi-static testing set-up	A-9
Figure A-10 - Load-deflection behaviour of quasi-static panel UCS2 and residual strength of panel UCI3	A-10
Figure A-11 - Impact hammer drop heights.....	A-11
Figure A-12 - Impact Hammer Test Set-up	A-12
Figure A-13 - Testing frame	A-13
Figure A-14 - Impact Hammer Test Set-up	A-14
Figure A-15 - Placement of high-speed cameras	A-14
Figure A-16 - Bolted connection of specimen to testing frame	A-15
Figure A-17 – Impact testing camera footage.....	A-16

LIST OF TABLES

Table 1-1 - Testing Schedule	4
Table 2-1 - UHPFRC Mix Design, adapted from [19].....	9
Table 3-1 – Specimen Description and Test Parameters	27
Table 3-2 – Hammer Drop Heights.....	29
Table 3-3 - Summary of Quasi-Static Test Results.....	31
Table 3-4 - Summary of Dynamic Test Results.....	31
Table 3-5 - Residual strength of FRP/SFRC panels.....	38
Table 3-6 - SDOF model comparison to actual data.....	45
Table 4-1 - Specimen Description and Test Parameters	51
Table 4-2 - Average Material Properties of UP-F4 Poly Mix.....	51
Table 4-3 - Hammer drop heights	52
Table 4-4 - Summary of Quasi-Static Test Results.....	55
Table 4-5 - Summary of Dynamic Test Results.....	55
Table 4-6 - Residual strength of UHPFRC panels	62
Table 4-7 - SDOF model comparison to actual data.....	68
Table A-1 - UP-F4 Poly Material Properties	A-2
Table A-2 - FRP Properties.....	A-2
Table A-3 - UP-F4 Mix Design	A-4
Table A-4 - Average Material Properties of UP-F4 Poly Mix.....	A-6
Table A-5 – Average Material Properties of SFRC Mix	A-7

LIST OF ABBREVIATIONS

ACI	American Concrete Institute
ASTM	American Society for Testing and Materials
CAF	Canadian Armed Forces
CFS	Canadian Forces Station
CFD	Computational Fluid Dynamics
CFRP	Carbon Fibre Reinforced Polymer
CoG	Centre of Gravity
CSA	Canadian Standards Association
FEM	Finite Element Model
FRP	Fibre Reinforced Polymer
HSS	Hollow Structural Section
LVDT	Linear Variable Differential Transducer
MPS	Modular Protective System
PVA	Polyvinyl Alcohol
RC	Reinforced Concrete
RMCC	Royal Military College of Canada
SDOF	Single Degree of Freedom
SFRC	Steel Fibre Reinforced Concrete
UHPC	Ultra High Performance Concrete
UHPFRC	Ultra High Performance Fibre Reinforced Concrete

LIST OF SYMBOLS

$^{\circ}\text{C}$	Degree Celsius
f'_c	Compressive strength of concrete
ε	Strain
E	Modulus of Elasticity
E_o	Maximum Available Energy
h_d	Hammer Drop Height
I_s	Impulse
g	Gram
g	Gravitational Constant
in	Inch
J	Joule
k	Spring Constant
K_{LM}	Load-mass Factor
m	Metre
M	Mass
min	Minute
N	Newton
Pa	Pascal
P_o	Ambient air pressure
P_{so}	Peak Incident Pressure
φ	Curvature
σ	Stress
t_A	Arrival Time
t_o	Positive Phase Duration
t_{o-}	Negative Phase Duration
t_{of}	Idealized Positive Phase Duration
V_i	Impact Velocity
W	Weight
\ddot{x}	Acceleration
\dot{x}	Velocity
x	Displacement
y	Displacement

1. INTRODUCTION

1.1 Project Background

Protective structures are used by the Canadian Armed Forces (CAF) during deployments to foreign territories and within domestic borders to protect key pieces of infrastructure. The CAF, along with its allies, primarily make use of earth filled gabions produced by the company Hesco®. These products consist of a collapsible wire mesh frame with a heavy-duty fabric liner [1]. These gabions are stackable which provides versatility and allows for perimeter walls, bunkers, and a variety of protective works to be created. While the units themselves are lightweight and collapsible, once filled with earth they are no longer reusable because the fabric often gets torn while being emptied, the wire mesh becomes twisted or tangled, and they must be emptied by hand as opposed to using heavy equipment.

To transition away from these costly, single use gabions, the CAF is seeking alternatives that are lightweight, modular, and reusable. The United States Army Corps of Engineers has created a system that generally fits these requirements, and which was an inspiration for this project. The U.S. Army Corps of Engineers system is called the Modular Protective System (MPS) and combines a lightweight metal spaceframe with armoured panels, as seen in Figure 1-1 [2]. This system consists of a rapidly erectable frame and armour panels which can be built in various configurations and optimized to protect against direct and indirect-fire threats. The modules can be stacked or connected side by side to form many different wall lengths and configurations. The components of the MPS are one or two-man portable and can be assembled with no special tools.

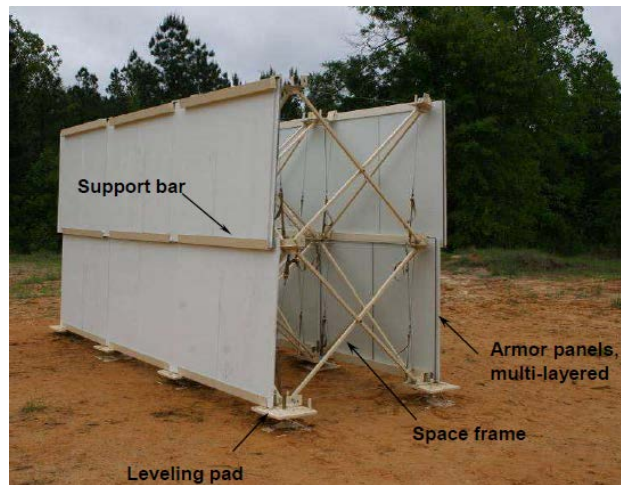


Figure 1-1 - Modular Protective System designed by U.S. Army ERDC [2]

In addition to finding a force protection system that satisfies the aforementioned criteria, it must be feasible and effective in all types of weather conditions, especially in cold temperature regions like Canada's Arctic. Since the publication of Canada's Northern Strategy in 2008, sovereignty in Northern Regions is one issue on which the Government of Canada is focused in order to advance its interests both domestically and internationally [3]. As a result of climate change and the possibility of accessing untapped natural resources, the Arctic region is becoming an area of geopolitical significance to not only our country, but also our Arctic neighbours. The *Canada First* Defence Strategy provides direction to the CAF that they must have the capacity to exercise control over and defend Canada's sovereignty in the Arctic [4]. The policy also directs that the military will play an increasingly vital role in demonstrating a

visible Canadian presence in this potentially resource-rich region. A modular protective system designed or procured by the CAF must be effective in Arctic conditions so that it can be utilized to protect key assets located at northern bases such as Canadian Forces Station (CFS) Alert.

1.2 Aim

The aim of this project was to design a lightweight, armour panel that could be utilized as part of a modular protective system. Two panels were designed and research was conducted to determine the response of these panels when subjected to dynamic loads caused by impact. The first type of panel is a steel fibre reinforced concrete (SFRC) panel strengthened with fibre reinforced polymer (FRP) straps. The second type is a panel made of ultra high performance fibre reinforced concrete (UHPFRC). The FRP straps were added to the SFRC panel to give it a similar design strength to the UHPFRC panel's design strength. The panels were tested at ambient laboratory temperatures and extreme cold temperatures to examine the differences in behaviour at the two different temperatures and to ensure the panels are effective at cold temperatures.

1.3 Scope

The scope of this project was restricted to focus solely on the ability of the two types of armoured panels to resist impact loads at ambient and cold temperatures. Although these panels would be installed in a spaceframe-type structure to provide sufficient protection, the design and testing of this type of structure was beyond the scope of this research.

Panels were cast and tested in the RMCC Structures Laboratory and were designed to be 1040 mm in length, 535 mm wide and 38 mm thick. These dimensions were selected to ensure that overall panel weight was kept under 100 lbs which would allow them to be carried and installed by two individuals. The FRP straps that were placed around the SFRC panels consisted of two layers of MBrace CF160 and were 100 mm in width. Panel dimensions and FRP placement details are found in Figure 1-2.

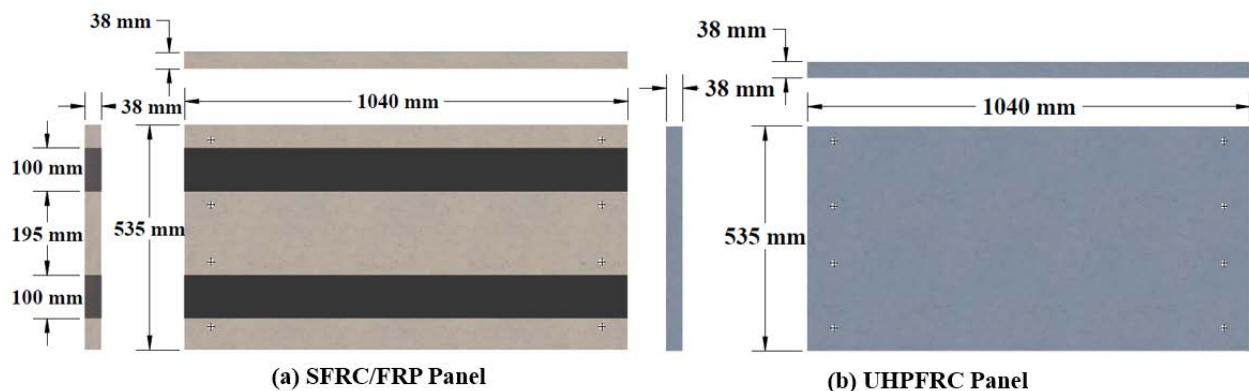


Figure 1-2 – Panel Dimensions

The experimental study in this thesis evaluated and compared the two types of panels. Two types of testing were completed, testing the static and dynamic qualities of the panels. Quasi-static three-point flexural bending tests were completed on untested panels to determine a baseline load-deflection behaviour, using the set-up shown in Figure 1-3. The three-point flexural bending test was also used to determine the residual strength of impact tested panels. The impact testing conducted as a part of this research used a pendulum-type impact hammer, shown in Figure 1-4. By varying the drop height of the impact hammer, the amount of impact energy could be altered. The initial impact energies were selected

based on the baseline data provided by initial quasi-static testing, and subsequent impact energies were chosen based on the results of previous impact tests.

Quasi-static testing was conducted using a MTS Model 322 machine. This machine was displacement-controlled and the head was set to displace at a rate of 2 mm/min. Panels were supported within the machine by triangular pins with bearing plates on top which would allow translation in the horizontal direction and limited rotation. The load was applied to the panel at midspan to simulate the same loading conditions as those found in the dynamic test.

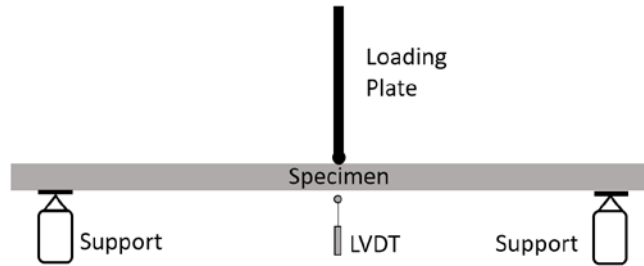


Figure 1-3 - Three-point flexural bending test set-up

Dynamic tests were conducted at varying hammer heights which altered the impact energy of the system. The same impact energies were used for tests of each type of panel and at each temperature, to have meaningful data. Once an impact test was completed, the residual strength of the panel was tested by using the same three-point flexural bending test setup that was used for the quasi-static testing. For the panels tested at cold temperatures, they were returned to the freezer following the impact test so they could return to the proper temperature. Once the correct temperature was reached, approximately -70°C , the panel was taken out of the freezer and installed in the flexural testing apparatus. By the time all the instrumentation was set up and the test was ready to commence, the panels had reached the proper testing temperature of -55°C .

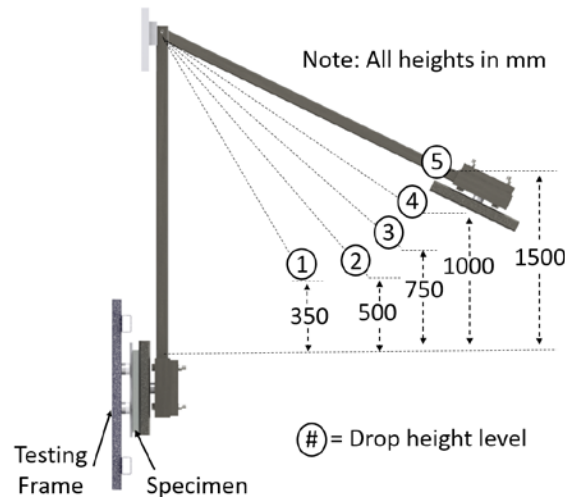

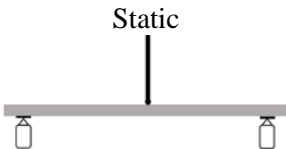






Figure 1-4 - Impact Hammer Drop Heights

All experimental testing in this research was conducted on each type of panel, at both ambient and extreme cold temperature. This was done to compare the behaviour of not only each type of panel, but to see the behavioural difference between panels tested at ambient laboratory temperature and extreme cold

temperature. In total, 23 panels were tested during this research project. The testing schedule can be seen in Table 1-1.

Table 1-1 - Testing Schedule

<u>Panel Material</u>	<u>Test Type</u>	<u>Temperature</u>	<u># of Specimens</u>
SFRC/FRP 	Static 	Ambient	2
		Cold	1
	Impact 	Ambient	4
		Cold	4
UHPFRC 	Static 	Ambient	2
		Cold	2
	Impact 	Ambient	4
		Cold	4

Numerical modeling for this research consists of single degree of freedom (SDOF) modeling, which is frequently used as a predictive modelling tool for the design of concrete members to resist impact loads. This model was validated using the experimental testing results and can predict panel behaviour based on the impact load to which they are subjected.

1.4 Thesis Organization

This document was written in the article-based format as laid out in the Royal Military College of Canada (RMCC) Thesis Preparation Guidelines [5] and has five chapters. Chapter 1 introduces the research project, establishes the aim and outlines the scope of the research. Chapter 2 provides a review of the current, relative literature that pertains to the topics discussed in this thesis. Chapter 3 consists of a stand-alone article that will be submitted for publication in a relevant engineering journal. This article

discusses the results and analysis of the experimental testing conducted on the FRP strengthened SFRC panels. Chapter 4 presents the second stand-alone article that will also be submitted for publication. The second article is presented in a similar manner to the first, but discusses the results and analysis of the experimental testing conducted on the UHPFRC panels. Both articles discuss the differences in panel behaviour when in ambient laboratory temperatures versus extreme cold temperatures. Chapter 5 concludes the research project by highlighting the key findings and providing recommendations for future work. Appendices follow Chapter 5.

Because the document is prepared in manuscript format, the references for Chapter 3 and Chapter 4 are contained within the chapters and the numbering of the references is initiated at 1 in these chapters. The references for Chapters 1, 2 and Appendix A are provided at the end of the document and are numbered independently of the two manuscript chapters.

1.5 Description of Appendices

As this thesis document is written in the manuscript format, information that was pertinent and essential to the individual papers was provided within those papers. The remainder of the information that was gathered in this research project is provided in the appendices that are located at the end of this document. The reader is highly encouraged to read Appendix A as it provides extensive information regarding the procedures followed during this research project.

Appendix B provides the preliminary calculations that were completed during the design process of these panels. The intent was to design panels from two different materials that had similar flexural strengths to be able to compare the behaviours of these two materials. As seen in the calculations, both types of panels were designed to have peak strengths of just over 12 kN but as testing showed, both materials exceeded these predicted strengths.

Appendix C includes drawings of the forms that were used for casting both types of panels. The SFRC panels were cast first and then once they were removed, the forms were used to cast the UHPFRC panels. The forms were built using standard framing lumber and the panel dimensions were selected to optimize the lumber sizes available.

Data collected from an impact test is provided in Appendix D. The time window where the impact event took place is included but the remainder of the data was removed to minimize the length of the appendix.

The moment-curvature model that was developed to predict the quasi-static flexural strength of the panels is included in Appendix E. The model was created in Microsoft Excel and several screenshots are found in the Appendix. This model is explained in Appendix A but is not referenced in either Chapter 3 or 4. Note that the spreadsheet has been condensed for proper formatting within the document.

The SDOF model was also created in Microsoft Excel and is found in Appendix F. The model was used to predict the behaviour of each panel tested dynamically but only the calculations for panel UAI3 are found in the Appendix. The graphs for all other panels can be found in Appendix H or I. Note that some of the data from the spreadsheet was cut out to enable printing.

Appendix G includes the conservation of energy spreadsheet that was used to make the conservation of energy graphs found in the papers. This spreadsheet was developed using the formulas that were included in the papers. The example spreadsheet that is found in the Appendix is for panel UAI3.

The final two appendices, H and I, include all graphs created for each panel. Appendix H displays graphs for the SFRC panels and the UHPFRC panel graphs are shown in Appendix I. The graphs for each panel are in the same order, from left to right, top to bottom: SDOF model, quasi-static three-point flexural bending, conservation of energy, and dynamic load-deflection.

2. LITERATURE REVIEW

2.1 General

This section will provide an in-depth review of current and relevant literature pertaining to the subject of ultra high performance fibre reinforced concrete (UHPFRC). It will also provide the reader with sufficient background knowledge of steel fibre reinforced concrete (SFRC), fibre-reinforced polymer (FRP) strengthening, and dynamic impact loading to provide a basic understanding of the materials and testing procedures used within this research. This literature review encompasses all topics covered in the manuscripts included within this document, serving as a review for the entire project. Each individual manuscript has its own brief literature review which summarizes the most important information from this review to provide the manuscript reader the required, pertinent background knowledge. References for this Chapter can be found after Chapter 5, while Chapters 3 and 4 have their own reference lists as they are stand-alone papers.

2.2 Steel Fibre Reinforced Concrete

SFRC is simply defined as normal strength concrete which contains randomly distributed steel fibres, such as those shown in Figure 2-1. These fibres are added to the mix prior to pouring and are intended to reinforce concrete, which on its own, is brittle and lacks tensile strength and ductility [6]. Much research has been done in this field over the past few decades to determine the key material properties and how it behaves within various structures.

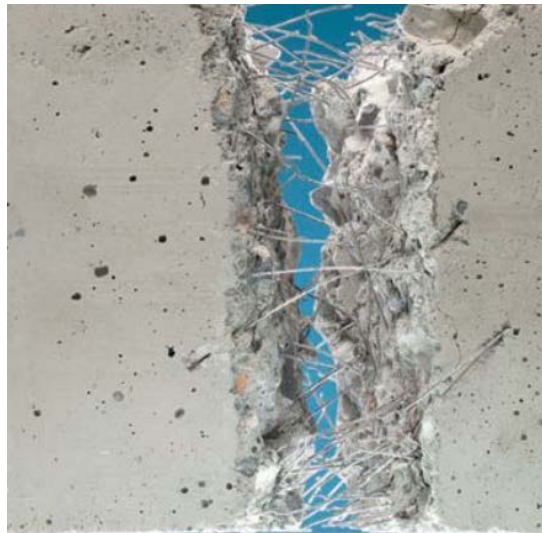


Figure 2-1 - Random fibre orientation in SFRC [7]

There are many different types of steel fibres that can be used in this application, with variations in length, width, and shape, as shown in Figure 2-2. The most common types of steel fibres are those cut from sheets, slit sheet fibres, fibres extracted from steel melt, and mill cut fibres [6]. These fibres have a random distribution in the mix which leads to an increase to both the ultimate strength and the toughness or ductility of the concrete structural component [8]. These fibres increase the tensile capacity of the member as they bridge the cracks that form in the tension regions of the member as loads increase. It is recommended that the aspect ratio of the fibres, the ratio between fibre length and diameter, be less than

100 and it typically ranges from 20 to 100 [8]. If the aspect ratio is larger than 100, the fibres tend to clump within the mix, reducing workability and preventing a uniform distribution within the mix.

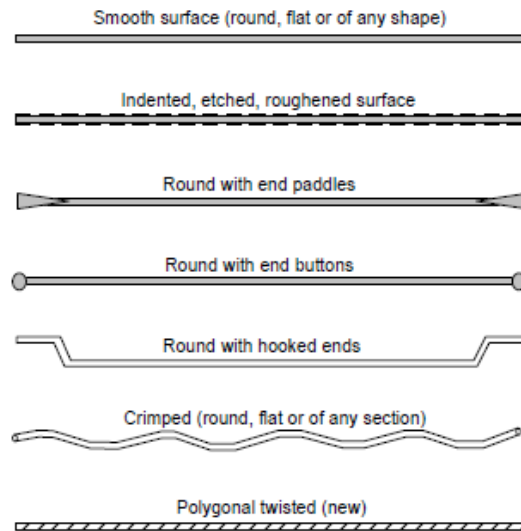


Figure 2-2 - Typical profiles of commonly used steel fibres in concrete [9]

In addition to selecting a proper aspect ratio of fibre, the proper dosage must be used. Fibre dosage is typically quantified as a percentage of the overall volume of the mix. The American Concrete Institute (ACI) recommends a dosage rate between 0.5 and 1.5% by volume [10]. Like the negative affects of a large fibre aspect ratio, having a fibre volume fraction greater than 1.5% can reduce the workability of the mix and cause balling or matting of the fibres.

Due to the water to cement ratio of a concrete mix being one of the key characteristics, adding water to improve workability is not feasible. Instead of adding water to the mix, an admixture known as superplasticizer is added which increases the workability of the mix while reducing the water amount by 12-30% [11]. Dosage amounts of superplasticizer to reduce the water to cement ratio range from 5-20 litres per cubic meter of concrete. All dosage recommendations depend on the type of superplasticizer used, with most manufacturers providing literature and instructions, but often several trial mix designs must be batched to determine an ideal mix.

Steel fibres are typically used as secondary reinforcement in addition to reinforcing steel bars. In many applications, fibres are used to control cracking caused by fatigue, impact, shrinkage, or thermal stresses [8]. Steel fibres can be the sole source of reinforcement in members that do not require continuous reinforcement for the structural integrity or safety that it provides. In thin sections that are not required by code to have continuous reinforcement, such as non-structural blast wall panels, steel fibres can be used to reduce the section depth but still provide improved toughness, flexural strength, and impact and fatigue resistance.

Research done by Banthia [12] shows that the addition of steel fibres increases the ductility of the concrete member both under static and dynamic loading conditions. He also found that hooked end steel fibres were superior to straight polypropylene fibres. A dramatic increase in the peak loads and fracture energies were also noted by adding steel fibres to the mix. The failure method noted was primarily steel fibre pull-out, with increasing numbers of fractured fibres as impact energy was increased. The addition of fibres reduced spalling and helped preserve the integrity of beams subjected to impact loads.

2.3 Ultra High Performance Fibre Reinforced Concrete

2.3.1 Definition

Ultra high performance fibre reinforced concrete (UHPFRC) is a material that can be characterized by the following ACI 239 definition, currently pending approval: “Ultra-High Performance Concrete (UHPC) is a cementitious, concrete material that has a minimum specified compressive strength of 150 MPa with specified durability, tensile ductility and toughness requirements; fibres are generally included to achieve specified requirements” [13]. The inclusion of steel fibres in some cases reduces the requirement for passive reinforcement such as normal steel reinforcing bars. The purpose of UHPFRC is to achieve high tensile strengths through the activation of the steel fibres within a matrix. This matrix still provides tensile strength even after first cracking due to the bond between the fibres and the concrete [14]. As this material is still relatively new and there are no existing North American design codes, CSA formed a working group in December of 2015 to develop a new annex on UHPC materials for their code, A23.1 [15].

Due to the relatively new nature of this material, there are a wide variety of both commercially available products and laboratory created mix-designs which claim to be ultra high performance concretes. There are no standard specifications outlining the material properties that must be satisfied to be classified as an UHPFRC with many manufactures and researchers focusing on achieving a high compressive strength [16] [17]. The penultimate property of a UHPFRC material is not only a high tensile strength, around 10 MPa, but that it exhibits strain hardening after reaching the ultimate strength and post-cracking. As each type of UHPFRC is unique, they all behave in slightly different manners but achieve the same basic properties.

2.3.2 Mix Design

There are many variations to the recipe or mix design for UHPFRC but all types are composed of the following constituents: cement, additives (powders), hard fine particles, water, admixtures, and steel fibres [18]. Each manufacturer or researcher alters the mix design in their own way to obtain specific material properties such as a higher compressive strength, better tensile properties, or more ductility. A standard UHPC mixture is list below in Table 2-1. Note that fibres are not included in this recipe, hence why it is referred to as UHPC as opposed to UHPFRC.

Table 2-1 - UHPFRC Mix Design, adapted from [19]

	Cement	GGBS ^{*1}	Silica fume	Silica sand	Superplasticizers	Water	Steel fibre 2% volume
[kg/m ³]	657	418	119	1051	40	185	157

^{*1} Ground granulated blast furnace slag (GGBS).

As with normal concrete mix designs, cement is the primary constituent with a dosage around 700-800 kg/m³ for most UHPFRC mixes [16] [20] [21] [22]. The amount of water included depends on the type of cement as each type has a different water demand. While the water to cement ratio of normal concrete is around 0.50, with UHPFRC the ratio is closer to 0.10-0.30. The solid particle materials that make up UHPFRC are all very fine particles, with no coarse aggregates. These particles allow a tight, cohesive matrix to form and this matrix, and the bond between the matrix and the steel fibres, is what gives UHPFRC its strength [14]. The ultra-fine particles such as silica fume and fine sands such as quartz or silica sand fill the matrix between the larger cement particles and are dispersed evenly using superplasticizers. Figure 2-3 shows the affect of superplasticizers on the concrete matrix, with a typical cement paste (A), a cement paste that has achieved more uniform packing using a superplasticizer (B),

and a concrete matrix that is formed with cement and ultrafine particles, such as silica fume, dispersed evenly using superplasticizer (C). UHPFRC is a flowing, self-consolidating type of concrete due in part to the addition of superplasticizers and the lack of coarse aggregates.

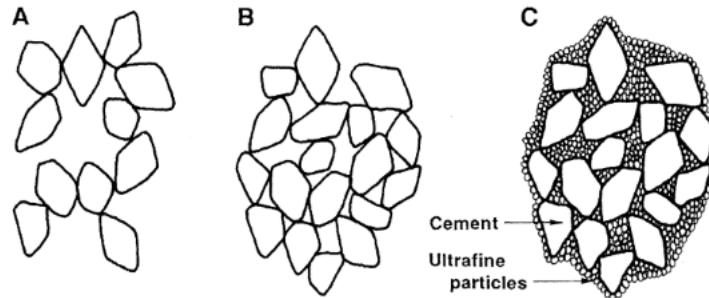


Figure 2-3 - Superplasticizer effect on concrete matrix [23]

The addition of fibres is what makes UHPFRC such an effective and strong material. The concrete material matrix can form a strong bond with the fibres that serves to solidify the overall strength of the material. While providing a large increase in the tensile strength of the material, fibres also increase the compressive strength of the material and prevent brittle failures and spalling [22]. The type of fibres added to the concrete mix have as much of an effect on the overall material properties as the types of cement and fines used [24]. There are a variety of different types of fibres used in UHPFRC applications, with materials such as high carbon steel, polyvinyl alcohol (PVA), and glass used to manufacture them [15]. The fibres are typically quite short, with those between 10-12 mm being the most commonly used. Certain mix designs call for a combination of fibres, sometimes containing up to three different sizes. In most dual-fibre mixes, there is a short fibre with a length less than 5 mm and a larger fibre with a length less than 30 mm [25]. The purpose of the short fibres is to prevent shrinkage cracks while the longer fibres provide the tensile strength, ductility, and toughness mandated of a UHPFRC. The majority of UHPFRC mix designs call for one type of fibre, with the most common being the in the range of 10-12 mm in length.

The proper dosage and correct type of fibres for a mix design are not the only important factors in producing a strong, ductile UHPFRC. The last critical step in producing effective UHPFRC members is ensuring there is an effective fibre orientation. Fibre orientation refers to the direction the fibres are oriented within the member. For a flexural beam for example, the fibres should be running in the same direction as the length of the beam, so that they will bridge the flexural cracks the will be located at the midspan. Since UHPFRC is a self-consolidating type of concrete, it flows well and requires no vibration during casting. Vibration during casting causes the fibres to orient themselves around the vibrator, leaving a fibreless area in the concrete. The fibres will orient themselves in the direction of flow so the casting method and production process must be carefully thought out to ensure the fibres are oriented properly for the required application [24].

2.3.3 Material Properties

Normal strength concretes are primarily categorized based on their compressive strength. While the compressive strength of UHPFRC is impressive, normally greater than 150 MPa, current design practices make it difficult to utilize this extremely high strength. In uniaxial compression, UHPFRC behaves differently than normal concrete because of the addition of the fibres and the tightly bonded matrix. There are six distinguishable phases of cracking in UHPFRC, as seen in Figure 2-4 and explained below:

1. elastic deformation between 0-40% of f'_c ;
2. development of microcracks parallel to the load between 40-70% of f'_c ;
3. development of microcracks perpendicular to the load between 79-90% of f'_c ;
4. localization of a macrocrack perpendicular to the load between 90-100% of f'_c ;
5. post-peak phase with the opening of the macrocrack;
6. complete rupture by lateral bursting.

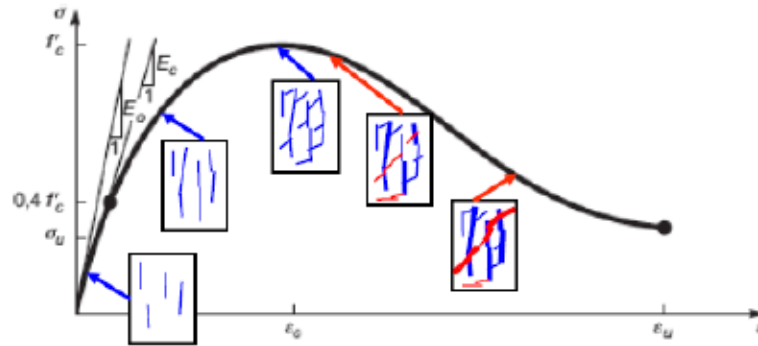


Figure 2-4 - Behaviour of UHPFRC under uniaxial compression [22]

The strain hardening behaviour of UHPFRC occurs due to the multiple cracks that form within the cross-section, as opposed to normal fibre reinforced concrete which will usually just have one large crack. The tensile response of UHPFRC is affected by the fibre properties such as their strength, stiffness, geometry, etc. as well as the concrete material matrix properties and the fibre-matrix interface properties. These variations in material properties, of both the steel fibres and the concrete material matrix, alter how the specimen will behave in tension, with several characteristic tensile responses shown below in Figure 2-5 [24].

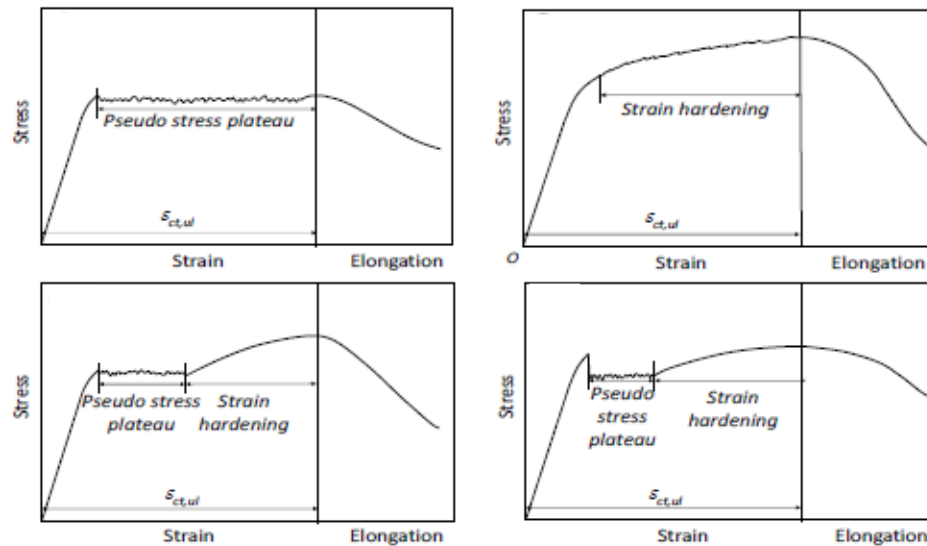


Figure 2-5 – Characteristic stress-strain behaviour of UHPFRC materials in tension [24]

A comparison between the tensile behaviour of normal SFRC and UHPFRC can be seen below in Figure 2-6. In this figure, the first region (I) is the elastic behaviour of the material up to point A. Point A is where the first crack occurs and the section continues to crack from point A to point B, during the

strain hardening phase. At point B, the primary crack opens and leads into a softening branch from point B to point C. This behaviour is much different than normal SFRC which, as shown in the figure, lacks a strain hardening phase after first cracking.

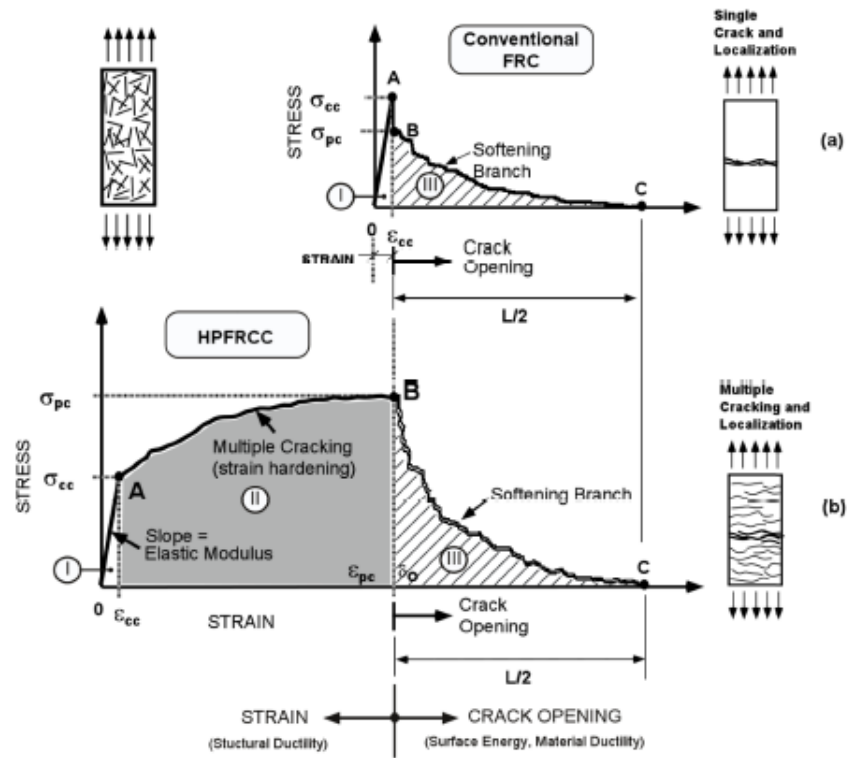


Figure 2-6 - Typical stress elongation response of fibre reinforced cement composites [9]

While the standard tests used for determining the compressive strength of normal strength concrete are suitable for finding the compressive strength and elastic modulus of UHPFRC, new testing standards must be made for determining the tensile strength. Studies have shown that the split-cylinder test (ASTM C496) and flexural test (ASTM C1609) do not accurately portray the tensile strength of UHPFRC [24] [26] [27]. A practice of making a dog bone shaped specimen, clamping it at the ends and placing a tension force on it has been found to be the most accurate test and is likely to be adopted as the standard test for determining the tensile strength of UHPFRC [28]. An example of the dog bone specimen tension test can be seen in Figure 2-7. The purpose of the smaller cross-section width at midspan is to ensure that failure occurs at this location, allowing it to be accurately recorded. This test is done to satisfy three important requirements for a pure tension test [29]:

- Application of load without eccentricity to the specimen, to achieve a pure tensile loading condition;
- Sufficient rigidity in the testing apparatus so that the crack opens uniformly across the width; and
- Sufficient stiffness so that after fracture, the post-crack response can be recorded.

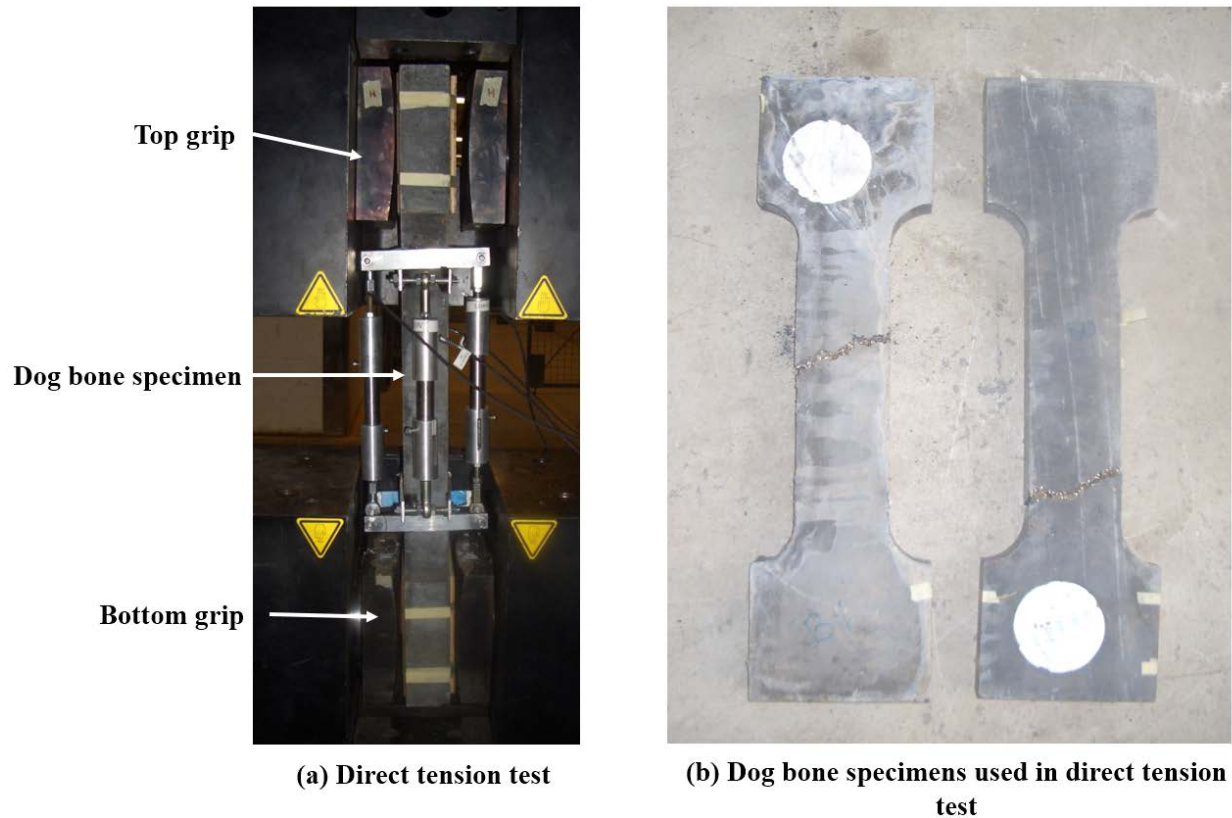


Figure 2-7 – Direct tension test for UHPFRC using dog bone specimens

UHPFRC is an innovative new material with key properties like ductility and post-crack strength which is giving designers the ability to create thinner structural components and is causing design codes to be rewritten to maximize the benefits of this material. The ductility provided by thin UHPFRC sections has attracted those who design structures which must be capable of surviving impact loading events such as those caused by explosive blasts.

2.4 FRP Strengthening

FRPs used for the strengthening of concrete members are composite materials made up of polymer matrices which are reinforced with fibres. The most common types of fibres used to reinforce the polymer matrix are glass, aramid, and carbon. This review will primarily focus on carbon fibre-reinforced polymer sheets. There are two design codes in Canada which deal with the use of FRPs in both construction and as a strengthening technique, Canadian Standards Association (CSA) Standard S806-12 [30] and CSA Standard S6-14 [31]. The advantage of using FRPs to strengthen existing concrete members is that they possess excellent properties such as high tensile strength and stiffness, they are lightweight, and they resist corrosion and chemicals [32].

Carbon FRPs (CFRPs) typically come in flexible, woven sheets but also exist as a cured material of fibre and epoxy both in sheet and reinforcing bar form. The flexible sheets are the most commonly used for external bonded strengthening because they are easily applied to a concrete member using a wet lay-up method, as shown in Figure 2-8. This method entails applying an epoxy to the concrete surface and laying the sheet over the epoxy. Once the sheet is flattened and smoothed against the concrete, an additional layer of epoxy is applied over to the outside surface to completely bond the FRP sheet to the

concrete member and to protect the fibres. Many studies have focused on the bond between the FRP sheet and the concrete member [32] [33] [34] [35] [36]. The wet lay-up method can be used to strengthen beams or columns in flexure or shear, and can help in confinement of concrete columns [37].



Figure 2-8 – FRP wet lay-up on concrete beam [38]

To strengthen a concrete member in flexure, strips of FRP are bonded to the tension face of the member using epoxy. Because most FRPs are unidirectional (the fibres run in one direction only), they can only provide strength in one direction. This means that the strips of FRP must be placed such that their fibres are oriented in the proper direction. For a simply-supported flexural beam, this means that the strips must run along the length of the bottom of the beam, as shown in Figure 2-9.



Figure 2-9 - FRP strips added to bottom of flexural beams [39]

Few studies have been done on the impact resistance of FRP strengthened members but research by Bhatti et al. [40] showed that the impact resistance of reinforced concrete slabs was increased by attaching an FRP sheet to the back surface of the slab, with the amount of strength added varying depending on the strengthening volume of the FRP sheet. A study by Yoo et al. [41] conducted experimental testing on normal strength concrete and SFRC slabs. Some slabs were strengthened with FRP sheets while some were left bare. This study found that when slabs were strengthened with FRP, the maximum deflections decreased by about 34% and the slabs could dissipate impact energies that were 2.3 - 2.7 times larger than normal RC and SFRC slabs.

While there is a large amount of published literature on the topics of FRP strengthening of reinforced concrete members, there is little research on the topic of FRP strengthening of SFRC members, especially when exposed to dynamic loading. Combining the ductility and crack control of SFRC with the tensile strength of FRP would likely lead to a very effective member.

2.5 Blast and Impact Loads

As defined by Cormie et al. [42], an explosion is a very fast chemical reaction producing transient air pressure waves called blast waves. An explosive blast produces thermal radiation in the form of a fireball and a large pressure and temperature gradient in the form of a blast wave front. This blast wave is a very compressed layer of air that is in disequilibrium with the air surrounding it. This disequilibrium causes the blast wave to expand outwards from the centre of the explosion towards the area of undisturbed air. The pressure variant between the undisturbed air and the blast wave reduces the further that the blast wave travels away from the centre of the explosion. The blast wave is propagated by the initial energy of the explosion and is forced to over-expand, causing the pressure of the air behind the blast wave to be lower than atmospheric conditions. This causes a negative phase to the blast, which results in a reversal in flow and a suction effect on particles and debris, bringing them back towards the centre of the explosion. The effects of the blast phases can be seen in Figure 2-10.

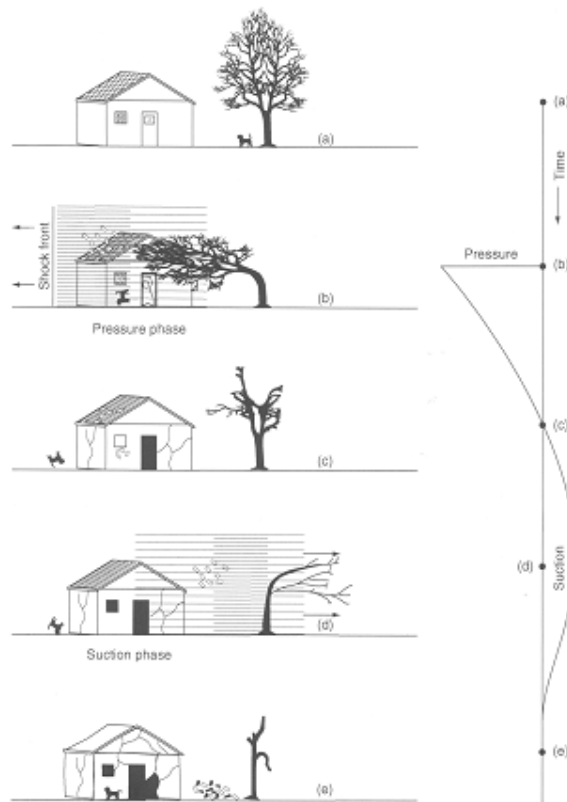


Figure 2-10 - Variations of blast effects associated with positive and negative phase pressures with time [42]

2.5.1 Blast Phases and Parameters

There are three phases to a blast which correspond to differences in pressure. The first phase is when the environment is in equilibrium and the air pressure is atmospheric. This phase is taking place until the blast occurs and leads all the way up until the blast wave arrives at the location in question. The time from detonation until the blast wave impacts the structure is known as the arrival time (t_A). When the blast wave contacts the structure, there is an immediate peak in pressure, the peak incident pressure (P_{so}), and the positive phase commences. The pressure begins to decay as soon as the blast wave passes and the duration of this pressure above atmospheric pressure is known as the positive phase duration (t_o). As the pressure continues to decay below atmospheric conditions, the negative pressure phase begins and continues until such time that the pressure returns to atmospheric (t_o^-). All phases of the blast can be seen in Figure 2-11 which is a typical pressure-time history. In addition to these parameters, the specific impulse (i_s), and negative specific impulse (i_s^-) are also important in blast analysis calculations. These values are simply the area under the incident pressure curve for both the positive and negative phase respectively [43].

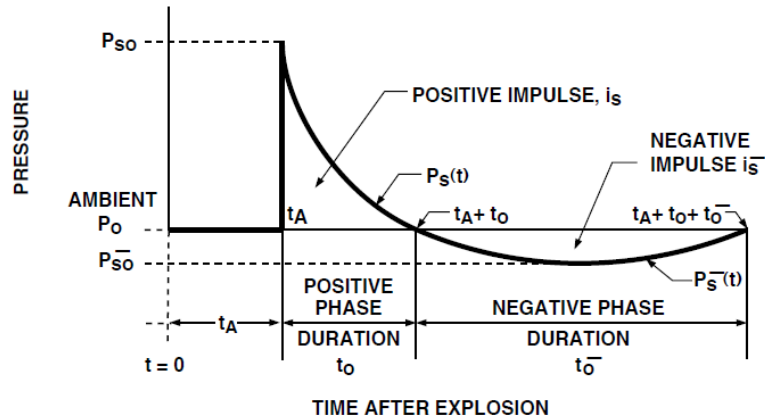


Figure 2-11 - Typical pressure-time history [43]

When designing a structural component to resist blast loads, the blast wave is simplified to be a triangular pressure load which idealizes the positive phase. The damage that is caused by an explosive blast occurs during the positive phase and is due to the punching characteristics of the peak positive pressure and impulse. To idealize the positive phase, which decays exponentially, the peak positive pressure is maintained but the positive phase duration is changed in order to maintain the same positive impulse. An idealized blast wave pressure-time history is shown in Figure 2-12.

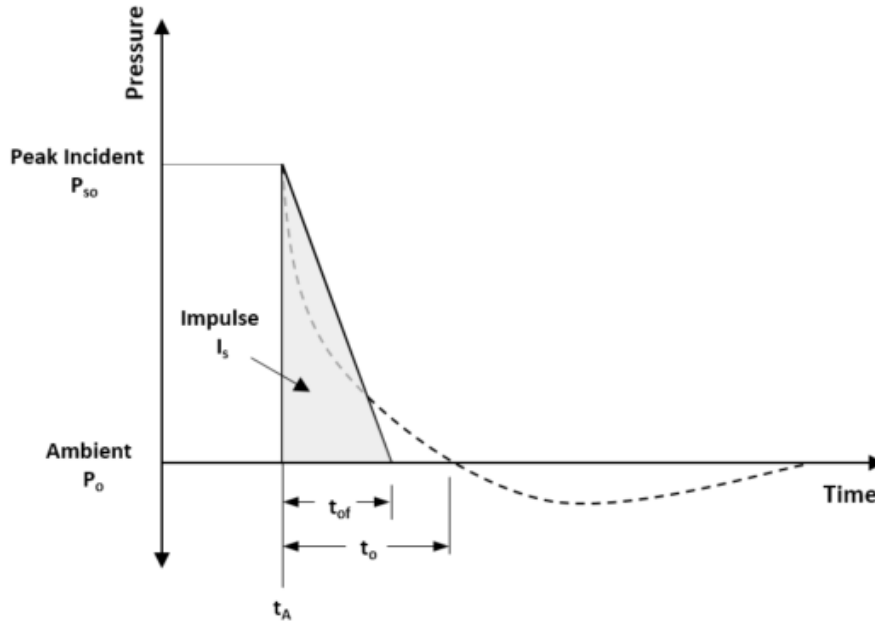


Figure 2-12 - Idealized pressure-time history

This triangular load represents the positive pressure phase can generally be replicated within a laboratory setting using an impact testing apparatus. Because of the impactor-specimen interaction the actual loading of an impact test may be more complex than this simplified representation.

2.5.2 Laboratory Impact Tests

Conducting explosive blast testing in the field is a very expensive and time-consuming process, and as such, other methods are required to simulate blast load conditions [44]. Concrete displays stress-rate sensitivity under compression, tension, and flexural loading conditions, which implies that the material properties determined through static laboratory testing cannot be used to predict the behaviour of concrete when it is subjected to high stress-rate loading conditions such as blast, impact or seismic events [45]. There is no generally accepted technique or practice to conduct impact load testing within a laboratory with various researchers using different testing set-ups. Researchers have typically used drop-weight impact machines, the Split Hopkinson bar, or a shock-tube apparatuses to simulate blast loads through impact events which have similar behaviour to a blast pressure wave [40] [46] [47] [48].

There are two basic types of impact loads which can be represented in a laboratory: single point impact loads, such as those caused by the impact of a projectile, and distributed impact loads, such as those caused by an explosive blast [12]. There are various set-ups that can be used to simulate distributed impact loads with many of them being used in the past at the Royal Military College of Canada. Pendulum-type impact hammers have been used in previous research investigating the effects of impact loads on RC columns, concrete sandwich panels, and GFRP panels [37] [49] [50]. An impact hammer was also used to test FRP sandwich panels that had a FRP catcher system, but in this case the hammer was designed to impact an inflated airbag to apply a distributed pressure load across the panel [51]. A vertical drop-weight hammer is an alternate arrangement for delivering an impact load to a structural specimen [40].

2.5.2.1 Effects of Testing Apparatus

Pendulum impact hammers and drop-weight impact devices are both adjustable by means of varying the amount of energy they can deliver. The amount of impact energy can be varied by altering either the drop height, or the mass, or both. The impact energy is governed by the following equation:

$$E_o = Mgh_d = \frac{1}{2}Mv_i^2 \quad (2-1)$$

Where E_o is the maximum available energy, M is the mass of the impact hammer, g is the gravitational constant, h_d is the drop height of the hammer and v_i is the impact velocity. The drop height of the hammer is difference between the point of impact and the height at which the hammer is dropped from, as shown in Figure 2-13.

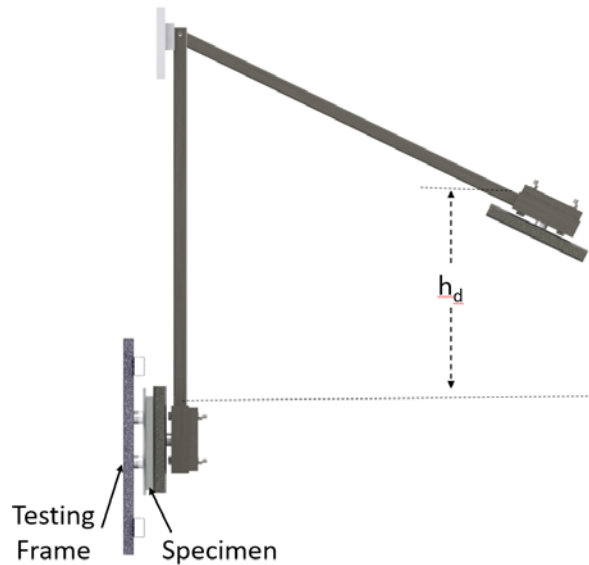


Figure 2-13 - Drop height of pendulum-type hammer

2.5.2.2 Transfer of Energy

Because of the inertial effects of the section's mass, some of the kinetic energy is lost when the impact device contacts the section. Very small amounts of energy are absorbed in forms of friction and heat loss while the remainder is absorbed by the section in the form of deformational energy or bending [49]. The inertial effects that prevent the full impact energy from being transferred to the section as deformational energy can be explained by D'Alembert's principle of dynamic equilibrium. This inertial force is a distributed load applied in the direction opposite of positive displacement, and is equal to the product of the section's mass and acceleration along its length, as shown in Figure 2-14. Per Banthia et al. [45], this distributed inertial load should be replaced with a generalized point inertial load ($P_i(t)$), which can then be subtracted from the tup impact load to obtain a generalized bending load ($P_b(t)$):

$$P_b(t) = P_t(t) - P_i(t) \quad (2-2)$$

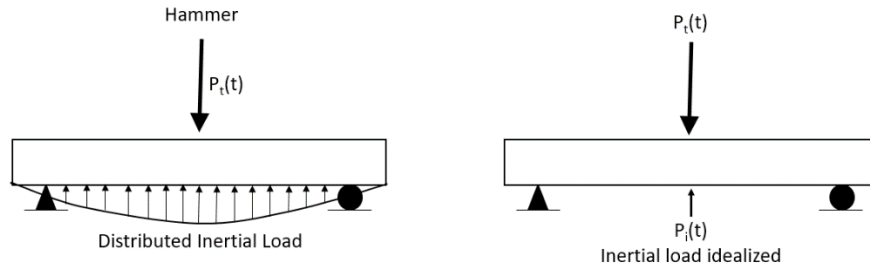


Figure 2-14 - Idealized inertial load, after [45]

Another method that can be used to compensate for the inertial loading effects of the specimen, which was used in this study, is to monitor the support reactions. By monitoring the support reactions, instead of just the hammer impact load, the load that is applied directly to the specimen can be measured directly, without the need for subtracting the inertial load.

2.5.3 Instrumentation of Impact Testing

The main parts of the testing apparatus which must be instrumented are the impacting face of the hammer, the support reactions, and the test specimen. The part of the hammer which contacts the specimen, the tup, can be instrumented with strain gauges or a force transducer to register the compressive force of the impact [45]. Strain gauges or force transducers can also be used to determine the reactions at the supports while a linear variable differential transducer (LVDT) is often used to ensure there is no deflection of the supports. Depending on the testing apparatus, the support reactions can be monitored solely on one side and then doubled to obtain the total reaction force, or they can be monitored from both sides. Accelerometers are typically placed on the impacting hammer to determine the impact velocity as well as on the specimen to determine deflection of the specimen. The specimen is also outfitted with strain gauges placed in areas of interest and a LVDT or similar measurement devices, such as a laser, to measure displacement at key locations, in most cases at the midspan.

2.5.4 Previous Experimental Impact Research

Studies have shown that both SFRC and UHPFRC have inherent material properties that make them ideal for use in blast loaded structural members. The increased ductility and tensile properties of both materials make them much more effective than normal reinforced concrete. Adding FRP to the external face of concrete members can also increase the impact resistance by providing additional flexural strength.

FRPs have been used to strengthen structural members to be able to resist blast or impact loads, and to strengthen structural members that have already sustained blast or impact loads. Research by Malvar et al. [52] showed that composites are effective for retrofitting key structural components such as columns, beams, and walls subjected to blast loading. Research done by Arndt [37] demonstrated that FRPs can effectively strengthen a concrete column that has been exposed to an explosive blast, and a study by Qasrawi et al. [53] showed that casting concrete columns in GFRP tubes increased their energy absorption when exposed to impact loads.

The impact resistance of concrete slabs has also been the subject of several studies. Research by Bhatti et al. [40] showed that the impact resistance of reinforced concrete slabs was increased by attaching an FRP sheet to the back surface of the slab, with the amount of strength added varying

depending on the strengthening volume of the FRP sheet. A study by Yoo et al. [41] conducted experimental testing on normal strength concrete and SFRC slabs. Some slabs were strengthened with FRP sheets while some were left bare. This study found that when slabs were strengthened with FRP, the maximum deflections decreased by about 34% and the slabs were able to dissipate impact energies that were 2.3 - 2.7 times larger than normal RC and SFRC slabs.

A number of research papers have investigated the qualities of ultra high performance fibre reinforced concrete (UHPFRC) to resist dynamic loading caused by explosive blasts and the fragmentation associated with these events. Xu et al. [54] conducted research on the behaviour of UHPFRC columns subjected to blast loading, concluding that they can effectively resist these types of load while reducing the maximum and residual displacements when compared to high strength reinforced concrete. In another study, Yi et al. [55] found that deflection, strain, and acceleration measurements during blast testing revealed that ultra-high strength concrete specimens have higher blast-resistant capacities than normal strength concrete. A study into the response of UHPFRC panels to blast loading by Ellis et al. [56] demonstrated that panels made of UHPFRC generated little debris and fragmentation. The ability of UHPFRC members to produce less fragmentation was also noted by Melancon et al. [57], who also found that during blast testing of columns, using UHPFRC enhanced the damage tolerance, increased the column capacity and reduced blast-induced deflections.

2.6 Cold Temperature Effects

The effects of cold temperatures on the blast and impact behaviour of normal reinforced concrete and the bond between reinforced concrete and FRP materials has had limited published literature [58] [59]. Unfortunately, there has been little, if any research done on the effects of cold temperatures on UHPFRC. The only relevant studies are on the effects of freeze-thaw cycles and de-icing chemicals, and the co-efficient of thermal expansion of UHPFRC [21] [60]. Numerous studies have looked at the effect of low temperatures on the curing of concrete and the evolution of concrete strength, but few have looked at the effect cold temperatures have on the impact resistance of concrete.

Green et al. [59] examined the effects of freeze-thaw cycling on the behaviour of reinforced concrete beams strengthened with FRP sheets in flexure. This study found that there are no significant adverse effects because of freeze-thaw cycling on RC beams strengthened with FRP sheets. While this study looked at the effects of freeze-thaw cycling, testing was conducted once the beams returned to ambient laboratory conditions and it did not investigate the behaviour of the beams when loaded under cold temperature conditions. A study by El-Hacha et al. [61] investigated concrete beams that were strengthened with prestressed CFRP sheets and were tested statically at room and low temperatures. This study concluded that cold temperatures did not negatively affect the behaviour of the CFRP strengthened beams.

An additional study by Green et al. [58] on the behaviour of FRP confined concrete columns demonstrated the effects that cold temperatures have on the behaviour of RC members strengthened with externally bonded FRP sheets. This study confirms two basic effects which occur when FRP materials are exposed to cold temperatures. The first effect is thermal incompatibility, which is related to the differences in the coefficients of thermal expansion between different materials, such as concrete and FRP. These differences cause internal stresses to develop between the concrete and FRP which can reduce the bond strength between the two materials. The second effect is polymer embrittlement which explains that while the polymer gains strength and stiffness at lower temperatures, the failure mode becomes more brittle because the increased stiffness reduces the ability of the matrix to transfer stresses between fibres.

2.7 Single Degree of Freedom Modeling

There are many numerical modeling techniques that can be used to analyze and predict the behaviour of structural members when exposed to blast or impact loads. The most common types of modeling used in literature and industry are computational fluid dynamics (CFD), finite element models (FEM) and single degree of freedom (SDOF) modeling. SDOF modeling may seem simplistic compared to the other methods of dynamic analysis, but it is common in the practice for the blast assessment of structural components due to its simplicity and validity [62]. Equivalent SDOF analysis simplifies the conditions within the environment and allows for structural elements such as beams, columns, and walls to be modelled as a simple spring-mass element, as shown in Figure 2-15. A typical SDOF system includes a forcing function, a mass, and a spring which resists the acceleration caused by the forcing function [63]. The forcing function is the blast pressure and the mass is the equivalent mass of the element in question. The resistance function for the element is determined based on its mass and stiffness and can include elastic, plastic, and elastoplastic regions. It is unique to each structural member and considers the cross-sectional dimensions, the amount and type of reinforcement, and the dynamic material properties. The parameters for the SDOF system are determined such that the maximum deflection within the system is equal to the maximum deflection that would occur within the actual structural member.

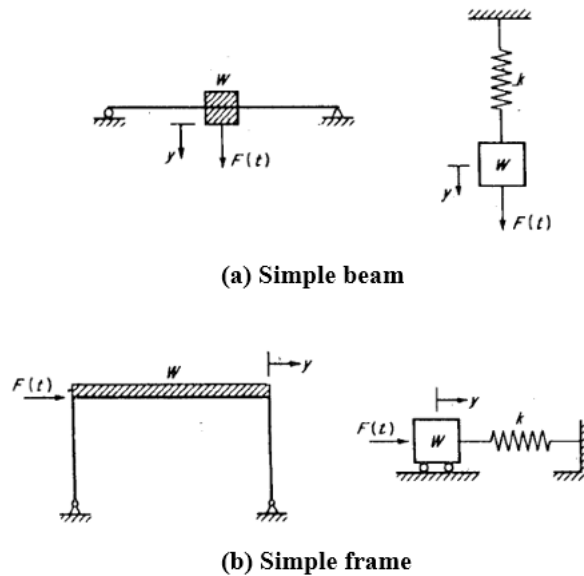


Figure 2-15 - Structures idealized as spring-mass systems [63]

In the case of impact loading, the inertial force must also be included as a force opposite to the forcing function, in addition to the mass and stiffness. A dynamic SDOF model is shown in Figure 2-16, where the forcing function, $F(t)$, is the impact load applied to the system by the hammer, which causes the mass, m , to move in the positive x -direction. The resisting function to this forcing function is made up of the stiffness of the structure, k , multiplied by the displacement, added to the inertial force which is equal to the product of the mass multiplied by the acceleration, $\ddot{x}(t)$. The governing equation for this SDOF model is:

$$F(t) = M\ddot{x} + kx \quad (2-3)$$

Research by Biggs [63] developed modification factors which allow the mass and stiffness of a specimen to be represented as a single element. The equation shown in 2-3 is modified using the

equivalent mass and stiffness determined by using the modification factors from Biggs to give equation 2-4, which is then modified using a load-mass factor to give the final governing equation shown in 2-5. This equation is valid while the specimen is exhibiting elastic behaviour and the second term, kx , is replaced with the ultimate resistance, R_u , once the elastic limit has been reached. A typical resistance function can be found in Figure 2-17.

$$F_e(t) = M_e \ddot{x} + k_e x \quad (2-4)$$

$$F(t) = K_{LM} \ddot{x} + kx \quad (2-5)$$

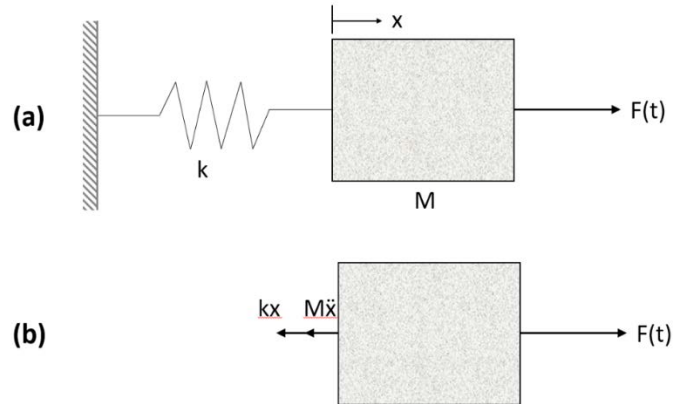


Figure 2-16 - Dynamic single degree of freedom model, adapted from [63]

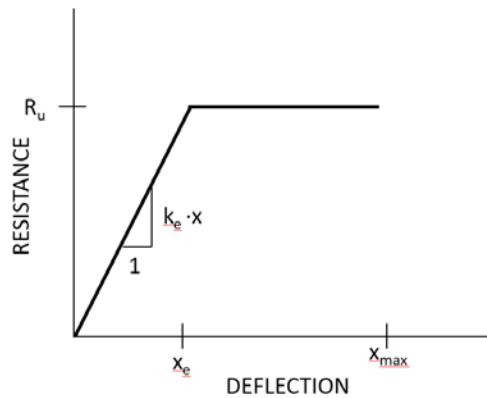


Figure 2-17 - Typical resistance function, adapted from [43]

The attractiveness of using SDOF modeling instead of CFD or FEM is the ability for these models to be done using a spreadsheet such as Microsoft Excel, or they can even be done by hand in some cases. More complex methods require specific computer programs that use a significant amount of computational power and can take a long time to run each iteration. A simple SDOF can be quickly built and run for different testing variations, while still providing accurate results. For those that require more accurate results, more complex programs may be preferred but in the realm of blast design, there are so many parameters and uncertainties that the increased accuracy of a complex program would likely be unwarranted.

2.8 Summary

There is a wide range of published literature available on the topics covered within this literature review. This review was intended to give a broad overview on the various elements that constitute this study and show that there is a gap in published research on the topic of the effect of cold temperatures on the blast and impact resistance of ultra high performance fibre reinforced concrete as well as FRP strengthened fibre reinforced concrete. Additional literature reviews are found at the beginning of each article within this document to provide specific, relevant details to the readers of those papers, allowing them to be sole-standing documents.

3. MANUSCRIPT #1: “COLD TEMPERATURE EFFECTS ON THE IMPACT RESISTANCE OF SFRC PANELS STRENGTHENED WITH FRP STRAPS”

3.1 Abstract

In this study, lightweight armour panels were designed using steel fibre reinforced concrete (SFRC) strengthened with fibre reinforced polymer (FRP) straps and experimental testing was conducted. Normal SFRC with a compressive strength of 40 MPa and a fibre dosage of 1% by volume was used. Fibres were Bekaert Dramix hooked-end fibres with a length of 60mm. Panels were cast with the dimensions of 1040 mm x 535 mm x 38 mm to limit their mass to approximately 50 kg and allow them to be carried by two individuals. These panels were designed to be a part of a modular protective system which could be used to protect key infrastructure and assets that may be exposed to extreme loading. Experimental quasi-static tests were conducted to determine a baseline loading capacity of the panels using three-point flexural bending. Dynamic testing was conducted using a pendulum-type impact hammer which could vary the amount of impact energy by altering the drop height of the hammer. Residual panel strength was determined after the panel was tested dynamically by using the same three-point flexural bending test that was used for quasi-static testing. All tests were conducted with panels at ambient laboratory temperatures and extreme cold temperatures to simulate Arctic conditions. Panels were tested at Arctic temperatures to determine their feasibility protecting critical infrastructure in Canada’s Arctic. The testing demonstrated that the FRP strengthened SFRC panels could resist impact loads with energies up to 2016 J without complete failure. Panels were not adversely affected by the extreme cold temperatures and in fact displayed increased effectiveness. Single degree of freedom (SDOF) modelling was used to estimate panel deflections based on various impact energies. The developed model appears to accurately predict peak displacements based on impact loading data.

3.2 Introduction

3.2.1 Protective Structures in Austere Environments

In an age of global terrorism, structures designed with the inherent ability to protect critical personnel and assets are of key importance to both the private and public sectors. There is an ever-present threat of accidental explosions in the oil and gas industry and deployed military forces are living under the constant threat of enemy offensive action. In Canada, the majority of the oil and gas industry is located in northern climates and the Canadian Armed Forces has several installations in Arctic regions where extreme cold temperatures are typical during the winter months. Being an extremely cold climate in the winter months, building materials and equipment intended for use in the Arctic must be tested under those cold weather conditions to ensure they are effective in the Arctic environment. Not only must these materials and equipment be functional at extreme cold temperatures, but they must also be effective during the summer months where temperatures are much warmer. While there has been research conducted in the fields of FRP strengthening of reinforced concrete (RC) structural components in cold temperatures [1] [2] and blast [3], there is a dearth of published literature on the topic of FRP strengthened SFRC exposed to the combined effects of blast or impact loads in extreme cold temperature environments.

3.2.2 Impact Resistant Properties of SFRC

Steel fibre reinforced concrete (SFRC) is simply defined as normal strength concrete that contains randomly distributed steel fibres. These fibres are added to the mix prior to pouring and are intended to reinforce concrete, which on its own, is brittle and lacks tensile strength and ductility [4]. There are many different types of steel fibres that can be used in this application, with variations in length, width, and shape. These fibres have a random distribution in the mix which leads to an increase to both the ultimate strength, toughness and the ductility of the concrete member [5]. These fibres increase the tensile capacity of the member as they bridge the cracks that form in the tension regions of the member as loads increase. Steel fibres can be the sole source of reinforcement in members that do not require continuous reinforcement for the structural integrity or safety that it provides. In thin sections that are not required by code to have continuous reinforcement, such as non-structural blast wall panels, steel fibres can be used to reduce the section depth but still provide improved toughness, flexural strength, and impact and fatigue resistance. Research done by Banthia [6] showed that the addition of steel fibres increases the ductility of the concrete member both under static and dynamic loading conditions. He also found that hooked end steel fibres were superior to straight polypropylene fibres. A dramatic increase in the peak loads and fracture energies were also noted by adding steel fibres to the mix. The failure method noted was primarily steel fibre pull-out, with increasing numbers of fractured fibres as impact energy was increased. The addition of fibres reduced spalling and helped preserve the integrity of beams subjected to impact loads.

3.2.3 FRP Strengthening

Fibre-reinforced polymers (FRPs) used in strengthening of concrete members are a composite material made up of a polymer matrix which is reinforced with fibres, typically fibres from glass, aramid, or carbon. The advantage of using FRPs to strengthen existing concrete members is that they possess excellent properties such as high tensile strength and stiffness, they are lightweight, and can resist corrosion and chemicals [7]. To strengthen a concrete member in flexure, strips of FRP are bonded to the tension face of the member using epoxy. Although externally bonded FRP strips do not enhance the ability of a member to carry its dead load, it has been shown that the application of FRP strips to a concrete beam or slab can significantly increase the live load capacity of that structural member [2] [8]. There have not been a lot of studies done on the impact resistance of FRP strengthened members but research by Bhatti et al. [9] showed that the impact resistance of reinforced concrete slabs was increased by attaching an FRP sheet to the back surface of the slab, with the amount of strength added varying depending on the strengthening volume of the FRP sheet. A study by Yoo et al. [10] conducted experimental testing on normal strength concrete and SFRC slabs. Some slabs were strengthened with FRP sheets while some were left bare. This study found that when slabs were strengthened with FRP, the maximum deflections decreased by about 34% and the slabs could dissipate impact energies that were 2.3 - 2.7 times larger than normal RC and SFRC slabs.

3.2.4 Pendulum-Type Impact Hammer Testing

Previous research has investigated the effects of blast loading on various types of structural components. As blast testing is an expensive and time-consuming endeavour, there have been numerous studies in literature that attempt to simulate blast loading in a laboratory setting. Researchers have typically used drop-weight impact machines, the Split Hopkinson bar, or a shock-tube apparatus to simulate blast loads through impact events which have similar behaviour to a blast pressure wave [11] [12] [13]. Several studies have been conducted using a pendulum-type impact hammer. This type of impact hammer provides the researcher with the ability to alter the amount of impact energy and the type of loading, either impulsive or dynamic, by changing the mass of the hammer and the drop height. Pendulum impact hammers as well as drop impact hammers have been used in a number of cases to

effectively apply severe, rapidly applied loading conditions within a laboratory setting with characteristics similar to projectile or blast loading conditions [14] [15].

3.3 Research Objectives and Scope

This research paper is part of a larger research project which focused on the ability of two types of armour panels to resist impact loads at ambient and cold temperatures. Although these panels would be installed in a spaceframe-type structure to provide sufficient protection, the design and testing of this type of structure is beyond the scope of this research.

The experimental study in this paper evaluated the armour panels made of SFRC that are strengthened with FRP straps. Two types of tests were conducted, testing the static and dynamic qualities of the panels. Quasi-static three-point flexural bending tests were completed on untested panels to determine a baseline load-deflection behaviour. The three-point flexural bending test was also used to determine the residual strength of impact tested panels. The impact testing conducted as a part of this research used a pendulum-type impact hammer. By varying the drop height of the impact hammer, the amount of impact energy could be altered. The initial impact energies were selected based on the baseline data provided by initial quasi-static testing, and subsequent impact energies were chosen based on the results of previous impact tests. All experimental testing in this research was conducted on panels at both ambient and extreme cold temperature. This was done to see the behavioural difference between panels tested at ambient laboratory temperature and extreme cold temperature.

Modeling for this research consisted of single degree of freedom (SDOF) modeling. This model was validated using the experimental testing results and can predict panel behaviour based on the impact load to which they are subjected.

3.4 Experimental Program

3.4.1 Specimens

A total of eleven specimens were tested in this experimental program. Four of those specimens were tested in a quasi-static manner using three-point flexural bending to determine baseline behavioural properties, and the remaining eight specimens were tested dynamically using a pendulum-type impact hammer. Panel dimensions can be found in Figure 3-1 and specimens were cast in plywood forms, following the recommended curing process outlined by the material supplier. All specimens have the same external dimensions; 1040 mm in length, 535 mm wide, and 38 mm thick. Panel dimensions were selected to keep the total panel mass around 50 kg, which would allow them to be carried by two persons.

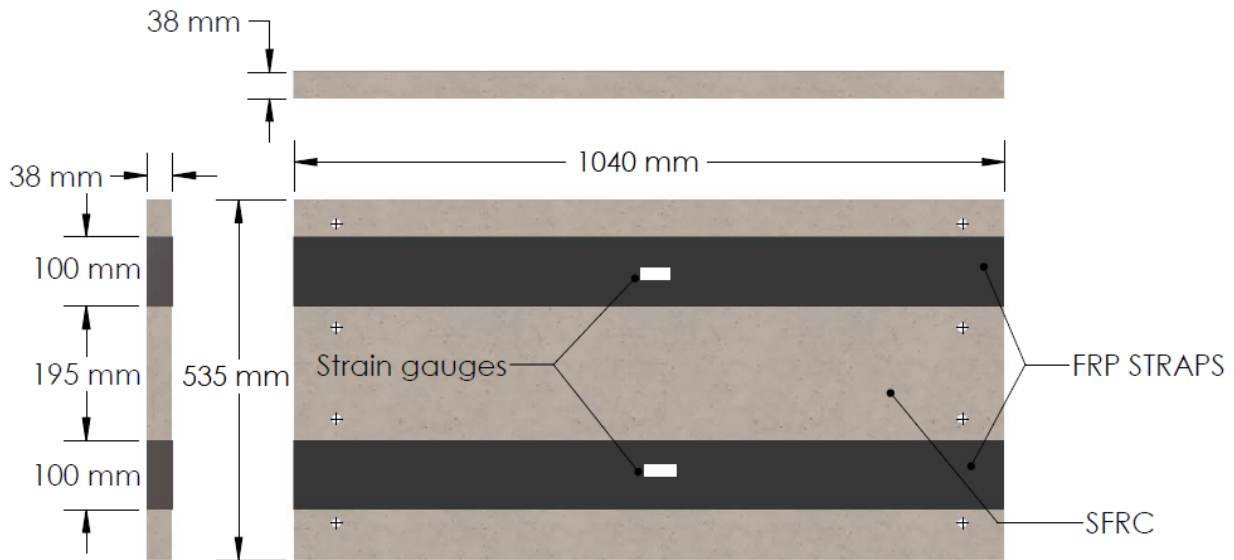


Figure 3-1 - Panel dimensions

Because this study is a part of a larger research project, a four-part specimen designation is used, with all test parameters shown in Table 3-1. The first letter refers to the type of material used with S referring to SFRC. The other panels used in this research project but not covered in this paper were made of ultra high performance fibre reinforced concrete, UHPFRC, and those panels are designated by the letter U. The second letter indicates whether the panel was tested at either ambient laboratory conditions, A, or cold temperature, C. The type of test is designated by the third term, with S referring to static testing and I indicating impact testing. Finally, the last term is the drop height level for the impact hammer.

Table 3-1 – Specimen Description and Test Parameters

Specimen Identification	Panel Material	Temperature	Test Type	Hammer drop height (mm)
SAS1	SFRC	Ambient	Static	-
SAS2	SFRC	Ambient	Static	-
SCS1	SFRC	Cold	Static	-
SAI1	SFRC	Ambient	Impact	500
SAI2	SFRC	Ambient	Impact	750
SAI3	SFRC	Ambient	Impact	1000
SAI4	SFRC	Ambient	Impact	1500
SCI1	SFRC	Cold	Impact	500
SCI2	SFRC	Cold	Impact	750
SCI3	SFRC	Cold	Impact	1000
SCI4	SFRC	Cold	Impact	1500

3.4.2 Materials

Ready mix air-entrained concrete with a steel fibre content of 1% by volume was used in this study. The fibres used in the study were Bekaert Dramix RC-65/60-BN fibres. These fibres are 60 mm in length with a 0.55 mm diameter and have a tensile strength of 1345 MPa [16]. Compression tests were carried out using cylinders with a 100 mm diameter and 200 mm height, and were conducted according to ASTM C39 [17]. Testing showed that the concrete provided had an average compressive strength of 40 MPa and an average modulus of elasticity of 22 GPa.

3.4.3 Test Setup, Instrumentation, Procedures

Quasi-static testing was conducted using a three-point flexural bending test on a MTS Model 322 machine. This machine was displacement-controlled and the head was set to displace at a rate of 2 mm/min. Panels were supported within the machine by triangular pins with bearing plates on top which would allow translation in the horizontal direction and limited rotation. The load was applied to the panel at midspan to simulate the same loading conditions as those found in the dynamic test. The loading setup can be seen in Figure 3-2. Midspan displacement was monitored by a 300 mm LVDT.

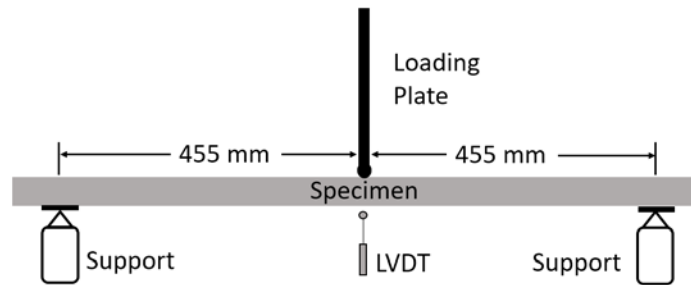


Figure 3-2 – Quasi-static three-point bending testing apparatus

Dynamic tests were conducted at varying hammer heights which altered the impact energy of the system. The same impact energies were used for tests of each type of panel and at each temperature, in order to have readily comparable data. An outline of the testing apparatus and testing schedule can be found in Table 3-2. The impact energy is calculated using the potential energy of the impact hammer which is based on the mass of the hammer, the drop height, and an acceleration of the gravitational constant, 9.81 m/s^2 . The drop height is calculated as the difference between the raised centre of gravity (CoG) and the at-rest CoG. Panels were secured to the testing frame using bolts which connected the panel through a steel rod to the reaction points on the test frame, as shown in Figure 3-3. The bolts were attached in such a manner to permit unrestrained rotation and limited translation of the tested specimen. Once an impact test was completed, the residual strength of the panel was tested by using the same three-point flexural bending test setup that was used for the quasi-static testing. For the panels tested at cold temperatures, they were returned to the freezer following the impact test so they could return to the proper temperature. Once the correct temperature was reached, approximately -70°C , the panel was taken out of the freezer and installed in the flexural testing apparatus. By the time all the instrumentation was set up and the test was ready to commence, the panels had reached a temperature of -60°C . Due to the duration of the test, the panels warmed to a temperature of -50°C by the end of the test.

Table 3-2 – Hammer Drop Heights

Specimen	Drop Height Level	Hammer drop height (mm)	Impact Energy (J)
SAI1	1	500	672
SAI2	2	750	1008
SAI3	3	1000	1344
SAI4	4	1500	2016
SCI1	1	500	672
SCI2	2	750	1008
SCI3	3	1000	1344
SCI4	4	1500	2016



Figure 3-3 - Bolted connection of specimen to testing frame

Strain gauges were installed on all panels, whether they were to be tested quasi-statically or dynamically. Gauges were applied to the FRP straps on the bottom face of the quasi-static panels and the back face of the dynamic panels, as shown in Figure 3-1. A type T thermocouple was applied to the surface of each cold temperature panel which provided constant temperature measurement throughout both the quasi-static and dynamic tests. Dynamic tests were highly instrumented to capture all relevant data. In addition to strain gauges, dynamic panels also had an accelerometer installed on the back of the panel at the midspan. Once the panels were installed in the impact testing frame, a laser was used to measure midspan displacement and an LVDT was placed at one support to monitor support deflections. The testing frame had three force transducers to measure loading data during the impact event. One force transducer was installed between the hammer arm and the hammer tip to measure the hammer force, and the other two force transducers were placed on the reaction points, one on the top left and one on the

bottom right, to determine the reactionary force. When using the reaction load for energy calculations, the data collected from each reaction point force transducer was doubled and then combined to obtain a complete reaction load. All testing frame instrumentation can be seen in Figure 3-4 and the test set-up can be seen in Figure 3-5.

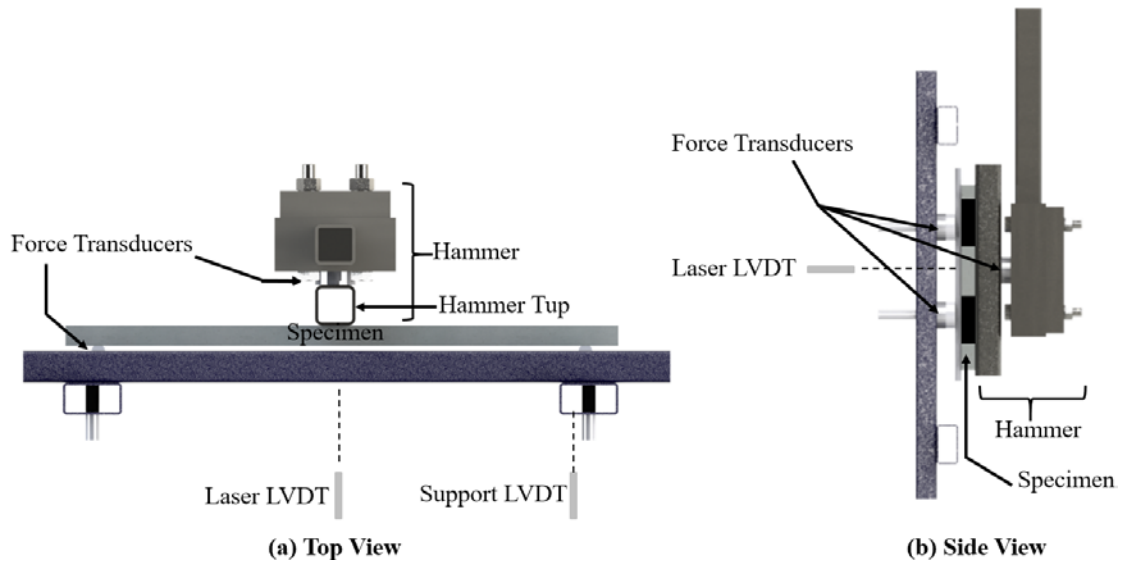


Figure 3-4 - Impact hammer instrumentation

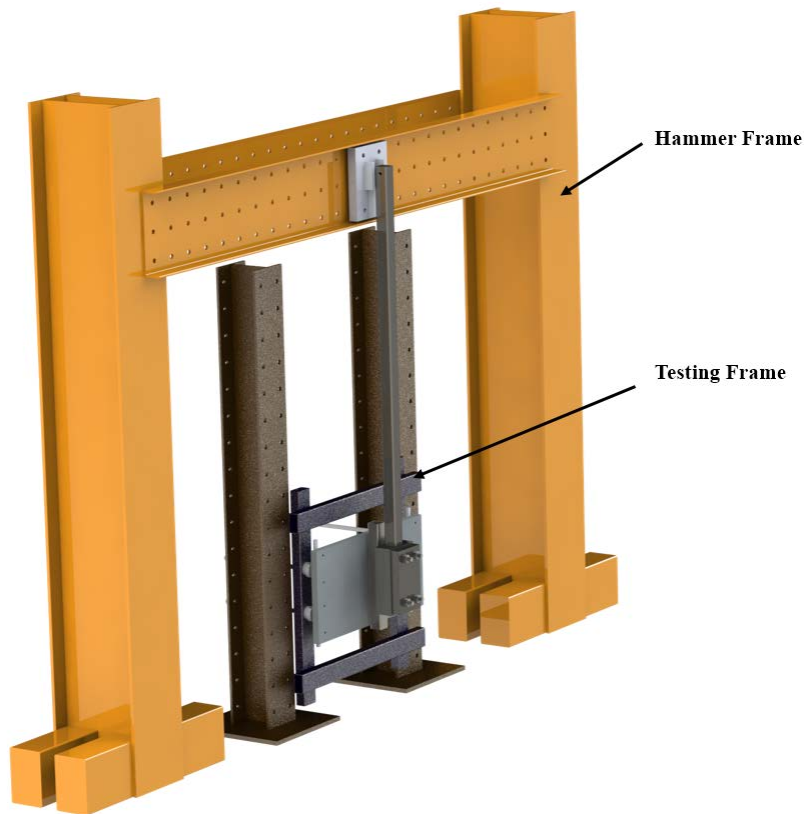


Figure 3-5 - Impact hammer test set-up

3.5 Test Results

Panel specimens were tested after at least 28 days of curing time. A summary of test results for quasi-static testing are found in Table 3-3, while the results from dynamic testing are presented in Table 3-4. Quasi-static results include the maximum load measured by the load cell in the MTS machine, P_{max} , the corresponding peak mid-span deflection measured by a LVDT, Δ_{max} , and the residual mid-span deflection $\Delta_{residual}$, measured once the load had been removed from the specimen. In addition to values of maximum load, peak and residual deflections, the dynamic testing results also include hammer potential energy, K_h , total work done by the hammer, W , and the amount of energy absorbed by the specimen, E_p . The maximum load for the dynamic tests is measured by the force transducer located on the hammer.

Table 3-3 - Summary of Quasi-Static Test Results

Specimen	Maximum Load P_{max} (kN)	Peak Deflection Δ_{max} (mm)	Residual Deflection $\Delta_{residual}$ (mm)
SAS1 ^a	18.0	39.7	--
SAS2	18.9	100.6	26.9
SCS1	15.8	122.0	25.8

^aPanel was not taken to maximum deflection before loading was removed. No data was obtained during re-loading.

Table 3-4 - Summary of Dynamic Test Results

Specimen	Drop height (mm)	Maximum load P_{max} (kN)	Peak deflection Δ_{max} (mm)	Residual deflection $\Delta_{residual}$ (mm)	Hammer kinetic energy K_h (J)	Work done by hammer W (J)	Energy absorbed by specimen E_p (J)
SAI1 ^a	500	45.2	40.8	1.4	672.0	482.8	420.5
SAI2	750	73.8	42.2	3.9	1007.8	687.1	642.8
SAI3	1000	82.8	45.2	7.2	1344.0	911.8	877.4
SAI4	1500	96.1	67.0	6.8	2016.0	2082.6	1309.8
SCI1	500	62.3	35.5	5.3	672.0	676.9	284.3
SCI2	750	76.6	44.6	6.0	1008.0	724.5	540.6
SCI3	1000	89.8	56.8	8.0	1344.0	1071.5	896.3
SCI4	1500	86.8	120.0	35.1	2015.9	3249.4	2866.9

^aPanel was hit 3 times. Data only acquired for 3rd hit.

A SFRC panel without FRP straps was the first panel to be tested quasi-statically to observe the effect that the steel fibres had on the strength and ductility of the panels. Three FRP strengthened panels were then tested. All tests were conducted in the same manner, with the ambient temperature panels being placed into the testing frame and the instrumentation hooked up and verified. Cold temperature panels were removed from the freezer at a temperature of -70°C and quickly placed into the testing apparatus. Testing was commenced as quickly as possible, so the temperature of the panel did not increase higher than -50°C by the end of the test. Cold temperature panels had their temperature range from -60°C at the beginning of the test to -50°C at the end of the test.

Dynamic testing began with a drop height of 500 mm for panel SAI1 and was increased to a height of 750 mm for panel SAI2 to study panel behaviour at various input energies. Upon seeing the results of those drop heights, it was decided that subsequent tests would be conducted at 1000 mm and 1500 mm to provide impact energies ranging from 672 J to 2016 J. Panel SAI1 was hit three separate times, with data being recorded the third time. Minor cracking occurred on the first two hits but the integrity of the FRP straps was not compromised.

3.5.1 General Behaviour

Three panels were tested quasi-statically using three-point flexural bending. Two ambient temperature panels and one cold temperature panel were tested. The ambient temperature panels displayed similar behaviour and data was only collected for one cold temperature test. All panels behaved in the same manner, with the FRP straps debonding and fracturing on the tension face of the panel before debonding on the compression face of the panel just before failure.

Eight panels were tested under impact loading, four panels were tested at ambient temperature and four panels were tested at extreme cold temperature. Each panel was subjected to impact loading from a different hammer drop height, ranging from 500mm to 1500mm. Cold temperature panels were tested at a temperature range of -50°C to -60°C , while ambient panels were tested at a temperature of approximately 20°C . Regardless of the drop height, all panels were very quick to crack due to the low strength of the concrete and the lack of standard steel reinforcement. At the lowest drop height, 500 mm, the FRP straps remained bonded to the concrete but as the drop height increased, the FRP straps began to debond. At the highest drop height, 1500 mm, the FRP straps completely debonded on the cold temperature panel but remained effective for the ambient temperature panel.

A typical impact event is shown in Figure 3-6 with photos captured from high-speed camera footage. As seen in the images, the hammer impacts the panel at midspan, immediately opening a crack which propagates from the back of the panel towards the front. In addition to the main crack, secondary cracks form and there is spalling of concrete from the back of the panel. The FRP straps on this panel, a 1500 mm drop height, debonded from the rear of the panel but remain bonded on the front. Once the impact event was over, the regions of FRP that remain bonded rebounded the panel back close to its original position, with a small residual deflection. All panels behaved in this way, with more debonding of FRP straps and larger residual deflections as the drop height was increased. Only panel SCI4 had complete debonding of the FRP, which resulted in a large residual deflection that was over four times larger than the previous largest residual deflection value.

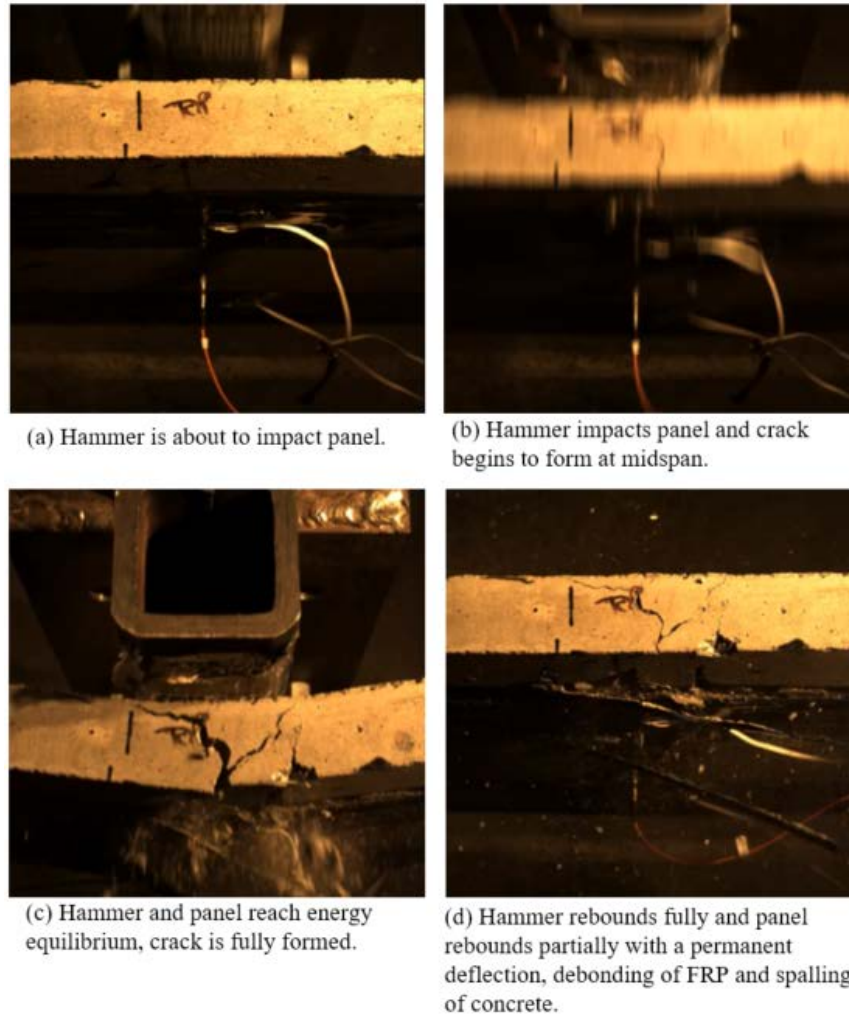


Figure 3-6 - Typical impact event captured by highspeed camera

3.5.2 Load-deflection behaviour and ductility

The load-deflection curves of the quasi-statically tested panels are shown in Figure 3-7. Each ambient temperature panel exhibited similar behaviour, with a distinct change in slope at first cracking of concrete and then a peak load of approximately 18 kN reached at a deflection of about 20 mm. Once the peak load was reached, the FRP straps began to debond at different locations on the panel, leading to drastic reductions in load-carrying capacity. After these rapid drops in capacity, the tension was redistributed to other parts of the FRP straps which allowed the load to increase again. Panel SAS2 was taken to its full deflection capacity and matched the behaviour of panel SAS1. For the cold temperature panels, panel SCS1 displayed a slightly different behaviour than those tested at ambient temperature, but still reached a similar plateau and had a higher maximum deflection. While the cold temperature panel also experienced drops in load-carrying capacity, these drops were not as significant as those experienced by the ambient temperature panels. The increased tensile strength of the SFRC at cold temperatures may allow the tension to be redistributed to other parts of the FRP straps quicker than the ambient temperature panels. It is assumed that all cold temperature panels will exhibit load-deflection behaviour like that of panel SCS1, depicted in Figure 3-7, but has not been verified experimentally.

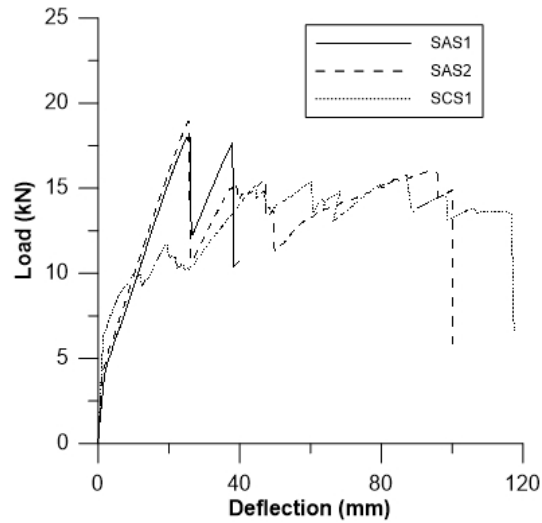


Figure 3-7 – Load-deflection behaviour of quasi-static panels

The load-deflection curves of the ambient temperature dynamic panels are shown in Figure 3-8. For each respective curve, the solid line represents an impact test, each graph designates which panel is represented, and the dashed line shows a comparison to a quasi-static load-deflection test. The loading data is sourced from the force transducers located on the reaction points of the panel. As seen in the graphs, there is an increase in deflection before there is a positive load recorded by the force transducers. This is due to the attachment of the panels to the testing frame and the fact that as the panel displaces at the midspan, the panel initially pries away from the supports which leads to a negative initial reaction load before it registers as a positive reaction load. The oscillations in the loading can be accredited to the oscillations of the panel after impact from the hammer and multiple impacts from the hammer. High-speed video shows the hammer impacting the panel, rebounding slightly and then continuing to impact the panel due to the kinetic energy of the hammer and is consistent with the multiple load peaks observed in Figure 3-8. Ambient temperature panels all displayed similar behaviour with similar peak loads from the hammer and increased maximum displacements as the drop height increased. The initial delay of load in the dynamic loaded panels is because the panel must deflect significantly and the inertia of the panel must be overcome before the reactions read a detectable load in the direction of the hammer's movement. The panels neither reached their maximum displacement as defined by the quasi-static tests nor completely failed.

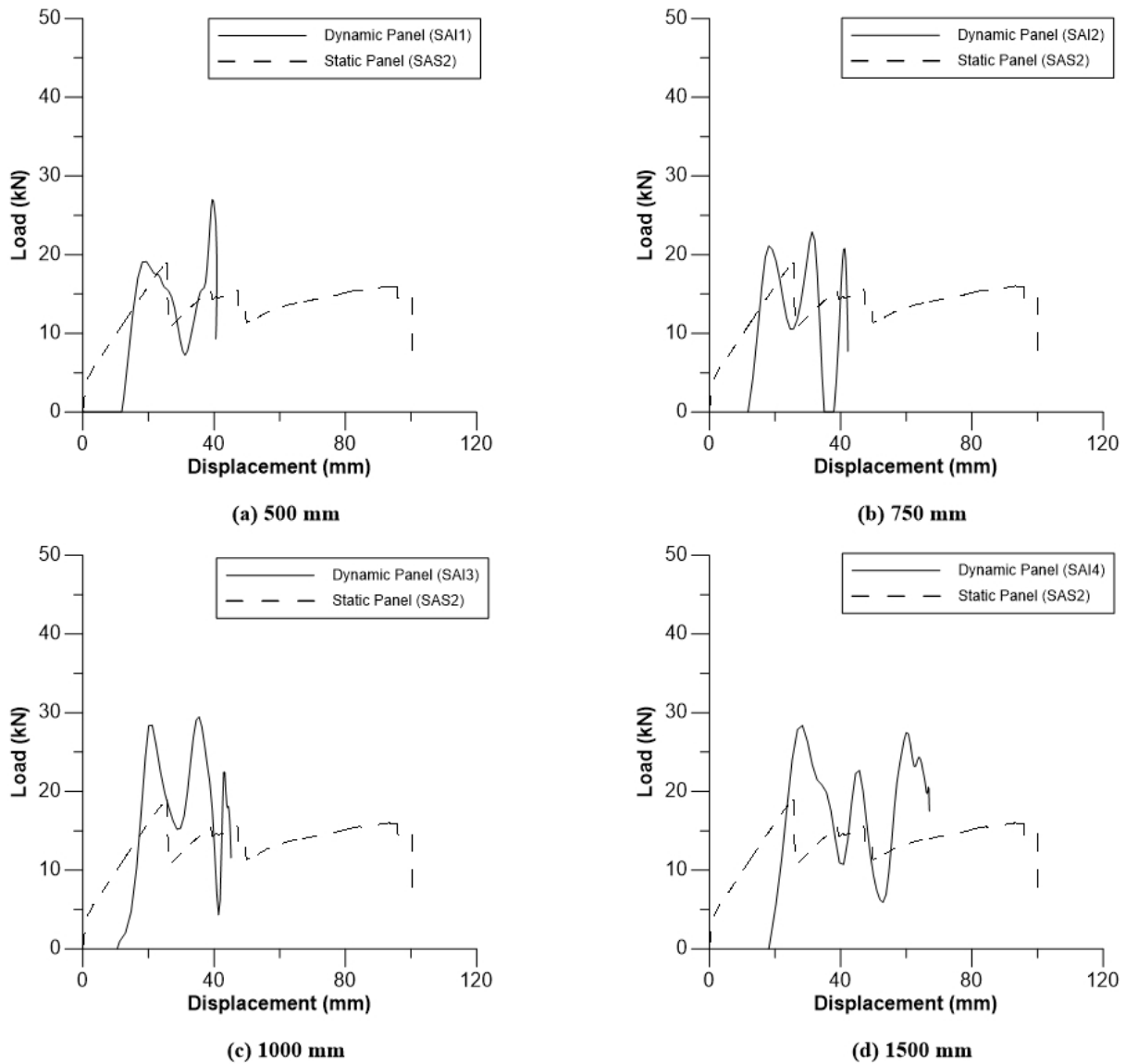


Figure 3-8 - Load-deflection behaviour of ambient temperature dynamic panels

The load-deflection curves of the cold temperature dynamic panels are shown in Figure 3-9. Cold temperature panels displayed similar behaviour to the ambient temperature panels, with similar panel oscillations, but the differences between adjacent peak loads and trough loads were lower than the room temperature tests. The lower loads differences are likely due to the increased tensile strength of the SFRC at cold temperatures. Cold temperature causes the concrete to have higher tensile strength, controlling and limiting the extent of debonding of the FRP. Furthermore, cold temperatures may cause the concrete to have increased bond strength on the steel fibres, increasing the tensile strength. This may cause cracks to be more effectively controlled, avoiding the greater intermittent losses observed in the room temperature panels. This effect was also noted in static tests where the drops in the load-deflection curve were less significant for the cold temperature panel than were noted for the room temperature tests. Panel SCI4 reached its maximum displacement and failed while all other panels had residual strength.

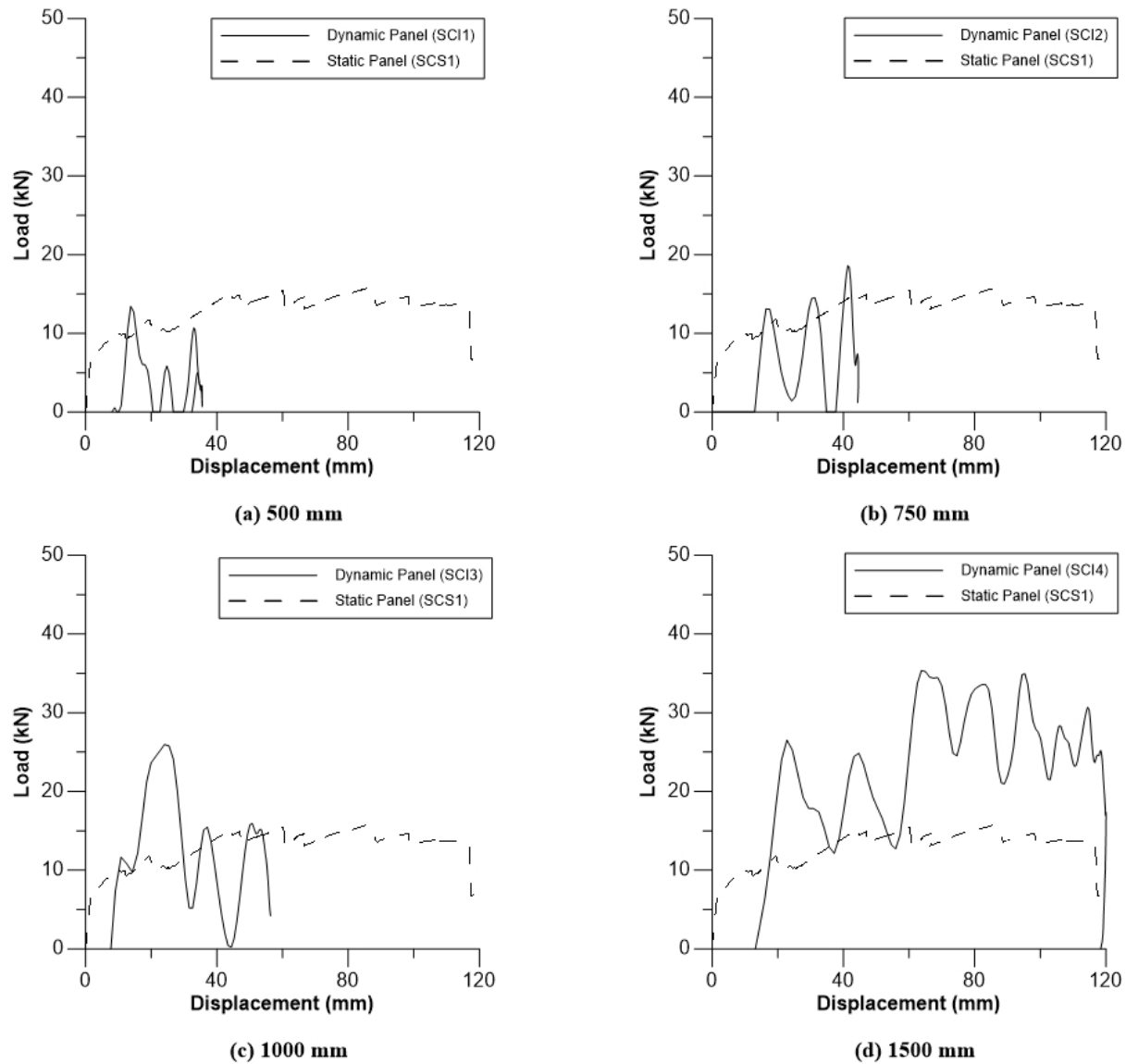


Figure 3-9 - Load-deflection behaviour of cold temperature dynamic panels

Although the general behaviour and shape of the load-deflection curves for impact tested ambient and cold temperature panels are similar, there are several differences in their behaviour. In addition to the differences in peak and trough loads, cold temperature panels generally experienced lower peak loads while reaching the same or greater maximum midspan displacements with the exception of the highest energy level at cold temperatures where the loads are highest at large deformations in panel SCI4. Again, this may be explained by the increased effectiveness of the concrete to bond both the FRP and steel fibre and to control the opening of cracks. There are slight differences in the load-deflection curves between ambient and cold temperature panels tested at the same drop heights which can be partially attributed to the panel's abilities to absorb energy, but it may be noted that there are uncertainties associated with the testing. If the same test was conducted multiple times, it is very likely that each load-deflection curve would be slightly different due to variables such as small differences in panel composition, installation of the panel in the testing frame, and the inconsistencies in the concrete-FRP bond.

3.5.3 Residual Strength of Dynamic Panels

Once dynamic testing of a panel was completed, the ambient temperature panels were immediately tested using the three-point flexural bending test used in quasi-static testing. The cold temperature panels were returned to the freezer until they once again reached at temperature of -70°C before being tested for residual strength. The load-deflection behaviour of the dynamically tested panels can be found in Figure 3-10. As shown in the graphs, each dynamic panel starts from the residual deflection caused by the impact test and then displays similar behaviour to the quasi-static panels, with peaks and valleys caused by fracturing and debonding of FRP. Table 3-5 lists the residual strengths of all panels that were tested dynamically. The cold temperature panels display more predictability than the ambient temperature panels, with all panels, regardless of their impact testing drop height, achieving a residual strength of 15 kN and reaching a displacement of 100mm - 200 mm. This may again be attributed to the higher concrete tensile and bond strength which better controlled the debonding of FRP and the pull-out of steel fibres. The ambient temperature panels display a much less predictable load-deflection behaviour, with a general observation that panels with a higher permanent deflection typically had lower residual strength.

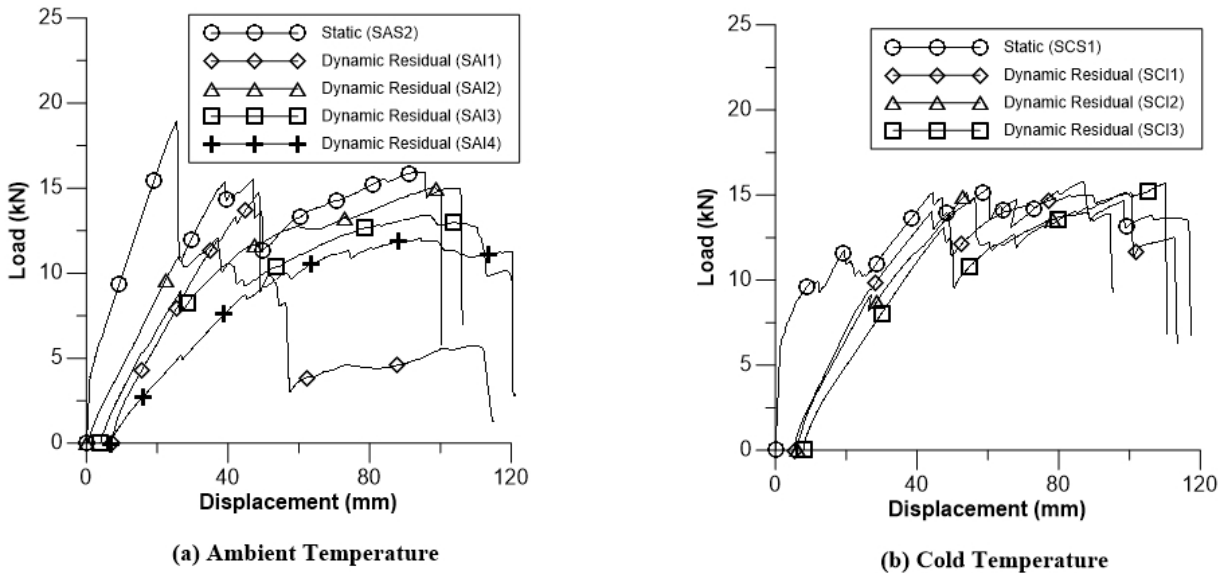


Figure 3-10 - Load-deflection behaviour of residual strength of FRP/SFRC panels

Table 3-5 - Residual strength of FRP/SFRC panels

Specimen	Drop height (mm)	Residual deflection $\Delta_{residual}$ (mm)	Residual Strength (kN)
SAI1	500	1.4	15.0
SAI2	750	3.9	13.4
SAI3	1000	7.2	14.8
SAI4	1500	6.8	12.0
SCI1	500	5.3	15.1
SCI2	750	6.0	15.1
SCI3	1000	8.0	15.7
SCI4 ^a	1500	35.1	--

^aComplete debonding of FRP straps and large cracking/spalling of concrete, no residual strength. Figure 3-11).

3.5.4 Failure Modes

All panels failed in the same manner, displaying a progression of failure. At lower impact energies, a crack would form at the midspan on the tension face (rear) of the panel. As the fibre dosage of the SFRC mix was quite low, few fibres bridged cracks and so spalling was an issue. As the impact energy increased, FRP fibres began to fracture and the FRP debonded from the concrete, causing the load to be redistributed. In all panels except for SCI4, some or all the FRP remained bonded to the concrete and had effective residual strength. Panel SCI4 had a complete failure and all FRP debonded from the back of the panel, leaving it with no residual strength, as shown in Figure 3-11.

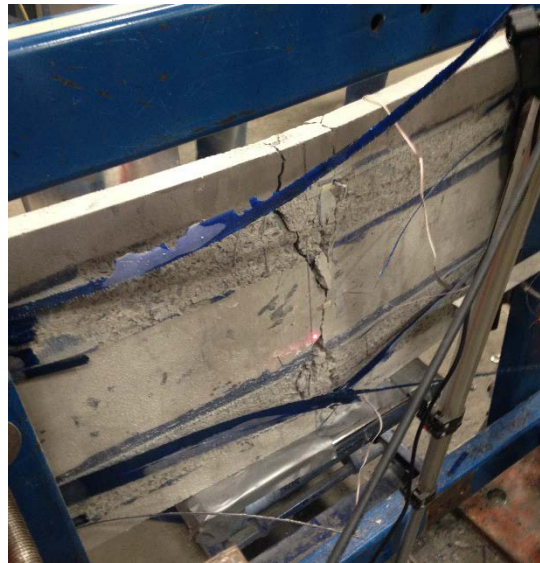


Figure 3-11 – Panel SCI4 post-impact. Complete debonding of FRP straps and cracking and spalling of concrete. No residual strength.

All panels, regardless of impact energy, displayed observable cracking and permanent, post-impact residual deflection. Panels tested at hammer drop heights of 500 mm and 750 mm exhibited behaviour such as that shown in Figure 3-12. These panels had noticeable cracking at the midspan but little fracturing and debonding of the FRP straps. Once the loading was complete, a small residual

deflection was observed. Panels impacted at higher drop heights, greater than 1000 mm, exhibited much more significant midspan cracking and had large portions of the FRP straps fracture and debond. These panels, like panel SCI4 shown in Figure 3-13, had larger permanent deflections due to the lack of FRP remaining bonded to the rear face of the panel post-impact.

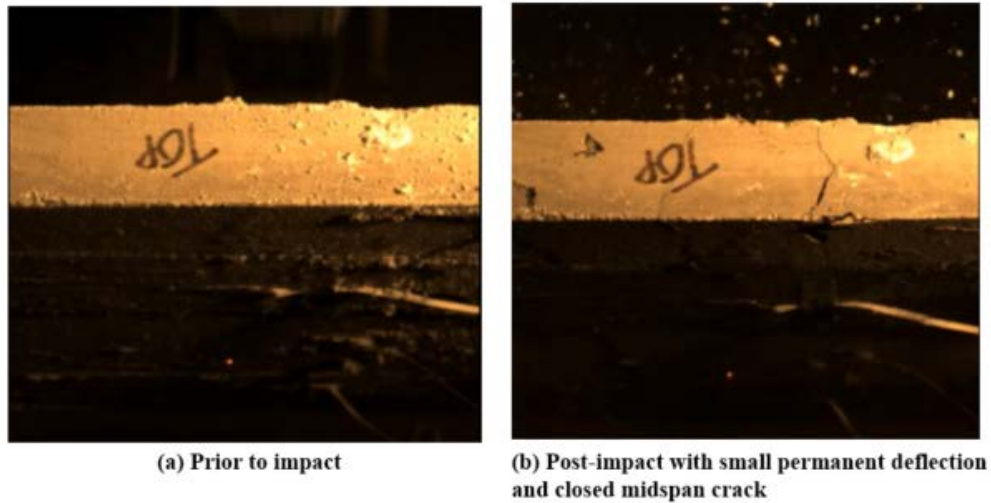


Figure 3-12 - Panel SCI2 pre- and post-impact

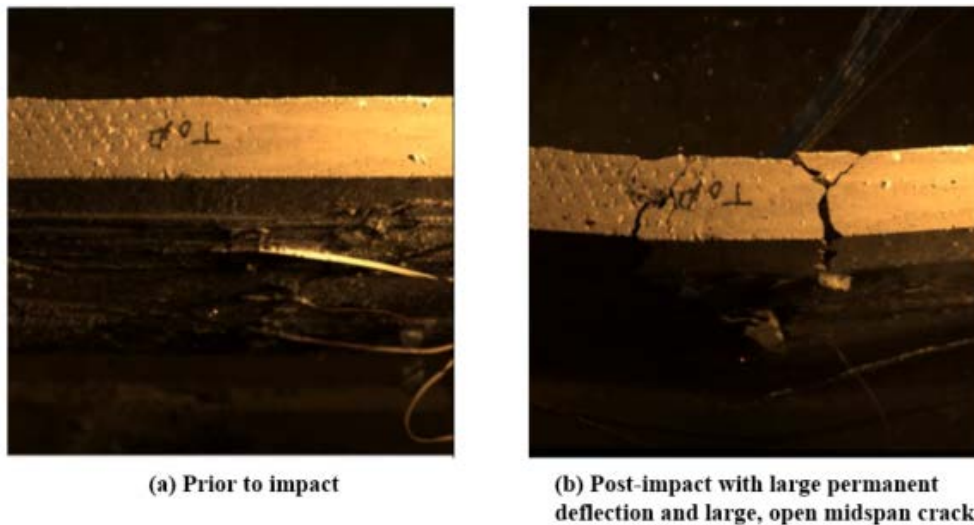


Figure 3-13 – Panel SCI4 pre- and post-impact

When tested for residual strength using the quasi-static testing apparatus, all panels failed in the same manner with a progression of the FRP straps debonding and fracturing on the tension face, debonding of FRP straps on the compression face, and finally complete fracturing of the tension face FRP straps. A typical post-residual testing panel is shown in Figure 3-14.

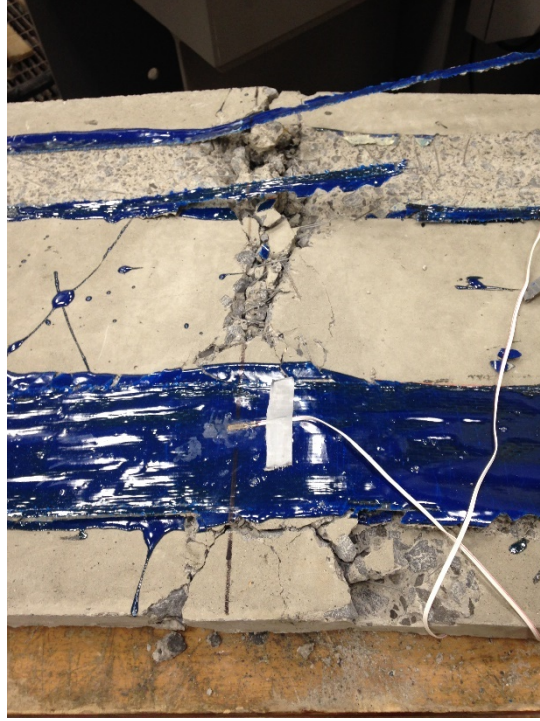


Figure 3-14 – Panel SAI2 post-residual strength testing. Fracture and debonding of one FRP strap, large cracks and spalling of concrete.

3.5.5 Conservation of Energy

Energy distribution is a key criterion in assessing the impact resistance of a structural element. In a closed system, such as the one in this study, the energy dissipated or absorbed by the system should equal the amount of energy that was introduced. In this study, the input energy is the kinetic energy lost by the impact hammer, which is calculated using the following equation [18]:

$$K_h(t_i) = \frac{1}{2} \cdot M_h \cdot \left[2 \cdot a_h \cdot h_h - \left(\sqrt{2 \cdot a_h \cdot h_h} - \frac{1}{M_h} \cdot I(t_i) \right)^2 \right] \quad (3-1)$$

Where M_h is the mass of the hammer, a_h is the hammer acceleration which could be measured but for this experiment the gravitational constant of 9.81 m/s^2 was used, h_h is the drop height of the hammer which is measured as the difference between the at-rest centre of gravity of the hammer and the raised centre of gravity, as was shown in Table 3-2. The final value used in the kinetic energy of the hammer equation is the impulse of the hammer, I , which is obtained based on integrating the hammer tup load.

The energy that is input into the system is transferred into kinetic and strain energy within the panel. The summation of these two energies is the amount of energy absorbed by the panel, which should be equal to the work done by the hammer. The kinetic energy of the panel is calculated using an equivalent mass and the midspan velocity of the panel (calculated from displacement data) while the strain energy of the panel is calculated by using the area under the reaction load-midspan deflection curve of the impact event. The work done by the hammer is calculated from the area under the load-displacement curve generated by the impact event and can be calculated using the following equation:

$$W(t_i) = W(t_{i-1}) + \frac{P_t(t_{i-1}) + P_t(t_i)}{2} \cdot [u(t_i) - u(t_{i-1})] \quad (3-2)$$

Where W , is the work done, P_t is the load measured from the hammer tup force transducer, and u is the midspan panel displacement at that time step.

For most of the panels in this study, the work done by the hammer is slightly less than the potential energy of the hammer, as seen in Table 3-4. For panel SCI4, the panel that failed completely, the work done by the hammer was higher than the potential energy of the hammer. The discrepancies between the potential energy and the work done by the hammer can be attributed to losses in the system due to elastic strains and vibrations and the manner in which the panels were secured to the testing frame.

Similar amounts of energy were absorbed by ambient and cold temperature panels impacted at the same hammer drop height, except for panel SCI4 which could absorb much more energy than the ambient temperature panel tested at a 1500 mm hammer drop height. This increase in panel energy absorption can be attributed to the FRP straps being pushed to failure and the increased bonding between the FRP strap and the concrete due to the higher tensile strength of the cold concrete.

An energy conservation graph for panel SAI1 is shown in Figure 3-15 which shows the relation between the work done by the hammer and the amount of energy absorbed by the panel. In this case, the correlation between the input and output energy from the system is very close but the same does not hold true for panels that are exposed to larger impact events, such as panel SAI4, shown in Figure 3-16. The amount of energy absorbed by panel SAI1 is nearly equivalent to the work done by the hammer but the energy absorbed by panel SAI4 is about 1000 J less than the work done by the hammer. This is because the energy absorption capacity of panel SAI4 was reached but panel SAI1 did not fully reach its energy absorption potential.

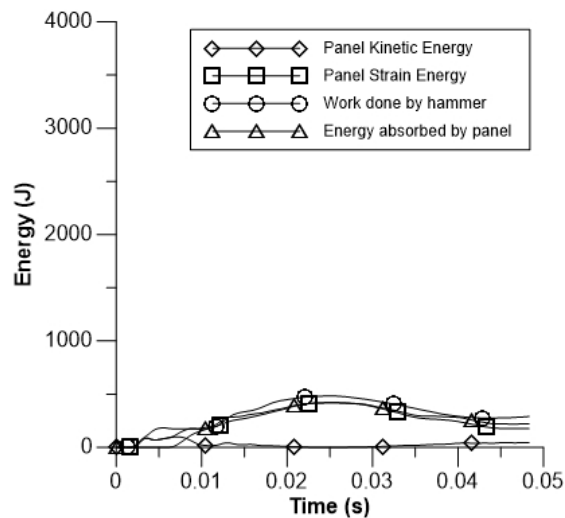


Figure 3-15 – Energy Conservation of Panel SAI1

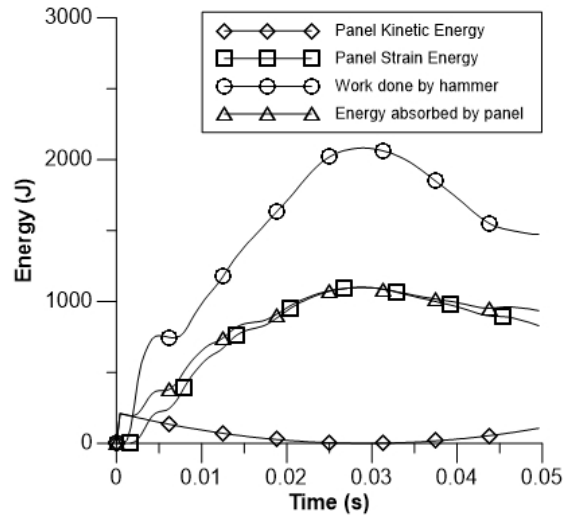


Figure 3-16 – Energy Conservation of Panel SAI4

3.6 SDOF Modelling

Single degree of freedom (SDOF) modelling is widely used in the practice of blast assessment of structural components due to its simplicity and validity [19]. Equivalent SDOF analysis simplifies the conditions within the environment and allows for structural elements such as beams, columns, and walls to be modelled as a simple spring-mass element. A typical SDOF system includes a forcing function, a mass, and a spring which resists the acceleration caused by the forcing function [20]. The forcing function is the blast pressure, or in this case it is the impact of the hammer, and the mass is the equivalent mass of the element in question. The resistance function for the element is determined based on its mass and stiffness and can include elastic, plastic, and elastoplastic regions. It is unique to each structural member and considers the cross-sectional dimensions, the amount and type of reinforcement, and the dynamic material properties. The parameters for the SDOF system are determined such that the maximum deflection within the system is equal to the maximum deflection that would occur within the actual structural member.

In this study, the resistance function for the FRP strengthened SFRC panels was determined based on idealizing the load-deflection curve found through quasi-static testing. A multi-linear load-deflection curve, shown in Figure 3-17, was created which could be used in the SDOF model to predict flexural behaviour.

The forcing function used in the model was provided by the force transducer that was located on the hammer tup. This transducer provided a forcing function, like the one found in Figure 3-18, that is similar in nature to the pressure-time history of an explosive blast. A different forcing function determined experimentally was used for each specimen as the impact load changed depending on the hammer drop height.

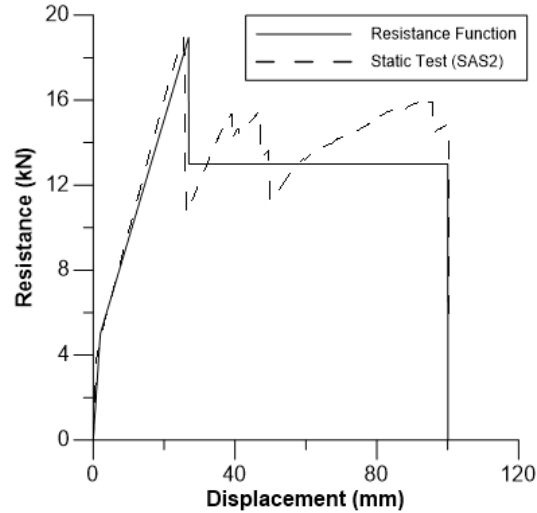


Figure 3-17 - Resistance Function for FRP/SFRC Panels

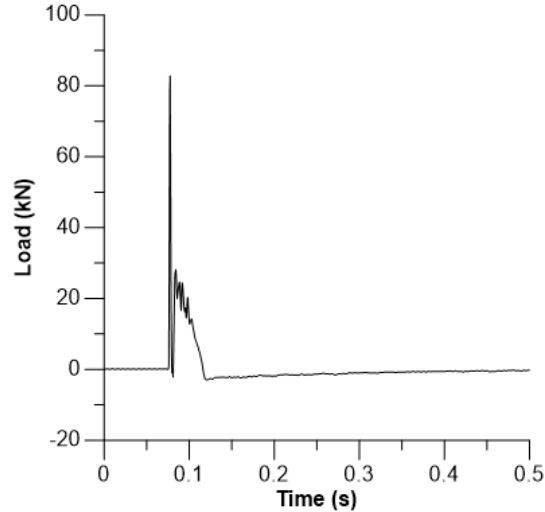


Figure 3-18 - Forcing Function (from hammer force transducer data of panel SAI1)

The SDOF model used in this study was based on the Predictor Method, established by Smith and Hetherington [21]. This method is based on constant acceleration throughout the time step and allows for accelerations, velocities, and displacements to be determined based upon a forcing function and resistance function. With the displacement and velocity set to zero at the beginning of the calculation, the initial acceleration can be determined by rearranging the equation of motion found below:

$$M\ddot{x} + R(x) = F(t) \quad (3-3)$$

Where $R(x)$ is the resistance function for the specimen, shown in Figure 3-17, $F(t)$ is the forcing function, such as the one shown in Figure 3-18, M is the mass of the specimen and \ddot{x} is the acceleration. Rearranging the equation of motion to determine the initial acceleration, the equation below is obtained:

$$\ddot{x} = \frac{F(0) - R(x_0)}{M} \quad (3-4)$$

Once the initial acceleration is known, since it remains constant throughout the time step, it can be used to find the velocity at the end of the time step using the equation below:

$$\dot{x}_1 = \dot{x}_0 + \ddot{x}_0 \Delta t \quad (3-5)$$

Where \dot{x} is the velocity of the specimen and Δt is the duration of the time step. The displacement is then given by:

$$x_1 = \dot{x}_0 \Delta t + \frac{1}{2} \ddot{x}_0 \Delta t^2 \quad (3-6)$$

Where x is the displacement and is based upon the velocity and acceleration at the previous time step. With the displacement known, the associated resistance value can be found from the resistance function and then the process can be continued until the complete displacement response is found, as shown in Figure 3-19. The figure shows plots of the resistance function, the displacement found by the SDOF model, and the actual displacement of panel SAI1 as measured by the laser. As seen in the figure, there is good correlation between the predicted displacement using the SDOF model and the actual measured displacement.

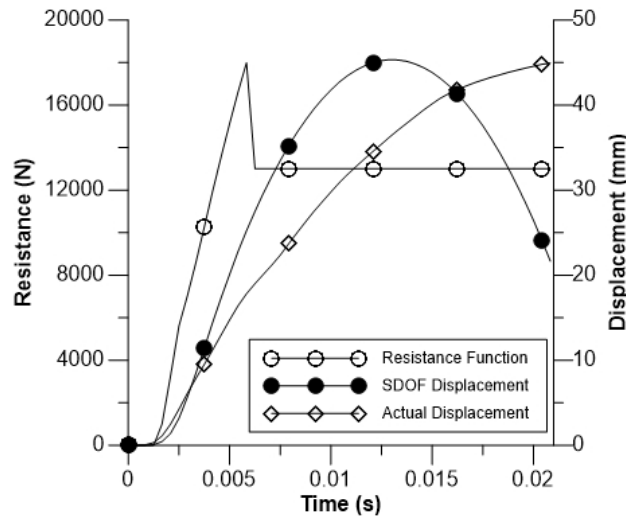


Figure 3-19 – SDOF Model for panel SAI1

Table 3-6 shows the results of the model for each panel and compares those results to the actual measured displacements from laboratory tests. As seen by the percent error, the model could accurately predict the panel midspan displacement for some specimens, particularly the ones tested with lower impact energies, but was off by as much as 42% for others. Panel SAI1 was hit three times from a 500 mm drop height due to data acquisition errors. While there was minimal visible cracking and damage to the FRP straps, the strength of this panel would have been reduced by the first two hits, reducing the strength for the final hit. This reduction in strength led to an increased peak deflection, making the SDOF prediction inaccurate. The predicted peak deflection from the SDOF model for panel SCI4 was off because the panel completely failed. The model did not predict complete failure, causing the deflection to be off by close to 40%.

The unpredictable behaviour of the FRP straps on the SFRC panels leads to the difficulty in predicting their behaviour. It is unknown at what load or deflection the FRP will begin to debond, and as such, predicting the peak deflection using a SDOF model is difficult. Utilizing a resistance function with

a flat plateau does not fully represent the actual behaviour of these types of panels. Although the flat plateau is an average of the panel strength throughout that deflection range, the load will instead fluctuate. The same resistance function was used for both ambient and cold temperature panels, which could also affect the accuracy of the model.

Table 3-6 - SDOF model comparison to actual data

Specimen	Drop height (mm)	Peak deflection (mm)	SDOF Peak deflection (mm)	% Error
SAI1 ^a	500	40.8	23.5	42.4
SAI2	750	42.2	33.5	20.6
SAI3	1000	45.2	45.3	0.2
SAI4	1500	67.0	65.0	3.0
SCI1	500	35.5	40.9	13.2
SCI2	750	44.6	47.6	6.3
SCI3	1000	56.8	57.1	0.5
SCI4	1500	120.0	73.0	39.2

^aPanel was hit 3 times. Data acquisition only worked for 3rd hit.

3.7 Conclusions

The experimental program outlined in this paper was created to design and test a lightweight, armour panel made of SFRC that was strengthened with FRP straps. These panels could be utilized as part of a modular protective system by military forces to form protective works which can withstand the effects of projectiles or an explosive blast.

1. Extreme cold temperatures do not appear to negatively affect the behaviour of SFRC panels strengthened with FRP straps. In particular, cold temperatures did not appear to reduce the energy absorption capacities of the panels.
2. Impact-tested cold temperature panels that did not reach ultimate failure, i.e. complete debonding of FRP straps, all had similar residual strength (15 kN) despite having absorbed various levels of impact energy.
3. Ambient temperature panels tested using the impact hammer had decreasing residual strength based on the amount of residual deflection. Those panels tested at higher impact energies displayed higher residual deflections and lower residual strength.
4. The presence of fibres may reduce the amount of spalling and cracking in the panels but unlikely provided any significant additional strength because the overall capacity of the panels is controlled by the FRP straps.
5. The strength of these panels is attributed to the FRP straps which were applied using a wet lay-up procedure. Despite the best efforts, inconsistencies between each panel were inevitable with varying levels of concrete panel smoothness and different amounts of epoxy used for each strap.
6. The SDOF model developed for these panels did a reasonable job representing the behaviour of the panels. It had an error of up to 42% for some panels, likely due to the unpredictable nature of the FRP straps. Developing an accurate resistance function is difficult to achieve due to the inconsistencies in FRP bonding. The model was most accurate at a drop height of 1000 mm and least accurate at a drop height of 500 mm. The inaccuracy of the model at a drop height of 500 mm can be accredited to a weakened SAI2 panel and is not indicative of the overall accuracy of the SDOF model. It did not predict

the failure of panel SCI4 but the predicted displacement of panel SAI4, also impacted from a drop height of 1500 mm, was only off by 2 mm from the actual displacement.

3.8 Acknowledgments

This research project was funded by the Natural Science and Engineering Research Council of Canada (NSERC) and the Department of National Defence (DND).

3.9 References

- [1] M. F. Green, L. A. Bisby, A. Z. Fam and V. K. Kodur, "FRP confined concrete columns: Behaviour under extreme conditions," *Cement & Concrete Composites*, no. 28, pp. 928-937, 2006.
- [2] M. F. Green, A. J. Dent and L. A. Bisby, "Effect of freeze-thaw cycling on the behaviour of reinforced concrete beams strengthened in flexure with fibre reinforced polymer sheets," *Canadian Journal of Civil Engineering*, no. 30, pp. 1081-1088, 2003.
- [3] L. J. Malvar, J. E. Crawford and K. B. Morrill, "Use of Composites to Resist Blast," *Journal of Composites for Construction*, vol. 11, no. 6, pp. 601-610, 2007.
- [4] W. Elsaigh, "Steel Fiber Reinforced Concrete Ground Slabs; A Comparative Evaluation of Plain and Steel Fiber Reinforced Concrete Ground Slabs," University of Pretoria, Pretoria, 2001.
- [5] M. V. Mohod, "Performance of Steel Fiber Reinforced Concrete," *International Journal of Engineering and Science*, vol. 1, no. 12, pp. 01-04, 2012.
- [6] N. P. Banthia, "Impact Resistance of Concrete," PhD Dissertation, 1987.
- [7] H. A. Toutanji and W. Gomez, "Durability characteristics of concrete beams externally bonded with FRP composite sheets," *Cement and Concrete Composites*, no. 19, pp. 351-358, 1997.
- [8] C. Bakis, L. Bank, V. Brown, E. Cosenza, J. Davalos, J. Lesko, A. Machida, S. Rizkalla and T. Triantafillou, "Fiber-Reinforced Polymer Composites for Construction - State-of-the-Art Review," *Journal of Composites for Construction*, vol. 6, no. 2, pp. 73-87, 2002.
- [9] A. Q. Bhatti, N. Kishi and K. H. Tan, "Impact resistance behaviour of RC slab strengthened with FRP sheet," *Materials and Structures*, vol. 44, pp. 1855-1864, 2011.
- [10] D.-Y. Yoo, K.-H. Min, J.-Y. Lee and Y.-S. Yoon, "Enhancing impact resistance of concrete slabs strengthened with FRPs and steel fibres," in *6th International Conference on FRP Composites in Civil Engineering*, Rome, 2012.
- [11] D.-Y. Yoo, N. Banthia, S.-T. Kang and Y.-S. Yoon, "Effect of fiber orientation on the rate-dependent flexural behavior of ultra-high-performance fiber-reinforced concrete," *Composite Structures*, vol.

157, pp. 62-70, 2016.

- [12] O. Millon, A. Kleemann and A. Stolz, "Influence of the fiber reinforcement on the dynamic behaviour of UHPC," in *First International Interactive Symposium on UHPC*, Des Moines, Iowa, 2016.
- [13] H. Aoude, F. P. Dagenais, R. P. Burrell and M. Saatcioglu, "Behavior of ultra-high performance fiber reinforced concrete columns under blast loading," *International Journal of Impact Engineering*, no. 80, pp. 185-202, 2015.
- [14] Y. Qasrawi, P. J. Heffernan and A. Fam, "Dynamic behaviour of concrete filled FRP tubes subjected to impact loading," *Engineering Structures*, vol. 100, pp. 212-225, 2015.
- [15] M. Zineddin and T. Krauthammer, "Dynamic response and behavior of reinforced concrete slabs under impact loading," *International Journal of Impact Engineering*, vol. 34, pp. 1517-1534, 2007.
- [16] Bekaert, "Dramix Fibre Data Sheet," Bekaert, 2010.
- [17] ASTM C39 / C39M - 16b, "Standard Test Method for Compressive Strength of Cylindrical Concrete Specimens," ASTM International, West Conshohocken, PA, 2016.
- [18] N. Banthia, S. Mindess, A. Bentur and M. Pigeon, "Impact Testing of Concrete Using Drop-Weight Impact Machine," *Experimental Mechanics*, pp. 63-69, 1989.
- [19] S. Astarlioglu and T. Krauthammer, "Response of normal-strength and ultra-high-performance fiber-reinforced concrete columns to idealized blast loads," *Engineering Structures*, no. 61, pp. 1-12, 2014.
- [20] J. M. Biggs, *Introduction to Structural Dynamics*, McGraw-Hill, Inc., 1964.
- [21] J. Hetherington and P. Smith, *Blast and Ballistic Loading of Structures*, CRC Press, 1994.

4. MANUSCRIPT #2: “COLD TEMPERATURE EFFECTS ON THE IMPACT RESISTANCE OF THIN, LIGHTWEIGHT UHPFRC PANELS.”

4.1 Abstract

In this study, lightweight armoured panels were designed using ultra high performance fibre reinforced concrete (UHPFRC) and experimental testing was conducted. Panels were cast with the dimensions of 1040 mm x 535 mm x 38 mm to limit their mass to approximately 50 kg and allow them to be carried by two individuals. These panels were designed to be a part of a modular protective system which could be used to protect key infrastructure and assets in a deployed military environment. Experimental quasi-static and dynamic tests were conducted. Quasi-static tests were done to determine a baseline loading capacity of the panels using three-point flexural bending. Dynamic testing was conducted using a pendulum-type impact hammer which could vary the amount of impact energy by altering the drop height of the hammer. Residual panel strength was determined after each panel was tested dynamically by using the same three-point flexural bending test that was used for quasi-static testing. All tests were conducted with panels at ambient laboratory temperatures and extreme cold temperatures to simulate Arctic conditions. Panels were tested at Arctic temperatures to determine their feasibility protecting critical infrastructure in Canada’s Arctic. The testing demonstrated that the UHPFRC panels could resist impact loads with energies up to 2000 J without complete failure. Panels were not adversely affected by the extreme cold temperatures and in fact displayed increased effectiveness at cold temperatures. Single degree of freedom (SDOF) modelling was used to predict panel deflections based on various impact energies. The model developed can accurately predict peak displacements based on impact loading data.

4.2 Introduction

4.2.1 Protective Works for Civilian and Military Applications

The threat of terrorism is currently a global issue, with numerous attacks in major metropolitan areas during the past three decades. The ability of terrorists to use improvised explosive devices to cause destruction to achieve some form of political or cultural gain is a very serious and real threat to military forces throughout the world. In addition, there is an ever-present threat of accidental explosions in the oil and gas industries. Protective structures have been used throughout the world to protect critical infrastructure from these types of attacks and accidental explosions and force protection measures, such as perimeter fencing, checkpoints, etc. provide standoff distance between a key asset and a vulnerable position. Modern military forces face a rapidly changing operational environment with a multitude of threats from a variety of hostile forces. Militaries are focusing on expeditionary forces that do not rely on a large logistical support framework but instead are mostly self sufficient with little reliance on assets such as heavy equipment to construct force protection barriers. To facilitate this, new types of barriers and protective structures, such as the U.S. Army Corps of Engineers Modular Protective Structure system, must be created to provide these deployed units the safety and security they require while conducting operations [1]. These structures consist of lightweight armoured panels installed within a spaceframe structure that is modular and allows the installation to be tailored to operational environment and security requirements. The Canadian Armed Forces (CAF) are focused on sovereignty operations, particularly in Arctic regions, as noted in the Canada First Defence Strategy [2]. In Canada, much of the oil and gas industries are located in northern climates, where extreme cold temperatures are typical during the winter months. Operating in the Arctic calls for the equipment and protective works to be effective in that

environment and at present, there is a lack of research into the subject of the blast resistance of UHPFRC in extreme cold temperatures.

4.2.2 Impact Resistant Properties of UHPFRC

A number of research papers have investigated the qualities of ultra high performance fibre reinforced concrete (UHPFRC) to resist dynamic loading caused by explosive blasts and the fragmentation associated with these events. Xu et al. [3] conducted research on the behaviour of UHPFRC columns subjected to blast loading, concluding that they can effectively resist these types of load while reducing the maximum and residual displacements when compared to high strength reinforced concrete. In another study, Yi et al. [4] found that deflection, strain, and acceleration measurements during blast testing revealed that ultra-high strength concrete specimens have higher blast-resistant capacities than normal strength concrete. A study into the response of UHPFRC panels to blast loading by Ellis et al. [5] demonstrated that panels made of UHPFRC generated little debris and fragmentation. The ability of UHPFRC members to produce less fragmentation was also noted by Melancon et al. [57], who also found that during blast testing of columns, using UHPFRC enhanced the damage tolerance, increased the column capacity and reduced blast-induced deflections.

4.2.3 Pendulum-Type Impact Hammer Testing

Previous research has investigated the effects of blast loading on various types of structural components. Because blast testing is an expensive and time-consuming endeavour, there have been numerous studies in literature that attempt to simulate blast loading in a laboratory setting. Researchers have typically used drop-weight impact machines, the Split Hopkinson bar, or a shock-tube apparatus to simulate blast loads through impact events which have similar behaviour to a blast pressure wave [7] [8] [9]. Research has also been conducted using a pendulum-type impact hammer which provides the researcher with the ability to alter the amount of impact energy and the type of loading, either impulsive or dynamic, by changing the mass of the hammer and the drop height. Pendulum impact hammers as well as drop impact hammers have been used in a number of cases to effectively apply severe, rapidly applied loading conditions within a laboratory setting with characteristics similar to projectile or blast loading conditions [10] [11].

4.2.4 Background Test Series

The experimental program described in this paper was designed based on the results found in the study outlined in Chapter 3 which examined the abilities of steel fibre reinforced concrete (SFRC) panels strengthened with fibre reinforced polymer (FRP) straps to resist impact loading. The panels in the previous study had the same dimensions and similar testing procedures were followed in both studies. This study was conducted in order to compare the two materials and provide recommendations on further research.

4.3 Research Objectives and Scope

This research paper is part of a larger research project which focused on the design and testing of two types of lightweight, armoured panels that could be utilized as part of a modular protective system for critical infrastructure protection or by military forces to form protective works which can withstand the effects of an explosive blast. The present paper addresses the ability of UHPFRC panels to resist impact loading when subjected to midspan loading and simply supported boundary conditions. Although these panels would be installed in a spaceframe-type structure to provide sufficient protection, the design and testing of this supporting structure is beyond the scope of this research.

The experimental study presented in this paper evaluated panels made of UHPFRC through quasi-static and impact testing. Quasi-static three-point flexural bending tests were completed on untested panels to determine a baseline load-deflection behaviour. The three-point flexural bending test was also used to determine the residual strength of impact tested panels. The impact testing conducted as a part of this research used a pendulum-type impact hammer. By varying the drop height of the impact hammer, the amount of impact energy could be altered. The initial impact energies were selected based on the baseline data provided by initial quasi-static testing, and subsequent impact energies were chosen based on the results of previous impact tests. All experimental testing in this research was conducted on panels at both ambient and extreme cold temperature. This was done to compare the behavioural difference between panels tested at ambient laboratory temperature and extreme cold temperature.

Modeling for this research consisted of single degree of freedom (SDOF) modeling. This model was validated using the experimental testing results and had the ability to predict panel behaviour based on the impact load to which they were subjected.

4.4 Experimental Program

4.4.1 Specimens

A total of twelve specimens were tested in this experimental program. Four of those specimens were tested in a quasi-static manner using three-point flexural bending to determine baseline behavioural properties, and the remaining eight specimens were tested dynamically using a pendulum-type impact hammer. Panel dimensions can be found in Figure 4-1 and specimens were cast in plywood forms, following the recommended curing process outlined by the material supplier. All specimens have the same external dimensions; 1040 mm in length, 535 mm wide, and 38 mm thick. There is no additional reinforcement within the panels, only the steel fibres which make up the UHPFRC mix. Panel dimensions were selected to keep the total panel mass around 50 kg, which would allow them to be carried by two persons.

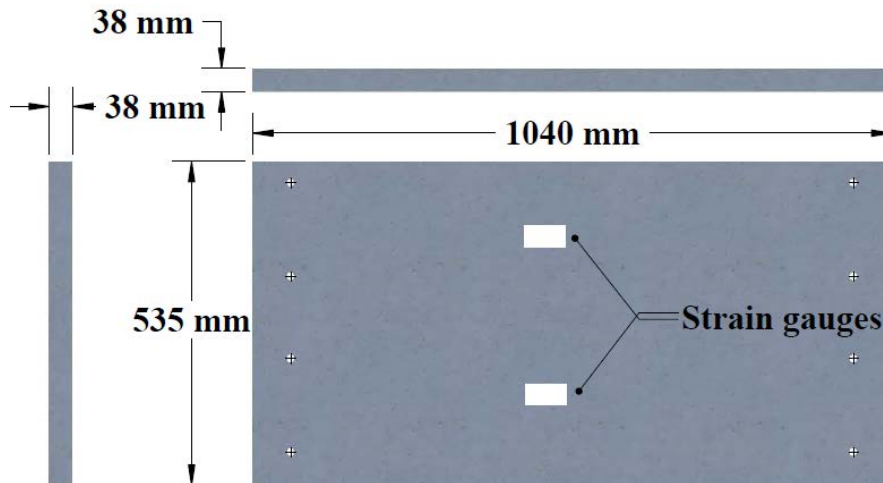


Figure 4-1 - Panel dimensions

As this study is a part of a larger research project, a four-part specimen designation is used, with all test parameters shown in Table 4-1. The first letter refers to the type of material used with U referring to UHPFRC. The second letter indicates whether the panel was tested at either ambient laboratory conditions, A, or cold temperature, C. The type of test is designated by the third term, with S referring to

static testing and I indicating impact testing. Finally, the last term is the test number for that type of test, with each number corresponding to a different drop height for the impact hammer.

Table 4-1 - Specimen Description and Test Parameters

Specimen Identification	Panel Material	Temperature	Test Type	Hammer drop height (mm)
UAS1	UHPFRC	Ambient	Static	-
UAS2	UHPFRC	Ambient	Static	-
UCS1	UHPFRC	Cold	Static	-
UCS2	UHPFRC	Cold	Static	-
UAI1	UHPFRC	Ambient	Impact	350
UAI2	UHPFRC	Ambient	Impact	500
UAI3	UHPFRC	Ambient	Impact	1000
UAI4	UHPFRC	Ambient	Impact	1500
UCI1	UHPFRC	Cold	Impact	350
UCI2	UHPFRC	Cold	Impact	500
UCI3	UHPFRC	Cold	Impact	1000
UCI4	UHPFRC	Cold	Impact	1500

4.4.2 Materials

The UHPFRC mix was provided by the King Construction Products branch of KPM Industries and is their UP-F4 Poly product [12]. This mix was developed by Ecole Polytechnique of Montreal [13] and is made of locally available materials, less the steel fibres. King’s UP-F4 consists of a bagged premix which consists of the cement, silica fume, and sand, as well as a super plasticizer, steel fibres, and water. The F4 designation in the name refers to the percent by volume of fibres, with 4% being used in this study. The steel fibres used in this mix are Bekaert Dramix fibres which are 10 mm in length with a diameter of 0.2 mm, and have a tensile strength of 2750 MPa. Material properties obtained by laboratory testing are listed in Table 4-2 along with the properties provided by the manufacturer [12]. Compression tests were carried out using cylinders with a 100 mm diameter and 200 mm height, and were conducted according to ASTM C39 [14].

Table 4-2 - Average Material Properties of UP-F4 Poly Mix

Mixture properties	Laboratory value	Manufacturer value
Compressive strength (MPa)	125	120
Elastic modulus (GPa)	27	37
Fibre volume (%)	4	4
Tensile strength (MPa)	-	11
Mass density (kg/m ³)	-	2450

4.4.3 Test Setup, Instrumentation, Procedures

Quasi-static testing was conducted using a three-point flexural bending test on a MTS Model 322 machine. This machine was displacement-controlled and the head was set to displace at a rate of 2 mm/min. Panels were supported within the machine by triangular pins with bearing plates on top which would allow translation in the horizontal direction and limited rotation. The load was applied to the panel at midspan to simulate the same loading conditions as those found in the dynamic test. The loading set-up can be seen in Figure 4-2. Midspan displacement was monitored by a 300 mm LVDT.

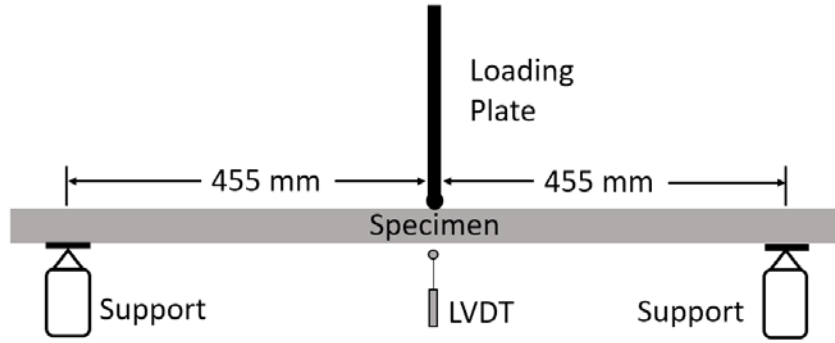


Figure 4-2 - Quasi-static three-point bending testing apparatus

Dynamic tests were conducted at varying hammer heights which altered the impact energy of the system. The same impact energies were used for tests of each type of panel and at each temperature. An outline of the testing apparatus and testing schedule can be found in Table 4-3. The impact energy is calculated using the potential energy of the impact hammer which is based on the mass of the hammer, the drop height, and an acceleration of the gravitational constant, 9.81 m/s^2 . The drop height is calculated as the difference between the raised centre of gravity (CoG) and the at-rest CoG. Panels were secured to the testing frame using bolts which connected the panel through a steel rod to the reaction points on the test frame, as shown in Figure 4-3. The bolts were attached in such a manner to permit unrestrained rotation and limited translation of the tested specimen. Once an impact test was completed, the residual strength of the panel was tested by using the same three-point flexural bending test setup that was used for the quasi-static testing. For the panels tested at cold temperatures, they were returned to the freezer following the impact test so they could return to the proper temperature. Once the correct temperature was reached, approximately -70°C , the panel was taken out of the freezer and installed in the flexural testing apparatus. By the time all the instrumentation was set up and the test was ready to commence, the panels had reached the proper testing temperature of -55°C .

Table 4-3 - Hammer drop heights

Specimen	Drop Height Level	Hammer drop height (mm)	Impact Energy (J)
UAI1	1	350	470
UAI2	2	500	672
UAI3	3	1000	1344
UAI4	4	1500	2016
UCI1	1	350	470
UCI2	2	500	672
UCI3	3	1000	1344
UCI4	4	1500	2016

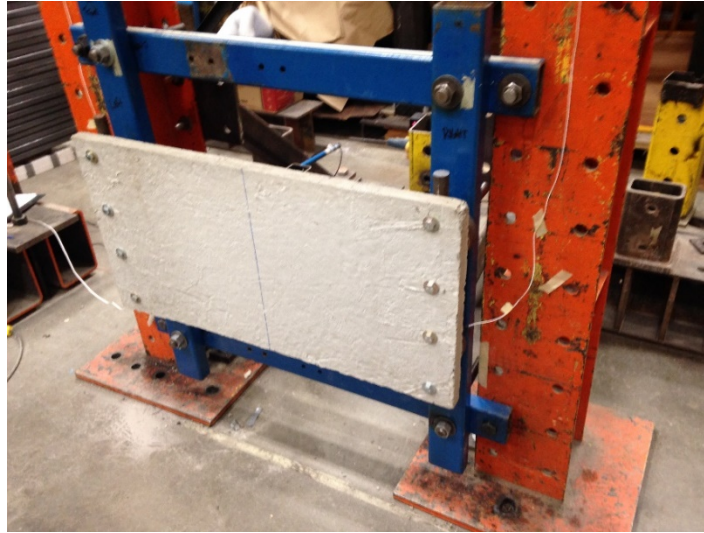


Figure 4-3 - Bolted connection of specimen to testing frame

Strain gauges were installed on all panels, on the bottom face of the quasi-static panels and the back face of the dynamic panels. A type T thermocouple was applied to the surface of each cold temperature panel which provided constant temperature measurement throughout both the quasi-static and dynamic tests. Dynamic tests were highly instrumented to capture all relevant data. In addition to strain gauges, dynamic panels also had an accelerometer installed on the back of the panel at the midspan. Once the panels were installed in the impact testing frame, a laser LVDT was used to measure midspan displacement and an LVDT was placed at one of the supports to monitor support deflections. The testing frame had three force transducers to measure loading data during the impact event. One force transducer was installed between the hammer arm and the hammer tip to measure the hammer force, and the other two force transducers were placed on the reaction points, one on the top left and one on the bottom right, in order to determine the reactionary force. When using the reaction load for energy calculations, the data collected from each reaction point force transducer was doubled and then added to the other one to obtain a complete reaction load. All testing frame instrumentation can be seen in Figure 4-4 and the test set-up can be seen in Figure 4-5.

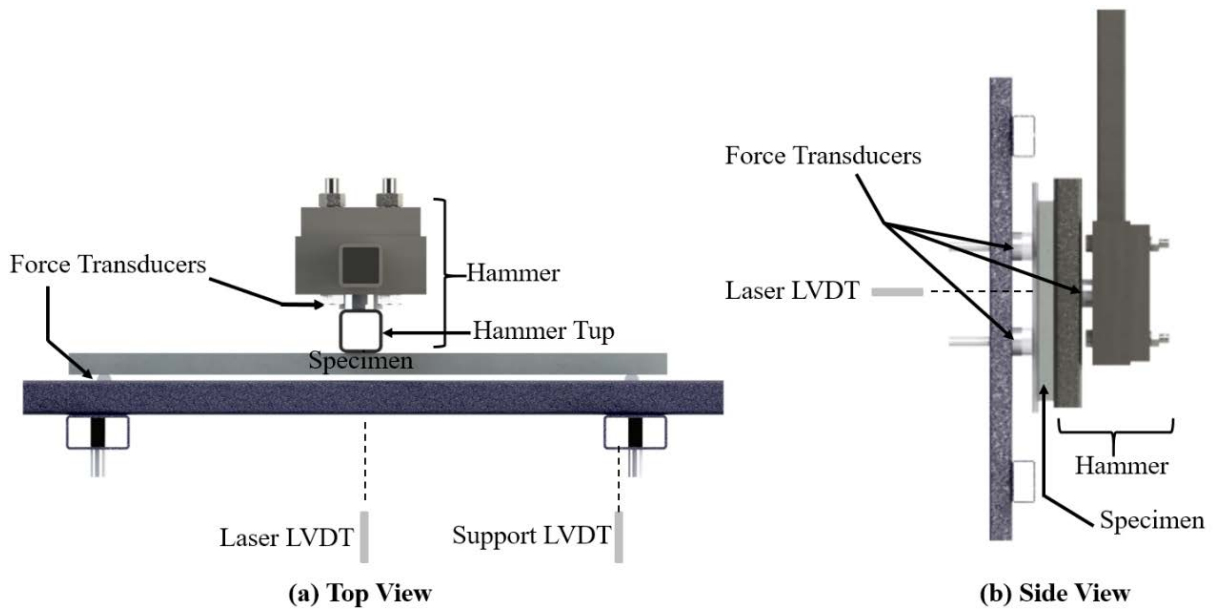


Figure 4-4 - Impact hammer instrumentation

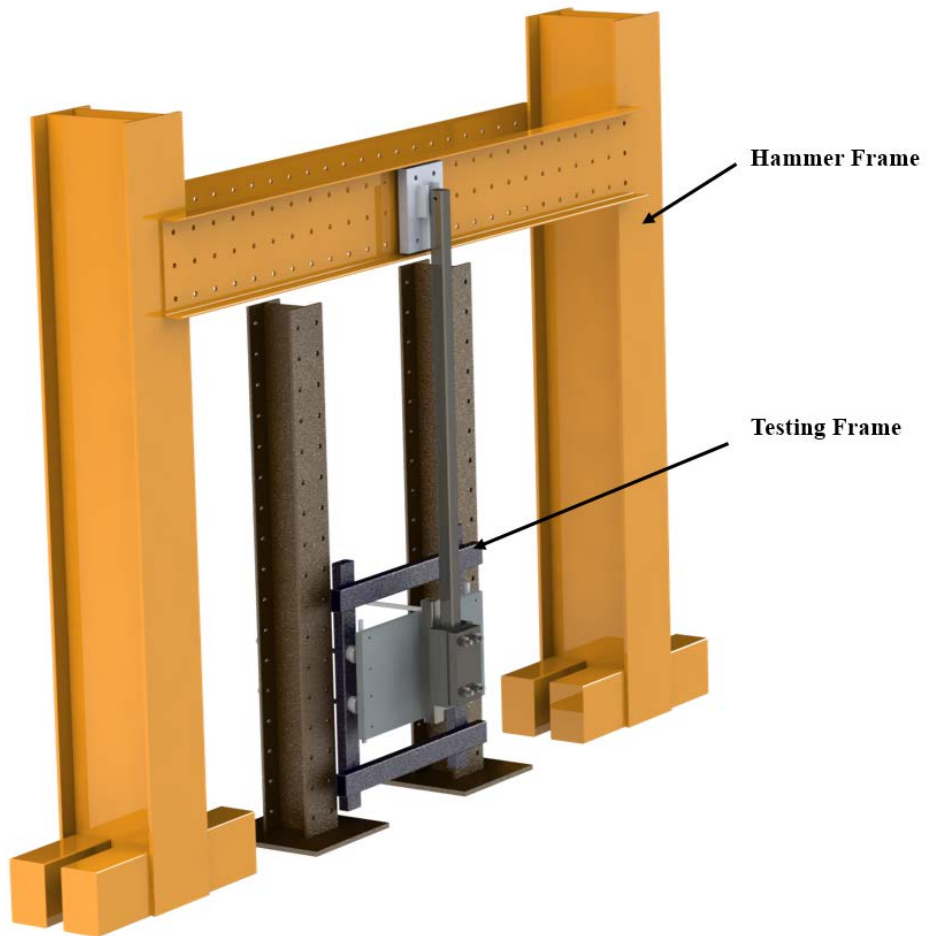


Figure 4-5 - Impact hammer test set-up

4.5 Test Results

Panel specimens were tested after at least 28 days of curing time. A summary of test results for quasi-static testing are found in Table 4-4, while the results from dynamic testing are presented in Table 4-5. Quasi-static results include the maximum load measured by the load cell in the MTS machine, P_{max} , the corresponding peak mid-span deflection measured by a LVDT, Δ_{max} , and the residual mid-span deflection $\Delta_{residual}$, measured once the load had been removed from the specimen. In addition to values of maximum load, peak and residual deflections, the dynamic testing results also include hammer potential energy, K_h , total work done by the hammer, W , and the amount of energy absorbed by the specimen, E_p . The maximum load for the dynamic tests was measured by the force transducer located on the hammer.

Table 4-4 - Summary of Quasi-Static Test Results

Specimen	Maximum Load P_{max} (kN)	Peak Deflection Δ_{max} (mm)	Residual Deflection $\Delta_{residual}$ (mm)
UAS1	20.4	45.3	42.9
UAS2	20.1	38.0	35.0
UCS1	20.7	47.5	43.6
UCS2	23.9	57.6	54.5

Table 4-5 - Summary of Dynamic Test Results

	Drop height (mm)	Maximum load P_{max} (kN)	Peak deflection Δ_{max} (mm)	Residual deflection $\Delta_{residual}$ (mm)	Hammer kinetic energy K_h (J)	Work done by hammer W (J)	Energy absorbed by specimen E_p (J)
UAI1	350	65.2	10.5	7.0	470.4	200.6	135.4
UAI2	500	66.7	24.1	9.7	671.9	487.1	478.8
UAI3	1000	101.8	36.9	21.0	1343.9	901.3	948.8
UAI4	1500	126.2	97.6	41.8	2016.0	2269.5	1042.6
UCI1	350	62.5	13.0	3.3	470.4	360.0	323.9
UCI2	500	71.0	25.0	6.8	672.0	642.2	584.1
UCI3	1000	97.9	43.0	27.6	1343.9	1146.5	1161.5
UCI4 ^a	1500	--	--	46.5	--	--	--

^aData acquisition error – no impact test data available.

4.5.1 General Behaviour

Four panels were tested at ambient temperature and four panels were tested at extreme cold temperature. Each panel was subjected to impact loading from a different hammer drop height, ranging from 350mm to 1500mm. Data was collected for all impact events except for the cold temperature panel at a drop height of 1500mm, due to an error with the data acquisition system, as shown in Table 4-5.

Tests conducted with lower impact energies, drop heights of 350mm and 500mm, failed to provide a distinct crack near the midspan of the panel but the panels did have a small residual deflection. Panels subjected to higher impact energies, those with drop heights of 1000mm and 1500mm, had a large crack form close to the midspan and experienced higher residual deflections as the crack was unable to

close after the loading event concluded. The cracks in these tests did not always occur straight along the midspan but the crack would meander across the section, as shown in Figure 4-6.

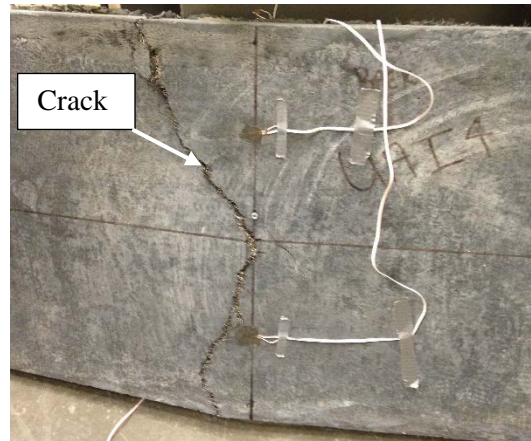


Figure 4-6 - Post-impact cracking of panel UAI4

A typical impact event is shown in Figure 4-7, with images captured from high-speed camera footage. The images show that as the hammer tup impacted the panel at midspan, the panel deflected and a crack formed until the energy within the panel was equal to that of the impact hammer, at which point the hammer rebounded and the panel tried to return to its original state. Due to the pulling out of fibres and the interlocking of those fibres, the panel was unable to return to its original state and was left with a residual or permanent deflection.

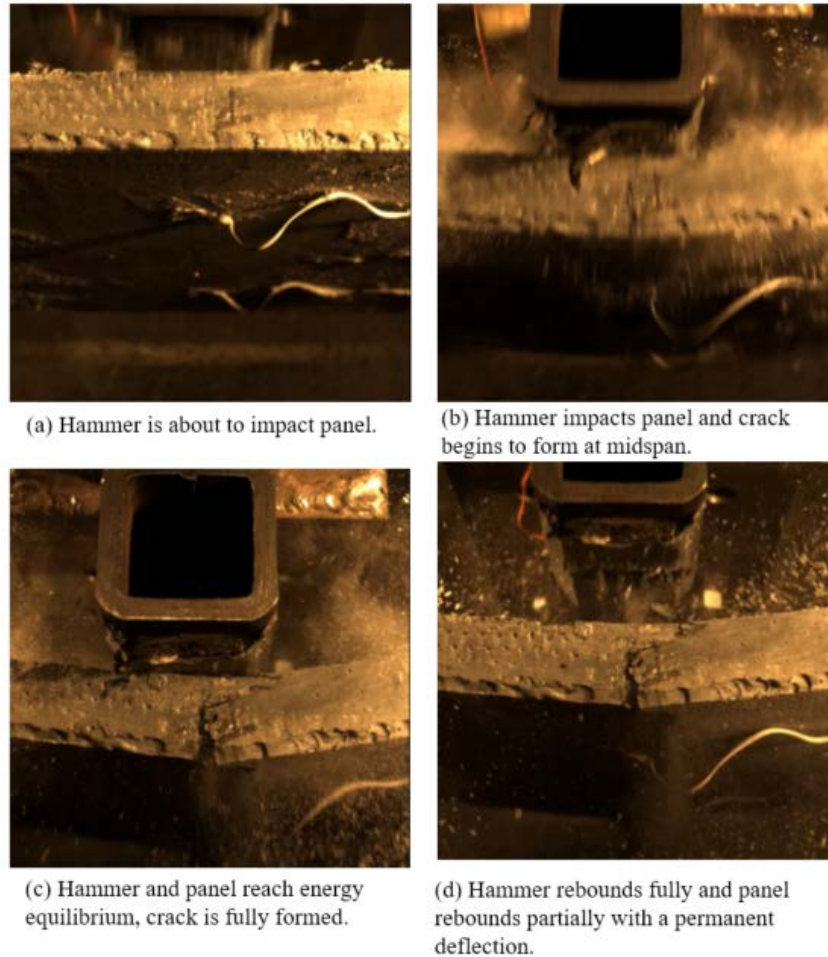


Figure 4-7 - Typical impact event captured by high-speed camera

The results of these tests have demonstrated the benefits of the ductility of UHPFRC and the effectiveness of the material to resist impact loads. Complete failure in this study was defined as a specimen breaking into two distinct pieces, and although significant cracking was found at higher impact energies, panels were able to maintain their form and resist complete failure at the impact energies tested in this study.

4.5.2 Load-deflection behaviour and ductility

The load-deflection curves of the quasi-static panels are shown in Figure 4-8. All panels exhibited similar behaviour with a distinct change in slope at first cracking and a gradual reduction in strength upon reaching the maximum load. The cold temperature panels, UCS1 and UCS2, had increased ductility and panel UCS2 had increased strength when compared to the ambient temperature panels. This increase in tensile strength and ductility occurs in all types of concrete exposed to cold temperatures due to the freezing and shrinkage of the material matrix. In UHPFRC, there is also improved bonding of the concrete matrix to the steel fibres at cold temperatures.

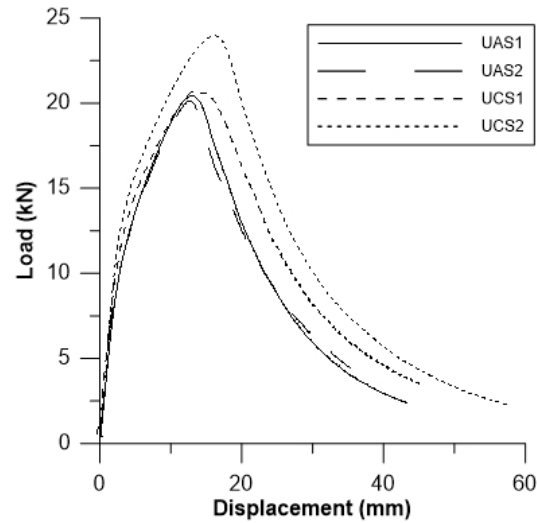


Figure 4-8 - Load-deflection behaviour of quasi-static panels

The load-deflection curves of the ambient temperature dynamic panels are shown in Figure 4-9. For each respective curve, the solid line represents an impact test, each graph designates which panel is represented, and the dashed line shows a comparison to a quasi-static load-deflection test. The loading data is sourced from the force transducers located on the reaction points of the panel. As seen in the graphs, there is an increase in deflection before there is a positive load recorded by the force transducers. This is due to the attachment of the panels to the testing frame and the fact that as the panel displaces at the midspan, the panel moves away from the supports which leads to a negative initial reaction load before it registers as a positive reaction load. The oscillations in the loading can be accredited to the hammer impacting the panel several times in rapid succession. High speed video shows the hammer impacting the panel, rebounding slightly and then continuing to impact the panel due to the kinetic energy of the hammer. In the cases of higher deflections, such as panel UAI4, there is a large immediate deflection of the panel which causes a separation between the panel and the hammer tup before the hammer tup continues its forward motion and impacts the panel again, causing more deflection.

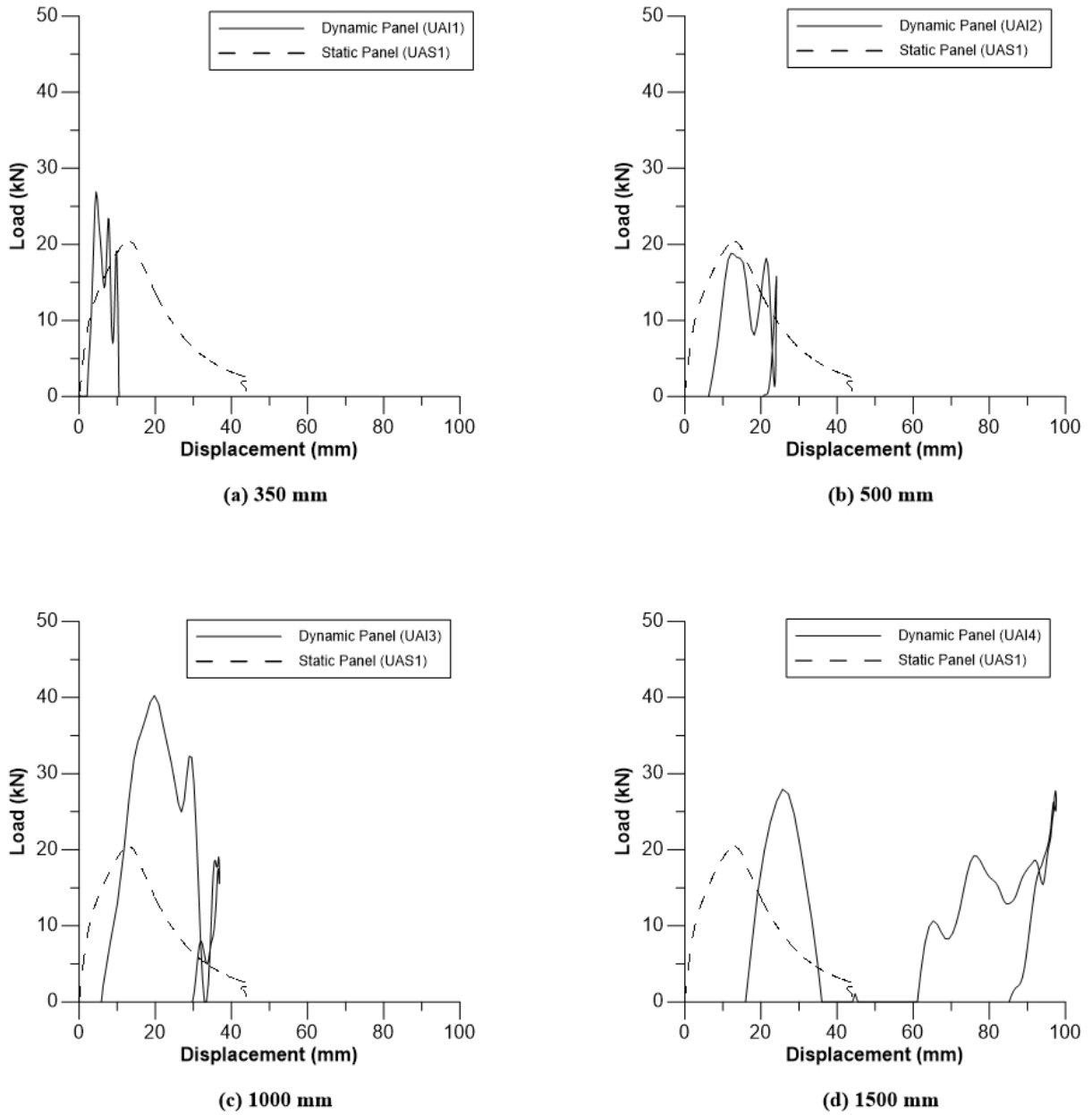


Figure 4-9 - Load-deflection behaviour of ambient temperature dynamic panels

The load-deflection curves of the cold temperature dynamic panels are shown in Figure 4-10. Cold temperature panels displayed similar behaviour to the ambient temperature panels, with oscillations caused by successive hammer hits. The cold temperature panels experienced lower midspan deflections at the same drop heights likely due to the increased tensile strength of UHPFRC at cold temperatures.

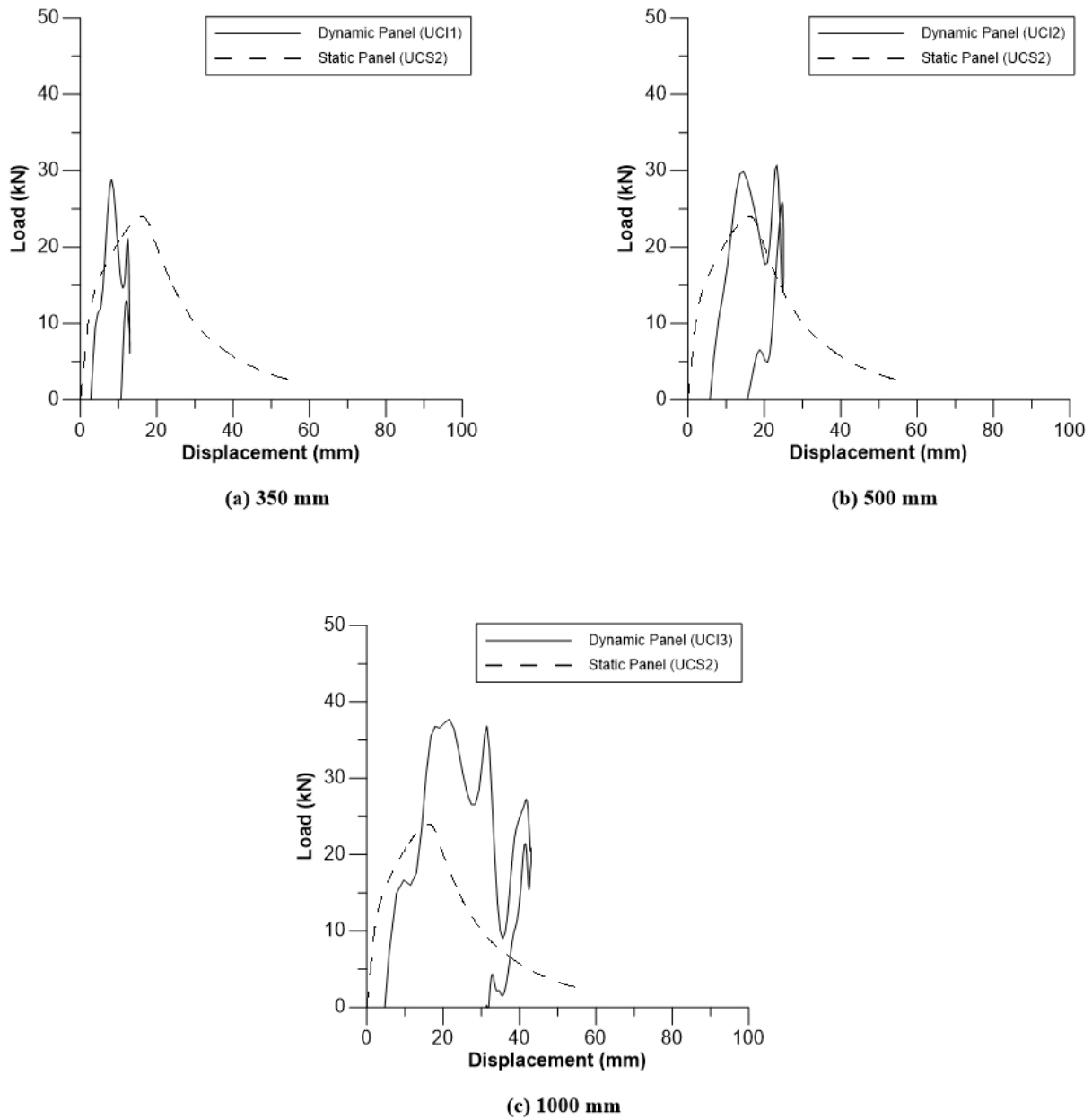


Figure 4-10 - Load-deflection behaviour of cold temperature dynamic panels

Although the general behaviour and shape of the load-deflection curves for impact tested ambient and cold temperature panels are similar, there are several differences in their behaviour. There are slight differences in the load-deflection curves between ambient and cold temperature panels tested at the same drop heights which can be partially attributed to the panels ability to absorb energy, but also to the uncertainties associated with the testing. If the same test was conducted multiple times, it is very likely that each load-deflection curve would be slightly different due to variables such as small differences in panel composition, installation of the panel in the testing frame, and the interaction of the impact hammer with the face of the panel.

4.5.3 Residual Strength of Dynamic Panels

Once dynamic testing of a panel was completed, the ambient temperature panels were immediately tested using the third-point flexural bending test used in quasi-static testing. The cold temperature panels were returned to the freezer until they once again reached at temperature of -70°C before being tested for residual strength. The load-deflection behaviour of the dynamically tested panels can be found in Figure 4-11. As shown in the graphs, each dynamic panel starts from the residual deflection caused by the impact test and then displays similar behaviour up to a maximum load as the quasi-static panels. The dynamic panels curves match up almost exactly with the quasi-static behaviour, which would allow a residual strength prediction based upon the amount of residual or permanent deflection observed for a panel.

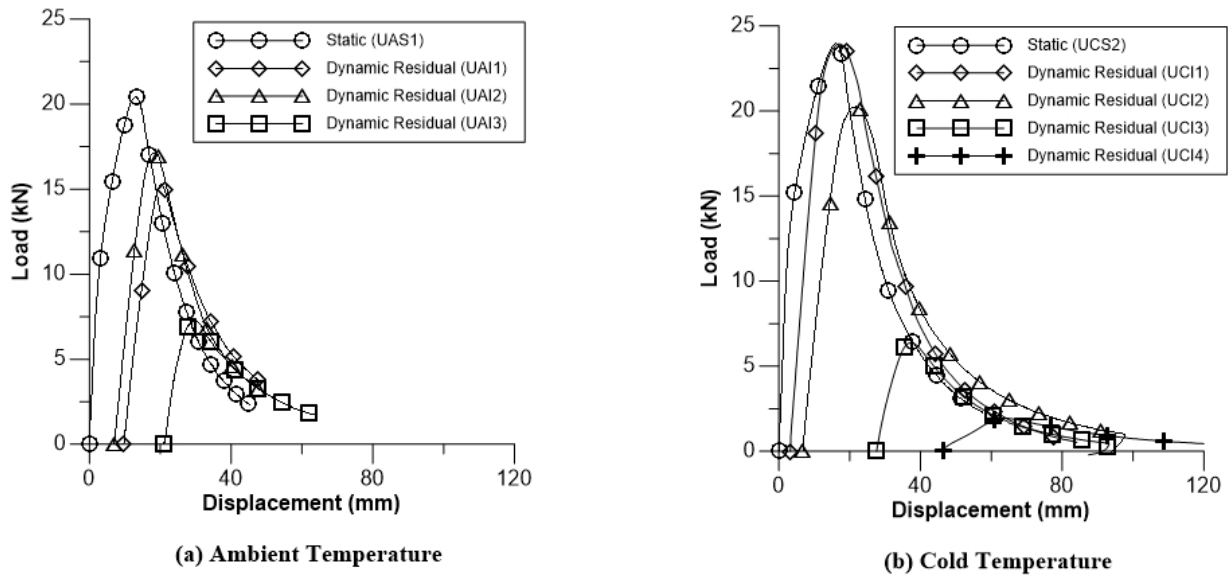


Figure 4-11 - Load-deflection behaviour of residual strength panels

Table 4-6 shows that ambient temperature panels had higher deflections at lower drop heights than the cold temperature panels and they also had lower residual strengths. At higher drop heights (1000 mm and 1500 mm), the ambient temperature panels had lower residual deflections and panel UAI3 had a slightly higher residual strength than the cold temperature panel tested at the same drop height. The behaviour cannot be verified for the 1500 mm drop height panels as the ambient temperature panel broke and was unable to be tested for residual strength.

Table 4-6 - Residual strength of UHPFRC panels

Specimen	Drop height (mm)	Residual deflection $\Delta_{residual}$ (mm)	Residual Strength (kN)
UAI1	350	7.0	17.1
UAI2	500	9.7	15.3
UAI3	1000	21.0	7.3
UAI4 ^a	1500	41.8	--
UCI1	350	3.3	23.9
UCI2	500	6.8	20.2
UCI3	1000	27.6	6.4
UCI4	1500	46.5	1.9

^aPanel broke while being carried to residual strength test apparatus.

4.5.4 Failure Modes

All panels tested could be characterized as having failed, since there was a quantifiable amount of permanent deflection after each test. Although most of the panels did not completely fracture into two pieces, they all had permanent deflection and those tested at higher impact energies had a large, visible crack around midspan. The permanent deflection was caused by the pulling out of fibres from the concrete-fibre matrix. As the panel deflects and the midspan crack forms, fibres at the cracking region are pulled out of the matrix and when the loading is removed, the fibres become interlocked and prevent the panel from returning to its original state. Even if a large, visible crack does not form during the loading, internally fibres are still elongating and pulling out of their original position within the matrix. Illustrations of both the loading case with permanent deflection but no visible cracking, and the loading case of permanent deflection with visible cracking can be seen in Figure 4-12 and Figure 4-13, respectively.

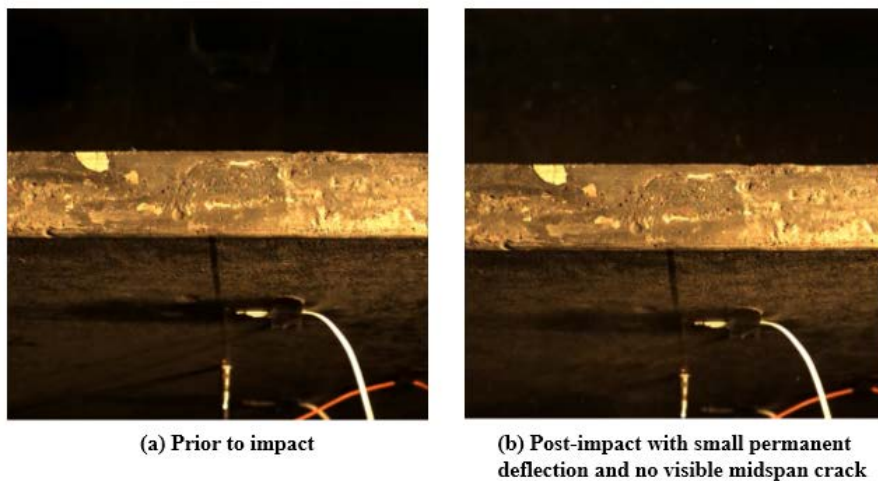


Figure 4-12 – Photos of panel UAI1 from high-speed camera

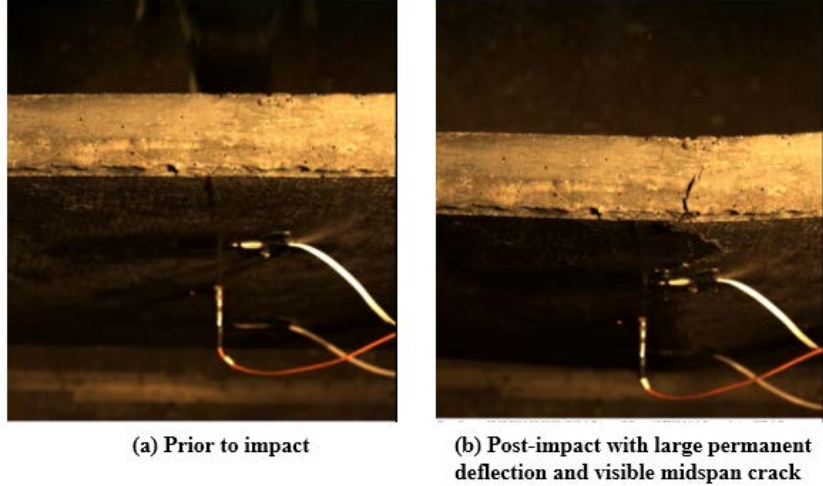


Figure 4-13 - Photos of panel UAI3 from high-speed camera

4.5.5 Conservation of Energy

Energy distribution is a key criterion in assessing the impact resistance of a structural element. In a closed system, such as the one in this study, the energy dissipated or absorbed by the system should equal the amount of energy that was introduced. In this study, the input energy is the kinetic energy lost by the impact hammer, which is calculated using the following equation [15]:

$$K_h(t_i) = \frac{1}{2} \cdot M_h \cdot \left[2 \cdot a_h \cdot h_h - \left(\sqrt{2 \cdot a_h \cdot h_h} - \frac{1}{M_h} \cdot I(t_i) \right)^2 \right] \quad (4-1)$$

Where M_h is the mass of the hammer, a_h is the hammer acceleration which could be measured but for this experiment the gravitational constant of 9.81 m/s^2 was used, h_h is the drop height of the hammer which is measured as the difference between the at-rest centre of gravity of the hammer and the raised centre of gravity, as was shown in Table 4-3. The final value used in the kinetic energy of the hammer equation is the impulse of the hammer, I , which is obtained based on integrating the hammer tup load.

The energy that is input into the system is transferred into kinetic and strain energy within the panel. The summation of these two energies is the amount of energy absorbed by the panel, which should be equal to the work done by the hammer. The kinetic energy of the panel is calculated using the midspan velocity of the panel while the strain energy of the panel is calculated by using the area under the reaction load-midspan deflection curve of the impact event. The work done by the hammer is calculated from the area under the load-displacement curve generated by the impact event and can be calculated using the following equation:

$$W(t_i) = W(t_{i-1}) + \frac{P_t(t_{i-1}) + P_t(t_i)}{2} \cdot [u(t_i) - u(t_{i-1})] \quad (4-2)$$

Where W , is the work done, P_t is the load measured from the hammer tup force transducer, and u is the midspan panel displacement at that time step.

In a perfect system, the work done by the hammer would equal the energy absorbed by the panel but there are losses in the system that prevent this from holding true. As seen in Table 4-5, the amount of work done by the hammer is lower than the potential energy of the hammer. This discrepancy shows that there are energy losses within the system and that it is not a perfect system. The amount of energy absorbed by the panels is almost equal to the work done by the hammer at lower impact energies. At higher impact energies, the panel is not able to absorb all the kinetic energy of the hammer and there are energy losses to other things such as local compression of the panel face and compression of the hammer tup material. At higher impact energies, due to the way panels are secured to the testing frame using bolts, there is the start of catenary action with friction losses caused by sliding of the panel along the supports. From testing, it appears that the maximum amount of energy that can be absorbed by the specimens is around 1200 J. There is good correlation between the amount of energy absorbed by the panels and the associated work done by the hammer for drop heights of 350 mm up until 1000 mm. Once the drop height exceeds 1000 mm, the amount of work done by the hammer exceeds 1200 J and the panel is unable to absorb that amount of energy. Therefore, panel UAI4 was damaged so severely that it could not be tested for residual strength and panel UCI4 had an extremely low residual strength.

An energy conservation graph for panel UAI3 is shown in Figure 4-14 which shows the relation between the work done by the hammer and the amount of energy absorbed by the panel. In this case, the correlation between the input and output energy from the system is very close but the same does not hold true for a panel that fails and has no residual strength, such as panel UAI4, shown in Figure 4-15. From the graph, panel UAI4 is only able to absorb just over 1000 J of energy while the work done by the energy is over 2000 J. This causes the large crack and permanent deflection in the panel and the lack of residual strength.

As was shown in Table 4-5, as the input energy of the impact hammer increases, the amount of energy absorbed by the panel increases. Panels that were tested at cold temperatures appear to absorb more energy than the panels tested at room temperature.

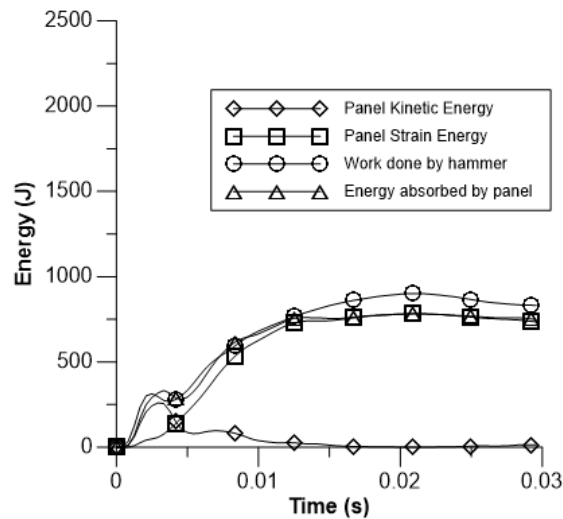


Figure 4-14 - Energy Conservation of Panel UAI3

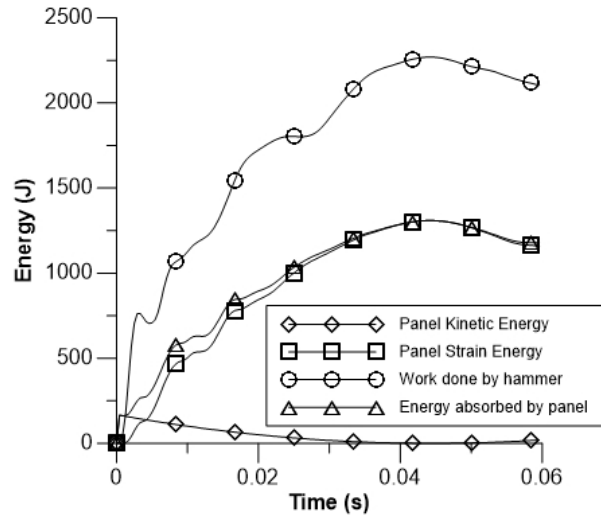


Figure 4-15 - Energy Conservation of Panel UAI4

4.6 SDOF Modelling

Single degree of freedom (SDOF) modelling is widely used in the practice of blast assessment of structural components due to its simplicity and validity [16]. Equivalent SDOF analysis simplifies the conditions within the environment and allows for structural elements such as beams, columns, and walls to be modelled as a simple spring-mass element. A typical SDOF system includes a forcing function, a mass, and a spring which resists the acceleration caused by the forcing function [17]. The forcing function is the blast pressure, or in this case it is the impact of the hammer, and the mass is the equivalent mass of the element in question. The resistance function for the element is determined based on its mass and stiffness and can include elastic, plastic, and elastoplastic regions. It is unique to each structural member and considers the cross-sectional dimensions, the amount and type of reinforcement, and the dynamic material properties. The parameters for the SDOF system are determined such that the maximum deflection within the system is equal to the maximum deflection that would occur within the actual structural member.

In this study, the resistance function for the UHPFRC panels was determined based on idealizing the load-deflection curve found through quasi-static testing. A multi-linear load-deflection curve, shown in Figure 4-16, was created which could be used in the SDOF model to predict flexural behaviour.

The forcing function used in the model was provided by the force transducer that was located on the hammer tup. This transducer provided a forcing function, like the one found in Figure 4-17, that is similar in nature to the pressure-time history of an explosive blast. A different forcing function was used for each specimen as the impact load changed depending on the hammer drop height.

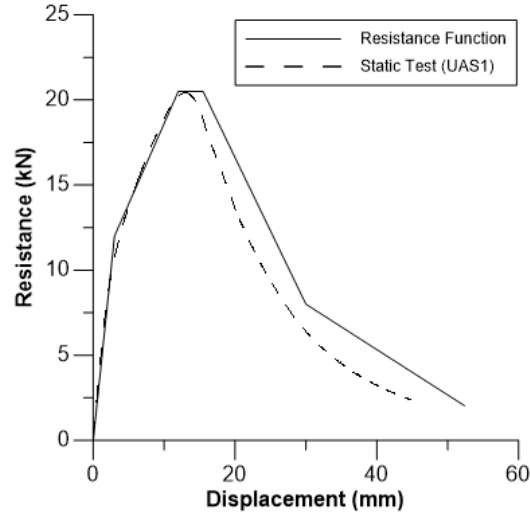


Figure 4-16 - Resistance Function for UHPFRC Panels

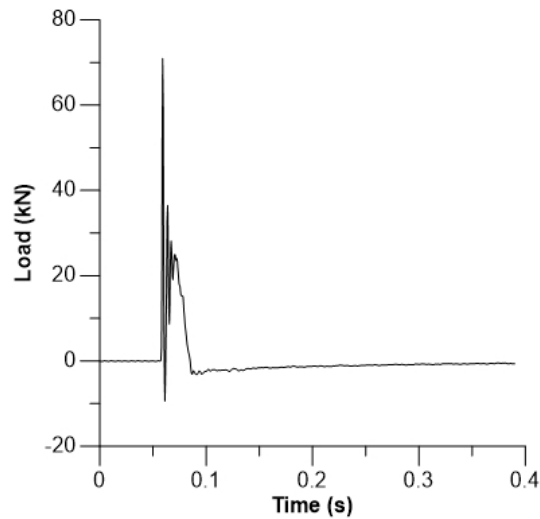


Figure 4-17 - Forcing Function (from hammer force transducer data of panel UCI2)

The SDOF model used in this study was based on the Predictor Method, established by Smith and Hetherington [18]. This method is based on constant acceleration throughout the time step and allows for accelerations, velocities, and displacements to be determined based upon a forcing function and resistance function. With the displacement and velocity set to zero at the beginning of the calculation, the initial acceleration can be determined by rearranging the equation of motion found below:

$$M\ddot{x} + R(x) = F(t) \quad (4-3)$$

Where $R(x)$ is the resistance function for the specimen, shown in Figure 4-16, $F(t)$ is the forcing function, such as the one shown in Figure 4-17, M is the mass of the specimen and \ddot{x} is the acceleration. Rearranging the equation of motion to determine the initial acceleration, the equation below is obtained:

$$\ddot{x} = \frac{F(0) - R(x_0)}{M} \quad (4-4)$$

Once the initial acceleration is known, since it remains constant throughout the time step, it can be used to find the velocity at the end of the time step using the equation below:

$$\dot{x}_1 = \dot{x}_0 + \ddot{x}_0 \Delta t \quad (4-5)$$

Where \dot{x} is the velocity of the specimen and Δt is the duration of the time step. The displacement is then given by:

$$x_1 = \dot{x}_0 \Delta t + \frac{1}{2} \ddot{x}_0 \Delta t^2 \quad (4-6)$$

Where x is the displacement and is based upon the velocity and acceleration at the previous time step. With the displacement known, the associated resistance value can be found from the resistance function and then the process can be continued until the complete displacement response is found, as shown in Figure 4-18. The figure shows plots of the resistance function, the displacement found by the SDOF model, and the actual displacement of panel UCI2 as measured by the laser. As seen in the figure, there is good correlation between the predicted displacement using the SDOF model and the actual measured displacement.

Table 4-7 shows the results of the model for each panel and compares those results to the actual measured displacements from laboratory tests. As seen by the percent error, the model was able to predict the panel midspan displacement within 20% for all specimens. This accuracy can be attributed to using the actual loading function from the hammer force transducer as opposed to using a generalized forcing function and the utilization of a multi-linear resistance function based off quasi-static flexural bending tests.

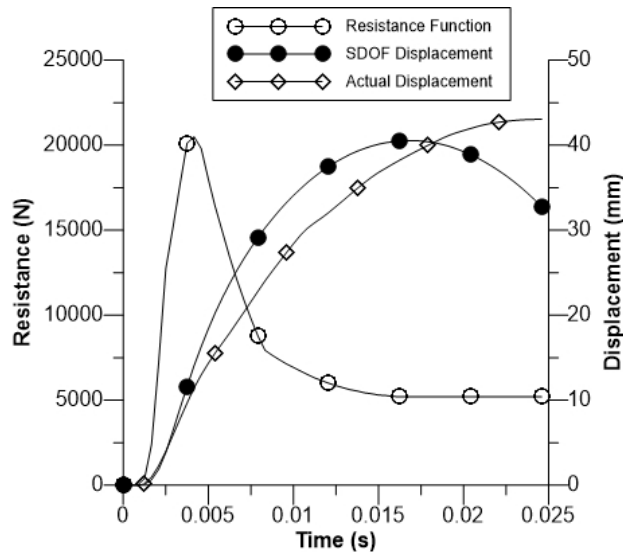


Figure 4-18 - SDOF Model for panel UCI3

Table 4-7 - SDOF model comparison to actual data

Specimen	Drop height (mm)	Peak deflection (mm)	SDOF deflection (mm)	% Error
UAI1	350	10.5	10.7	1.9
UAI2	500	24.1	22.4	7.0
UAI3	1000	36.9	32.9	10.9
UAI4	1500	97.6	88.5	9.3
UCI1	350	13.0	13.9	6.5
UCI2	500	25.0	19.9	20.6
UCI3	1000	43.0	40.5	5.7
UCI4 ^a	1500	--	88.5	--

^aData acquisition error – no impact test data available.

4.7 Comparison to FRP Strengthened SFRC Panels

As explained earlier in the paper, this study into the impact resistance of UHPFRC panels is a part of a larger research program. The first stage of this program was to evaluate the impact resistance of steel fibre reinforced concrete (SFRC) panels that were strengthened with straps of fibre reinforced polymer (FRP), as reported in Chapter 3. The same testing protocol was carried out for both studies, with each study having four panels tested in quasi-static three-point flexural bending, and eight panels tested dynamically using a pendulum-type impact hammer. Once impact testing was completed, those eight panels were tested for residual strength using the quasi-static three-point flexural bending test.

Plots are shown below to compare the two types of panels. Figure 4-19 shows the load-deflection behaviour of each type of panel tested quasi-statically. As seen in the graph, there is a distinct difference in the behaviour of the two types of panels. The UHPFRC panels behave in a very smooth and predictable manner, compared with the FRP strengthened SFRC panels which are much less predictable. The drastic drops in the load of the FRP strengthened SFRC panels represent the debonding of FRP fibres which causes the load to redistribute after which the panel is subsequently able to sustain additional load. The FRP strengthened SFRC panels are able to carry close to their peak load until complete failure at a deflection of around 100 mm for the ambient temperature panels and 120 mm for the cold temperature panels. The UHPFRC panels are able to achieve a higher peak load, but once reaching that peak and having a flexural crack open, they quickly lose that load capacity as they continue to deflect. They are able to reach large deflections but are not able to carry much load while deflecting.

When tested quasi-statically at cold temperatures, both types of panels display different types of behaviour. While the cold temperature UHPFRC panels have similar load-deflection behaviour when compared to room temperature panels, they are able to achieve a higher peak load as well as sustain higher loads with lower deflections. The cold temperature FRP strengthened SFRC panel displays the typical jagged load-deflection behaviour of the other FRP strengthened SFRC panels, but sustains less of a load-capacity drop than the ambient temperature panels. In both cases, the additional load-capacity can be attributed to the increased tensile strength in the concrete and improved bonding of steel fibres and FRP caused by the cold temperatures. The increase in tensile strength is more significant in the UHPFRC panels but the FRP strengthened SFRC panels are also able to take advantage of this benefit.

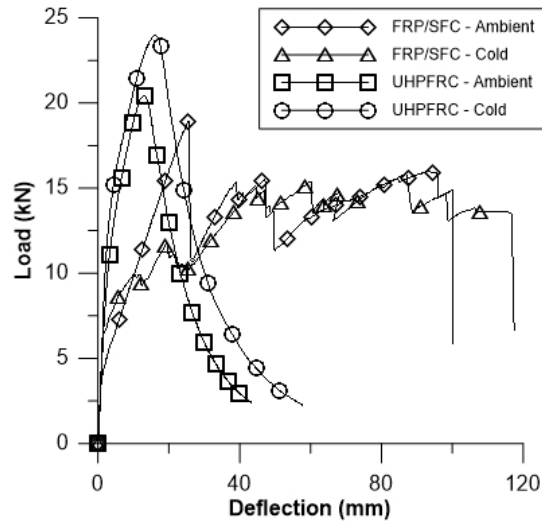


Figure 4-19 - Load-deflection behaviour of FRP/SFRC Panels and UHPFRC Panels

The residual strength of these panels is an important criterion to evaluate as the ability to reuse the panels after a blast event is a key feature. As shown in Figure 4-20, the residual strength of UHPFRC panels is much easier to predict than the FRP strengthened SFRC panels. Contrary to the UHPFRC panels, which almost perfectly line up with the quasi-static load-deflection curve, the residual strength of FRP strengthened SFRC panels is very erratic, but some conclusions can still be drawn from it. On the UHPFRC graph, the residual strength is based on the residual deflection of the panel. The maximum load a panel can take after sustaining an impact load decreases based on how much residual deflection it has. For FRP strengthened SFRC panels, the amount of residual deflection observed in a panel is typically much less than the UHPFRC panels. This is due to the strength of the elastic FRP straps and the amount of tension reinforcement they provide. The FRP strengthened SFRC reach similar loading plateaus to an untested panel, just with a lower peak load. This means that although a FRP strengthened SFRC panel may have significant cracking to the concrete and some debonding of the FRP, the panel can still achieve a strength of close to 15 kN until the FRP becomes completely debonded.

Cold temperature panels once again display increased tensile strength and load-capacity during residual strength tests. As shown in Figure 4-11(b), the cold temperature UHPFRC panel tested at a drop height of 350 mm, panel UCI1, had the same strength as a panel tested quasi-statically without being exposed to an impact load. The panel tested at a drop height of 500 mm, panel UCI2, had the same residual strength as the ambient temperature quasi-static tested panels, despite having a residual deflection of 6.8 mm at the start of the test. This once again displays the increased tensile strength of the cold temperature panels and shows that cold temperatures do not negatively affect panel behaviour but instead may actual improve their performance. The cold temperature FRP strengthened SFRC panels also display improved cold temperature behaviour, with each impact tested cold temperature panel achieving the same residual strength despite having various amounts of residual deflection. While the ambient temperature panels had decreasing residual strengths as the residual deflection increased, the cold temperature panels had the same residual strength.

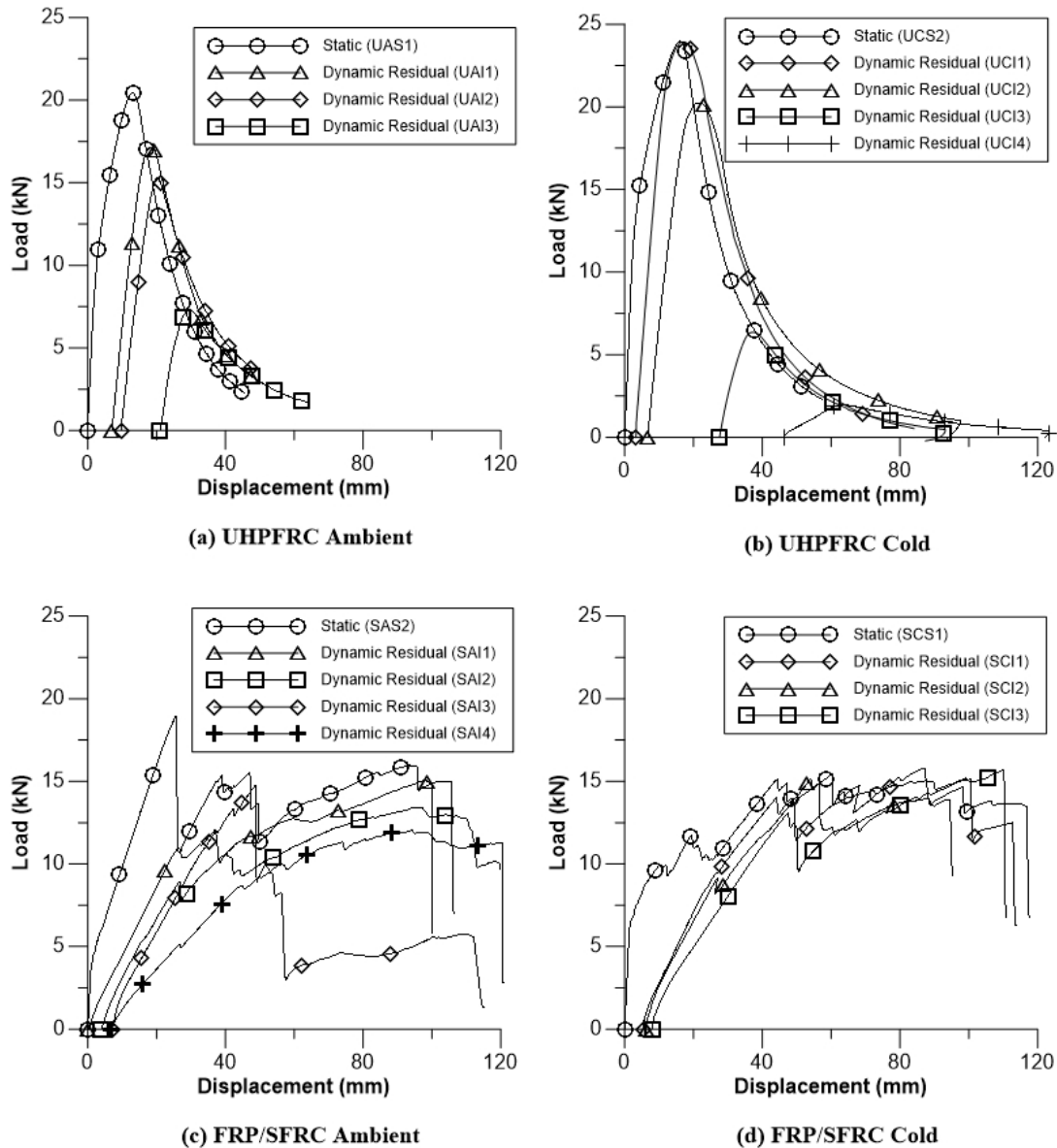


Figure 4-20 – Comparison of Residual Strength Behaviour of Panels

4.8 Conclusions

The experimental program outlined in this chapter was created to design and test two types of lightweight, armoured panels that could be utilized as part of a modular protective system by military forces to form protective works which can withstand the effects of an explosive blast. This paper outlined the results of the panels constructed out of UHPFRC while the previous chapter outlined the results of the FRP strengthened SFRC panels. The following conclusions are related to the study described in this paper and the summary found in the following section explains the conclusions drawn from a comparison of the two types of panels.

1. Cold temperatures did not negatively affect panel behaviour, instead increasing their quasi-static load-capacity, residual strength and ability to absorb energy.
2. The 4% fibre dosage used in this study provided a high peak strength, but also provided ductility which allowed for very large deformations (greater than 100 mm)
3. Panels tested at cold temperatures had a higher load capacity when tested in a quasi-static manner than the ambient temperature panels.
4. Cold temperature panels had a smaller residual deflection than ambient temperature panels at lower impact energies (470 J and 672 J) but had a larger residual deflection at higher impact energies (1344 J and 2016 J).
5. A SDOF model was developed based on the experimental results of this study. The model uses a resistance function based on the load-deflection curve of the panels tested in quasi-static flexural bending and uses the loading data from the force transducer located on the hammer tup to provide the forcing function. The model achieved good results with all predicted midspan deflections within 20% of the actual deflections measured from testing.
6. Residual strength testing showed an excellent correlation between residual deflection caused by the impact test and the residual strength of the panel. Due to the behaviour of the panels during the residual strength testing and the fact that they match up with the quasi-static load-deflection curve almost perfectly, a panel's residual strength can easily be predicted based upon observed permanent deflection.

4.9 Acknowledgments

This research project was funded by the Natural Science and Engineering Research Council of Canada (NSERC) and the UHPFRC materials were graciously provided by KPM Industries. The authors are extremely grateful for the hard work and contributions by the technical staff of the Royal Military College of Canada Structure's Laboratory and the assistance of a few undergraduate Officer Cadets whose help in constructing the testing frame was greatly appreciated.

4.10 References

- [1] O. G. Flores, "Development of a lightweight, modular protective structure for contingency environments," U.S. Army - ERDC, Vicksburg, 2009.
- [2] Government of Canada, "Canada First Defence Strategy," Government of Canada, Ottawa, 2008.
- [3] J. Xu, C. Wu, H. Xiang, Y. Su, Z.-X. Li, Q. Fang, H. Hao, Z. Liu, Y. Zhang and J. Li, "Behaviour of ultra high performance fibre reinforced concrete columns subjected to blast loading," *Engineering Structures*, no. 118, pp. 97-107, 2016.
- [4] N.-H. Yi, J.-H. J. Kim, T.-S. Han, Y.-G. Cho and J. H. Lee, "Blast-resistant characteristics of ultra-high strength concrete and reactive powder concrete," *Construction and Building Materials*, no. 28, pp. 694-707, 2012.
- [5] B. Ellis, B. DiPaolo, D. McDowell and M. Zhou, "Experimental investigation and multiscale modeling of ultra-high-performance concrete panels subject to blast loading," *International Journal*

- of Impact Engineering*, no. 69, pp. 95-103, 2014.
- [6] C. Melancon, S. De Carufel and H. Aoude, "Effect of High-Performance Materials on the Blast Response of Reinforced Concrete Structural Components," in *Proceedings of the 4th International Symposium on Ultra-High Performance Concrete and High Performance Materials*, Kassel, 2016.
- [7] D.-Y. Yoo and N. Banthia, "Size-dependent impact resistance of ultra-high-performance fiber-reinforced concrete beams," *Construction and Building Materials*, vol. 142, pp. 363-375, 2017.
- [8] O. Millon, A. Kleemann and A. Stolz, "Influence of the fiber reinforcement on the dynamic behaviour of UHPC," in *First International Interactive Symposium on UHPC*, Des Moines, Iowa, 2016.
- [9] H. Aoude, F. P. Dagenais, R. P. Burrell and M. Saatcioglu, "Behavior of ultra-high performance fiber reinforced concrete columns under blast loading," *International Journal of Impact Engineering*, no. 80, pp. 185-202, 2015.
- [10] Y. Qasrawi, P. J. Heffernan and A. Fam, "Dynamic behaviour of concrete filled FRP tubes subjected to impact loading," *Engineering Structures*, vol. 100, pp. 212-225, 2015.
- [11] M. Zineddin and T. Krauthammer, "Dynamic response and behavior of reinforced concrete slabs under impact loading," *International Journal of Impact Engineering*, vol. 34, pp. 1517-1534, 2007.
- [12] King Packaged Materials Company, "UP-F4 Poly Technical Data Sheet," King Packaged Materials Company, Boisbriand, QC, 2016.
- [13] S. Braike, "Design of precast bridge elements made with high and ultrahigh-performance fiber reinforced concrete," M.Sc. thesis, Polytechnique Montreal, QC, Canada (in French), 2007.
- [14] ASTM C39 / C39M - 16b, "Standard Test Method for Compressive Strength of Cylindrical Concrete Specimens," ASTM International, West Conshohocken, PA, 2016.
- [15] N. Banthia, S. Mindess, A. Bentur and M. Pigeon, "Impact Testing of Concrete Using Drop-Weight Impact Machine," *Experimental Mechanics*, pp. 63-69, 1989.
- [16] S. Astarlioglu and T. Krauthammer, "Response of normal-strength and ultra-high-performance fiber-reinforced concrete columns to idealized blast loads," *Engineering Structures*, no. 61, pp. 1-12, 2014.
- [17] J. M. Biggs, *Introduction to Structural Dynamics*, McGraw-Hill, Inc., 1964.
- [18] J. Hetherington and P. Smith, *Blast and Ballistic Loading of Structures*, CRC Press, 1994.

5. CONCLUSIONS AND RECOMMENDATIONS

5.1 General

This research project focused on the ability of two types of concrete panels to resist blast loads at ambient and cold temperatures. These panels could be utilized within a modular force protection system which could be deployed to austere environments to provide protective measures for Canadian Armed Forces personnel.

The first type of panel designed and tested in this study was composed of SFRC that was strengthened with external FRP straps. These straps were applied to the panel once cured using a wet lay-up method. The FRP straps provided a significant boost in overall strength of the panel and allowed it to behave in a ductile manner, demonstrating large deflections while maintaining an applied load.

The second type of panel that was investigated in this project was made of UHPFRC. This panel did not require external strengthening as the UHPFRC mix used provided a peak strength which exceeded the FRP strengthened SFRC panel.

The objectives of this research were to compare the two types of panels in their ability to resist blast loads, to evaluate if the panels behaved differently at ambient and extreme cold temperatures, and to develop a single-degree-of-freedom model to simulate laboratory tests and accurately predict results.

5.2 Summary of Research Program

Both the UHPFRC and FRP strengthened SFRC panels provided similar peak strengths but their load-deflection behaviour is significantly different. While the UHPFRC panels display higher strength, they quickly lose capacity to hold this strength and as they continue to deflect, their strength decreases significantly. The FRP strengthened SFRC panels have a lower peak strength but as the FRP begins to fracture and debond in certain regions, the load is redistributed allowing the panel to continue to hold strength throughout the duration of its deflection capacity.

The FRP straps reduce the amount of permanent deflection each panel has. UHPFRC panels tested quasi-statically had permanent deflections that were close to 95% of the maximum measured deflection while quasi-statically tested FRP strengthened SFRC panels had permanent deflections of only 25%. Dynamically tested UHPFRC panels had permanent deflections that ranged from 25-65% of their peak deflections while FRP strengthened SFRC panels had permanent deflections around 10-15% of their peak deflections caused by impact loading.

It is hypothesized that a combination of UHPFRC panel with FRP straps or highly ductile steel bars could provide a superior panel with a high peak strength and predictable residual strength behaviour. As such, it is recommended that further research be conducted in the area of combining UHPFRC panels with FRP straps and with ductile steel bars in order to investigate their behaviour. Based on preliminary calculations to predict the strength of these hybrid panels, the UHPFRC panel reinforced with FRP straps would have a predicted strength of 42 kN. In comparison, both the UHPFRC and FRP strengthened SFRC panels had a predicted strength of 12 kN but actual laboratory testing proved that they were in fact stronger than predicted.

5.3 Conclusions

A summary of the conclusions found in each article are presented below as they represent the conclusions found from the entire research project.

1. Extreme cold temperatures do not appear to negatively affect the behaviour of either the SFRC panels strengthened with FRP straps or the UHPFRC panels and the energy absorption ability of both panels were not reduced. Generally, cold temperatures positively affected UHPFRC panel behaviour increasing their quasi-static load-capacity residual strength and ability to absorb energy.
2. Impact-tested cold temperature FRP strengthened SFRC panels that did not reach ultimate failure, i.e. complete debonding of FRP straps, all had similar residual strength (15 kN) despite having absorbed various levels of impact energy.
3. Ambient temperature FRP strengthened SFRC panels tested using the impact hammer had decreasing residual strength based on the amount of residual deflection. Those panels tested at higher impact energies displayed higher residual deflections and lower residual strength.
4. UHPFRC panels tested at cold temperatures had a higher load capacity when tested in a quasi-static manner than the ambient temperature panels.
5. Cold temperature UHPFRC panels had a smaller residual deflection than ambient temperature panels at lower impact energies (470 J and 672 J) but had a larger residual deflection at higher impact energies (1344 J and 2016 J).
6. The SDOF model developed for each type of panel produced good results, with predicted midspan deflections within 20% of actual measured midspan deflections.
7. Residual strength testing of UHPFRC panels showed an excellent correlation between residual deflection caused by the impact test and the residual strength of the panel. Due to the behaviour of the panels during the residual strength testing and the fact that they match up with the quasi-static load-deflection curve almost perfectly, a panel's residual strength can easily be predicted based upon the permanent deflection it has.

Overall, it can be concluded that extreme cold temperatures do not negatively affect the performance of either type of panel tested in this research project. From the testing conducted, both FRP strengthened SFRC panels and UHPFRC panels showed similar or improved behaviour when exposed to extreme cold temperatures.

5.4 Recommendations

Based on the findings of this research project, the following recommendations are made for future work in the use of UHPFRC for blast resistant protective works:

1. The use of FRP straps or highly ductile steel reinforcement to strengthen a UHPFRC panel is recommended in an attempt to blend the high peak compressive strength provided by the UHPFRC with the high tensile strength provided by the FRP straps or highly ductile steel bars. Preliminary calculations of a hybrid UHPFRC-FRP panel predict that it would have a strength of 42 kN, compared to the UHPFRC panel which had a predicted strength of 12 kN using the same calculation method.
2. A spaceframe should be developed which can hold the armoured panels. The frame must be easily modified to form different shaped structures depending on the operational requirement. The frame should consist of man-portable components and not require special tools or equipment to assemble.
3. Explosive blast testing should be conducted to confirm the accuracy of laboratory impact testing and verify this method of conducting impact testing as well as to test the panels in a blast environment.

References

- [1] K. Scherbatiuk and N. Rattanawangcharoen, "A hybrid rigid-body rotation model with sliding for calculating the response of a temporary soil-filled wall subjected to blast loading," *International Journal of Impact Engineering*, no. 38, pp. 637-652, 2011.
- [2] O. G. Flores, "Development of a lightweight, modular protective structure for contingency environments," U.S. Army Engineer Research and Development Center, Vicksburg, 2009.
- [3] Government of Canada, "Statement on Canada's Arctic Foreign Policy; Exercising Sovereignty and Promoting Canada's NORTHERN STRATEGY Abroad," Government of Canada, Ottawa, 2008.
- [4] Government of Canada, "Canada First Defence Strategy," Government of Canada, Ottawa, 2008.
- [5] Royal Military College of Canada, "Thesis Preparation Guidelines," Royal Military College of Canada, Kingston, 2015.
- [6] W. Elsaigh, "Steel Fiber Reinforced Concrete Ground Slabs; A Comparative Evaluation of Plain and Steel Fiber Reinforced Concrete Ground Slabs," University of Pretoria, Pretoria, 2001.
- [7] "Steel Fiber Reinforced Concrete," Bright Hub Engineering, 2012-2016. [Online]. Available: <http://www.brighthubengineering.com/concrete-technology/52076-steel-fiber-reinforced-concrete/>. [Accessed 25 11 2016].
- [8] M. V. Mohod, "Performance of Steel Fiber Reinforced Concrete," *International Journal of Engineering and Science*, vol. 1, no. 12, pp. 01-04, 2012.
- [9] A. E. Naaman, "Engineered steel fibers with optimal properties for reinforcement of cement composites," *Journal of Advanced Concrete Technology*, vol. 1, no. 3, pp. 241-252, 2003.
- [10] ACI Committee 544, "544.3R-08: Guide for Specifying, Proportioning, and Production of Fiber-Reinforced Concrete," p. 14, 2008.
- [11] T. Handojo, "Use of Water Reducers, Retarders, and Superplasticizers," [Online]. Available: <http://www.engr.psu.edu/ce/courses/ce584/concrete/library/materials/Admixture/AdmixturesMain.htm>. [Accessed 25 11 2016].
- [12] N. P. Banthia, "Impact Resistance of Concrete," PhD Dissertation, 1987.
- [13] ACI - 239 Committee in Ultra-High Performance Concrete, "Minutes of Committee Meeting October 2012," ACI Annual Conference 2012, Toronto, ON, Canada, 2012.
- [14] AFGC Scientific and Technical Committee, "Ultra High Performance Fibre-Reinforced Concretes -

- Interim Recommendations," Service d'études techniques des routes et autoroutes, France, 2002.
- [15] V. Perry, P. White and T. M. Ahlborn, "The First North American Broad Based Structural Design Guide on UHPC - ACI 239C," in *First International Interactive Symposium on UHPC*, Des Moines, Iowa, 2016.
- [16] P. Hadl, H. Kim and N. V. Tue, "Influence of cement type and type of aggregate on the fresh and hardened properties of UHPC and HPC," in *First International Interactive Symposium on UHPC*, Des Moines, Iowa, 2016.
- [17] R. Zhong and K. Wille, "Material efficiency in the design of UHPC paste," in *First International Interactive Symposium on UHPC*, Des Moines, Iowa, 2016.
- [18] E. Bruhwiler, "Structural UHPFRC: Welcome to the post-concrete era!," in *First International Interactive Symposium on UHPC*, Des Moines, Iowa, 2016.
- [19] A. Hassan, S. Jones and G. Mahmud, "Experimental test methods to determine the uniaxial tensile and compressive behaviour of ultra high performance fibre reinforced concrete (UHPFRC)," *Construction and Building Materials*, no. 37, pp. 874-882, 2012.
- [20] H. K. Shehab El-Din, H. A. Mohamed, M. A. El-Hak Khater and S. Ahmed, "Effect of steel fibres on behavior of ultra high performance concrete," in *First International Interactive Symposium on UHPC*, Des Moines, Iowa, 2016.
- [21] S. Rehacek, I. Simunek, J. Kolisko and D. Citek, "UHPC and FRC in severe environment conditions, resistance against freeze-thaw cycles, aggressive chemical agents and dynamic loading," in *First International Interactive Symposium on UHPC*, Des Moines, IO, 2016.
- [22] M.-A. Dagenais, "Réhabilitation sismique des jointes de chevauchement de piles de ponts par chemisage en béton fibré à ultra-haute performance," École Polytechnique de Montréal, Montréal, 2014.
- [23] D. M. Roy, "New strong cement materials: chemically bonded ceramics," *Science*, vol. 235, pp. 651-658, 1987.
- [24] L. F. Maya Duque, I. De La Varga and B. A. Graybeal, "Fiber reinforcement influence on the tensile response of UHPFRC," in *First International Interactive Symposium on UHPC*, Des Moines, Iowa, 2016.
- [25] E. Parent, P. Rossi and F. Le Maou, "Durability of a multiscale fibre reinforced cement composite in aggressive environment under service load," *Cement and Concrete Research*, no. 37, pp. 1106-1114, 2007.
- [26] ASTM C496/C496M-11, "Standard Test Method for Splitting Tensile Strength of Cylindrical Concrete Specimens," ASTM International, West Conshohocken, PA, 2011.

- [27] ASTM C1609/C1609M-12, "Standard Test Method for Flexural Performance of Fiber-Reinforced Concrete (Using Beam with Third-Point Loading)," ASTM International, West Conshohocken, PA, 2012.
- [28] L. F. Maya Duque and B. Graybeal, "Fiber orientation distribution and tensile mechanical response in UHPFRC," *Materials and Structures*, vol. 50, 2017.
- [29] M. J. Roth, "Flexural and tensile properties of thin, very high-strength, fiber-reinforced concrete panels," U.S. Army Engineer Research and Development Center, Vicksburg, MS, 2008.
- [30] Canadian Standards Association, "S806-12 - Design and construction of building structures with fibre-reinforced polymers," CSA, 2012.
- [31] Canadian Standards Association, "S6-14 - Canadian Highway Bridge Design Code," CSA, 2014.
- [32] H. A. Toutanji and W. Gomez, "Durability characteristics of concrete beams externally bonded with FRP composite sheets," *Cement and Concrete Composites*, no. 19, pp. 351-358, 1997.
- [33] O. Buyukozturk, O. Gunes and E. Karaca, "Progress on understanding debonding problems in reinforced concrete and steel members strengthened using FRP composites," *Construction and Building Materials*, no. 18, pp. 9-19, 2004.
- [34] L. Li, Y. Guo and F. Liu, "Test analysis for FRC beams strengthened with externally bonded FRP sheets," *Construction and Building Materials*, no. 22, pp. 315-323, 2008.
- [35] H. Toutanji and G. Ortiz, "The effect of surface preparation on the bond interface between FRP sheets and concrete members," *Composite Structures*, no. 53, pp. 457-462, 2001.
- [36] H. Yuan, J. Teng, R. Seracino, Z. Wu and J. Yao, "Full-range behavior of FRP-to-concrete bonded joints," *Engineering Structures*, no. 26, pp. 553-565, 2004.
- [37] M. Arndt, "FRP Rehabilitation of Blast and Impact Damaged Reinforced Concrete," Masters Thesis, Kingston, On, Aug 2009.
- [38] T. Alkhrdaji, "Strengthening of Concrete Structures Using FRP Composites," *Structure Magazine*, vol. 05, pp. 18-20, 2015.
- [39] R. Wight, "CE505 Course Notes," RMCC Civil Engineering Department, Kingston, 2016.
- [40] A. Q. Bhatti, N. Kishi and K. H. Tan, "Impact resistance behaviour of RC slab strengthened with FRP sheet," *Materials and Structures*, vol. 44, pp. 1855-1864, 2011.
- [41] D.-Y. Yoo, K.-H. Min, J.-Y. Lee and Y.-S. Yoon, "Enhancing impact resistance of concrete slabs strengthened with FRPs and steel fibres," in *6th International Conference on FRP Composites in Civil Engineering*, Rome, 2012.

- [42] D. Cormie, G. Mays and P. Smith, Blast effects on buildings, Second edition, London: Thomas Telford Limited, 2009.
- [43] United States Army Corps of Engineers, "UFC 3-340-01 Design and Analysis of Hardened Structures to Conventional Weapons Effects," Washington DC, USA, 2002.
- [44] L. Mao, S. Barnett, D. Begg, G. Schleyer and G. Wight, "Numerical simulation of ultra high performance fibre reinforced concrete panel subjected to blast loading," *International Journal of Impact Engineering*, no. 64, pp. 91-100, 2014.
- [45] N. Banthia, S. Mindess, A. Bentur and M. Pigeon, "Impact Testing of Concrete Using Drop-Weight Impact Machine," *Experimental Mechanics*, pp. 63-69, 1989.
- [46] D.-Y. Yoo, K.-H. Min, J.-Y. Lee and Y.-S. Yoon, "Enhancing impact resistance of concrete slabs strengthened with FRPs and steel fibers," in *6th International Conference on FRP Composites in Civil Engineering*, Rome, 2012.
- [47] O. Millon, A. Kleemann and A. Stolz, "Influence of the fiber reinforcement on the dynamic behaviour of UHPC," in *First International Interactive Symposium on UHPC*, Des Moines, Iowa, 2016.
- [48] H. Aoude, F. P. Dagenais, R. P. Burrell and M. Saatcioglu, "Behavior of ultra-high performance fiber reinforced concrete columns under blast loading," *International Journal of Impact Engineering*, no. 80, pp. 185-202, 2015.
- [49] M. W. Runge, "Precast concrete sandwich panels subjected to impact loading," Master's Thesis, Kingston, ON, 2012.
- [50] V. Boivin, "GFRP panels subjected to impact loads at room and arctic temperatures," Master's Thesis, Kingston, ON, 2016.
- [51] A. Benko, "FRP Sandwich Panel and Catcher System to Resist an Internal Blast," Master's Thesis, Kingston, ON, 2016.
- [52] L. J. Malvar, J. E. Crawford and K. B. Morrill, "Use of Composites to Resist Blast," *Journal of Composites for Construction*, vol. 11, no. 6, pp. 601-610, 2007.
- [53] Y. Qasrawi, P. J. Heffernan and A. Fam, "Dynamic behaviour of concrete filled FRP tubes subjected to impact loading," *Engineering Structures*, vol. 100, pp. 212-225, 2015.
- [54] J. Xu, C. Wu, H. Xiang, Y. Su, Z.-X. Li, Q. Fang, H. Hao, Z. Liu, Y. Zhang and J. Li, "Behaviour of ultra high performance fibre reinforced concrete columns subjected to blast loading," *Engineering Structures*, no. 118, pp. 97-107, 2016.
- [55] N.-H. Yi, J.-H. J. Kim, T.-S. Han, Y.-G. Cho and J. H. Lee, "Blast-resistant characteristics of ultra-high strength concrete and reactive powder concrete," *Construction and Building Materials*, no. 28, pp. 694-707, 2012.

- [56] B. Ellis, B. DiPaolo, D. McDowell and M. Zhou, "Experimental investigation and multiscale modeling of ultra-high-performance concrete panels subject to blast loading," *International Journal of Impact Engineering*, no. 69, pp. 95-103, 2014.
- [57] C. Melancon, S. De Carufel and H. Aoude, "Effect of High-Performance Materials on the Blast Response of Reinforced Concrete Structural Components," in *Proceedings of the 4th International Symposium on Ultra-High Performance Concrete and High Performance Materials*, Kassel, 2016.
- [58] M. F. Green, L. A. Bisby, A. Z. Fam and V. K. Kodur, "FRP confined concrete columns: Behaviour under extreme conditions," *Cement & Concrete Composites*, no. 28, pp. 928-937, 2006.
- [59] M. F. Green, A. J. Dent and L. A. Bisby, "Effect of freeze-thaw cycling on the behaviour of reinforced concrete beams strengthened in flexure with fibre reinforced polymer sheets," *Canadian Journal of Civil Engineering*, no. 30, pp. 1081-1088, 2003.
- [60] H. H. Hussein, K. K. Walsh, S. M. Sargand and E. P. Steinberg, "Effect of extreme temperatures on the coefficient of thermal expansion for ultra-high performance concrete," in *First International Interactive Symposium on UHPC*, Des Moines, IO, 2016.
- [61] R. El-Hacha, R. G. Wight and M. F. Green, "Prestressed Carbon Fiber Reinforced Polymer Sheets for Strengthening Concrete Beams at Room and Low Temperatures," *Journal of Composites for Construction*, vol. 8, no. 1, 2004.
- [62] S. Astarlioglu and T. Krauthammer, "Response of normal-strength and ultra-high-performance fiber-reinforced concrete columns to idealized blast loads," *Engineering Structures*, no. 61, pp. 1-12, 2014.
- [63] J. M. Biggs, *Introduction to Structural Dynamics*, McGraw-Hill Book Company, 1964.
- [64] King Packaged Materials Company, "UP-F4 Poly Technical Data Sheet," King Packaged Materials Company, Boisbriand, QC, 2016.
- [65] ASTM C39 / C39M - 16b, "Standard Test Method for Compressive Strength of Cylindrical Concrete Specimens," ASTM International, West Conshohocken, PA, 2016.
- [66] ASTM C469 / C469M - 14, "Standard Test Method for Static Modulus of Elasticity and Poisson's Ratio of Concrete in Compression," ASTM International, West Conshohocken, PA, 2014.
- [67] M. P. Collins and D. Mitchell, *Prestressed Concrete Structures*, Toronto: Response Publications, 1997.

APPENDICES

Appendix A Complimentary Information

1. Appendix A

The studies presented in the Chapters 2 and 3 are presented as individual papers but are a part of the larger research program which is the topic of this thesis. The studies, although presented separately, were conducted simultaneously using similar apparatuses and procedures. Chapter 3 and Chapter 4 summarized the principal information from the studies, while this appendix will provide complimentary information about the design and fabrication of both the specimens and the testing apparatuses.

1.1 Design of Experimental Specimens

As the panels created in this project would be utilized as a part of a modular protective system (MPS) which is adaptable to many different types of terrain and environments, a standard size had to be determined. With the intent of the MPS to not require heavy equipment or local resources to construct, all components must be man-portable. To create an armour panel that could provide sufficient resistance to potential explosive events, the dimensions of the panel were determined based on a maximum panel mass. The mass selected for this research was 50 kg as it was assessed that two individuals would be able to easily carry and install 50 kg panels.

With the mass of the panel known, the next key parameter was selecting a suitable panel thickness. It was attempted to keep the panel as thin as possible in order to allow the length and width of the panel to be larger. Based on previous research into thin panels for impact testing, a panel thickness of 38 mm, or 1.5 in, was selected. Other studies had used thicknesses as low as 12 mm, 0.5 in, but preliminary calculations showed these panels would be too weak for this project. A panel thickness of 38 mm also made the fabrication of concrete forms easier, as nominal construction lumber such as 2 x 4's are 38 mm thick.

Based on a weight of 50 kg and a thickness of 38 mm, and with a known approximate density of concrete being 2450 kg/m^3 , it was calculated that the panels could have a surface area of about 0.5 m^2 . A rectangular shape panel was determined to be the most suitable shape and so a 2:1 ratio of length to width was selected. Based on these criteria, panel dimensions of 1040 mm x 535 mm x 38 mm were chosen, as shown below in Figure 1-1.

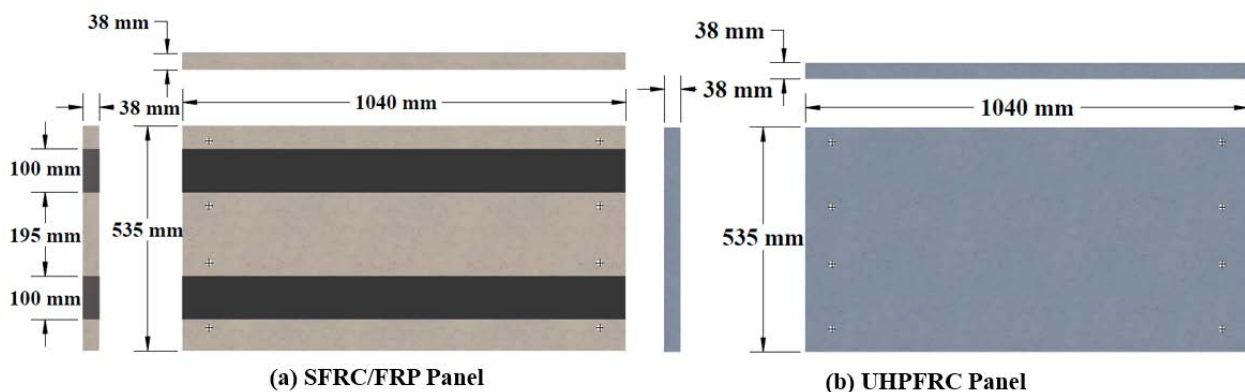


Figure 1-1 - Panel Dimensions

Appendix A Complimentary Information

1.1.1 UHPFRC Panels

The UHPFRC used in this study was provided by the King Construction Products branch of KPM Industries and is their UP-F4 Poly product. Preliminary panel strength calculations were completed based on the material properties provided by the company [64]. A summary of these properties can be found in Table 1-1. Based on these specifications, the strength of these panels in three-point flexural bending was calculated to be around 12.6 kN. Calculations can be found in Appendix B and were completed based on a simple equilibrium of forces calculation. Another strength prediction model, a moment-curvature model developed by the author, was used to predict panel strength and from that model, the strength of the UHPFRC panels was predicted to be 12.1 kN. The moment-curvature model will be described later in this appendix and is located Appendix D.

Table 1-1 - UP-F4 Poly Material Properties

Mixture properties	Manufacturer value
Compressive strength (MPa)	120
Elastic modulus (GPa)	37
Fibre volume (%)	4
Tensile strength (MPa)	11
Mass density (kg/m ³)	2450

1.1.2 SFRC Panels Strengthened with FRP Straps

The SFRC panels used in this research project were intended to be used as a baseline comparison to the UHPFRC panels to essentially see the improvement associated with UHPFRC panels. The concrete used in the SFRC panels was ordered from Lafarge Canada and was requested to have a compressive strength of 40 MPa, air-entrainment, and a steel fibre dosage of 2% by volume. A lack of experience working with SFRC led the supplier to not have enough fibres on hand and the actual fibre dosage of the concrete mix was just under 1% by volume, greatly reducing the overall strength and behaviour of the panels. In order to have panels that could be compared to the UHPFRC panels, it was decided to add FRP straps to the SFRC panels to increase their strength and ductility. Preliminary calculations were completed to determine how much FRP to add to the panels to achieve a similar strength of around 12.6 kN. These calculations, provided in Appendix B, established that two straps of MBrace CF160 CFRP, with the material properties and dimensions shown in Table 1-2, would provide a panel with approximately the same strength as the UHPFRC panels. The moment-curvature model predicted a panel strength of 15.4 kN, which turned out to be closer to the actual strength as determined from laboratory testing.

Table 1-2 - FRP Properties

MBrace CF160 Properties	Value
Ultimate tensile strength (MPa)	3800
Tensile elastic modulus (GPa)	227
Strain at failure (%)	1.7
Material thickness (mm)	0.33
Strap width (mm)	100

Appendix A Complimentary Information

1.2 Fabrication of Experimental Specimens

As explained earlier in the chapter, the panel dimensions were selected primarily to achieve a panel mass close to 50 kg. However, to ease the fabrication process of the forms, the length, width and thickness of the panels were selected based on nominal lumber dimensions. The forms were built using $\frac{3}{4}$ -in thick plywood and 2-in x 4-in framing lumber, some of which were ripped to be 2-in by 2-in to obtain the required panel dimensions. A photo of one form is shown in Figure 1-2, and sixteen of these forms were constructed. Form drawings can be found in Appendix C and dimensions are shown in Figure 1-3.



Figure 1-2 - Forms used to cast specimens

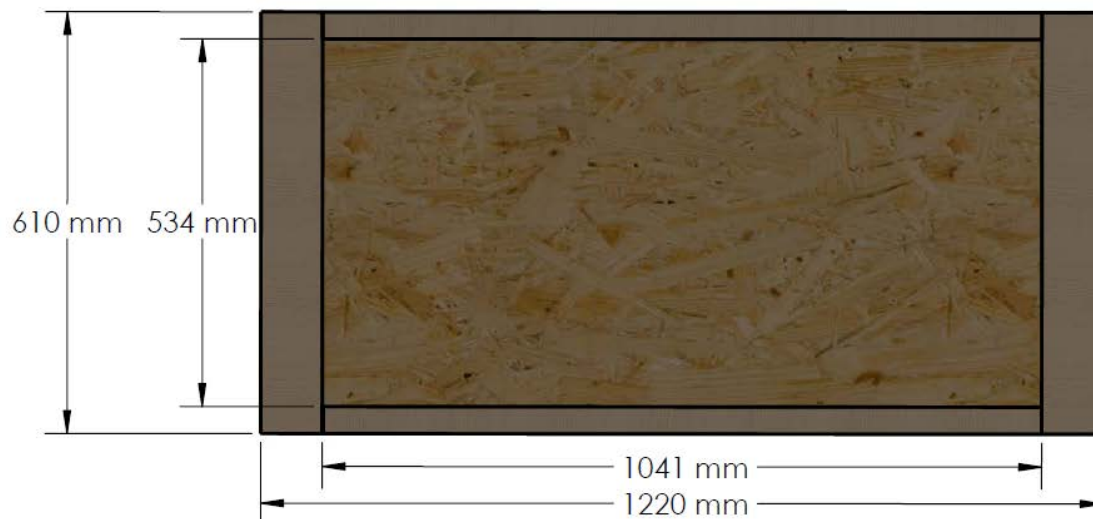


Figure 1-3 - Form dimensions

As can be seen in Figure 1-2, $\frac{3}{4}$ -in dowels were placed in the forms so that once the concrete panels were removed, there would be four holes at each end of the panel. These holes were required to secure the panels in the testing frame using bolts.

Appendix A Complimentary Information

1.2.1 UHPFRC Panels

Prior to the mixing and pouring of the UHPFRC panels, additional work had to be done to ensure the forms were watertight. UHPFRC is a self-consolidating concrete and is very fluid, so all form joints were sealed using silicone sealant. The sealant was applied using an applicator gun and was given a few days to cure before the UHPFRC was mixed. Immediately prior to pouring the concrete, a coat of oil was applied to the forms to ease the removal of the forms once the concrete had cured.

The UP-F4 Poly mix from King Construction Products was mixed in the RMCC Structures Laboratory using the Cumflow RP100XD HD Rotating Pan Mixer, shown in Figure 1-4. King was generous enough to provide the materials required for the research project and their technical sales engineer, Mr. Julian Pena Cruz, to travel to Kingston to ensure the product was mixed correctly. The mix design used in this study is shown in Table 1-3 and a total of six batches were mixed to provide enough material for the panels as well as some extra for ancillary testing such as cylinders and beams. Each batch varied in size to determine the optimum amount for the mixer. The mix design shown in Table 1-3 is based on one bag of UP-F4 Poly premix and this amount increased to four bags for some batches. The steel fibres used in the UHPFRC are Bekaert Dramix fibres which are 10 mm in length with a diameter of 0.2 mm, and have a tensile strength of 2750 MPa.



Figure 1-4 - Cumflow RP100XD HD Rotating Pan Mixer

Table 1-3 - UP-F4 Mix Design

Ingredient	Mass (kg)
UP-F4 Poly Premix	25.00
Water	2.825
Superplasticizer	0.893
Steel fibres	16.83

Appendix A Complimentary Information

A crew of six helped with the mixing and pouring process which reduced the amount of time it took to get all the specimens cast. Each batch of UHPFRC was mixed in an identical manner by Mr. Julian Pena Cruz and the author to reduce the variations between batches. The same procedure was followed for each batch, with the amount of premix, water, superplasticizer, and steel fibres being prepared and weighed before being added to the mixer. The premix was added to the mixer first, followed by the water and superplasticizer. These ingredients were mixed together for five minutes before the steel fibres were slowly added. The steel fibres were poured onto a wire mesh and a concrete vibrator was used to pass the fibres through the mesh, as shown in Figure 1-5. This was done to prevent clumping of fibres within the concrete and allow for uniform distribution. Once all the fibres were added to the mixer, it was mixed for another five minutes before being transferred to buckets. The buckets were brought to the forms and the UHPFRC was poured into the forms using a smooth, back and forth motion to make sure the fibres are properly orientated. The steel fibres orient themselves with the direction of flow so it is critical to ensure the concrete is poured properly to get the required orientation. If the fibres are incorrectly oriented, they will not perform to their capacity.



Figure 1-5 - Adding steel fibres to the UHPFRC mix

Once all the specimens were cast, the forms were covered with plastic and allowed to cure. The forms were removed after 48hrs and the panels were wrapped in plastic and watered for the remainder of the first week. After 7 days of curing, the plastic was removed and the panels were left to cure in ambient laboratory conditions for the remainder of the 28 days required for proper curing.

Ancillary tests were conducted after 28 days of curing to determine the material properties of the UHPFRC mix used in this research project. Compression tests were carried out using cylinders with a 100 mm diameter and 200 mm height, and were conducted according to ASTM C39 [65]. Modulus of elasticity tests were completed according to ASTM C469 [66], shown in Figure 1-6. The results of the ancillary testing are shown alongside the manufacturer values in Table 1-4.

Appendix A Complimentary Information



Figure 1-6 - Modulus of Elasticity Testing Setup

Table 1-4 - Average Material Properties of UP-F4 Poly Mix

Mixture properties	Laboratory value	Manufacturer value
Compressive strength (MPa)	125	120
Elastic modulus (GPa)	27	37
Fibre volume (%)	4	4
Tensile strength (MPa)	-	11
Mass density (kg/m ³)	-	2450

1.2.2 SFRC Panels Strengthened with FRP Straps

Unlike the UHPFRC which had to be mixed in the RMCC Structures Laboratory, Lafarge could deliver the SFRC using a ready-mix truck. The steel fibres were added to the truck once on site and the concrete was mixed for five minutes to ensure proper distribution of fibres throughout the mixture. Once the fibres had been distributed and mixed, the concrete was poured into wheelbarrows and moved into the laboratory. Once in the lab, the forms were filled with the concrete mix and covered with plastic for the first week of curing. The panels remained in the forms for the first week and were watered each day. After 7 days, the forms were removed and the panels were left to cure in ambient laboratory conditions.

After 28 days of curing, ancillary tests were completed to determine the material properties of the SFRC mix. Based on the compression and modulus of elasticity tests, the material properties listed in Table 1-5 were determined.

Appendix A Complimentary Information

Table 1-5 – Average Material Properties of SFRC Mix

Mixture Property	Laboratory Value
Compressive strength (MPa)	40
Elastic modulus (GPa)	22

As explained in Section A.1.2.1, the SFRC panels were intended to have sufficient strength to be compared to the UHPFRC panels. After an initial quasi-static three-point flexural bending test was conducted on the first SFRC panel, it was determined that they did not have sufficient strength to be testable. FRP straps were suggested as a solution to this flexural weakness and so preliminary calculations were completed to determine the required amount of FRP to provide adequate flexural strength.

To prepare the SFRC panels for the application of the FRP straps, they had to be pressure washed to expose the aggregate and remove the surface layer of concrete. The difference between the pressure washed section and the typical concrete surface can be seen in Figure 1-7. Once the panels were prepared, the FRP straps were applied using a wet lay-up procedure. A two-part epoxy was mixed following the manufacturer instructions and was applied to one side of the panel. The FRP strap, previously measured and cut from a larger sheet, was laid on the wet epoxy and smoothed out, ensuring it was in uniform contact with the entire length of the panel. A final coat of epoxy was applied to the top of the FRP strap before being covered with plastic to cure for two days. Once the FRP straps on the one side of the panel had cured, the panel was flipped over and the strap was applied to the ends and the other side of the panel.



Figure 1-7 - Exposed Aggregate of SFRC Panels

Appendix A Complimentary Information

1.3 Experimental Setup and Procedure

While this research project focused on the dynamic response of each type of panel when exposed to impact loads at both ambient and cold temperatures, quasi-static testing was carried out on four specimens of each type of panel to obtain baseline behavioural information. Once the static load-deflection curves had been developed for the ambient and cold temperature panels, dynamic testing was completed.

Each panel that was tested dynamically as part of this research project went through a process of two tests. Cold temperature panels were first placed in a Panasonic MDF-794-PE ultra-low freezer, which was capable of cooling the panels to a temperature of -70°C . Ambient temperature panels were left in the laboratory prior to testing to maintain their temperature of approximately 20°C . Each panel was subjected to an impact load from the pendulum-type drop hammer before being testing for residual strength using the same testing set-up that was used for quasi-static testing.

1.3.1 Quasi-static Testing Apparatus

The quasi-static testing apparatus was used for both static testing and the residual strength testing of impact tested panels. The same procedure and set-up was used for both tests. Three-point flexural bending was used to determine the flexural behaviour of the panels in an effort to keep the loading set-up consistent with the impact testing. The only difference between the boundary conditions in the quasi-static test and the impact test are that the panels are not bolted to the supports. The loading set-up can be seen in Figure 1-8. Boundary conditions of the testing set-up are best described as simply supported due to the triangular supports with bearing plates between the support and the panel. These support conditions allow for rotation at both supports and displacement in the horizontal direction.

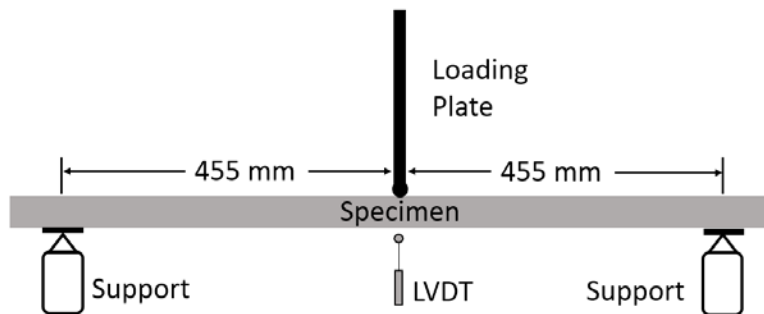


Figure 1-8 - Quasi-static three-point bending testing apparatus

1.3.1.1 Testing Machine

A MTS model 322 machine, shown in Figure 1-9, was used for quasi-static testing. The MTS machine consisted on a 500 kN hydraulic head that applied the load to the midspan of the panel with a constant head speed of 2mm/min.

Appendix A Complimentary Information



Figure 1-9 - Three-point flexural bending quasi-static testing set-up

1.3.1.2 Instrumentation

Quasi-statically tested panels were instrumented with two 10 mm Kyowa strain gauges on the bottom of the panel. In addition to the strain gauges, the MTS machine monitored the load which was applied to the midspan of the panel, as well as the displacement of the machine head. To confirm the head displacement, a 300 mm LVDT was placed under the midspan of the panel, measuring midspan displacement of the panel. To monitor the temperature of the cold temperature panels, Type T thermocouples were placed on the face of the panels.

1.3.1.3 Testing Procedure

Once strain gauges were installed on the panels, ambient temperature panels could be tested immediately while the cold temperature panels had to be placed in the freezer until reaching a temperature of -70°C . Once the cold temperature panels reached the desired temperature, the same procedure was followed for both the ambient and cold temperature quasi-static testing.

Panels were placed in the testing apparatus with the bearing plates centred on the triangular supports. Strain gauges, and the thermocouple for cold temperature panels, were hooked up to the data acquisition system and the LVDT was positioned under the midspan of the panel. Once the data acquisition system was checked to ensure all instrumentation was being monitored, the loading head was lowered and testing commenced.

The data acquisition system provided a live view of the load-deflection curve for each panel, allowing the testers to determine when the test could be terminated. For the first few tests, due to inexperience of the testers, testing was halted prematurely, preventing the full load-deflection behaviour from being acquired. After realizing that testing should be conducted until there was complete failure of the panel, subsequent tests were conducted in this manner to obtain the proper load-deflection curves.

Residual strength tests were performed in the same manner as the quasi-static tests, with one alteration. As most the panels already had a permanent deflection resulting from the impact test, this

Appendix A Complimentary Information

residual deflection was taken as the initial deflection of the panel. This means that instead of the load-deflection curve starting from a deflection of 0 mm, it started from further along the x-axis depending on the residual deflection. An example of load-deflection curves of a quasi-static test compared with a residual strength test can be found in Figure 1-10.

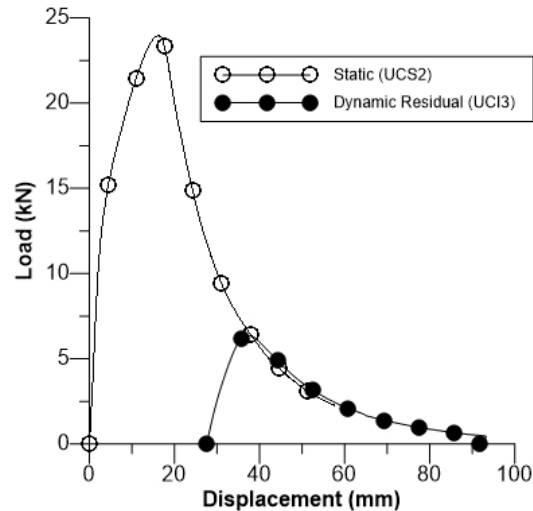


Figure 1-10 - Load-deflection behaviour of quasi-static panel UCS2 and residual strength of panel UCI3

1.3.2 Dynamic Testing Apparatus

The dynamic testing conducted in this research project used panels that had not previously been tested, ensuring they had their full strength. The ability of these panels to resist multiple impact events was not tested in this study but instead their residual strength was tested post-impact.

1.3.2.1 Pendulum Hammer

To apply an impact load, a pendulum-type impact hammer was used. In other published literature, drop weight impact machines are often used but previous research at RMCC has been completed using a similar pendulum hammer to the one used in this study. This hammer was selected because of its ability to alter the amount of energy transferred to the specimen by adjusting the drop height and the mass of the hammer. The drop height was measured as the difference between the centre of gravity of the hammer at rest and the centre of gravity of the hammer at the raised position, as shown in Figure 1-11.

Appendix A Complimentary Information

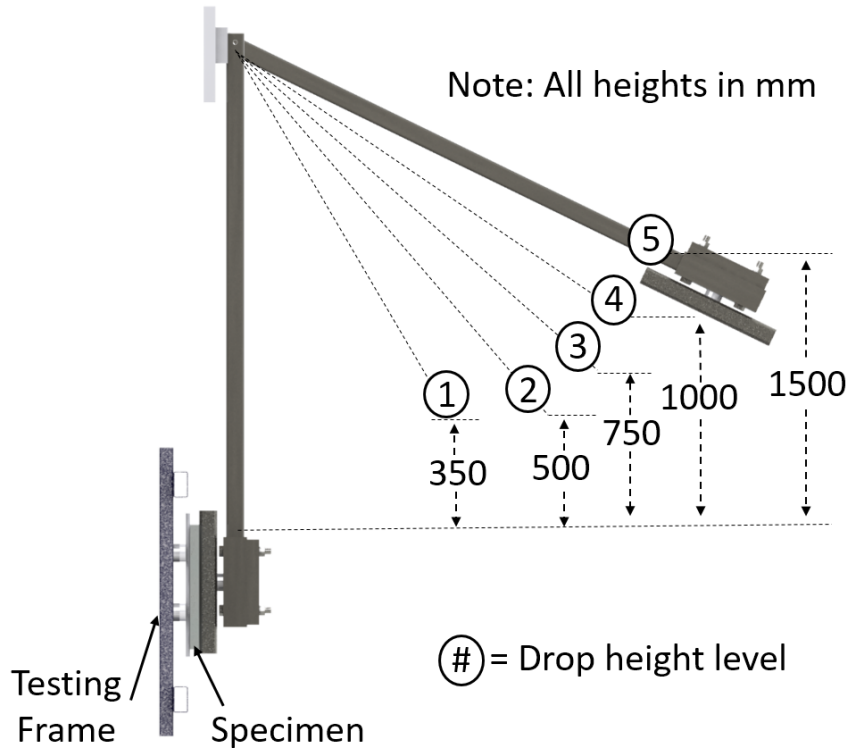


Figure 1-11 - Impact hammer drop heights

The impact hammer was connected to a frame of steel I-beams and C-channels that were bolted together and connected to the floor of the RMCC Structures Laboratory. The testing set-up is presented in Figure 1-12. The hammer consisted of an arm made of a hollow structural section (HSS) connected to a solid steel plate that served as the head of the hammer. Additional plates could be added to the hammer head to increase the mass of the hammer. The hammer tup, the part of the hammer that impacts the panel, consisted of another HSS piece that was the same length as the width of the panel, ensuring that the entire face of the panel was impacted. Once the testing frame was constructed within the hammer frame, the entire hammer had to be levelled to ensure the tup evenly contacted the entire panel.

Appendix A Complimentary Information

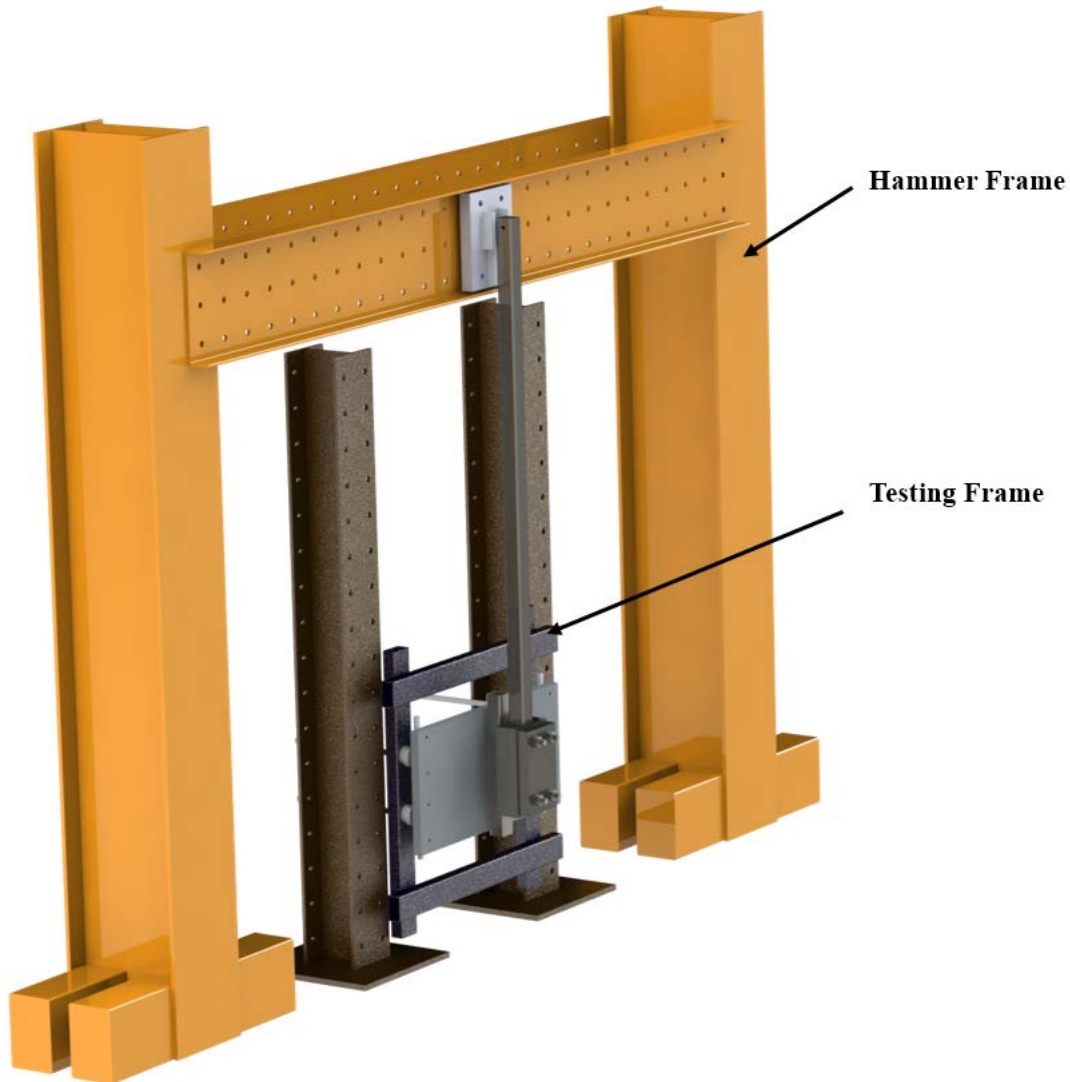


Figure 1-12 - Impact Hammer Test Set-up

1.3.2.2 Impact Frame Construction

The testing frame which held the panels was constructed within the existing hammer frame. This caused several issues during the manufacturing process as the testing frame had to be perfectly aligned within the hammer frame to make sure the hammer would impact the midspan of the panel. HSS pieces were used to make a frame that would allow the panels to be mounted and provide the ability for the panels to deflect within the frame without impacting any part of the frame. These HSS pieces were attached together to form a rectangular shape and the four corners were bolted to steel I-beams that were bolted to the floor of the lab. Holes were drilled in the HSS pieces to allow panel supports to be attached. The panel supports were constructed of steel rods that were welded onto length of threaded rod. The threaded rod allowed the supports to be connected to the HSS testing frame. The steel rods had holes drilled into them to allow the panels to be secured using bolted connections. Spacers were placed on the threaded rods to provide a contact surface for the force transducers that would be used to measure the reaction forces. The testing frame can be seen in Figure 1-13.

Appendix A Complimentary Information

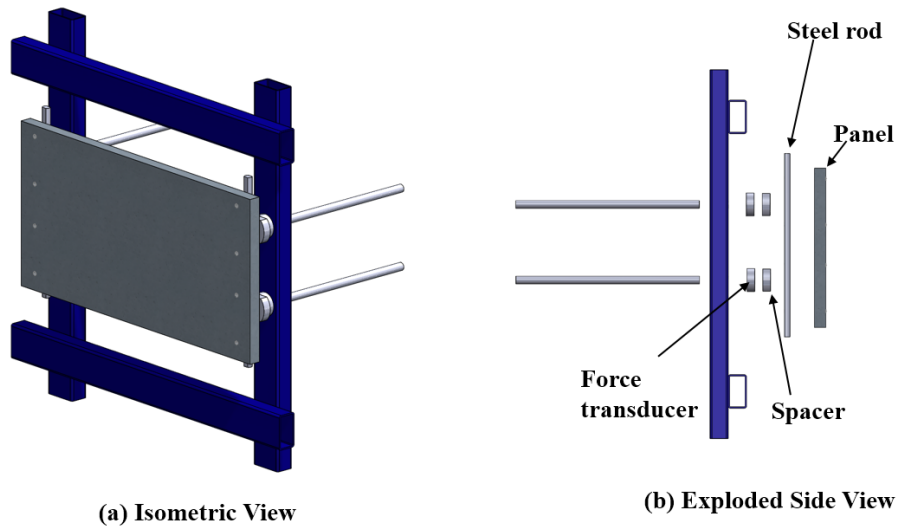


Figure 1-13 - Testing frame

1.3.2.3 Instrumentation

Similar to the quasi-statically tested panels, dynamically tested panels had strain gauges installed on their tension face, and they were located in the same manner. Dynamic tests were highly instrumented to capture all relevant data. In addition to strain gauges, dynamic panels also had an accelerometer installed on the back of the panel at the midspan. Once the panels were installed in the impact testing frame, a laser LVDT was used to measure midspan displacement and an LVDT was placed the supports to monitor support deflections. The testing frame had three force transducers to measure loading data during the impact event. One force transducer was installed between the hammer arm and the hammer tup to measure the hammer force, and the other two force transducers were placed on the reaction points, one on the top left and one on the bottom right, in order to determine the reactionary force. All testing frame instrumentation can be seen in Figure 1-14.

Appendix A Complimentary Information

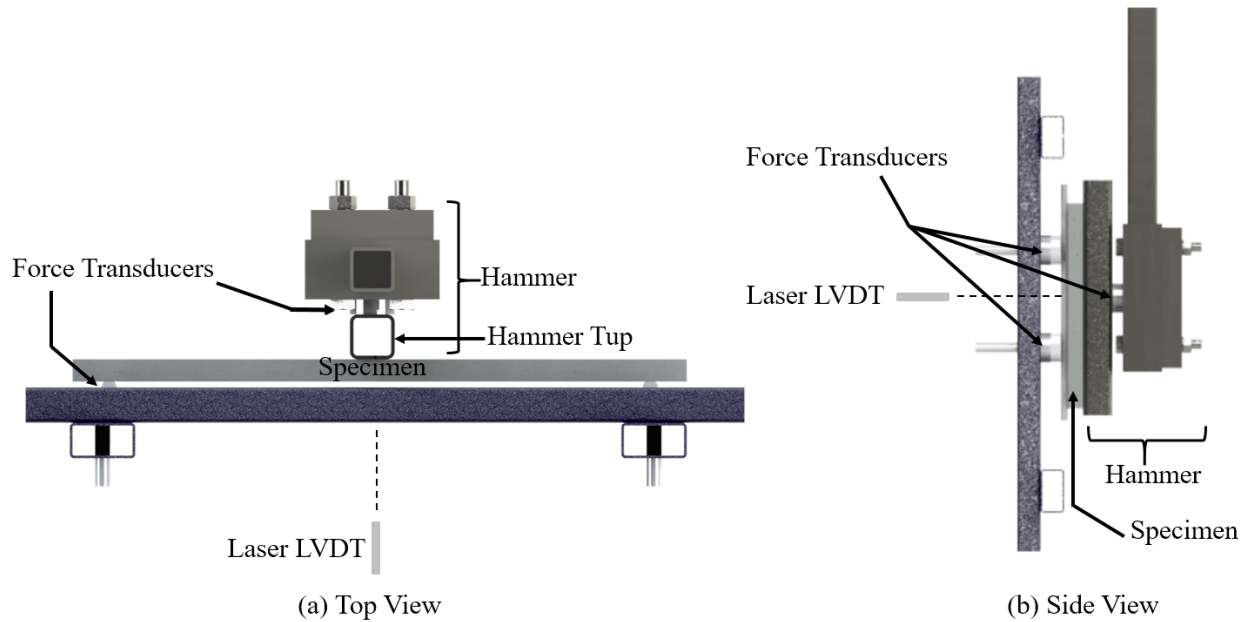


Figure 1-14 - Impact Hammer Test Set-up

To capture the panel behaviour during the impact testing, high-speed cameras were set up to capture the impact of the hammer with the panel. One camera was placed to the side of the testing frame while the other camera provided a top view. Both cameras were set up on tripods and placed in the same location for every test. The cameras used were MotionBLITZ Cube high speed cameras produced by Mikrotron. These cameras were connected to laptops through the provided software and were triggered using external trigger cables. The cameras were set to continuously record at a frame rate of 500 fps and then a set time before and after the trigger point could be saved by the program. The system was set up so the trigger would be the hammer impacting the panel and the program would save a video that lasted from 2 seconds before the trigger to 2 seconds after. This duration was enough to record the impact of the hammer and the response of the panel.



Figure 1-15 - Placement of high-speed cameras

Appendix A Complimentary Information

1.3.2.4 Testing Procedure

Dynamic tests were conducted at varying hammer heights which altered the impact energy of the system. The same impact energies were used for tests of each type of panel and at each temperature, in order to have comparable data. Panels were secured to the testing frame using bolts which connected the panel through a steel rod to the reaction points on the test frame, as shown in Figure 1-16. Once panels were connected to the testing frame, the strain gauges and accelerometer were connected to the data acquisition system and all the instrumentation was zeroed and checked to make sure it was working properly. The hammer was raised using the 10-ton overhead crane that is in the structures lab. The hammer height was measured from the laboratory floor to the centre of gravity of the hammer using a tape measure. Once the hammer was raised to the desired height and the data acquisition and high-speed cameras were ready to record, the command was given to drop the hammer and the pin was released, allowing the hammer to fall and impact the panel. Once the hammer impacted the panel and rebounded, a member of the testing team would grab the hammer to prevent it from impacting the panel a second time. Screenshots of a video depicting the testing are shown in Figure 1-17.



Figure 1-16 - Bolted connection of specimen to testing frame

Appendix A Complimentary Information

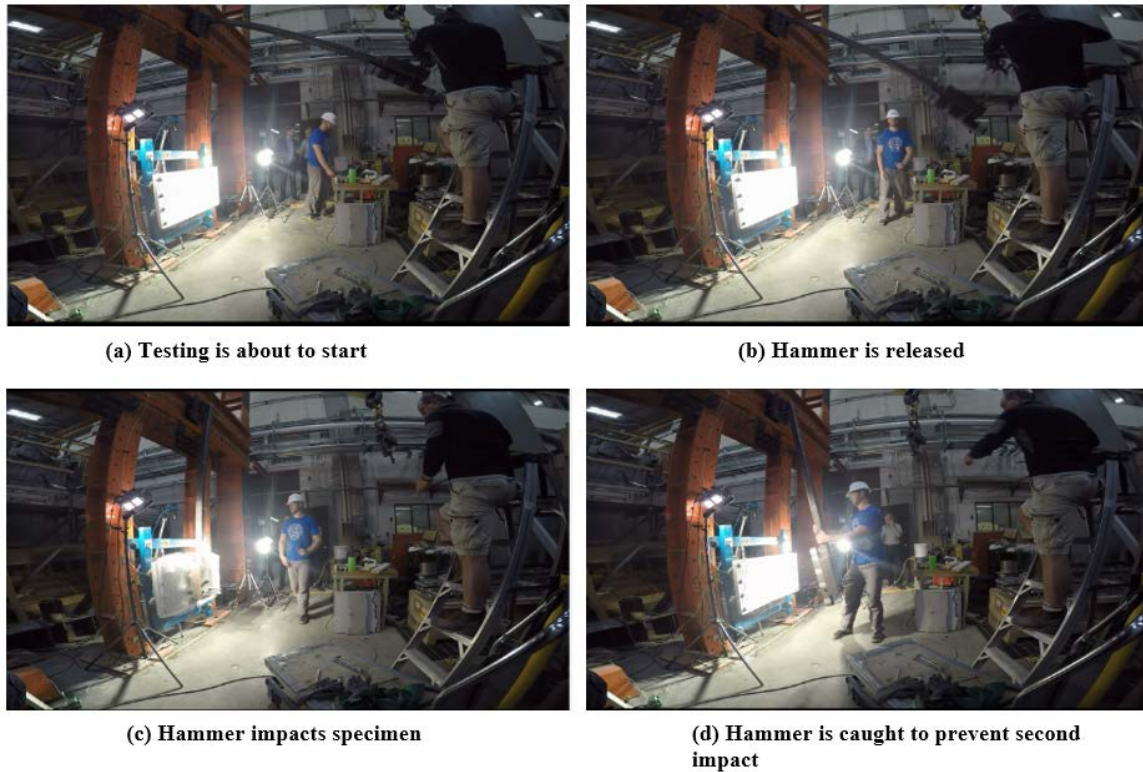


Figure 1-17 – Impact testing camera footage

1.4 Moment-Curvature Model

As stated earlier in this appendix, Microsoft Excel was used to create a spreadsheet that once programmed, could predict the behaviour of both types of panels. The cross-section of the panel was split into 40 layers and by using strain compatibility and force equilibrium, the model was able to determine the stresses in each of these layers. For the SFRC panels, the strain at the top of the cross-section was increased incrementally and the strains in the rest of the cross-section were determined to satisfy the equilibrium of forces. For the UHPFRC panels, the strain at the bottom was increased incrementally and then the strain for the rest of the cross-section was determined based on equilibrium. The driving value of the spreadsheet was changed from the top strain to the bottom strain for the UHPFRC panels to not overpredict the amount of compression in the top part of the cross-section. The resulting moment and force that were required to cause this stress distribution were recorded and the model then proceeded to the next increment of strain at the top of the cross-section. The curvature for each increment of top strain was determined using Equation A-1 and once all the increments of top strain were analyzed, a moment-curvature diagram was created.

$$\varphi = \frac{\varepsilon_t + \varepsilon_b}{d} \quad (\text{A-1})$$

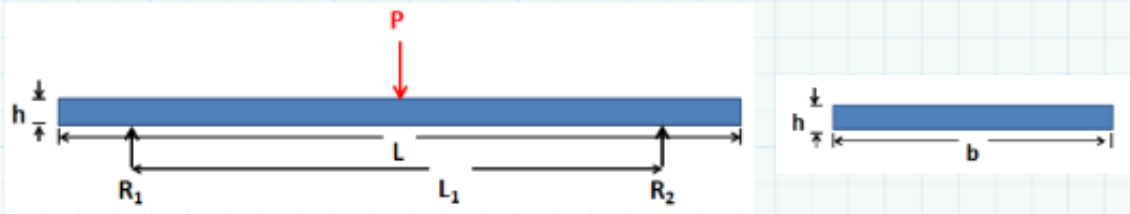
To develop theoretical load-deflection curves for each of the type of panels, the curvature and loading data from the moment-curvature relationship were used. The deflection at 100 mm intervals along the length of the beam was determined using the moment and curvature at that point. The approximated approach determined by Collins and Mitchell [67] was used and the load-deflection curves for each type of panel were determined.

Appendix B Preliminary Calculations

CONCRETE PANEL STRENGTH CALCULATIONS

1. STEEL FIBRE REINFORCED CONCRETE (SFRC)

(a) Cross-Section Properties.



$$h := 38 \text{ mm}$$

$$b := 534 \text{ mm}$$

$$L := 1041 \text{ mm}$$

$$L_1 := 915 \text{ mm}$$

$$A_g := b \cdot h = 20292 \text{ mm}^2$$

$$I_g := \frac{b \cdot h^3}{12} = 2441804 \text{ mm}^4$$

$$V_g := b \cdot h \cdot L = 0.021 \text{ m}^3$$

$$M := V_g \cdot \gamma_c = 51.754 \text{ kg}$$

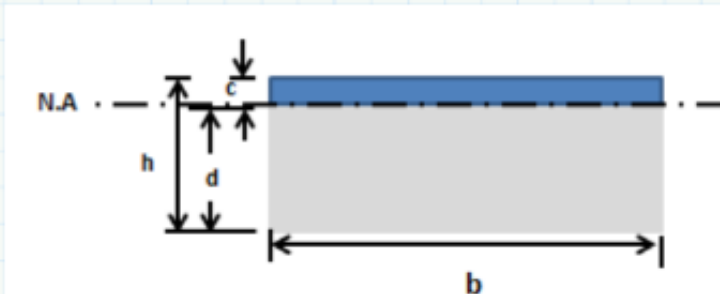
$$f'_c := 38 \text{ MPa} \quad \gamma_c := 2450 \frac{\text{kg}}{\text{m}^3}$$

$$f_r := 0.6 \cdot \sqrt{\frac{f'_c}{\text{MPa}}} \cdot \text{MPa} = 3.699 \text{ MPa}$$

$$\alpha_1 := 0.85 - 0.0015 \cdot \frac{f'_c}{\text{MPa}}$$

$$\beta_1 := 0.97 - 0.0025 \cdot \frac{f'_c}{\text{MPa}}$$

(b) Determine flexural strength.



$$C = T$$

$$C = f'_c \cdot b \cdot c$$

$$T = f_r \cdot b \cdot d$$

Guess value of c to determine equilibrium forces:

$$c := 3.37 \text{ mm}$$

$$d := h - c$$

$$C := f'_c \cdot b \cdot c = 68.384 \text{ kN}$$

$$T := f_r \cdot b \cdot d = 68.397 \text{ kN}$$

$$M_r := C \cdot \left(\frac{\beta_1 \cdot d}{2} - \frac{\beta_1 \cdot c}{2} \right) = 935.237 \text{ J}$$

Appendix B Preliminary Calculations

$$M = \frac{P}{2} \cdot \frac{L_1}{2} \quad @\text{midspan} \quad P = \frac{4 \cdot M}{L_1}$$

$$P_r := \frac{4 \cdot M_r}{L_1} = 4.088 \text{ kN}$$

(c) Add FRP straps to increase strength.

FRP Properties:

$$E_{frp} := 227 \text{ GPa}$$

$$\varepsilon_{frp} := 0.006$$

$$\#_{layers} := 1 \quad b_{frp} := 100 \text{ mm} \quad \#_{straps} := 2$$

$$t_{frp} := 0.33 \text{ mm} \quad \text{MBrace CF160}$$

$$A_{frp} := \#_{layers} \cdot t_{frp} \cdot b_{frp} \cdot \#_{straps} = 66 \text{ mm}^2$$

Guess value of c to determine equilibrium forces:

$$c := 5.61 \text{ mm}$$

$$C := f'_c \cdot b \cdot c = 113.838 \text{ kN} \quad T := \varepsilon_{frp} \cdot E_{frp} \cdot A_{frp} = 89.892 \text{ kN}$$

$$M_r := T \cdot \left(d - \frac{\beta_1 \cdot c}{2} \right) = 2.892 \text{ kN} \cdot \text{m}$$

$$P_{SFRC} := \frac{4 \cdot M_r}{L_1} = 12.644 \text{ kN}$$

2. ULTRA HIGH PERFORMANCE FIBRE REINFORCED CONCRETE (UHPRC)

(a) Cross-Section Properties.

$$f'_c := 120 \text{ MPa}$$

$$f_r := 11 \text{ MPa}$$

**Values from UP-F4 specs.

No other properties changed.

Guess value of c to determine equilibrium forces:

$$c := 3.19 \text{ mm}$$

$$d := h - c$$

$$C := f'_c \cdot b \cdot c = 204.415 \text{ kN} \quad T := f_r \cdot b \cdot d = 204.474 \text{ kN}$$

$$M_r := C \cdot \left(\frac{\beta_1 \cdot d}{2} - \frac{\beta_1 \cdot c}{2} \right) = 2.828 \text{ kN} \cdot \text{m}$$

$$M = \frac{P}{2} \cdot \frac{L_1}{2} \quad @\text{midspan} \quad P = \frac{4 \cdot M}{L_1}$$

$$P_{UHPRC} := \frac{4 \cdot M_r}{L_1} = 12.362 \text{ kN}$$

Appendix B Preliminary Calculations

3. PREDICTED STRENGTHS

$$P_{SFRC} = 12.644 \text{ kN}$$

$$P_{UHPRC} = 12.362 \text{ kN}$$

It is predicted that the two types of concrete panels will have comparable strength when tested using quasi-static three-point flexural bending.

4. FRP STRAPS ADDED TO UHPRC PANELS

Guess value of c to determine equilibrium forces:

$$c := 4.6 \text{ mm}$$

$$C := f'_c \cdot b \cdot c = 294.768 \text{ kN} \quad T := f_r \cdot b \cdot d + \varepsilon_{frp} \cdot E_{frp} \cdot A_{frp} = 294.366 \text{ kN}$$

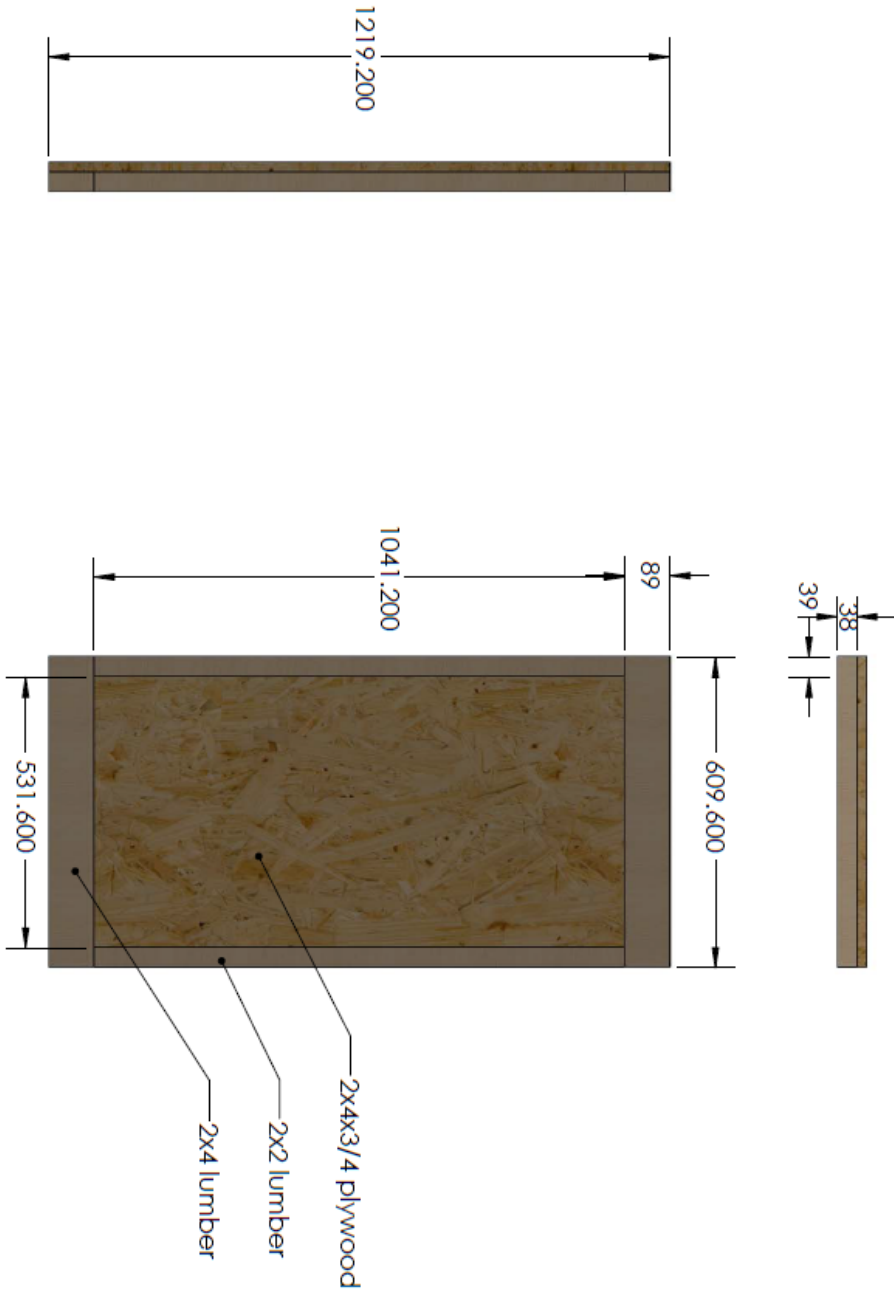
$$M_r := T \cdot \left(d - \frac{\beta_1 \cdot c}{2} \right) = 9.654 \text{ kN} \cdot \text{m}$$



$$P_{combo} := \frac{4 \cdot M_r}{L_1} = 42.205 \text{ kN}$$

If FRP straps are added to the UHPRC panels, it is estimated that there will be a 3.5 x increase in panel strength when tested in three-point flexural bending.

Appendix C Form Drawings

Note: All dimensions in mm.



NATIONAL MATERIAL	WISCONSIN	lbs
STATE PROJECT CONTRACT NUMBER		
LAND OWNER		
PROJECT NUMBER		
 BMC ENGINEERING FACILITY CMRC FACILITE D'INGENIERIE		
 SCALE 1:12 INCH / FEET POUCE / MÈTRE		
TOLERANCES: X.X = ± 0.05 X.XX = ± 0.005 X.XXX = ± 0.001		
TITLE	NAME	DATE
Concrete Forms	M. Beirnes	Form 3A
NUMBER	SHEET	DATE
G-6794	1 OF 1	
DESIGN #	001	

Appendix D Data from Dynamic Test Panel SCI2

5.72792	-15.6167	-11.875	-0.0043	0.03138	-0.01842	0.0888	-0.14386	-0.01656	0.02809	5.72792	-57.0581
5.72833	-14.925	-12.025	-0.00488	0.03424	-0.00996	0.0739	-0.12892	-0.0157	0.02484	5.72833	-57.0752
5.72875	-10.3417	-7.99167	-0.00566	0.03763	0.0073	0.06641	-0.10471	-0.01352	0.02406	5.72875	-57.0923
5.72917	-3.94167	-1.85833	-0.00501	0.0401	0.04043	0.11305	-0.06174	-0.01102	0.02234	5.72917	-57.080
5.72958	0.36667	2.21867	-0.00514	0.04004	0.07726	0.14595	-0.01425	-0.00867	0.02031	5.72958	-57.0752
5.73	1.15	2.90933	-0.00694	0.03757	0.07552	0.1412	-0.01969	-0.00391	0.01734	5.73	-57.0667
5.73042	-0.40633	1.71867	-0.0071	0.03529	0.05687	0.11722	-0.04923	-0.0007	0.01687	5.73042	-57.0581
5.73083	2.7	0.125	-0.0052	0.03444	0.05328	0.10888	-0.05757	0.00091	0.01891	5.73083	-57.0453
5.73125	-0.01667	-1.15	-0.00514	0.03348	0.0556	0.1083	-0.05467	0.00234	0.01884	5.73125	-57.0411
5.73167	-4.25	-1.99167	-0.00443	0.03138	0.04819	0.09846	-0.06116	0.0067	0.01894	5.73167	-57.0539
5.73208	-4.4	-2.95833	-0.00488	0.0304	0.03174	0.07865	-0.08259	0.00883	0.01687	5.73208	-57.0752
5.7325	-5.00833	-4	-0.0054	0.03158	0.01552	0.05684	-0.10888	0.01	0.01219	5.7325	-57.0667
5.73292	-5.94167	-5.19167	-0.00423	0.03197	0.00486	0.03915	-0.1295	0.00891	0.01078	5.73292	-57.0581
5.73333	-6.8	-6.55	-0.00273	0.0304	0.00023	0.02792	-0.13854	0.00781	0.01547	5.73333	-57.0624
5.73375	-7.35	-7.33333	-0.00195	0.02813	0.00068	0.0249	-0.13942	0.00703	0.02	5.73375	-57.0667
5.73417	-7.59333	-7.49167	-0.00345	0.02305	0.00405	0.0271	-0.13274	0.00578	0.02320	5.73417	-57.0667
5.73458	-7.575	-7.53333	-0.00573	0.0179	0.00903	0.03104	-0.1229	0.00383	0.02703	5.73458	-57.0709
5.735	-6.925	-7.31667	-0.00625	0.01452	0.02305	0.0468	-0.10216	0.0018	0.02719	5.735	-57.0837
5.73542	-5.16667	-5.825	-0.00501	0.01315	0.05085	0.07969	-0.06556	-0.00172	0.02437	5.73542	-57.088
5.73583	-2.475	-2.875	-0.00378	0.01263	0.07263	0.11027	-0.03487	-0.0043	0.02062	5.73583	-57.0752
5.73625	-0.10833	-0.20833	-0.00345	0.01107	0.05664	0.10135	-0.05073	-0.00582	0.01875	5.73625	-57.0709
5.73667	-0.45	-0.33333	-0.00326	0.00984	0.04517	0.09047	-0.0686	-0.00687	0.01812	5.73667	-57.0837
5.73708	-0.85833	-0.20833	-0.0028	0.00858	0.05681	0.09552	-0.05016	-0.00977	0.01781	5.73708	-57.1008
5.7375	-10.825	-10.0333	-0.00458	0.00443	0.07135	0.12139	-0.03127	-0.01148	0.01734	5.7375	-57.1051
5.73792	-15.5917	-14.4	-0.00765	0.00163	0.0644	0.12058	-0.03857	-0.01258	0.01422	5.73792	-57.0965
5.73833	-16.9593	-15.8593	-0.00775	-0.00078	0.03982	0.10321	-0.07089	-0.01375	0.01297	5.73833	-57.0795
5.73875	-15.5667	-14.4083	-0.00658	-0.00124	0.0085	0.08027	-0.10772	-0.01641	0.01781	5.73875	-57.0837
5.73917	-13.1667	-12.1917	-0.00547	8.5E-05	-0.01471	0.06207	-0.13552	-0.01898	0.02016	5.73917	-57.1008
5.73958	-11.4417	-10.45	-0.00449	-6.5E-05	-0.0271	0.05421	-0.14931	-0.02055	0.02172	5.73958	-57.1008
5.74	-10.5093	-9.375	-0.00456	-0.00215	-0.02676	0.05963	-0.15325	-0.02203	0.02219	5.74	-57.0837
5.74042	-10.1083	-8.64167	-0.00527	-0.0028	-0.0212	0.05745	-0.14977	-0.02381	0.02172	5.74042	-57.0867
5.74083	-9.525	-8.14167	-0.00514	-0.00328	-0.01714	0.06533	-0.14143	-0.02582	0.01969	5.74083	-57.0624
5.74125	-9.1	-7.63333	-0.00501	-0.00508	-0.0117	0.07811	-0.12429	-0.02773	0.02125	5.74125	-57.0581
5.74167	-8.10833	-7.525	-0.0043	-0.00658	0.00602	0.10425	-0.09209	-0.02883	0.02234	5.74167	-57.0581
5.74208	-8.725	-8.06667	-0.00404	-0.00651	0.04355	0.14398	-0.04297	-0.03023	0.01875	5.74208	-57.0709
5.7425	-7.81667	-6.09167	-0.00417	-0.00619	0.07891	0.17919	-0.00490	-0.02891	0.01312	5.7425	-57.088
5.74292	-6.9	-5.39833	-0.0041	-0.00612	0.06672	0.17027	-0.02502	-0.02437	0.00853	5.74292	-57.1051
5.74333	-7.20833	-5.46667	-0.00488	-0.00558	0.04263	0.14238	-0.0822	-0.02078	0.01862	5.74333	-57.1051
5.74375	-8.4	-7.34167	-0.00551	-0.0041	0.03209	0.12464	-0.07853	-0.02008	0.01375	5.74375	-57.0837
5.74417	-13.0417	-10.0417	-0.00651	-0.00592	0.02919	0.11711	-0.07784	-0.01953	0.01828	5.74417	-57.0624
5.74458	-16.1583	-13.525	-0.00547	-0.00384	0.02212	0.10888	-0.08864	-0.01684	0.01781	5.74458	-57.0539
5.745	-15.8583	-13.2417	-0.00534	-0.00423	0.0088	0.09475	-0.10657	-0.01312	0.01859	5.745	-57.0581
5.74542	-11.2	-8.71667	-0.00547	-0.00137	-0.00486	0.07077	-0.12626	-0.01078	0.01844	5.74542	-57.0667
5.74583	-4.56667	-2.10333	-0.00605	0.00423	-0.01483	0.06417	-0.13865	-0.00852	0.01687	5.74583	-57.0752
5.74625	0.225	2.49167	-0.00592	0.00989	-0.01819	0.05458	-0.14317	-0.00422	0.01531	5.74625	-57.0937
5.74667	1.64167	3.65833	-0.00488	0.01293	-0.01239	0.05108	-0.14009	-0.00023	0.01547	5.74667	-57.098
5.74708	0.28333	2.45	-0.0041	0.01478	-0.0029	0.05384	-0.13182	-0.00187	0.01734	5.74708	-57.088
5.7475	-1.825	-0.40833	-0.00332	0.01803	0.0088	0.0622	-0.11456	0.00234	0.01812	5.7475	-57.0795
5.74792	-3.83333	-1.6	-0.00417	0.01979	0.02873	0.07893	-0.08734	0.00227	0.01891	5.74792	-57.0667
5.74833	-5.40833	-3.06667	-0.00547	0.01914	0.0629	0.10529	-0.04402	0.00203	0.02031	5.74833	-57.0581
5.74875	-6.2	-4.13333	-0.00514	0.01992	0.08525	0.12484	-0.01274	0.00148	0.02084	5.74875	-57.0667
5.74917	-6.26333	-5.025	-0.00482	0.02325	0.0685	0.1083	-0.03405	0.00281	0.01844	5.74917	-57.0752
5.74958	-6.35	-5.64167	-0.00488	0.02708	0.05525	0.09313	-0.05421	0.005	0.01703	5.74958	-57.0752
5.75	-6.58333	-6.58333	-0.00553	0.02891	0.06194	0.08558	-0.04888	0.00516	0.01422	5.75	-57.0837
5.75042	-7.19167	-6.43333	-0.00475	0.02898	0.08915	0.09695	-0.04077	0.00547	0.01203	5.75042	-57.088
5.75083	-8.04167	-8.85833	-0.00417	0.03088	0.06267	0.09502	-0.05085	0.00489	0.01547	5.75083	-57.0837
5.75125	-8.425	-7.30833	-0.00371	0.0321	0.04089	0.06579	-0.08062	0.00367	0.02187	5.75125	-57.0837
5.75167	-7.85833	-7.325	-0.0043	0.03327	0.01471	0.04541	-0.11525	0.00328	0.02484	5.75167	-57.0837
5.75208	-5.975	-5.81667	-0.00586	0.03333	-0.00463	0.02988	-0.13981	0.00187	0.02281	5.75208	-57.0837
5.7525	-3.025	-2.69167	-0.00547	0.03419	-0.01274	0.02525	-0.14896	0.00016	0.01806	5.7525	-57.0923
5.75292	-0.525	-0.15	-0.00397	0.03548	-0.01147	0.02638	-0.14711	-0.00195	0.01844	5.75292	-57.0923
5.75333	-0.88167	-0.4	-0.00332	0.03584	-0.00556	0.03452	-0.14039	-0.00477	0.01812	5.75333	-57.0795
5.75375	-4.875	-4.44167	-0.00443	0.03464	0.00174	0.04274	-0.13089	-0.00646	0.01891	5.75375	-57.0667
5.75417	-11.3167	-10.3583	-0.00521	0.03242	0.01378	0.05898	-0.11143	-0.00787	0.01787	5.75417	-57.0539
5.75458	-16.1093	-14.825	-0.00527	0.03255	0.03788	0.09895	-0.0724	-0.01148	0.0175	5.75458	-57.0624
5.755	-17.2593	-15.9417	-0.00553	0.0334	0.06927	0.1324	-0.02317	-0.01805	0.01806	5.755	-57.0837
5.75542	-15.6917	-14.1	-0.00592	0.03346	0.06857	0.14479	-0.01413	-0.02156	0.02234	5.75542	-57.088
5.75583	-13.583	-11.3833	-0.00566	0.03385	0.04587	0.12614	-0.03718	-0.02287	0.02344	5.75583	-57.0795
5.75625	-12.0417	-9.64167	-0.00508	0.03288	0.03939	0.11838	-0.04749	-0.02406	0.02109	5.75625	-57.0709
5.75667	-11.1667	-9.14167	-0.00469	0.03132	0.0388	0.12325	-0.04785	-0.02521	0.01891	5.75667	-57.0752
5.75708	-10.3667	-8.8	-0.00443	0.0291	0.02838	0.12081	-0.05887	-0.02602	0.01841	5.75708	-57.0837
5.7575	-8.58167	-8.25	-0.00443	0.02878	0.01042	0.10842	-0.07833	-0.02608	0.01856	5.7575	-57.088
5.75792	-8.29167	-7.68333	-0.00508	0.02378	-0.0086	0.09151	-0.09869	-0.02602	0.01734	5.75792	-57.088
5.75833	-8.25	-7.08333	-0.00547	0.02005	-0.01876	0.07714	-0.11927	-0.02414	0.01578	5.75833	-57.0837
5.75875	-9.25	-6.45	-0.0056	0.01621	-0.0271	0.06889	-0.13101	-0.02289	0.01391	5.75875	-57.0795
5.75917	-8.8	-5.90833	-0.0056	0.01283	-0.03012	0.06417	-0.13402	-0.02273	0.01719	5.75917	-57.088
5.75958	-7.85833	-5.21667	-0.00553	0.01016	-0.02898	0.06718	-0.128	-0.02227	0.02084	5.75958	-57.0837
5.76	-7.375	-6.29167	-0.00449	0.00931	-0.02004	0.07564	-0.11864	-0.02172	0.02084	5.76	-57.0795
5.76042	-6.66667	-5.975	-0.00397	0.00814	-0.0051	0.09162	-0.09765	-0.02078	0.01828	5.76042	-57.0667
5.76083	-11.475	-9.58333	-0.00469	0.00671	0.02039	0.11595	-0.06802	-0.02047	0.01825	5.76083	-57.0624
5.76125	-14.2917	-12.0667	-0.00599	0.00328	0.04863	0.14108	-0.03104	-0.02	0.01825	5.76125	-57.0667
5.76167	-14.65	-12.3583	-0.00645	-0.00033	0.04321	0.13031	-0.03938	-0.01687	0.01719	5.76167	-57.0667
5.76208	-11.05	-8.875	-0.00812	-0.00241	0.02803	0.10587	-0.06035	-0.01273	0.01875	5.76208	-57.0624
5.7625	-5.04167	-3.08667	-0.0056	-0.00475	0.03894	0.10781	-0.048	-0.00888	0.02018	5.7625	-57.0581
5.76292	-0.275	1.45933	-0.00632	-0.00592							

Appendix D

Data from Dynamic Test Panel SCI2

5.78917	-2.85	-3.39167	-0.00573	0.00169	0.05004	0.07911	-0.05881	-0.00305	0.01875	5.78917	-57.0795
5.78958	-0.325	-0.44167	-0.0054	0.00234	0.04413	0.07575	-0.08826	-0.00398	0.01859	5.78958	-57.0985
5.77042	-4.25	-3.18667	-0.00599	0.00651	0.01785	0.08408	-0.09182	-0.00648	0.01703	5.77042	-57.0837
5.77083	-10.35	-8.93333	-0.00812	0.01042	0.00116	0.05155	-0.10954	-0.00711	0.01734	5.77083	-57.0752
5.77125	-15.125	-13.4833	-0.00632	0.01408	-0.01124	0.04158	-0.12128	-0.00906	0.01859	5.77125	-57.0837
5.77167	-18.85	-15.2083	-0.00645	0.01621	-0.01982	0.03799	-0.12765	-0.01234	0.01937	5.77167	-57.0923
5.77208	-15.7167	-14.275	-0.0054	0.01634	-0.0205	0.04205	-0.12718	-0.01648	0.01844	5.77208	-57.0923
5.7725	-13.325	-12.2833	-0.00573	0.01654	-0.01714	0.05201	-0.12255	-0.01945	0.01703	5.7725	-57.0795
5.77292	-11.25	-10.4417	-0.00716	0.01921	-0.00707	0.06776	-0.11074	-0.02125	0.01631	5.77292	-57.0795
5.77333	-10.0083	-9.3	-0.00781	0.02207	0.011	0.08931	-0.08608	-0.0243	0.0125	5.77333	-57.0752
5.77375	-9.33333	-8.7	-0.00871	0.0248	0.04019	0.12139	-0.04506	-0.02789	0.01484	5.77375	-57.0687
5.77417	-8.05	-8.23333	-0.00482	0.02665	0.06973	0.15558	-0.0051	-0.03016	0.01853	5.77417	-57.0687
5.77458	-8.78333	-7.55	-0.0043	0.03171	0.08035	0.15278	-0.01402	-0.02875	0.02203	5.77458	-57.0752
5.775	-8.10833	-6.84167	-0.00443	0.03398	0.03981	0.13576	-0.03948	-0.02766	0.02141	5.775	-57.0752
5.77542	-7.275	-5.875	-0.00489	0.03477	0.02683	0.13703	-0.03417	-0.02952	0.02016	5.77542	-57.0795
5.77583	-6.88333	-5.425	-0.00482	0.03633	0.04158	0.14444	-0.02595	-0.02773	0.01806	5.77583	-57.0752
5.77625	-7.025	-5.85	-0.00558	0.03685	0.03521	0.13773	-0.03568	-0.02523	0.01662	5.77625	-57.0824
5.77667	-7.86667	-6.33333	-0.00814	0.03542	0.01748	0.1156	-0.06278	-0.0218	0.01172	5.77667	-57.0581
5.77708	-9.925	-8.09333	-0.00755	0.03301	-0.00313	0.0895	-0.0922	-0.01789	0.01281	5.77708	-57.0687
5.7775	-12.2333	-10.8	-0.00638	0.03197	-0.019	0.08889	-0.11282	-0.01437	0.01828	5.7775	-57.0752
5.77792	-15.725	-12.7083	-0.00599	0.03177	-0.02919	0.06676	-0.12371	-0.01148	0.02188	5.77792	-57.0752
5.77833	-16.9833	-12.175	-0.00729	0.03218	0.03452	0.0949	-0.13054	-0.01847	0.01864	5.77833	-57.0752
5.77875	-10.45	-8.34167	-0.00677	0.03405	-0.03162	0.04772	-0.12892	-0.01082	0.01872	5.77875	-57.0752
5.77917	-3.94167	-2.48333	-0.00488	0.03483	-0.0205	0.0512	-0.11873	-0.01047	0.01516	5.77917	-57.0637
5.77958	0.8	2.05933	-0.00475	0.03359	-0.00489	0.05915	-0.10066	-0.00759	0.01656	5.77958	-57.0985
5.78	1.80833	3.20833	-0.00592	0.02988	0.01853	0.07657	-0.06741	-0.00398	0.01937	5.78	-57.0923
5.78042	0.275	1.84167	-0.00586	0.02885	0.05444	0.11004	-0.01891	-0.02026	0.02312	5.78042	-57.0923
5.78083	-2.08333	-0.31667	-0.00586	0.02604	0.07508	0.12973	0.00985	-0.00172	0.02219	5.78083	-57.0795
5.78125	-3.83333	-2.14167	-0.00645	0.02493	0.0651	0.1156	-0.00922	0.00148	0.0175	5.78125	-57.0581
5.78167	-4.7	-3.33333	-0.00632	0.02385	0.03587	0.10031	-0.02583	0.00481	0.01841	5.78167	-57.0539
5.78208	-4.96667	-4.01667	-0.0054	0.02378	0.0534	0.09301	-0.02919	0.00687	0.01719	5.78208	-57.0687
5.7825	-5.24167	-4.49167	-0.00378	0.02327	0.04599	0.08016	-0.03788	0.00906	0.01531	5.7825	-57.0637
5.78292	-5.075	-5.03333	-0.00319	0.02005	0.02942	0.08	-0.06023	0.01023	0.01408	5.78292	-57.0923
5.78333	-6.51667	-5.69333	-0.00371	0.0153	0.01251	0.03973	-0.09757	0.00977	0.01375	5.78333	-57.0637
5.78375	-7.33333	-6.26667	-0.00489	0.01191	-0.00151	0.0249	-0.10950	0.00758	0.01297	5.78375	-57.0752
5.78417	-7.85	-6.59333	-0.00612	0.00905	-0.00985	0.01584	-0.12278	0.0068	0.01672	5.78417	-57.0752
5.78458	-8.15	-6.725	-0.00638	0.00845	-0.01193	0.01237	-0.12889	0.00625	0.02266	5.78458	-57.088
5.785	-7.98333	-6.43333	-0.00579	0.00527	-0.01019	0.01425	-0.12872	0.00234	0.02406	5.785	-57.1051
5.78542	-8.025	-6.79167	-0.00508	0.00443	-0.00591	0.02178	-0.11734	-0.00109	0.02359	5.78542	-57.1051
5.78583	-2.46667	-1.95	-0.00488	0.00241	0.00591	0.03637	-0.09985	-0.00227	0.02219	5.78583	-57.1008
5.78625	0.58333	0.25	-0.00508	0.00078	0.02537	0.06023	-0.07135	-0.0032	0.02125	5.78625	-57.1008
5.78667	0.85833	-0.19167	-0.00599	-0.00143	0.05502	0.09417	-0.03116	-0.00602	0.01804	5.78667	-57.1008
5.78708	-3.45	-3.94167	-0.00658	-0.00423	0.06371	0.109	-0.01811	-0.00958	0.01705	5.78708	-57.0923
5.7875	-9.91667	-9.20833	-0.00664	-0.00599	0.06108	0.09930	-0.03707	-0.01109	0.01829	5.7875	-57.0795
5.78792	-14.725	-13.475	-0.00736	-0.00729	0.0527	0.10251	-0.03556	-0.01482	0.02070	5.78792	-57.0709
5.78833	-18.225	-14.9833	-0.00782	-0.00749	0.06384	0.11908	-0.01942	-0.01897	0.02047	5.78833	-57.0687
5.78875	-15.0083	-13.7583	-0.00638	-0.00547	0.05989	0.12603	-0.0168	-0.02125	0.01809	5.78875	-57.0752
5.78917	-12.85	-11.85	-0.00573	-0.00462	0.03718	0.10958	-0.04077	-0.02203	0.01422	5.78917	-57.0923
5.78958	-11.0667	-10.0083	-0.0056	-0.00605	0.00857	0.08352	-0.07506	-0.02141	0.01662	5.78958	-57.1008
5.79	-10.1917	-9.18667	-0.00501	-0.00703	-0.01517	0.08359	-0.10784	-0.02088	0.01797	5.79	-57.0923
5.79042	-10.25	-8.93333	-0.00462	-0.00664	-0.03035	0.05409	-0.1295	-0.02133	0.02047	5.79042	-57.0752
5.79083	-10.35	-8.74167	-0.00456	-0.00716	-0.03683	0.0527	-0.14004	-0.02287	0.02219	5.79083	-57.0752
5.79125	-9.925	-8.18667	-0.00521	-0.00833	-0.03637	0.05502	-0.14004	-0.02482	0.02172	5.79125	-57.0795
5.79167	-9.05833	-7.16	-0.0071	-0.00723	-0.03324	0.05973	-0.13229	-0.02586	0.02203	5.79167	-57.0923
5.79208	-7.93333	-6.075	-0.00697	-0.00247	-0.02629	0.08798	-0.11899	-0.02625	0.02156	5.79208	-57.0923
5.7925	-7.00833	-5.375	-0.00508	0.00299	-0.01008	0.08995	-0.09232	-0.02586	0.01869	5.7925	-57.0837
5.79292	-6.75833	-5.16833	-0.00221	0.0054	0.01894	0.11491	-0.05502	-0.02547	0.01703	5.79292	-57.0795
5.79333	-7.39167	-5.40833	-0.00189	0.0054	0.05942	0.15325	-0.00533	-0.02684	0.01856	5.79333	-57.0752
5.79375	-8.36667	-6.925	-0.00456	0.00365	0.06992	0.16251	0.00822	-0.0243	0.02031	5.79375	-57.0687
5.79417	-12.35	-8.7	-0.00671	0.00378	0.04599	0.13634	-0.02363	-0.01719	0.0225	5.79417	-57.0581
5.79458	-15.025	-12.1583	-0.00716	0.00723	0.02985	0.11398	-0.04691	-0.01258	0.02047	5.79458	-57.0581
5.795	-14.7083	-11.9167	-0.00632	0.01009	0.0249	0.10309	-0.05294	-0.0125	0.01872	5.795	-57.0624
5.79542	-10.2417	-8.24167	-0.0058	0.01224	0.02015	0.09287	-0.05931	-0.01344	0.01344	5.79542	-57.0709
5.79583	-3.69333	-2.16667	-0.00592	0.01536	0.0117	0.08027	-0.07274	-0.01039	0.01809	5.79583	-57.0985
5.79625	1.05	1.89333	-0.00596	0.01829	0.00081	0.06589	-0.08985	-0.00492	0.02141	5.79625	-57.1008
5.79667	1.725	2.98333	-0.0056	0.02064	-0.00996	0.04819	-0.10881	-0.00125	0.02406	5.79667	-57.1008
5.79708	-0.275	1.45833	-0.00449	0.02298	-0.01645	0.03579	-0.11757	0.00211	0.02234	5.79708	-57.0795
5.7975	-2.46667	-0.74167	-0.00345	0.02715	-0.01726	0.02907	-0.11931	0.00477	0.01766	5.7975	-57.0709
5.79792	-3.8	-2.36667	-0.00395	0.03132	-0.01378	0.02897	-0.11444	0.00539	0.01625	5.79792	-57.0709
5.79833	-4.33333	-3.03333	-0.0041	0.03405	-0.00637	0.02965	-0.10159	0.0043	0.01869	5.79833	-57.0795
5.79875	-4.70833	-3.53333	-0.00384	0.03542	0.0085	0.04355	-0.07714	0.00359	0.02547	5.79875	-57.0709
5.79917	-5.38333	-4.33333	-0.00404	0.03542	0.03788	0.08799	-0.04089	0.00281	0.02867	5.79917	-57.0824
5.79958	-6.20833	-5.10833	-0.00501	0.03498	0.07425	0.09882	0.00232	0.00281	0.02453	5.79958	-57.0687
5.8	-6.81667	-5.825	-0.00579	0.03457	0.07807	0.10379	0.00579	0.00508	0.02125	5.8	-57.088
5.80042	-7.15833	-6	-0.00527	0.03535	0.05977	0.08352	-0.0205	0.00719	0.02016	5.80042	-57.088
5.80083	-7.49167	-6.025	-0.00378	0.03613	0.05572	0.0793	-0.02826	0.00578	0.01884	5.80083	-57.0837
5.80125	-7.525	-6.24167	-0.00358	0.03777	0.0622	0.08684	-0.01876	0.00336	0.02	5.80125	-57.0837
5.80167	-6.99167	-6.25	-0.00521	0.03874	0.06046	0.0878	-0.02015	0.00016	0.02078	5.80167	-57.088
5.80208	-5.26667	-5.24167	-0.00445	0.03928	0.04367	0.0724	-0.04193	-0.00117	0.02125	5.80208	-57.088
5.8025	-4.45	-3.00833	-0.00579	0.03997	0.01876	0.04823	-0.07147	-0.00102	0.02141	5.8025	-57.088
5.80292	-0.03333	-0.58333	-0.00534	0.03919	-0.00232	0.03232	-0.09672	-0.00242	0.02219	5.80292	-57.0985
5.80333	-0.00833	-0.2	-0.00568	0.03737	-0.0161	0.02328	-0.11271	-0.00414	0.02094	5.80333	-57.088
5.80375	-3.74167	-3.425	-0.00618	0.0349	-0.02548	0.01853	-0.12118	-0.00437	0.01844	5.80375	-57.0837
5.80417	-9.80833	-8.19333	-0.00579	0.03294	-0.02792	0.02082	-0.12429	-0.00469	0.01797	5.80417	-57.098
5.80458	-14.8917	-13.9583	-0.0041	0.03099	-0.02409	0.02788	-0.11989	-			

Appendix D Data from Dynamic Test Panel SCI2

5.81042	-8.95	-8.875	-0.00489	-0.00117	-0.03707	0.05375	-0.12174	-0.01797	0.01828	5.81042	-57.0539
5.81083	-11.8333	-8.5	-0.00417	-0.00247	-0.03104	0.05896	-0.11595	-0.01547	0.01891	5.81083	-57.0539
5.81125	-14.135	-11.9833	-0.00287	-0.00241	-0.01853	0.06811	-0.10135	-0.01547	0.02187	5.81125	-57.0709
5.81167	-14.1333	-11.8333	-0.00208	-0.0028	-0.00185	0.08097	-0.07786	-0.01841	0.02547	5.81167	-57.0823
5.81208	-9.91667	-8.29333	-0.00241	-0.0043	0.02757	0.10576	-0.04089	-0.01633	0.02609	5.81208	-57.1008
5.8125	-3.59167	-2.825	-0.00226	-0.00851	0.04885	0.12393	-0.01598	-0.01393	0.0225	5.8125	-57.988
5.81282	1.21667	1.70933	-0.00492	-0.00972	0.02544	0.10541	-0.03765	-0.00734	0.01797	5.81282	-57.0709
5.81333	2.91667	2.71667	-0.00534	0.0089	0.02355	0.09838	-0.04877	-0.00125	0.01344	5.81333	-57.0624
5.81375	0.55	1.3	-0.00436	-0.01048	0.05108	0.09776	-0.02853	0.00034	0.01422	5.81375	-57.0624
5.81417	-1.83333	-0.70933	-0.00352	-0.00918	0.06371	0.10899	-0.00753	0.0007	0.01781	5.81417	-57.0539
5.81458	-3.48333	-2.4	-0.00378	-0.00592	0.05294	0.09938	-0.01953	0.00187	0.01869	5.81458	-57.0498
5.815	-4.20833	-3.53333	-0.00501	-0.00345	0.02722	0.07367	-0.0534	0.00477	0.02031	5.815	-57.0581
5.81542	-4.475	-4.05833	-0.00534	-0.00078	0.00232	0.0439	-0.09128	0.00727	0.02078	5.81542	-57.0687
5.81583	-4.7	-4.45833	-0.00482	-0.00038	-0.01552	0.01834	-0.11514	0.00891	0.02084	5.81583	-57.0752
5.81625	-5.24167	-5.03333	-0.00443	-0.00189	-0.0234	0.0086	-0.12417	0.00894	0.02156	5.81625	-57.0752
5.81667	-6.325	-6.03333	-0.00458	-0.00265	-0.02444	0.00243	-0.12814	0.00961	0.02107	5.81667	-57.0627
5.81708	-7.42333	-6.725	-0.00495	-0.00458	-0.02015	0.00488	-0.12464	0.00836	0.02156	5.81708	-57.088
5.8175	-7.95833	-6.775	-0.00385	-0.00345	-0.01274	0.01135	-0.11514	0.00594	0.02125	5.8175	-57.0795
5.81792	-8.05	-8.89167	-0.00371	-0.00048	-0.00151	0.02212	-0.09568	0.00211	0.01837	5.81792	-57.0752
5.81833	-7.50833	-6.85833	-0.0041	0.00339	0.02189	0.04494	-0.06174	-0.00062	0.02016	5.81833	-57.0837
5.81875	-5.84167	-5.75	-0.00423	0.00756	0.06151	0.08803	-0.0073	-0.00281	0.02141	5.81875	-57.0985
5.81917	-2.96333	-3.075	-0.00371	0.01185	0.08711	0.1207	0.02886	-0.00609	0.02	5.81917	-57.1093
5.81958	-4.35	-3.18667	-0.00293	0.01458	0.06789	0.10437	0.0044	-0.00895	0.01872	5.81958	-57.1093
5.82	-0.225	0.08667	-0.00228	0.0153	0.03904	0.07688	-0.03012	-0.0057	0.01582	5.82	-57.1008
5.82042	-4.05	-3.18333	-0.00384	0.01585	0.02478	0.06765	-0.04332	-0.00672	0.0175	5.82042	-57.0985
5.82083	-10.3667	-8.70933	-0.00618	0.01777	0.01946	0.06927	-0.04668	-0.00891	0.01853	5.82083	-57.1008
5.82125	-15.1333	-13.125	-0.00716	0.01908	0.01274	0.06569	-0.05653	-0.01094	0.02094	5.82125	-57.0985
5.82167	-16.7167	-14.8083	-0.00684	0.02135	0.00058	0.0578	-0.07274	-0.01281	0.02344	5.82167	-57.0752
5.82208	-16.7083	-13.775	-0.00755	0.02552	-0.01438	0.04819	-0.09894	-0.01516	0.02266	5.82208	-57.0687
5.8225	-13.225	-12.2167	-0.00748	0.02878	-0.02676	0.04112	-0.09986	-0.01781	0.02312	5.8225	-57.0709
5.82292	-11.1417	-10.8867	-0.00618	0.02923	0.03451	0.03986	-0.10484	-0.02117	0.02489	5.82292	-57.0752
5.82333	-9.55833	-8.575	-0.00475	0.02858	-0.02919	0.04781	-0.10483	-0.02359	0.02391	5.82333	-57.0795
5.82375	-8.05833	-8.575	-0.00482	0.02975	-0.02317	0.05894	-0.0995	-0.02516	0.02234	5.82375	-57.0823
5.82417	-8.41667	-7.775	-0.00534	0.03089	-0.01541	0.07147	-0.09433	-0.02641	0.01812	5.82417	-57.1008
5.82458	-7.74167	-7.125	-0.0056	0.03289	0.00127	0.09023	-0.05409	-0.02697	0.01422	5.82458	-57.0985
5.825	-7.25933	-6.73333	-0.00586	0.03679	0.03127	0.12408	-0.00486	-0.02612	0.01579	5.825	-57.0823
5.82542	-7.20833	-6.575	-0.00586	0.04141	0.04911	0.14942	0.02583	-0.02888	0.01828	5.82542	-57.0837
5.82583	-6.96667	-6.13333	-0.00573	0.04318	0.03208	0.13552	0.0029	-0.02672	0.01859	5.82583	-57.0795
5.82625	-6.8	-6.44167	-0.00586	0.04089	0.01795	0.11942	-0.01819	-0.02538	0.02281	5.82625	-57.0709
5.82667	-7.44167	-5.13333	-0.00547	0.03802	0.02169	0.12128	-0.01332	-0.02422	0.02375	5.82667	-57.0709
5.82708	-8.63333	-6.575	-0.00475	0.03548	0.02676	0.12267	-0.00753	-0.02039	0.02031	5.82708	-57.0752
5.8275	-13.025	-8.05833	-0.00448	0.0332	0.01853	0.11108	-0.01981	-0.01672	0.01562	5.8275	-57.0752
5.82792	-15.95	-13.0417	-0.00371	0.0321	0.00046	0.08977	-0.04881	-0.01381	0.01562	5.82792	-57.0687
5.82833	-15.7167	-13.2583	-0.00378	0.03151	-0.019	0.08753	-0.0781	-0.01218	0.01837	5.82833	-57.0624
5.82875	-10.9933	-9.175	-0.00488	0.03105	-0.03185	0.04953	-0.09707	-0.01117	0.02141	5.82875	-57.0795
5.82917	-4.06667	-2.9	-0.00495	0.02809	-0.03895	0.03407	-0.10622	-0.00814	0.02125	5.82917	-57.0985
5.82958	0.93333	1.78333	-0.00345	0.02871	-0.03934	0.02884	-0.11939	-0.00516	0.02047	5.82958	-57.1061
5.83	2.06667	2.95833	-0.0028	0.0285	-0.03579	0.02687	-0.11097	-0.00076	0.01806	5.83	-57.0985
5.83042	0.5	1.54167	-0.00288	0.02409	-0.02722	0.03093	-0.10228	0.00164	0.01703	5.83042	-57.0985
5.83083	-1.73333	-0.325	-0.00352	0.02122	-0.0088	0.04332	-0.07946	0.00312	0.01766	5.83083	-57.0923
5.83125	-3.275	-1.725	-0.00527	0.01849	0.02282	0.06884	-0.03986	0.00273	0.02172	5.83125	-57.0795
5.83167	-4.05	-2.75	-0.00579	0.01589	0.06023	0.09873	0.00741	0.00109	0.02437	5.83167	-57.0581
5.83208	-4.45	-3.36667	-0.00553	0.0151	0.06359	0.10425	0.01077	0.0025	0.02156	5.83208	-57.0539
5.8325	-4.725	-4.1867	-0.00547	0.01529	0.04448	0.08082	-0.01807	0.0057	0.01703	5.8325	-57.0752
5.83292	-5.04167	-4.19167	-0.00532	0.01302	0.03934	0.08911	-0.03093	0.0075	0.01562	5.83292	-57.0795
5.83333	-5.05	-4.25	-0.00651	0.0097	0.04193	0.0895	-0.02757	0.00742	0.01859	5.83333	-57.0752
5.83375	-7.19167	-6.63333	-0.00592	0.0056	0.03985	0.06895	-0.03127	0.00648	0.02266	5.83375	-57.0752
5.83417	-8.01667	-6.6	-0.00534	0.00182	0.02571	0.05294	-0.05108	0.00547	0.0225	5.83417	-57.0837
5.83458	-8.58333	-7.11667	-0.00534	-0.00124	0.0044	0.0329	-0.07738	0.00508	0.02109	5.83458	-57.088
5.835	-9.13333	-7.60933	-0.0056	-0.00371	-0.01239	0.0139	-0.09811	0.00406	0.02	5.835	-57.0823
5.83542	-9.925	-8.4	-0.00482	-0.00488	-0.02073	0.0088	-0.10935	0.00242	0.02016	5.83542	-57.1093
5.83583	-2.8	-3.65833	-0.00404	-0.00339	-0.02395	0.01038	-0.11284	-0.00023	0.02094	5.83583	-57.1136
5.83625	0.275	-1.05	-0.00475	-0.00254	-0.02201	0.01888	-0.11201	-0.00273	0.02172	5.83625	-57.1008
5.83667	0.00333	-0.78333	-0.00553	-0.00345	-0.01587	0.02915	-0.10332	-0.00477	0.02156	5.83667	-57.0837
5.83708	-4.39333	-4.09167	-0.00449	-0.00397	-0.00301	0.04355	-0.09263	-0.00758	0.02187	5.83708	-57.0795
5.8375	-10.9593	-9.75933	-0.00358	-0.00391	0.01934	0.06869	-0.04981	-0.01008	0.02187	5.8375	-57.0837
5.83792	-15.7167	-14.2833	-0.00469	-0.00488	0.04633	0.09804	-0.01193	-0.01398	0.02381	5.83792	-57.088
5.83833	-16.775	-15.3917	-0.00632	-0.00697	0.04205	0.10147	-0.01781	0.01	0.025	5.83833	-57.0837
5.83875	-15.3667	-14.1333	-0.00592	-0.00716	0.02514	0.0907	-0.04019	-0.02117	0.02609	5.83875	-57.0795
5.83917	-13.0417	-12.3417	-0.00534	-0.00573	0.03174	0.10112	-0.02977	-0.02228	0.02119	5.83917	-57.0795
5.83958	-11.4417	-11.2333	-0.00729	-0.00365	0.04784	0.12023	-0.00802	-0.02414	0.02609	5.83958	-57.0923
5.84	-10.5867	-10.3083	-0.00827	-0.00247	0.04681	0.12429	-0.00382	-0.02445	0.02172	5.84	-57.1093
5.84042	-10.2417	-9.18333	-0.00638	-0.00288	0.02629	0.1112	-0.02884	-0.02422	0.01872	5.84042	-57.1136
5.84083	-9.83333	-7.91667	-0.00443	-0.00143	-0.0028	0.08734	-0.06707	-0.02523	0.01437	5.84083	-57.1008
5.84125	-9.06667	-6.85833	-0.00397	0.00158	-0.02938	0.06637	-0.10135	-0.02586	0.01437	5.84125	-57.0837
5.84167	-8.23333	-6.29833	-0.00534	0.00319	-0.04344	0.05433	-0.12267	-0.02469	0.01734	5.84167	-57.0752
5.84208	-7.89167	-6.11667	-0.00729	0.00438	-0.04958	0.05802	-0.12684	-0.02336	0.01822	5.84208	-57.0795
5.8425	-7.28333	-5.95833	-0.00612	0.00768	-0.04785	0.05156	-0.12055	-0.02258	0.01844	5.8425	-57.0923
5.84292	-7	-5.68333	-0.00397	0.01278	-0.04112	0.05548	-0.11062	-0.02141	0.01786	5.84292	-57.0837
5.84333	-7.16667	-5.64167	-0.00365	0.01771	-0.02826	0.06209	-0.08927	-0.02108	0.01869	5.84333	-57.0709
5.84375	-8.86667	-6.825	-0.00385	0.02038	-0.00789	0.07833	-0.07888	-0.02211	0.02359	5.84375	-57.0752
5.84417	-12.0333	-9.30333	-0.00391	0.02057	0.02467	0.10622	-0.0351	-0.02273	0.02594	5.84417	-57.0795
5.84458	-15.0083	-11.925	-0.00482	0.02181	0.06232	0.14607	0.0212	-0.02218	0.02841	5.84458	-57.0752
5.845	-15.1667	-12.1583	-0.00534	0.02402	0.08243	0.14873	0.02757	-0.01781	0.02589	5.845	-57.0752
5.84542	-10										

Appendix D Data from Dynamic Test Panel SCI2

5.85167	89902.9	89902.9	-12.8309	2.79557	-0.96559	-2.84355	-2.84998	-0.02727	9.93141	5.85187	-57.3184
5.85208	89902.9	89902.9	-24.3292	2.0873	0.16587	-2.37007	0.83952	-0.04195	11.5209	5.85208	-57.2544
5.85256	89902.9	89902.9	-27.8232	0.75664	1.2005	-1.15045	0.24626	-0.05852	12.9784	5.85256	-57.2208
5.85292	89902.9	89902.9	-20.3498	1.4627	2.28307	0.49218	3.41268	-0.07608	14.2456	5.85292	-57.2075
5.85333	89902.9	89902.9	-5.44219	2.59753	3.25225	1.87698	8.00099	-0.09586	15.3602	5.85333	-57.1891
5.85375	89902.9	89902.9	7.5403	1.84468	3.8054	2.67085	11.9272	-0.11719	16.432	5.85375	-57.1435
5.85417	89902.9	89902.9	9.73112	1.14188	3.63056	2.90348	15.2389	-0.1382	17.539	5.85417	-57.1392
5.85458	89902.9	89902.9	5.33704	2.30293	2.90323	3.09731	21.2459	0.14466	18.6877	5.85458	-57.152
5.855	89902.9	89902.9	0.40345	3.83828	0.52964	3.43515	24.861	-0.10437	19.8484	5.855	-57.1477
5.85542	89902.9	89902.9	-3.94427	4.35814	-0.83933	3.44141	23.1273	0.00633	20.9856	5.85542	-57.1349
5.85583	89902.9	89902.9	-6.211	4.25977	-1.24521	2.92954	20.3009	0.17906	22.095	5.85583	-57.1284
5.85625	89902.9	89902.9	-3.41849	4.13431	-0.82103	1.88113	17.9944	0.38281	23.1844	5.85625	-57.1093
5.85667	89902.9	89902.9	0.37259	3.9252	-0.06313	0.76323	14.4376	0.58922	24.2722	5.85667	-57.0795
5.85708	89902.9	89902.9	-2.88828	3.73802	0.83226	0.15823	8.80432	0.78211	25.3766	5.85708	-57.0411
5.8575	89902.9	89902.9	-8.80978	4.15892	1.75385	0.29558	8.92164	1.00125	26.4808	5.8575	-57.0227
5.85792	89902.9	89902.9	-10.2531	5.31204	2.44937	1.11015	9.82905	1.2269	27.5394	5.85792	-56.9956
5.85833	89902.9	89902.9	-5.70195	6.32715	2.68938	2.54532	13.3484	1.46062	28.5162	5.85833	-56.9984
5.85875	89902.9	89902.9	-1.87435	6.38061	2.46331	4.04397	16.7375	1.69184	29.4341	5.85875	-57.0283
5.85917	89902.9	89902.9	-1.30879	5.93988	2.07828	5.13408	18.267	1.91387	30.3437	5.85917	-57.0453
5.85958	89902.9	89902.9	-2.65977	4.40319	1.74236	5.53069	19.4667	1.22666	31.2837	5.85958	-57.0453
5.86	89902.9	89902.9	-2.89187	2.82741	1.57788	4.98153	20.1118	2.32039	32.2319	5.86	-57.0453
5.86042	89902.9	89902.9	-3.09928	1.25872	1.51811	3.3982	19.0989	2.50867	33.1364	5.86042	-57.0411
5.86093	89902.9	89902.9	-5.71949	0.39122	1.44039	1.10713	17.6996	2.89844	33.9792	5.86093	-57.0411
5.86125	89902.9	89902.9	-6.50111	0.44883	1.18799	-1.0681	17.8173	2.98552	34.7736	5.86125	-57.0498
5.86167	89902.9	89902.9	-6.25267	1.2803	0.71701	-2.33208	18.0437	3.03547	35.5302	5.86167	-57.0539
5.86208	89902.9	89902.9	-6.25625	2.51556	0.12406	-2.3957	20.1369	3.20219	36.2455	5.86208	-57.0496
5.8625	89902.9	89902.9	-6.53548	3.63249	-0.35375	-1.38992	21.2105	3.36258	36.9233	5.8625	-57.0453
5.86292	89902.9	89902.9	-6.28001	4.3778	-0.5553	0.15556	22.6813	3.51836	37.5666	5.86292	-57.0411
5.86333	89902.9	89902.9	-5.83744	5.01992	-0.43148	1.83318	23.7817	3.68652	38.1808	5.86333	-57.0325
5.86375	89902.9	89902.9	-5.21126	5.87389	-0.08792	3.37098	23.9457	3.81528	38.7731	5.86375	-57.0112
5.86417	89902.9	89902.9	-4.85958	6.72292	0.41688	4.55422	23.3198	3.95258	39.3541	5.86417	-57.0027
5.86458	89902.9	89902.9	-3.91335	6.96165	1.09312	5.39841	22.720	4.08281	39.9195	5.86458	-57.0155
5.865	89902.9	89902.9	-3.80215	6.32578	1.82959	5.98499	21.7228	4.20586	40.448	5.865	-57.0197
5.86542	89902.9	89902.9	-3.53184	5.01847	2.38888	6.99489	20.0058	4.32477	40.9266	5.86542	-57.024
5.86583	89902.9	89902.9	-3.42214	3.3	2.60683	6.70549	19.0283	4.36325	41.3634	5.86583	-57.0368
5.86625	89902.9	89902.9	-3.85001	1.51471	2.4854	6.74195	16.3012	4.53906	41.7716	5.86625	-57.0325
5.86667	89902.9	89902.9	-5.48288	0.38159	2.14917	6.27654	15.2206	4.83414	42.1583	5.86667	-57.0112
5.86708	89902.9	89902.9	-7.09453	0.24642	1.85009	5.19316	15.5914	4.72975	42.5294	5.86708	-56.9941
5.8675	89902.9	89902.9	-5.9923	0.64134	1.82503	2.7347	17.8458	4.80625	42.8941	5.8675	-56.9941
5.86792	89902.9	89902.9	-3.71687	0.91471	1.44155	2.48069	20.0704	4.87703	43.2424	5.86792	-57.0027
5.86833	89902.9	89902.9	-2.87305	1.15775	1.80111	1.92457	21.3936	4.93781	43.5164	5.86833	-57.0089
5.86875	89902.9	89902.9	-3.2429	1.72617	0.78326	2.1682	21.1874	4.98482	43.7162	5.86875	-57.0089
5.86917	89902.9	89902.9	-3.74881	2.53945	0.30441	2.8634	19.7687	5.05258	43.8864	5.86917	-57.0112
5.86958	89902.9	89902.9	-4.08478	3.40501	-0.07438	3.51193	17.8797	5.1107	44.0152	5.86958	-57.0089
5.87	89902.9	89902.9	-4.38932	4.37863	-0.13784	3.79118	16.3367	5.16461	44.1789	5.87	-57.0089
5.87042	89902.9	89902.9	-4.73014	5.2847	0.12325	3.59469	15.5548	5.21039	44.3316	5.87042	-57.0027
5.87083	89902.9	89902.9	-4.78134	5.63865	0.52587	2.94877	15.8083	5.25008	44.4541	5.87083	-56.9989
5.87125	89902.9	89902.9	-4.58354	5.28939	0.93084	2.1523	16.5067	5.2807	44.5384	5.87125	-56.9813
5.87167	89902.9	89902.9	-4.28529	4.6194	1.06312	1.41131	17.9833	5.30109	44.5866	5.87167	-56.9813
5.87208	89902.9	89902.9	-4.38197	3.85527	0.86458	0.87498	19.3479	5.31508	44.5417	5.87208	-56.9941
5.8725	89902.9	89902.9	-4.82895	2.98516	0.42789	0.82619	20.2158	5.32711	44.4842	5.8725	-57.0112
5.87292	89902.9	89902.9	-4.63086	2.29173	-0.03544	0.64125	20.504	5.33633	44.3302	5.87292	-57.0155
5.87333	89902.9	89902.9	-4.56834	2.08698	-0.38074	0.85028	20.1725	5.34055	44.1383	5.87333	-57.0155
5.87375	89902.9	89902.9	-4.72292	2.12324	-0.48472	1.08953	19.1161	5.33859	43.800	5.87375	-57.0089
5.87417	89902.9	89902.9	-4.88037	1.05639	-0.4831	1.29095	17.5859	5.33156	43.6527	5.87417	-57.0027
5.87458	89902.9	89902.9	-4.54805	2.03581	-0.30962	1.53977	16.2199	5.32039	43.3899	5.87458	-56.9941
5.875	89902.9	89902.9	-3.77227	2.28829	-0.11549	1.93187	15.3134	5.30555	43.1412	5.875	-56.9899
5.87542	89902.9	89902.9	-3.13008	2.55308	0.22259	2.56976	14.5898	5.29055	42.8658	5.87542	-57.0027
5.87583	89902.9	89902.9	-2.81751	2.661	0.06093	3.37399	13.8671	5.27383	42.5683	5.87583	-57.0155
5.87625	89902.9	89902.9	-2.85072	2.76556	0.01484	4.17269	13.2717	5.25242	42.25	5.87625	-57.0155
5.87667	89902.9	89902.9	-2.5568	3.0873	-0.07088	4.73191	12.7816	5.22787	41.92	5.87667	-57.0027
5.87708	89902.9	89902.9	-2.58029	3.4584	-0.11189	4.81508	12.2923	5.20453	41.5741	5.87708	-56.9956
5.8775	89902.9	89902.9	-2.72598	3.55137	-0.01378	4.93867	11.821	5.17852	41.1942	5.8775	-56.9856
5.87792	89902.9	89902.9	-2.87702	3.33027	0.23388	3.58002	11.816	5.14383	40.7709	5.87792	-56.9941
5.87833	89902.9	89902.9	-3.07402	2.98178	0.54982	2.49937	12.2402	5.10234	40.3012	5.87833	-57.0089
5.87875	89902.9	89902.9	-3.40404	2.43411	0.81049	1.44399	12.7391	5.05805	39.7875	5.87875	-57.0283
5.87917	89902.9	89902.9	-3.85547	1.69277	0.89891	0.83894	13.3421	5.01227	39.2659	5.87917	-57.0388
5.87958	89902.9	89902.9	-3.85195	0.98125	0.74191	0.13228	13.8816	4.96802	38.7078	5.87958	-57.0388
5.88	89902.9	89902.9	-3.45293	0.71797	0.33719	-0.1712	13.9841	4.92125	38.1944	5.88	-57.0283
5.88042	89902.9	89902.9	-3.19924	1.08959	0.24406	-0.42233	13.4097	4.87734	37.5733	5.88042	-57.0112
5.88083	89902.9	89902.9	-2.92389	1.91558	-0.88358	-0.70357	12.3861	4.82981	37.0431	5.88083	-56.9984
5.88125	89902.9	89902.9	-2.55215	2.75824	-1.46819	-1.02559	11.2387	4.77516	36.5344	5.88125	-57.0089
5.88167	89902.9	89902.9	-2.1793	3.18854	-1.95889	-1.30892	10.1994	4.71039	36.0138	5.88167	-57.0283
5.88208	89902.9	89902.9	-1.90547	3.09063	-2.383	-1.42	9.33028	4.6357	35.4445	5.88208	-57.0325
5.8825	89902.9	89902.9	-1.89786	2.69941	-2.70726	-1.33417	8.74623	4.55828	34.9191	5.8825	-57.0197
5.88292	89902.9	89902.9	-1.81576	2.22194	-2.97981	-1.14248	8.49224	4.48586	34.1442	5.88292	-57.024
5.88333	89902.9	89902.9	-1.83918	1.70137	-3.17615	-0.99709	8.42908	4.41719	33.4411	5.88333	-57.0325
5.88375	89902.9	89902.9	-1.86923	1.23477	-3.25306	-0.99732	8.46475	4.34872	32.7359	5.88375	-57.0453
5.88417	89902.9	89902.9	-1.73240	0.97513	-3.17024	-1.12937	8.47668	4.26938	32.0236	5.88417	-57.0411
5.88458	89902.9	89902.9	-1.92006	0.88411	-2.96174	-1.35065	8.35216	4.17531	31.289	5.88458	-57.0283
5.885	89902.9	89902.9	-2.14297	0.74935	-2.70401	-1.82968	8.1125	4.07914	30.5355	5.885	-57.024
5.88542	89902.9	89902.9	-2.11973	0.48712	-2.45347	-1.85264	7.81829	3.98187	29.7725	5.88542	-57.0325
5.88583	89902.9	89902.9	-1.89329	0.18725	-2.23975	-1.93592	7.39353	3.88358	28.9994	5.88583	-57.0498
5.88625	89902.9	89902.									

Appendix D Data from Dynamic Test Panel SCI2

5.89292	69902.9	69902.9	0.70723	-0.21224	-3.7891	-4.4473	-1.37868	3.24398	14.5758	5.89292	-57.1008
5.89333	69902.9	69902.9	1.15085	-0.42793	-3.94042	-4.56013	-1.95191	3.26375	13.727	5.89333	-57.1093
5.89375	69902.9	69902.9	1.55618	-0.59427	-4.09668	-4.62418	-2.45466	3.28109	12.0661	5.89375	-57.0923
5.89417	69902.9	69902.9	1.94883	-0.46465	-4.22734	-4.636	-2.918	3.29492	12.0569	5.89417	-57.0624
5.89458	69902.9	69902.9	2.32298	-0.10755	-4.30437	-4.64607	-3.2709	3.30227	11.2428	5.89458	-57.0388
5.895	69902.9	69902.9	2.67819	0.17715	-4.309	-4.72079	-3.45149	3.30187	10.4277	5.895	-57.0389
5.89542	69902.9	69902.9	3.11397	0.01139	-4.24031	-4.88817	-3.49643	3.29508	9.80359	5.89542	-57.0581
5.89583	69902.9	69902.9	3.55124	-0.638	-4.10984	-5.13049	-3.41847	3.28664	8.79828	5.89583	-57.0709
5.89625	69902.9	69902.9	3.90814	-1.27318	-3.87644	-5.3925	-3.2858	3.28023	8.01094	5.89625	-57.0667
5.89667	69902.9	69902.9	4.25404	-1.39811	-3.87323	-5.59745	-3.19932	3.2725	7.28937	5.89667	-57.0581
5.89708	69902.9	69902.9	4.71406	-1.0849	-3.76354	-5.82408	-3.27055	3.25914	6.82047	5.89708	-57.0581
5.8975	69902.9	69902.9	5.3776	-0.80794	-3.83022	-5.51147	-3.31214	3.24227	5.97922	5.8975	-57.0624
5.89792	69902.9	69902.9	6.22083	-0.91419	-3.50257	-5.33658	-3.26395	3.22305	5.34422	5.89792	-57.0667
5.89833	69902.9	69902.9	6.98808	-1.39525	-3.42114	-5.18637	-3.25908	3.20242	4.72062	5.89833	-57.0667
5.89875	69902.9	69902.9	7.49115	-1.96777	-3.44604	-5.05205	-3.2392	3.18055	4.13234	5.89875	-57.0667
5.89917	69902.9	69902.9	7.87611	-2.1875	-3.63219	-5.0094	-3.23709	3.15625	3.60562	5.89917	-57.0667
5.89958	69902.9	69902.9	7.75228	-1.74264	-3.97679	-5.02404	-3.18576	3.13	3.14766	5.89958	-57.0624
5.9	69902.9	69902.9	7.80384	-0.75338	-4.40757	-5.06064	-3.25955	3.10156	2.75375	5.9	-57.0539
5.90042	69902.9	69902.9	7.79779	0.20833	-4.81185	-5.07338	-3.33693	3.07047	2.41484	5.90042	-57.0667
5.90083	69902.9	69902.9	7.71494	0.61129	-5.10469	-5.05462	-3.29592	3.03773	2.12719	5.90083	-57.0709
5.90125	69902.9	69902.9	7.52982	0.41217	-5.24493	-5.03689	-3.24403	3.00802	1.8814	5.90125	-57.0667
5.90167	69902.9	69902.9	7.20385	-0.11725	-5.24227	-5.0567	-3.22842	2.97408	1.67906	5.90167	-57.0709
5.90208	69902.9	69902.9	6.78242	-0.6895	-5.16848	-5.14824	-3.1392	2.93206	1.52297	5.90208	-57.0795
5.9025	69902.9	69902.9	6.34082	-1.06582	-5.12238	-5.34683	-3.05410	2.90055	1.41234	5.9025	-57.088
5.90292	69902.9	69902.9	5.84635	-1.05758	-5.11566	-5.64514	-3.09857	2.88039	1.35187	5.90292	-57.0923
5.90333	69902.9	69902.9	5.30514	-0.82526	-5.08382	-5.94697	-3.16352	2.91602	1.33953	5.90333	-57.0795
5.90375	69902.9	69902.9	4.74316	-0.73392	-4.98987	-6.17542	-3.13167	2.77039	1.36287	5.90375	-57.0624
5.90417	69902.9	69902.9	4.24323	-0.99043	-4.83268	-6.28975	-3.07897	2.72555	1.40881	5.90417	-57.0539
5.90458	69902.9	69902.9	3.85534	-1.34635	-4.62488	-6.27643	-3.08881	2.6818	1.47719	5.90458	-57.0539
5.905	69902.9	69902.9	3.54909	-1.54251	-4.38084	-6.15353	-3.07132	2.63789	1.58062	5.905	-57.0524
5.90542	69902.9	69902.9	3.28177	-1.82793	-4.15193	-5.98196	-3.03978	2.59172	1.74047	5.90542	-57.0795
5.90583	69902.9	69902.9	2.97435	-1.65807	-3.92926	-5.89274	-3.10167	2.54164	1.97062	5.90583	-57.0837
5.90625	69902.9	69902.9	2.68084	-1.42448	-3.69323	-5.93699	-3.08761	2.48914	2.28719	5.90625	-57.0985
5.90667	69902.9	69902.9	2.24284	-0.80697	-3.42751	-5.0757	-3.03784	2.43711	2.81375	5.90667	-57.1051
5.90708	69902.9	69902.9	1.93607	-0.03229	-3.12982	-4.72704	-3.06739	2.38312	2.97875	5.90708	-57.1008
5.9075	69902.9	69902.9	1.67227	0.60326	-2.82726	-4.36508	-3.10329	2.3275	3.3275	5.9075	-57.0923
5.90792	69902.9	69902.9	1.42337	0.88898	-2.55575	-4.00054	-3.07132	2.26945	3.64578	5.90792	-57.0795
5.90833	69902.9	69902.9	1.13757	0.59355	-2.32787	-3.59813	-2.99719	2.20773	3.93812	5.90833	-57.0795
5.90875	69902.9	69902.9	0.75158	-0.16335	-2.18181	-3.3572	-2.91958	2.14195	4.22109	5.90875	-57.1093
5.90917	69902.9	69902.9	0.30298	-0.94063	-2.09763	-3.1326	-2.83768	2.07555	4.51109	5.90917	-57.1126
5.90958	69902.9	69902.9	-0.17487	-1.24753	-2.10597	-2.97159	-2.78494	2.00895	4.82158	5.90958	-57.1051
5.91	69902.9	69902.9	-0.8444	-1.03444	-2.15883	-2.82958	-2.74502	1.93484	5.14375	5.91	-57.1093
5.91042	69902.9	69902.9	-1.1054	-0.62662	-2.24149	-2.71258	-2.73008	1.86148	5.46875	5.91042	-57.1126
5.91083	69902.9	69902.9	-1.58922	-0.30381	-2.34678	-2.62027	-2.68942	1.78789	5.79562	5.91083	-57.1051
5.91125	69902.9	69902.9	-2.08889	-0.13763	-2.4354	-2.52189	-2.71513	1.71227	6.13406	5.91125	-57.0985
5.91167	69902.9	69902.9	-2.44492	-0.08411	-2.47501	-2.42497	-2.82749	1.63399	6.48312	5.91167	-57.1008
5.91208	69902.9	69902.9	-2.74567	0.10748	-2.47118	-2.37281	-2.90488	1.5493	6.92594	5.91208	-57.1093
5.9125	69902.9	69902.9	-3.00358	-0.20052	-2.43273	-2.40968	-2.92537	1.48219	7.15578	5.9125	-57.1179
5.91292	69902.9	69902.9	-3.2457	-0.32995	-2.38061	-2.54127	-2.98939	1.37242	7.47047	5.91292	-57.1179
5.91333	69902.9	69902.9	-3.48922	-0.45578	-2.33091	-2.71829	-2.99914	1.28094	7.75922	5.91333	-57.1198
5.91375	69902.9	69902.9	-3.76335	-0.48893	-2.26558	-2.87429	-2.93985	1.18841	8.01562	5.91375	-57.1051
5.91417	69902.9	69902.9	-4.02324	-0.33053	-2.15728	-2.97437	-2.88645	1.09896	8.23889	5.91417	-57.1008
5.91458	69902.9	69902.9	-4.20748	-0.08003	-1.99038	-3.00031	-2.89589	0.99164	8.44498	5.91458	-57.1051
5.915	69902.9	69902.9	-4.32278	-0.0249	-1.78788	-2.98894	-2.88250	0.88516	8.63158	5.915	-57.1051
5.91542	69902.9	69902.9	-4.41224	-0.42257	-1.60742	-2.99487	-2.81127	0.78625	8.80062	5.91542	-57.1008
5.91583	69902.9	69902.9	-4.45938	-1.06428	-1.45487	-2.99001	-2.77421	0.69109	8.93703	5.91583	-57.0985
5.91625	69902.9	69902.9	-4.50951	-1.52493	-1.34517	-2.93093	-2.74432	0.57937	9.03391	5.91625	-57.088
5.91667	69902.9	69902.9	-4.52598	-1.56764	-1.32745	-2.83629	-2.69567	0.46875	9.09344	5.91667	-57.0837
5.91708	69902.9	69902.9	-4.50306	-1.22148	-1.41641	-2.76726	-2.67992	0.36281	9.12141	5.91708	-57.0965
5.9175	69902.9	69902.9	-4.42279	-0.65417	-1.5656	-2.76205	-2.74199	0.26195	9.12375	5.9175	-57.0965
5.91792	69902.9	69902.9	-4.28738	-0.10048	-1.6892	-2.80293	-2.82426	0.17	9.08964	5.91792	-57.0923
5.91833	69902.9	69902.9	-4.04803	-0.2234	-1.73043	-2.85043	-2.87313	0.09125	9.01625	5.91833	-57.088
5.91875	69902.9	69902.9	-3.71573	0.26091	-1.70344	-2.86143	-2.90881	0.025	8.91806	5.91875	-57.0965
5.91917	69902.9	69902.9	-3.27474	0.18368	-1.68047	-2.81104	-2.83581	-0.03812	8.80375	5.91917	-57.1093
5.91958	69902.9	69902.9	-2.83493	0.11329	-1.64159	-2.69938	-2.85904	-0.1075	8.66297	5.91958	-57.1126
5.92	69902.9	69902.9	-2.52376	-0.01855	-1.64089	-2.54717	-2.89418	-0.185	8.49062	5.92	-57.1126
5.92042	69902.9	69902.9	-2.31055	-0.28177	-1.67008	-2.39902	-3.01132	-0.28734	8.28312	5.92042	-57.1051
5.92083	69902.9	69902.9	-2.07786	-0.60215	-1.68781	-2.28875	-2.9541	-0.35094	8.04484	5.92083	-57.088
5.92125	69902.9	69902.9	-1.78009	-0.91654	-1.69985	-2.2028	-2.85988	-0.43516	7.78822	5.92125	-57.088
5.92167	69902.9	69902.9	-1.35703	-1.22005	-1.73101	-2.13759	-2.78719	-0.51989	7.53141	5.92167	-57.098
5.92208	69902.9	69902.9	-0.96419	-1.44837	-1.8319	-2.14604	-2.77236	-0.6025	7.27547	5.92208	-57.0985
5.9225	69902.9	69902.9	-0.61927	-1.48301	-1.85793	-2.23618	-2.79483	-0.68484	7.01578	5.9225	-57.1093
5.92292	69902.9	69902.9	-0.28841	-1.33581	-2.04643	-2.39022	-2.84860	-0.76809	6.74489	5.92292	-57.1221
5.92333	69902.9	69902.9	0.05378	-1.15742	-2.08881	-2.60602	-2.9022	-0.84538	6.45837	5.92333	-57.1179
5.92375	69902.9	69902.9	0.38892	-1.03704	-2.14394	-2.87278	-2.90849	-0.92477	6.17297	5.92375	-57.1284
5.92417	69902.9	69902.9	0.82656	-0.90684	-2.22504	-3.16489	-2.89576	-1.00586	5.88719	5.92417	-57.1307
5.92458	69902.9	69902.9	0.81556	-0.70289	-2.35339	-3.44187	-2.89923	-1.08625	5.58844	5.92458	-57.1349
5.925	69902.9	69902.9	0.92426	-0.49115	-2.48934	-3.66389	-2.89471	-1.165	5.27266	5.925	-57.1349
5.92542	69902.9	69902.9	1.03262	-0.35547	-2.62467	-3.90814	-2.84996	-1.24477	4.8575	5.92542	-57.1284
5.92583	69902.9	69902.9	1.23789	-0.33945	-2.70112	-3.87926	-2.83818	-1.33062	4.68826	5.92583	-57.1179
5.92625	69902.9	69902.9	1.53132	-0.47843	-2.72741	-3.89374	-2.85147	-1.41787	4.40781	5.92625	-57.1051
5.92667	69902.9	69902.9	1.86523	-0.78185	-2.73158	-3.86999	-2.83664	-1.48641	4.17141	5.92667	-57.1093
5.92708	69902.9	69902.9	2.12715	-1.02311	-2.76193	-3.82189	-2.7829	-1.51555	3.9475	5.92708	-57.1221
5.9275	69902.9	69902.9									

Appendix D Data from Dynamic Test Panel SCI2

5.93417	69902.9	69902.9	2.48053	-0.26934	-2.46181	-3.84701	-2.58111	-0.19109	3.44125	5.93417	-57.1392
5.93458	69902.9	69902.9	2.03763	-0.39727	-2.49134	-3.82373	-2.58362	-0.10887	3.64562	5.93458	-57.1392
5.935	69902.9	69902.9	1.84089	-0.55228	-2.57127	-3.85628	-2.58003	-0.02258	3.06016	5.935	-57.1583
5.93542	69902.9	69902.9	1.31204	-0.68204	-2.64019	-3.85802	-2.53805	0.05388	4.00884	5.93542	-57.1681
5.93583	69902.9	69902.9	0.98898	-0.8347	-2.65072	-3.86888	-2.51894	0.12047	4.33547	5.93583	-57.1776
5.93625	69902.9	69902.9	0.63328	-0.98069	-2.62223	-3.89716	-2.51138	0.18141	4.59547	5.93625	-57.1733
5.93667	69902.9	69902.9	0.29785	-0.32038	-2.52075	-3.20522	-2.51254	0.24078	4.86719	5.93667	-57.152
5.93708	69902.9	69902.9	0.06009	-0.14147	-2.38383	-3.04618	-2.54416	0.28805	5.14858	5.93708	-57.1425
5.9375	69902.9	69902.9	-0.11224	0.04284	-2.15936	-2.94193	-2.61188	0.34703	5.43887	5.9375	-57.152
5.93792	69902.9	69902.9	-0.32786	0.12728	-1.96222	-2.90174	-2.6844	0.39492	5.73016	5.93792	-57.1648
5.93833	69902.9	69902.9	-0.85658	0.01797	-1.82275	-2.90383	-2.67332	0.41344	6.02484	5.93833	-57.1648
5.93875	69902.9	69902.9	-1.06582	-0.22845	-1.75487	-2.91634	-2.68312	0.43841	6.31422	5.93875	-57.1648
5.93917	69902.9	69902.9	-1.47982	-0.47658	-1.72928	-2.9102	-2.64989	0.4557	6.59855	5.93917	-57.1648
5.93958	69902.9	69902.9	-1.78036	-0.84048	-1.69788	-2.87255	-2.62525	0.46914	6.84281	5.93958	-57.1583
5.94	69902.9	69902.9	-1.95202	-0.70749	-1.63001	-2.80444	-2.58585	0.47742	7.07234	5.94	-57.1348
5.94042	69902.9	69902.9	-2.01049	-0.89473	-1.53294	-2.70007	-2.53817	0.48031	7.26172	5.94042	-57.1221
5.94083	69902.9	69902.9	-2.11322	-0.8334	-1.46691	-2.58644	-2.51034	0.47977	7.48625	5.94083	-57.1136
5.94125	69902.9	69902.9	-2.29212	-0.5765	-1.48313	-2.45645	-2.53362	0.48164	7.70469	5.94125	-57.1179
5.94167	69902.9	69902.9	-2.48874	-0.59023	-1.53224	-2.28759	-2.54578	0.48102	7.94219	5.94167	-57.1348
5.94208	69902.9	69902.9	-2.5972	-0.68698	-1.57406	-2.09102	-2.52065	0.47453	8.19016	5.94208	-57.152
5.9425	69902.9	69902.9	-2.84095	-0.80028	-1.61414	-1.93395	-2.48482	0.46848	8.42875	5.9425	-57.152
5.94292	69902.9	69902.9	-2.70814	-0.84635	-1.6607	-1.8575	-2.46588	0.45891	8.635	5.94292	-57.1435
5.94333	69902.9	69902.9	-2.94898	-0.78668	-1.61851	-1.86594	-2.47385	0.45375	8.80531	5.94333	-57.1392
5.94375	69902.9	69902.9	-2.9698	-0.53737	-1.68433	-1.95376	-2.4932	0.44888	8.94875	5.94375	-57.1392
5.94417	69902.9	69902.9	-3.02904	-0.19078	-1.64136	-2.10631	-2.51312	0.44602	9.075	5.94417	-57.1348
5.94458	69902.9	69902.9	-3.05156	0.13704	-1.58147	-2.29292	-2.53779	0.44781	9.19172	5.94458	-57.1264
5.945	69902.9	69902.9	-3.11621	0.28203	-1.52786	-2.49018	-2.55737	0.45484	9.25625	5.945	-57.1221
5.94542	69902.9	69902.9	-3.23717	0.18451	-1.48417	-2.67146	-2.55957	0.46828	9.29703	5.94542	-57.1083
5.94583	69902.9	69902.9	-3.34271	-0.08704	-1.438	-2.81588	-2.52525	0.48887	9.31719	5.94583	-57.0985
5.94625	69902.9	69902.9	-3.37839	-0.42441	-1.37885	-2.9051	-2.54277	0.50719	9.33297	5.94625	-57.088
5.94667	69902.9	69902.9	-3.34453	-0.78668	-1.31089	-2.92721	-2.51034	0.52633	9.34512	5.94667	-57.0837
5.94708	69902.9	69902.9	-3.25143	-0.89342	-1.26876	-2.88685	-2.44068	0.54387	9.33825	5.94708	-57.0709
5.9475	69902.9	69902.9	-3.08302	-0.9625	-1.25957	-2.77838	-2.38721	0.56242	9.29869	5.9475	-57.0453
5.94792	69902.9	69902.9	-2.80449	-0.89208	-1.36347	-2.70494	-2.40319	0.58047	9.23453	5.94792	-57.0283
5.94833	69902.9	69902.9	-2.52311	-1.00729	-1.54186	-2.64123	-2.42926	0.60445	9.15359	5.94833	-57.0369
5.94875	69902.9	69902.9	-2.26875	-0.98431	-1.76148	-2.58482	-2.44084	0.62102	9.06328	5.94875	-57.0453
5.94917	69902.9	69902.9	-2.06895	-0.90718	-2.00809	-2.56883	-2.48447	0.63422	8.95344	5.94917	-57.0411
5.94958	69902.9	69902.9	-1.88385	-0.7903	-2.25087	-2.60521	-2.48517	0.64225	8.81531	5.94958	-57.0325
5.95	69902.9	69902.9	-1.69375	-0.67868	-2.44989	-2.64988	-2.51242	0.64684	8.64679	5.95	-57.0187
5.95042	69902.9	69902.9	-1.48759	-0.62578	-2.57034	-2.80363	-2.52818	0.64569	8.45172	5.95042	-57.0187
5.95083	69902.9	69902.9	-1.28151	-0.63314	-2.80023	-2.9117	-2.54198	0.63735	8.24703	5.95083	-57.0283
5.95125	69902.9	69902.9	-1.0125	-0.63717	-2.53501	-3.00796	-2.52841	0.66414	8.03658	5.95125	-57.0283
5.95167	69902.9	69902.9	-0.88724	-0.57819	-2.39926	-3.08363	-2.48972	0.67375	7.82016	5.95167	-57.024
5.95208	69902.9	69902.9	-0.78028	-0.48055	-2.24219	-3.14395	-2.45011	0.67944	7.60547	5.95208	-57.024
5.9525	69902.9	69902.9	-0.14609	-0.34141	-2.11315	-3.18005	-2.40134	0.67555	7.39562	5.9525	-57.024
5.95292	69902.9	69902.9	0.03014	-0.30391	-2.04214	-3.21388	-2.3301	0.67109	7.19494	5.95292	-57.024
5.95333	69902.9	69902.9	0.23246	-0.38793	-2.02141	-3.23005	-2.2588	0.67117	6.99887	5.95333	-57.0325
5.95375	69902.9	69902.9	0.51393	-0.57788	-2.04052	-3.23708	-2.22284	0.67687	6.79891	5.95375	-57.0187
5.95417	69902.9	69902.9	0.88841	-0.73053	-2.1128	-3.20901	-2.28026	0.68887	6.60016	5.95417	-57.0084
5.95458	69902.9	69902.9	1.26204	-0.77734	-2.19891	-3.24043	-2.31988	0.6975	6.4	5.95458	-57.0084
5.955	69902.9	69902.9	1.5827	-0.69822	-2.28981	-3.45658	-2.37088	0.70648	6.20297	5.955	-57.0084
5.95542	69902.9	69902.9	1.77786	-0.52077	-2.41779	-3.50824	-2.40458	0.71687	6.01266	5.95542	-57.0187
5.95583	69902.9	69902.9	1.91693	-0.33878	-2.60637	-3.57172	-2.41708	0.72883	5.83703	5.95583	-57.0283
5.95625	69902.9	69902.9	2.00309	-0.24818	-2.82853	-3.64844	-2.42788	0.74012	5.67625	5.95625	-57.0383
5.95667	69902.9	69902.9	2.04863	-0.25742	-3.0273	-3.73829	-2.43702	0.76047	5.52812	5.95667	-57.0411
5.95708	69902.9	69902.9	2.09421	-0.33151	-3.1553	-3.82331	-2.42404	0.77742	5.39297	5.95708	-57.0453
5.9575	69902.9	69902.9	2.14779	-0.45566	-3.2065	-3.89281	-2.40285	0.78094	5.26266	5.9575	-57.0411
5.95792	69902.9	69902.9	2.1916	-0.60534	-3.20603	-3.92849	-2.38613	0.80258	5.13872	5.95792	-57.0383
5.95833	69902.9	69902.9	2.21688	-0.73568	-3.18646	-3.92466	-2.38825	0.81422	5.02031	5.95833	-57.0283
5.95875	69902.9	69902.9	2.26055	-0.83197	-3.16457	-3.8964	-2.38578	0.82617	4.91828	5.95875	-57.024
5.95917	69902.9	69902.9	2.3321	-0.89108	-3.14152	-3.8547	-2.34088	0.83565	4.83203	5.95917	-57.0187
5.95958	69902.9	69902.9	2.38928	-0.88667	-3.10364	-3.80061	-2.30717	0.84156	4.76531	5.95958	-57.0283
5.96	69902.9	69902.9	2.39115	-0.71758	-3.04807	-3.7274	-2.25331	0.84225	4.71828	5.96	-57.0325
5.96042	69902.9	69902.9	2.33388	-0.47533	-3.02337	-3.66763	-2.22886	0.84266	4.68094	5.96042	-57.0325
5.96083	69902.9	69902.9	2.23789	-0.20671	-3.039	-3.6411	-2.25284	0.84391	4.69422	5.96083	-57.0383
5.96125	69902.9	69902.9	2.15423	0.03464	-3.03286	-3.614	-2.27277	0.84297	4.70703	5.96125	-57.0411
5.96167	69902.9	69902.9	2.08861	0.19225	-2.96417	-3.57137	-2.28585	0.83945	4.76828	5.96167	-57.0383
5.96208	69902.9	69902.9	2.00755	0.23218	-2.83537	-3.52261	-2.3147	0.83488	4.86484	5.96208	-57.0325
5.9625	69902.9	69902.9	1.9612	0.17658	-2.67737	-3.47975	-2.34887	0.82727	4.97594	5.9625	-57.024
5.96292	69902.9	69902.9	1.84258	0.06673	-2.52829	-3.44863	-2.37386	0.81711	5.07853	5.96292	-57.0283
5.96333	69902.9	69902.9	1.70171	-0.07533	-2.4186	-3.43448	-2.38489	0.8093	5.1875	5.96333	-57.0325
5.96375	69902.9	69902.9	1.11148	-0.23867	-2.35386	-3.42809	-2.37829	0.80141	5.25809	5.96375	-57.0325
5.96417	69902.9	69902.9	0.85436	-0.41113	-2.31806	-3.40828	-2.35593	0.7893	5.36219	5.96417	-57.0283
5.96458	69902.9	69902.9	0.60482	-0.5778	-2.27802	-3.34889	-2.30218	0.77187	5.4875	5.96458	-57.0187
5.965	69902.9	69902.9	0.38086	-0.68665	-2.21485	-3.23221	-2.31945	0.75109	5.62281	5.965	-57.0187
5.96542	69902.9	69902.9	0.19512	-0.67813	-2.13573	-3.07693	-2.30138	0.72844	5.75859	5.96542	-57.024
5.96583	69902.9	69902.9	0.02298	-0.58112	-2.0638	-2.90707	-2.27207	0.70328	5.89016	5.96583	-57.0411
5.96625	69902.9	69902.9	-0.15104	-0.50202	-2.01888	-2.75602	-2.23929	0.67536	6.02344	5.96625	-57.0484
5.96667	69902.9	69902.9	-0.33685	-0.5041	-2.03218	-2.67332	-2.23526	0.64273	6.17344	5.96667	-57.0484
5.96708	69902.9	69902.9	-0.54888	-0.564	-2.11071	-2.6571	-2.25527	0.61626	6.31884	5.96708	-57.0411
5.9675	69902.9	69902.9	-0.80588	-0.62539	-2.16979	-2.63451	-2.25041	0.59686	6.46719	5.9675	-57.0325
5.96792	69902.9	69902.9	-1.06419	-0.61699	-2.16527	-2.58331	-2.22829	0.57805	6.61344	5.96792	-57.0484
5.96833	69902.9	69902.9	-1.2502	-0.47272	-2.08461	-2.52588	-2.21334	0.56031	6.75872	5.96833	-57.0709
5.96875	69902.9	69902.9	-1.384	-0.22467	-1.96805	-2.48532	-2.22041	0.54258	6.89406	5.96875	-57.0

Appendix D Data from Dynamic Test Panel SCI2

5.97542	69902.9	69902.9	-1.8888	-0.7653	-1.58217	-2.2335	-2.28234	0.06508	7.55797	5.97542	-57.0388
5.97583	69902.9	69902.9	-1.89023	-0.80879	-1.6351	-2.20871	-2.2813	0.03352	7.45937	5.97583	-57.0453
5.97625	69902.9	69902.9	-1.48022	-0.80371	-1.65665	-2.16608	-2.28141	0.00531	7.35312	5.97625	-57.0539
5.97667	69902.9	69902.9	-1.31113	-0.76667	-1.64811	-2.12298	-2.27242	-0.0193	7.24570	5.97667	-57.0539
5.97708	69902.9	69902.9	-1.12945	-0.7198	-1.62039	-2.10087	-2.27277	-0.04305	7.13281	5.97708	-57.0388
5.9775	69902.9	69902.9	-0.93464	-0.69544	-1.60881	-2.11014	-2.25354	-0.06336	7.01297	5.9775	-57.0293
5.97792	69902.9	69902.9	-0.73281	-0.68072	-1.62398	-2.14072	-2.23419	-0.09477	6.89825	5.97792	-57.0224
5.97833	69902.9	69902.9	-0.53454	-0.62875	-1.64485	-2.18045	-2.21045	-0.11937	6.75234	5.97833	-57.0368
5.97875	69902.9	69902.9	-0.33197	-0.4847	-1.64657	-2.22342	-2.18689	-0.14328	6.60719	5.97875	-57.0411
5.97917	69902.9	69902.9	-0.16211	-0.29447	-1.61611	-2.25724	-2.11512	-0.1667	6.45079	5.97917	-57.0368
5.97958	69902.9	69902.9	-0.01126	-0.13997	-1.59132	-2.30207	-2.09068	-0.1832	6.29953	5.97958	-57.0283
5.98	69902.9	69902.9	0.14577	-0.08776	-1.61113	-2.38758	-2.09902	-0.19484	6.13156	5.98	-57.0204
5.98042	69902.9	69902.9	0.32617	-0.15938	-1.64414	-2.47395	-2.09218	-0.20625	5.98172	5.98042	-57.0368
5.98083	69902.9	69902.9	0.52533	-0.30059	-1.62923	-2.54671	-2.07318	-0.22016	5.83016	5.98083	-57.0453
5.98125	69902.9	69902.9	0.87754	-0.41152	-1.74759	-2.62432	-2.05589	-0.23617	5.68094	5.98125	-57.0368
5.98167	69902.9	69902.9	1.25202	-0.44689	-1.8465	-2.70989	-2.05164	-0.25078	5.53912	5.98167	-57.0411
5.98208	69902.9	69902.9	1.74467	-0.44748	-1.9628	-2.79425	-2.07712	-0.26445	5.39937	5.98208	-57.0496
5.9825	69902.9	69902.9	2.31654	-0.47487	-2.07585	-2.87116	-2.11373	-0.27805	5.26109	5.9825	-57.0581
5.98292	69902.9	69902.9	2.92129	-0.5377	-2.16875	-2.94054	-2.12577	-0.2943	5.11937	5.98292	-57.0624
5.98333	69902.9	69902.9	3.59945	-0.59965	-2.24068	-3.0024	-2.12357	-0.31445	4.97579	5.98333	-57.0539
5.98375	69902.9	69902.9	4.3507	-0.57702	-2.28443	-3.05302	-2.134	-0.33734	4.83678	5.98375	-57.0453
5.98417	69902.9	69902.9	5.18678	-0.47849	-2.31921	-3.08198	-2.15662	-0.36059	4.705	5.98417	-57.0453
5.98458	69902.9	69902.9	6.11973	-0.32319	-2.30181	-3.07109	-2.10481	-0.38396	4.58703	5.98458	-57.0539
5.985	69902.9	69902.9	7.10176	-0.1853	-2.23813	-3.01699	-2.08149	-0.40802	4.48297	5.985	-57.0687
5.98542	69902.9	69902.9	8.15117	-0.08898	-2.13573	-2.93139	-2.00859	-0.42945	4.39375	5.98542	-57.0762
5.98583	69902.9	69902.9	9.26217	0.06091	-2.02049	-2.84129	-1.92781	-0.45375	4.32203	5.98583	-57.0937
5.98625	69902.9	69902.9	10.43292	0.10781	-1.94936	-2.78842	-1.89179	-0.47508	4.26281	5.98625	-57.0937
5.98667	69902.9	69902.9	11.7641	-0.1543	-1.93303	-2.80027	-1.91843	-0.49414	4.21922	5.98667	-57.0937
5.98708	69902.9	69902.9	13.2534	-0.16732	-1.93685	-2.79845	-1.92944	-0.51359	4.19016	5.98708	-57.0795
5.9875	69902.9	69902.9	14.9014	-0.14414	-1.96129	-2.76205	-1.90789	-0.53414	4.17329	5.9875	-57.088
5.98792	69902.9	69902.9	16.7199	-0.11009	-2.02038	-2.70992	-1.90959	-0.55453	4.17312	5.98792	-57.1008
5.98833	69902.9	69902.9	18.70887	-0.10885	-2.11407	-2.6578	-1.94322	-0.57082	4.18875	5.98833	-57.1051
5.98875	69902.9	69902.9	19.9454	-0.16408	-2.21985	-2.61189	-1.98982	-0.58344	4.21869	5.98875	-57.1008
5.98917	69902.9	69902.9	21.71855	-0.25345	-2.30253	-2.57741	-1.98585	-0.59306	4.26494	5.98917	-57.088
5.98958	69902.9	69902.9	23.2259	-0.32064	-2.32744	-2.55494	-2.00982	-0.59992	4.32197	5.98958	-57.0937
5.99	69902.9	69902.9	24.493	-0.32806	-2.27346	-2.54254	-2.01979	-0.60227	4.39375	5.99	-57.088
5.99042	69902.9	69902.9	26.41718	-0.28935	-2.13666	-2.53988	-2.00542	-0.60125	4.48328	5.99042	-57.0937
5.99083	69902.9	69902.9	28.50746	-0.2459	-1.94345	-2.54335	-1.99755	-0.59937	4.59406	5.99083	-57.088
5.99125	69902.9	69902.9	30.76139	-0.23139	-1.74144	-2.55447	-1.99905	-0.59859	4.72494	5.99125	-57.0762
5.99167	69902.9	69902.9	33.2448	-0.25091	-1.57105	-2.58397	-1.99029	-0.6007	4.81062	5.99167	-57.0581
5.99208	69902.9	69902.9	35.9754	-0.29811	-1.45811	-2.55588	-1.94797	-0.60437	4.93172	5.99208	-57.0411
5.9925	69902.9	69902.9	38.9527	-0.22207	-1.36133	-1.43413	-2.55401	-1.95677	5.05266	5.9925	-57.0411
5.99292	69902.9	69902.9	42.0643	-0.41802	-1.47038	-2.551	-1.98504	-0.5975	5.17312	5.99292	-57.0453
5.99333	69902.9	69902.9	45.4124	-0.48502	-1.52147	-2.49679	-1.97195	-0.59336	5.29641	5.99333	-57.0581
5.99375	69902.9	69902.9	49.0012	-0.5112	-1.54359	-2.39565	-1.94589	-0.59297	5.42806	5.99375	-57.0539
5.99417	69902.9	69902.9	52.8367	-0.55052	-1.56672	-2.29446	-1.94125	-0.59172	5.57437	5.99417	-57.0453
5.99458	69902.9	69902.9	56.9429	-0.49429	-1.51428	-1.59445	-2.1945	-1.95561	5.72494	5.99458	-57.0411
5.995	69902.9	69902.9	61.337	-0.55781	-1.61356	-2.09705	-1.99002	-0.57605	5.87125	5.995	-57.0453
5.99542	69902.9	69902.9	66.0027	-0.65827	-1.60197	-2.0221	-2.03909	-0.56867	6.00875	5.99542	-57.0539
5.99583	69902.9	69902.9	70.9203	-0.57454	-1.56945	-1.96478	-2.06461	-0.55945	6.13953	5.99583	-57.0581
5.99625	69902.9	69902.9	76.0574	-0.52884	-1.48789	-1.93372	-2.06959	-0.5493	6.26547	5.99625	-57.0453
5.99667	69902.9	69902.9	81.497	-0.48483	-1.4068	-1.92851	-2.08616	-0.53703	6.39437	5.99667	-57.0325
5.99708	69902.9	69902.9	87.2351	-0.47118	-1.31911	-1.935	-2.11338	-0.52242	6.47853	5.99708	-57.0411
5.9975	69902.9	69902.9	93.2781	-0.48151	-1.22111	-1.93905	-2.13843	-0.50773	6.59172	5.9975	-57.0453
5.99792	69902.9	69902.9	99.739	-0.50293	-1.12775	-1.93108	-2.14049	-0.49326	6.69906	5.99792	-57.0453
5.99833	69902.9	69902.9	106.617	-0.52985	-1.04667	-1.92098	-2.1055	-0.47719	6.78531	5.99833	-57.0368
5.99875	69902.9	69902.9	113.933	-0.54883	-0.9825	-1.89735	-2.0104	-0.4607	6.82225	5.99875	-57.0368
5.99917	69902.9	69902.9	121.687	-0.55879	-0.96113	-1.87708	-1.93071	-0.44383	6.86641	5.99917	-57.0496
5.99958	69902.9	69902.9	129.98	-0.58569	-1.04099	-1.87326	-1.93951	-0.42516	6.90812	5.99958	-57.0496
6	69902.9	69902.9	138.725	-0.63828	-1.11003	-1.84905	-1.97114	-0.40578	6.95547	6	-57.0453
6.00042	69902.9	69902.9	147.964	-0.70864	-1.16625	-1.80654	-1.978	-0.38641	7.00489	6.00042	-57.0453
6.00083	69902.9	69902.9	157.639	-0.7541	-1.19749	-1.77355	-1.98156	-0.36758	7.0475	6.00083	-57.0368
6.00125	69902.9	69902.9	167.765	-0.7319	-1.25621	-1.79449	-2.00507	-0.34998	7.09031	6.00125	-57.0155
6.00167	69902.9	69902.9	178.346	-0.81439	-1.33405	-1.85611	-2.02106	-0.32937	7.09822	6.00167	-57.0112
6.00208	69902.9	69902.9	189.367	-0.43652	-1.41641	-1.95631	-2.02994	-0.30914	7.10266	6.00208	-57.0325
6.0025	69902.9	69902.9	200.843	-0.27643	-1.49475	-2.07596	-2.05013	-0.29016	7.09	6.0025	-57.0539
6.00292	69902.9	69902.9	212.843	-0.20423	-1.5224	-2.18774	-2.06172	-0.27375	7.05828	6.00292	-57.0624
6.00333	69902.9	69902.9	225.249	-0.2444	-1.50884	-2.26744	-2.04399	-0.25836	7.005	6.00333	-57.0539
6.00375	69902.9	69902.9	238.064	-0.35846	-1.43853	-2.29616	-2.025	-0.24393	6.93187	6.00375	-57.0453
6.00417	69902.9	69902.9	251.299	-0.46191	-1.33058	-2.27242	-2.01666	-0.22944	6.85531	6.00417	-57.0411
6.00458	69902.9	69902.9	264.967	-0.49967	-1.22285	-2.2123	-1.99108	-0.22758	6.79094	6.00458	-57.0368
6.005	69902.9	69902.9	279.048	-0.94408	-0.49674	-1.14976	-2.14118	-1.94739	6.73578	6.005	-57.0411
6.00542	69902.9	69902.9	293.546	-0.49004	-1.15045	-2.10459	-1.93581	-0.21636	6.69266	6.00542	-57.0411
6.00583	69902.9	69902.9	308.458	-0.47875	-1.26888	-2.13434	-1.98994	-0.20742	6.62016	6.00583	-57.0411
6.00625	69902.9	69902.9	323.783	-0.45957	-1.41537	-2.17997	-1.99353	-0.19817	6.54244	6.00625	-57.0411
6.00667	69902.9	69902.9	339.527	-0.42879	-1.56213	-2.21128	-1.99754	-0.18773	6.45859	6.00667	-57.0453
6.00708	69902.9	69902.9	355.694	-0.36634	-1.6914	-2.24369	-1.94635	-0.17914	6.36981	6.00708	-57.0581
6.0075	69902.9	69902.9	372.289	-0.25789	-1.78186	-2.26817	-1.93001	-0.16805	6.27875	6.0075	-57.0539
6.00792	69902.9	69902.9	389.315	-0.15163	-1.81221	-2.33752	-1.93468	-0.15742	6.19172	6.00792	-57.0624
6.00833	69902.9	69902.9	406.791	-0.12422	-1.78488	-2.37759	-1.95989	-0.14836	6.10375	6.00833	-57.0762
6.00875	69902.9	69902.9	424.613	-0.19518	-1.72916	-2.40298	-1.95781	-0.13887	6.01187	6.00875	-57.0795
6.00917	69902.9	69902.9	442.788	-0.30605	-1.68734	-2.41721	-1.93198	-0.12937	5.91825	6.00917	-57.0709
6.00958	69902.9	69902.9	461.315	-0.39421	-1.68804	-2.42474	-1.91299	-0.12039	5.81225	6.00958	-57.0624
6.01	69902.9	69902									

Appendix D Data from Dynamic Test Panel SCI2

6.01867	69902.9	69902.9	0.85111	-0.36738	-1.79878	-2.87633	-1.87129	-0.05734	5.19922	6.01867	-57.0411
6.01708	69902.9	69902.9	0.75775	-0.34434	-1.80468	-2.82652	-1.88758	-0.06047	5.25016	6.01708	-57.0368
6.0175	69902.9	69902.9	0.85723	-0.31491	-1.8114	-2.54209	-1.83909	-0.06396	5.30044	6.0175	-57.0368
6.01782	69902.9	69902.9	0.55845	-0.28786	-1.80202	-2.4298	-1.79381	-0.06727	5.37109	6.01782	-57.0411
6.01833	69902.9	69902.9	0.47624	-0.28068	-1.79878	-2.33335	-1.798	-0.06786	5.43609	6.01833	-57.0539
6.01875	69902.9	69902.9	0.41081	-0.29159	-1.77689	-2.26093	-1.83283	-0.06617	5.50687	6.01875	-57.0524
6.01917	69902.9	69902.9	0.35775	-0.27441	-1.6907	-2.18987	-1.94997	-0.06719	5.58219	6.01917	-57.0709
6.01958	69902.9	69902.9	0.28941	-0.26393	-1.58549	-2.07029	-1.87372	-0.06898	5.66312	6.01958	-57.0752
6.02	69902.9	69902.9	0.18206	-0.25592	-1.45128	-1.99789	-1.81785	-0.07008	5.74856	6.02	-57.0539
6.02042	69902.9	69902.9	0.08926	-0.26504	-1.3769	-1.96498	-1.95283	-0.06969	5.83031	6.02042	-57.0325
6.02083	69902.9	69902.9	-0.01895	-0.32741	-1.35316	-1.9592	-1.97438	-0.06786	5.91703	6.02083	-57.0197
6.02125	69902.9	69902.9	-0.14622	-0.45176	-1.36182	-1.98048	-1.99094	-0.06828	6.00594	6.02125	-57.024
6.02187	69902.9	69902.9	-0.30299	-0.58861	-1.38919	-1.95747	-1.97554	-0.06852	6.09406	6.02187	-57.0368
6.02208	69902.9	69902.9	-0.4735	-0.87324	-1.42741	-1.94838	-1.92989	-0.06769	6.17806	6.02208	-57.0453
6.0225	69902.9	69902.9	-0.63145	-0.67868	-1.46892	-1.94113	-1.89121	-0.06781	6.26328	6.0225	-57.0453
6.02292	69902.9	69902.9	-0.76302	-0.60085	-1.51301	-1.93465	-1.86561	-0.07039	6.34516	6.02292	-57.0453
6.02333	69902.9	69902.9	-0.86973	-0.47721	-1.54939	-1.92805	-1.83156	-0.07234	6.42422	6.02333	-57.0368
6.02375	69902.9	69902.9	-0.96615	-0.35811	-1.56352	-1.9204	-1.80132	-0.07305	6.50172	6.02375	-57.0411
6.02417	69902.9	69902.9	-1.00055	-0.28833	-1.53481	-1.90682	-1.77318	-0.07588	6.57797	6.02417	-57.0453
6.02458	69902.9	69902.9	-1.18087	-0.27272	-1.46101	-1.88507	-1.72325	-0.07859	6.64828	6.02458	-57.0581
6.025	69902.9	69902.9	-1.28146	-0.3161	-1.38116	-1.89187	-1.69785	-0.07922	6.71158	6.025	-57.0624
6.02542	69902.9	69902.9	-1.33783	-0.38809	-1.33915	-1.9409	-1.72974	-0.07734	6.76225	6.02542	-57.0498
6.02583	69902.9	69902.9	-1.34688	-0.44842	-1.26081	-1.9099	-1.75453	-0.075	6.80675	6.02583	-57.0325
6.02625	69902.9	69902.9	-1.29258	-0.481	-1.15181	-2.01098	-1.73892	-0.07312	6.8475	6.02625	-57.024
6.02667	69902.9	69902.9	-1.24049	-0.44824	-1.05292	-2.01087	-1.7183	-0.07219	6.87156	6.02667	-57.024
6.02708	69902.9	69902.9	-1.23711	-0.43809	-1.0052	-2.00632	-1.71653	-0.07047	6.89609	6.02708	-57.0293
6.0275	69902.9	69902.9	-1.26387	-0.44189	-1.0235	-2.01052	-1.71514	-0.06711	6.895	6.0275	-57.024
6.02792	69902.9	69902.9	-1.26758	-0.46708	-1.08474	-2.01307	-1.70715	-0.06387	6.88853	6.02792	-57.0089
6.02833	69902.9	69902.9	-1.23385	-0.49878	-1.18948	-2.00426	-1.71144	-0.0607	6.80187	6.02833	-56.9984
6.02875	69902.9	69902.9	-1.17617	-0.50397	-1.27993	-1.96258	-1.72001	-0.05908	6.89406	6.02875	-57.0089
6.02917	69902.9	69902.9	-1.10189	-0.46764	-1.34085	-1.97924	-1.71842	-0.05703	6.87852	6.02917	-57.024
6.02958	69902.9	69902.9	-0.99512	-0.40814	-1.3622	-1.78484	-1.70843	-0.05453	6.85078	6.02958	-57.024
6.03	69902.9	69902.9	-0.85716	-0.339	-1.35201	-1.6541	-1.69785	-0.05266	6.81359	6.03	-57.0197
6.03042	69902.9	69902.9	-0.71328	-0.28354	-1.33185	-1.68015	-1.68258	-0.05125	6.78578	6.03042	-57.0112
6.03083	69902.9	69902.9	-0.59678	-0.19525	-1.3132	-1.51811	-1.60649	-0.0507	6.71203	6.03083	-57.0027
6.03125	69902.9	69902.9	-0.47989	-0.14753	-1.32675	-1.53305	-1.5988	-0.04953	6.65187	6.03125	-56.9956
6.03167	69902.9	69902.9	-0.39004	-0.12363	-1.38328	-1.62236	-1.60987	-0.04984	6.58719	6.03167	-56.9813
6.03208	69902.9	69902.9	-0.32122	-0.12747	-1.4207	-1.72047	-1.60719	-0.04453	6.52844	6.03208	-56.9884
6.0325	69902.9	69902.9	-0.23903	-0.16408	-1.41015	-1.79715	-1.59857	-0.04376	6.47375	6.0325	-57.0155
6.03292	69902.9	69902.9	-0.2474	-0.21578	-1.38544	-1.86503	-1.57545	-0.04328	6.41378	6.03292	-57.0197
6.03333	69902.9	69902.9	-0.19044	-0.26188	-1.30718	-1.94195	-1.57522	-0.04422	6.35125	6.03333	-57.0112
6.03375	69902.9	69902.9	-0.05352	-0.29835	-1.25459	-2.03345	-1.58282	-0.04625	6.28822	6.03375	-56.9984
6.03417	69902.9	69902.9	0.01797	-0.31953	-1.22621	-2.12938	-1.62584	-0.04555	6.22547	6.03417	-56.9984
6.03458	69902.9	69902.9	0.05845	-0.30352	-1.23513	-2.2145	-1.64958	-0.04516	6.18172	6.03458	-57.0089
6.035	69902.9	69902.9	0.0735	-0.2543	-1.26262	-2.28228	-1.69986	-0.04773	6.09703	6.035	-57.024
6.03542	69902.9	69902.9	0.12233	-0.19909	-1.35201	-2.32176	-1.87912	-0.05391	6.02691	6.03542	-57.0325
6.03583	69902.9	69902.9	0.22729	-0.1515	-1.41982	-2.32408	-1.89486	-0.05853	5.95408	6.03583	-57.0325
6.03625	69902.9	69902.9	0.36823	-0.12383	-1.46786	-2.28296	-1.88202	-0.06391	5.88016	6.03625	-57.0368
6.03667	69902.9	69902.9	0.51152	-0.13262	-1.48973	-2.19956	-1.66406	-0.06828	5.81375	6.03667	-57.024
6.03708	69902.9	69902.9	0.64264	-0.16745	-1.48023	-2.08743	-1.65074	-0.07312	5.75734	6.03708	-57.0089
6.0375	69902.9	69902.9	0.73852	-0.2	-1.46205	-1.98152	-1.61808	-0.07908	5.70158	6.0375	-56.9984
6.03792	69902.9	69902.9	0.80387	-0.22552	-1.49881	-1.8794	-1.60814	-0.08539	5.64359	6.03792	-57.0027
6.03833	69902.9	69902.9	0.86237	-0.25404	-1.58831	-1.85888	-1.63408	-0.09281	5.59281	6.03833	-57.0155
6.03875	69902.9	69902.9	0.91608	-0.28522	-1.67657	-1.85739	-1.65132	-0.10187	5.55281	6.03875	-57.0155
6.03917	69902.9	69902.9	0.9237	-0.31237	-1.74816	-1.87013	-1.63846	-0.11021	5.52328	6.03917	-57.0089
6.03958	69902.9	69902.9	0.97786	-0.33275	-1.80051	-1.91148	-1.63035	-0.11742	5.49797	6.03958	-57.0089
6.04	69902.9	69902.9	0.82357	-0.33628	-1.82032	-1.98527	-1.64588	-0.12422	5.47031	6.04	-57.0112
6.04042	69902.9	69902.9	0.84342	-0.31445	-1.78152	-2.07573	-1.6592	-0.13141	5.44703	6.04042	-57.0197
6.04083	69902.9	69902.9	0.9224	-0.28255	-1.68132	-2.1479	-1.66719	-0.13836	5.42822	6.04083	-57.0325
6.04125	69902.9	69902.9	0.97611	-0.2668	-1.54255	-2.18184	-1.68352	-0.14641	5.41766	6.04125	-57.0325
6.04167	69902.9	69902.9	0.96784	-0.27272	-1.39	-2.1708	-1.89808	-0.15508	5.41359	6.04167	-57.0293
6.04208	69902.9	69902.9	0.92598	-0.29134	-1.25714	-2.12309	-1.87305	-0.16381	5.42078	6.04208	-57.0197
6.0425	69902.9	69902.9	0.87604	-0.31387	-1.17617	-2.05548	-1.87869	-0.17289	5.43125	6.0425	-57.024
6.04292	69902.9	69902.9	0.81992	-0.32031	-1.18401	-1.98909	-1.87819	-0.1807	5.43891	6.04292	-57.024
6.04333	69902.9	69902.9	0.75951	-0.30801	-1.20907	-1.93778	-1.84935	-0.18609	5.46225	6.04333	-57.0155
6.04375	69902.9	69902.9	0.70169	-0.31139	-1.28598	-1.89434	-1.89502	-0.18984	5.50641	6.04375	-57.0112
6.04417	69902.9	69902.9	0.62832	-0.34349	-1.40378	-1.87627	-1.87985	-0.19148	5.55853	6.04417	-57.0089
6.04458	69902.9	69902.9	0.52513	-0.35905	-1.52783	-1.86829	-1.89016	-0.19148	5.61084	6.04458	-57.0112
6.045	69902.9	69902.9	0.39121	-0.32585	-1.58935	-1.82553	-1.89908	-0.19273	5.66187	6.045	-57.0197
6.04542	69902.9	69902.9	0.23945	-0.27331	-1.5934	-1.77789	-1.84895	-0.19445	5.72447	6.04542	-57.024
6.04583	69902.9	69902.9	0.08088	-0.2599	-1.5781	-1.77213	-1.6486	-0.19477	5.77875	6.04583	-57.0112
6.04625	69902.9	69902.9	-0.0686	-0.32378	-1.55159	-1.81893	-1.58248	-0.19234	5.83562	6.04625	-56.9984
6.04667	69902.9	69902.9	-0.19389	-0.48128	-1.50986	-1.8926	-1.59028	-0.18742	5.89031	6.04667	-57.0027
6.04708	69902.9	69902.9	-0.28451	-0.62734	-1.42622	-1.95098	-1.62954	-0.18338	5.94203	6.04708	-57.0155
6.0475	69902.9	69902.9	-0.33372	-0.7554	-1.30034	-1.97473	-1.64819	-0.18125	5.99156	6.0475	-57.0155
6.04792	69902.9	69902.9	-0.35352	-0.78932	-1.15082	-1.96164	-1.64506	-0.17984	6.04359	6.04792	-57.0155
6.04833	69902.9	69902.9	-0.27012	-0.70814	-1.02093	-1.916	-1.64993	-0.17838	6.09809	6.04833	-57.0027
6.04875	69902.9	69902.9	-0.40859	-0.47269	-0.97081	-1.85838	-1.65665	-0.17687	6.15578	6.04875	-56.9984
6.04917	69902.9	69902.9	-0.47305	-0.34831	-1.00034	-1.78627	-1.63916	-0.17586	6.20656	6.04917	-57.0089
6.04958	69902.9	69902.9	-0.5418	-0.21784	-1.08802	-1.72221	-1.60429	-0.17695	6.25329	6.04958	-56.9984
6.05	69902.9	69902.9	-0.59284	-0.18216	-1.18243	-1.65815	-1.5819	-0.17984	6.29531	6.05	-56.9984
6.05042	69902.9	69902.9	-0.63971	-0.22389	-1.24509	-1.59514	-1.49506	-0.18312	6.33625	6.05042	-57.0089
6.05083	69902.9	69902.9	-0.70221	-0.30215	-1.29374	-1.5729	-1.45255	-0.18422	6.37281	6.05083	-57.0155
6.05125	69902.9	69902.9	-0.7588								

Appendix D Data from Dynamic Test Panel SCI2

8.05792	89902.9	89902.9	-0.47813	-0.23073	-1.59039	-1.70136	-1.409	-0.20492	8.275	8.05792	-56.9984
8.05833	89902.9	89902.9	-0.42507	-0.19473	-1.53016	-1.73715	-1.38487	-0.20586	8.23887	8.05833	-57.0027
8.05875	89902.9	89902.9	-0.32129	-0.18177	-1.43158	-1.77966	-1.36579	-0.20625	8.21016	8.05875	-57.0027
8.05917	89902.9	89902.9	-0.18678	-0.20306	-1.34297	-1.83319	-1.3512	-0.20538	8.18	8.05917	-56.9899
8.05958	89902.9	89902.9	-0.07767	-0.2188	-1.26505	-1.89187	-1.3571	-0.20326	8.13837	8.05958	-56.9858
8.06	89902.9	89902.9	-0.01471	-0.17324	-1.25669	-1.94137	-1.39046	-0.19889	8.09609	8.06	-56.9771
8.06042	89902.9	89902.9	0.02939	-0.08751	-1.24544	-1.97577	-1.41583	-0.19641	8.02908	8.06042	-56.9643
8.06083	89902.9	89902.9	0.086	0.05469	-1.2437	-1.99709	-1.41884	-0.19453	8.07780	8.06083	-56.9643
8.06125	89902.9	89902.9	0.18751	0.12789	-1.2605	-2.01017	-1.42452	-0.19312	8.03359	8.06125	-56.9643
8.06167	89902.9	89902.9	0.2625	0.11738	-1.2949	-2.02778	-1.43274	-0.19141	8.09109	8.06167	-56.96
8.06208	89902.9	89902.9	0.37448	0.03555	-1.34193	-2.05303	-1.42139	-0.1893	8.04672	8.06208	-56.9728
8.0625	89902.9	89902.9	0.489	-0.07285	-1.38676	-2.07017	-1.39986	-0.18684	8.04066	8.0625	-56.9813
8.06292	89902.9	89902.9	0.57598	-0.15931	-1.41432	-2.06218	-1.37425	-0.18312	8.07659	8.06292	-56.9899
8.06333	89902.9	89902.9	0.80851	-0.20345	-1.42746	-2.0198	-1.32583	-0.17858	8.07854	8.06333	-56.9858
8.06375	89902.9	89902.9	0.611	-0.22415	-1.43085	-1.9804	-1.30182	-0.17148	8.03720	8.06375	-56.9771
8.06417	89902.9	89902.9	0.61901	-0.24779	-1.47294	-1.98963	-1.33197	-0.16047	8.07547	8.06417	-56.9695
8.06458	89902.9	89902.9	0.63249	-0.28238	-1.48228	-1.95909	-1.35768	-0.15102	8.05156	8.06458	-56.96
8.065	89902.9	89902.9	0.64922	-0.32658	-1.48761	-1.95088	-1.35154	-0.14562	8.02806	8.065	-56.9643
8.06542	89902.9	89902.9	0.67721	-0.37507	-1.50074	-1.94681	-1.34795	-0.14125	8.00837	8.06542	-56.9899
8.06583	89902.9	89902.9	0.69993	-0.39727	-1.51	-1.94689	-1.37274	-0.13562	8.05941	8.06583	-57.0069
8.06625	89902.9	89902.9	0.70143	-0.35697	-1.5261	-1.9418	-1.40008	-0.12902	8.059047	8.06625	-57.0069
8.06667	89902.9	89902.9	0.69548	-0.26578	-1.54568	-1.9343	-1.41896	-0.12547	8.05031	8.06667	-56.9984
8.06708	89902.9	89902.9	0.64115	-0.17383	-1.56259	-1.93349	-1.43364	-0.12141	8.05244	8.06708	-56.9941
8.0675	89902.9	89902.9	0.57683	-0.11558	-1.58841	-1.94832	-1.44819	-0.11844	8.00802	8.0675	-57.0027
8.06792	89902.9	89902.9	0.51393	-0.08598	-1.5485	-1.97716	-1.43853	-0.11887	8.05156	8.06792	-56.9984
8.06833	89902.9	89902.9	0.46349	-0.11419	-1.50259	-2.01017	-1.42626	-0.12211	8.03641	8.06833	-56.9984
8.06875	89902.9	89902.9	0.42467	-0.15345	-1.4251	-2.02523	-1.41432	-0.1257	8.06094	8.06875	-57.0069
8.06917	89902.9	89902.9	0.38342	-0.18893	-1.32201	-2.01735	-1.37946	-0.12937	8.00802	8.06917	-57.0155
8.06958	89902.9	89902.9	0.35755	-0.22862	-1.20617	-1.99189	-1.33533	-0.13219	8.07265	8.06958	-57.0224
8.07	89902.9	89902.9	0.31302	-0.30652	-1.13053	-1.97982	-1.34135	-0.13287	8.07644	8.07	-57.0283
8.07042	89902.9	89902.9	0.25137	-0.42051	-1.01028	-1.9811	-1.3783	-0.13287	8.07878	8.07042	-57.0187
8.07083	89902.9	89902.9	0.17376	-0.53307	-1.0795	-1.94102	-1.37216	-0.13641	8.02484	8.07083	-57.0080
8.07125	89902.9	89902.9	0.08648	-0.58603	-1.12186	-1.86237	-1.35073	-0.14156	8.05820	8.07125	-57.0027
8.07167	89902.9	89902.9	0.00458	-0.58112	-1.18053	-1.77818	-1.35380	-0.14406	8.00047	8.07167	-57.0112
8.07208	89902.9	89902.9	-0.06354	-0.49577	-1.2064	-1.70689	-1.37042	-0.14344	8.05904	8.07208	-57.0325
8.0725	89902.9	89902.9	-0.10598	-0.38913	-1.23478	-1.6497	-1.39811	-0.14281	8.00570	8.0725	-57.0283
8.07292	89902.9	89902.9	-0.1332	-0.32598	-1.23617	-1.59854	-1.43969	-0.14287	8.00381	8.07292	-57.0224
8.07333	89902.9	89902.9	-0.1623	-0.33878	-1.21853	-1.55758	-1.46413	-0.14289	8.11768	8.07333	-57.0155
8.07375	89902.9	89902.9	-0.22077	-0.40417	-1.19992	-1.52946	-1.45956	-0.14287	8.05544	8.07375	-57.0224
8.07417	89902.9	89902.9	-0.30723	-0.48132	-1.18775	-1.518	-1.4544	-0.14352	8.09889	8.07417	-57.0453
8.07458	89902.9	89902.9	-0.38971	-0.51849	-1.17073	-1.52989	-1.45452	-0.14336	8.22869	8.07458	-57.0581
8.075	89902.9	89902.9	-0.4401	-0.49829	-1.13366	-1.55275	-1.44166	-0.14256	8.25806	8.075	-57.0496
8.07542	89902.9	89902.9	-0.46992	-0.4459	-1.06254	-1.56722	-1.41988	-0.14078	8.20875	8.07542	-57.0380
8.07583	89902.9	89902.9	-0.50851	-0.4028	-0.95933	-1.55101	-1.39452	-0.13922	8.31829	8.07583	-57.0197
8.07625	89902.9	89902.9	-0.54473	-0.37169	-0.8384	-1.49413	-1.34123	-0.13703	8.34484	8.07625	-57.0027
8.07667	89902.9	89902.9	-0.59288	-0.34492	-0.75681	-1.43077	-1.29374	-0.13312	8.36859	8.07667	-56.9984
8.07708	89902.9	89902.9	-0.63522	-0.30462	-0.74678	-1.42046	-1.30811	-0.12594	8.38825	8.07708	-56.9884
8.0775	89902.9	89902.9	-0.62985	-0.23242	-0.785	-1.41985	-1.33509	-0.11883	8.40287	8.0775	-57.0112
8.07792	89902.9	89902.9	-0.67832	-0.13945	-0.84709	-1.42197	-1.33567	-0.11344	8.41687	8.07792	-57.0069
8.07833	89902.9	89902.9	-0.7403	-0.07773	-0.92064	-1.42718	-1.3373	-0.10922	8.43141	8.07833	-57.0112
8.07875	89902.9	89902.9	-0.78828	-0.08898	-0.98586	-1.43781	-1.35919	-0.10482	8.44812	8.07875	-57.0155
8.07917	89902.9	89902.9	-0.80397	-0.15449	-1.01632	-1.4412	-1.37888	-0.10039	8.46344	8.07917	-57.0089
8.07958	89902.9	89902.9	-0.78079	-0.23874	-1.00439	-1.43992	-1.38881	-0.09531	8.47787	8.07958	-57.0069
8.08	89902.9	89902.9	-0.73987	-0.29897	-0.98394	-1.44818	-1.40308	-0.09055	8.49031	8.08	-57.0197
8.08042	89902.9	89902.9	-0.69477	-0.30394	-0.91335	-1.45985	-1.40934	-0.08781	8.49141	8.08042	-57.0325
8.08083	89902.9	89902.9	-0.63291	-0.25573	-0.8713	-1.48498	-1.39588	-0.08617	8.47812	8.08083	-57.0283
8.08125	89902.9	89902.9	-0.60104	-0.19468	-0.84583	-1.5122	-1.38062	-0.08484	8.45562	8.08125	-57.0197
8.08167	89902.9	89902.9	-0.57402	-0.15897	-0.83539	-1.52812	-1.37019	-0.08406	8.43406	8.08167	-57.0155
8.08208	89902.9	89902.9	-0.53366	-0.16452	-0.82937	-1.53259	-1.33753	-0.08352	8.41344	8.08208	-57.0027
8.0825	89902.9	89902.9	-0.47865	-0.23646	-0.81651	-1.51383	-1.281	-0.08469	8.39	8.0825	-56.9941
8.08292	89902.9	89902.9	-0.41327	-0.36315	-0.8179	-1.48707	-1.24729	-0.08469	8.36108	8.08292	-56.9899
8.08333	89902.9	89902.9	-0.34238	-0.47487	-0.85274	-1.47808	-1.28339	-0.08312	8.32625	8.08333	-56.9884
8.08375	89902.9	89902.9	-0.28576	-0.49188	-0.87620	-1.44711	-1.2722	-0.08383	8.29287	8.08375	-57.0197
8.08417	89902.9	89902.9	-0.18125	-0.38783	-0.88126	-1.39885	-1.26258	-0.08617	8.26489	8.08417	-57.0325
8.08458	89902.9	89902.9	-0.11348	-0.18991	-0.90628	-1.35571	-1.25941	-0.0882	8.24234	8.08458	-57.0325
8.085	89902.9	89902.9	-0.09516	0.02282	-0.97288	-1.35316	-1.26756	-0.09016	8.21703	8.085	-57.0283
8.08542	89902.9	89902.9	-0.05404	0.15586	-1.06173	-1.38757	-1.29548	-0.09184	8.19	8.08542	-57.0325
8.08583	89902.9	89902.9	0.01003	0.16595	-1.13864	-1.44201	-1.33243	-0.09312	8.16872	8.08583	-57.0411
8.08625	89902.9	89902.9	0.07643	0.07843	-1.18231	-1.49564	-1.34737	-0.09594	8.14078	8.08625	-57.0496
8.08667	89902.9	89902.9	0.11569	-0.05234	-1.19888	-1.53375	-1.33741	-0.09789	8.10887	8.08667	-57.0453
8.08708	89902.9	89902.9	0.14141	-0.17617	-1.16517	-1.55888	-1.32803	-0.09922	8.06703	8.08708	-57.0283
8.0875	89902.9	89902.9	0.18014	-0.23945	-1.12636	-1.57904	-1.31702	-0.10242	8.02109	8.0875	-57.0112
8.08792	89902.9	89902.9	0.24954	-0.22148	-1.08964	-1.60183	-1.29829	-0.10875	8.07864	8.08792	-57.0089
8.08833	89902.9	89902.9	0.31751	-0.16203	-1.05885	-1.62689	-1.27509	-0.11718	8.04078	8.08833	-57.0155
8.08875	89902.9	89902.9	0.34095	-0.11621	-1.03439	-1.64077	-1.2488	-0.12453	8.00719	8.08875	-57.0325
8.08917	89902.9	89902.9	0.32747	-0.10877	-1.01111	-1.65873	-1.19783	-0.13148	8.04547	8.08917	-57.0539
8.08958	89902.9	89902.9	0.31623	-0.14805	-1.01551	-1.67564	-1.1794	-0.13516	8.07844	8.08958	-57.0624
8.09	89902.9	89902.9	0.33887	-0.21068	-1.05025	-1.70194	-1.21081	-0.13625	8.05203	8.09	-57.0581
8.09042	89902.9	89902.9	0.40339	-0.26458	-1.0732	-1.7031	-1.23397	-0.13789	8.05707	8.09042	-57.0539
8.09083	89902.9	89902.9	0.4908	-0.28509	-1.07609	-1.87333	-1.22702	-0.13884	8.07406	8.09083	-57.0624
8.09125	89902.9	89902.9	0.5347	-0.27174	-1.08154	-1.83082	-1.22891	-0.14258	8.07631	8.09125	-57.0687
8.09167	89902.9	89902.9	0.55052	-0.23587	-1.11316	-1.80877	-1.24463	-0.14489	8.04489	8.09167	-57.0581
8.09208	89902.9	89902.9	0.54818	-0.18908	-1.17098	-1.54885	-1.25957	-0.14856	8.07570	8.09208	-57.0380
8.0925	89902.9	89902.9	0.54								

Appendix D Data from Dynamic Test Panel SCI2

8.09917	89902.9	89902.9	-0.13581	-0.41719	-1.08833	-1.51881	-1.32791	-0.17656	5.98656	8.09917	-57.0824
8.09958	89902.9	89902.9	-0.18542	-0.40832	-1.16239	-1.49054	-1.32177	-0.17477	6.02375	8.09958	-57.0539
6.1	89902.9	89902.9	-0.22155	-0.42214	-1.24034	-1.46302	-1.31265	-0.17492	6.05869	6.1	-57.0411
8.10042	89902.9	89902.9	-0.25755	-0.42802	-1.27938	-1.49182	-1.30231	-0.17594	6.09281	8.10042	-57.0453
8.10083	89902.9	89902.9	-0.3127	-0.39811	-1.26837	-1.49935	-1.27981	-0.17838	6.11984	8.10083	-57.0581
6.10125	89902.9	89902.9	-0.36222	-0.35202	-1.2071	-1.49208	-1.25227	-0.18184	6.14172	6.10125	-57.0709
8.10167	89902.9	89902.9	-0.39737	-0.30964	-1.10227	-1.46597	-1.22077	-0.18359	6.15969	8.10167	-57.0709
6.10208	89902.9	89902.9	-0.37885	-0.26504	-0.98964	-1.42035	-1.16378	-0.1857	6.17797	6.10208	-57.0667
6.1025	89902.9	89902.9	-0.36834	-0.22988	-0.85612	-1.39174	-1.11744	-0.18578	6.19203	6.1025	-57.0539
6.10292	89902.9	89902.9	-0.39531	-0.2056	-0.81282	-1.41757	-1.13796	-0.19398	6.20406	6.10292	-57.0411
8.10333	89902.9	89902.9	-0.4498	-0.1778	-0.8106	-1.45778	-1.172	-0.18281	6.21828	8.10333	-57.0388
6.10375	89902.9	89902.9	-0.48542	-0.12982	-0.82184	-1.47884	-1.17524	-0.18082	6.23094	6.10375	-57.0411
8.10417	89902.9	89902.9	-0.48288	-0.07754	-0.84767	-1.47398	-1.17189	-0.17719	6.23375	8.10417	-57.0539
8.10458	89902.9	89902.9	-0.48081	-0.05189	-0.89238	-1.48101	-1.1793	-0.17516	6.23047	8.10458	-57.0752
6.105	89902.9	89902.9	-0.42594	-0.06494	-0.94856	-1.4434	-1.18741	-0.17469	6.23375	6.105	-57.0637
8.10542	89902.9	89902.9	-0.42122	-0.11081	-1.00462	-1.42359	-1.19957	-0.17578	6.25266	8.10542	-57.0795
8.10583	89902.9	89902.9	-0.41569	-0.17548	-1.05605	-1.40656	-1.21926	-0.17672	6.26906	8.10583	-57.0709
6.10625	89902.9	89902.9	-0.42643	-0.23262	-1.10795	-1.39568	-1.22482	-0.17687	6.25812	6.10625	-57.0667
6.10667	89902.9	89902.9	-0.45293	-0.25283	-1.16216	-1.3986	-1.21982	-0.17672	6.23531	6.10667	-57.0624
6.10708	89902.9	89902.9	-0.46942	-0.22806	-1.20177	-1.41027	-1.20894	-0.1775	6.21516	6.10708	-57.0709
8.1075	89902.9	89902.9	-0.44803	-0.17552	-1.20061	-1.43425	-1.20814	-0.17828	6.19719	8.1075	-57.0752
8.10792	89902.9	89902.9	-0.40039	-0.12824	-1.15161	-1.45348	-1.18914	-0.17877	6.18084	8.10792	-57.0539
8.10833	89902.9	89902.9	-0.35938	-0.10378	-1.08439	-1.44537	-1.15254	-0.1816	6.16391	8.10833	-57.0411
8.10875	89902.9	89902.9	-0.33218	-0.10718	-0.97659	-1.42048	-1.1325	-0.1832	6.14844	8.10875	-57.0539
8.10917	89902.9	89902.9	-0.28652	-0.11847	-0.84346	-1.4348	-1.16181	-0.1818	6.13703	8.10917	-57.0667
6.10959	89902.9	89902.9	-0.20332	-0.12692	-0.93281	-1.45197	-1.1932	-0.17893	6.12469	6.10959	-57.0539
6.11	89902.9	89902.9	-0.11439	-0.11914	-0.91881	-1.44745	-1.20131	-0.17672	6.10887	6.11	-57.0411
8.11042	89902.9	89902.9	-0.05911	-0.09303	-0.92794	-1.43749	-1.19505	-0.17375	6.08516	8.11042	-57.0283
8.11083	89902.9	89902.9	-0.03359	-0.08816	-0.97601	-1.44201	-1.1815	-0.16891	6.06287	8.11083	-57.0112
8.11125	89902.9	89902.9	-0.00769	-0.07195	-1.04748	-1.45579	-1.18301	-0.16291	6.04312	8.11125	-57.0069
8.11167	89902.9	89902.9	0.04584	-0.10378	-1.11038	-1.48784	-1.20594	-0.1575	6.02469	8.11167	-57.024
8.11208	89902.9	89902.9	0.11582	-0.12824	-1.14779	-1.47317	-1.22588	-0.15273	6.00453	8.11208	-57.0539
8.1125	89902.9	89902.9	0.18145	-0.13184	-1.16262	-1.47583	-1.2349	-0.14656	5.97781	8.1125	-57.0709
8.11292	89902.9	89902.9	0.23558	-0.1235	-1.16517	-1.48614	-1.24728	-0.13883	5.94062	8.11292	-57.0709
8.11333	89902.9	89902.9	0.23789	-0.11211	-1.16343	-1.4924	-1.26293	-0.13195	5.91109	8.11333	-57.0624
8.11375	89902.9	89902.9	0.21992	-0.11349	-1.16717	-1.49927	-1.26907	-0.12727	5.88672	8.11375	-57.0581
8.11417	89902.9	89902.9	0.20812	-0.14577	-1.1398	-1.48093	-1.28186	-0.12286	5.85219	8.11417	-57.0453
8.11458	89902.9	89902.9	0.22441	-0.20111	-1.10189	-1.47398	-1.29884	-0.11789	5.85406	8.11458	-57.0197
8.115	89902.9	89902.9	0.27533	-0.24229	-1.03937	-1.48321	-1.1985	-0.11576	5.84669	8.115	-57.0069
8.11542	89902.9	89902.9	0.32863	-0.24805	-0.98998	-1.46519	-1.14528	-0.11359	5.83375	8.11542	-57.024
8.11583	89902.9	89902.9	0.34874	-0.2308	-0.9882	-1.49216	-1.18123	-0.10773	5.81156	8.11583	-57.0539
8.11625	89902.9	89902.9	0.34408	-0.21901	-0.98478	-1.5012	-1.17937	-0.10437	5.79806	8.11625	-57.0709
8.11667	89902.9	89902.9	0.35072	-0.23457	-0.99582	-1.48174	-1.16343	-0.10383	5.79822	8.11667	-57.0709
8.11708	89902.9	89902.9	0.3582	-0.2789	-1.00312	-1.48135	-1.15011	-0.10484	5.80625	8.11708	-57.0667
6.1175	89902.9	89902.9	0.34082	-0.32995	-1.03219	-1.45911	-1.15981	-0.10562	5.81266	6.1175	-57.0667
8.11792	89902.9	89902.9	0.2972	-0.35352	-1.07988	-1.46772	-1.1727	-0.10648	5.82703	8.11792	-57.0752
8.11833	89902.9	89902.9	0.24622	-0.33314	-1.12728	-1.49128	-1.18082	-0.10789	5.84719	8.11833	-57.0709
8.11875	89902.9	89902.9	0.211	-0.28359	-1.15636	-1.48008	-1.19586	-0.11039	5.86856	8.11875	-57.0496
8.11917	89902.9	89902.9	0.19421	-0.23633	-1.15891	-1.48834	-1.20293	-0.1125	5.88156	8.11917	-57.0453
8.11959	89902.9	89902.9	0.16478	-0.21361	-1.13968	-1.47808	-1.18991	-0.11484	5.89734	8.11959	-57.0624
6.12	89902.9	89902.9	0.12181	-0.21582	-1.11327	-1.48193	-1.17328	-0.11684	5.91809	6.12	-57.0667
8.12042	89902.9	89902.9	0.08941	-0.23112	-1.08513	-1.44907	-1.16282	-0.11742	5.93625	8.12042	-57.0496
8.12083	89902.9	89902.9	0.06055	-0.25944	-1.05185	-1.42558	-1.14028	-0.11884	5.95406	8.12083	-57.0453
8.12125	89902.9	89902.9	0.02715	-0.30124	-1.0027	-1.38015	-1.10215	-0.12477	5.97109	8.12125	-57.0453
8.12167	89902.9	89902.9	-0.01087	-0.33268	-0.95157	-1.33011	-1.09385	-0.12937	5.99094	8.12167	-57.0496
8.12208	89902.9	89902.9	-0.03581	-0.33457	-0.91894	-1.31031	-1.11188	-0.13227	6.01437	8.12208	-57.0539
6.1225	89902.9	89902.9	-0.03301	-0.31283	-0.86064	-1.28749	-1.12266	-0.13594	6.04766	6.1225	-57.0581
6.12292	89902.9	89902.9	-0.01771	-0.29788	-0.77898	-1.24046	-1.1025	-0.14039	6.08687	6.12292	-57.0624
8.12333	89902.9	89902.9	-0.0237	-0.3054	-0.71272	-1.20038	-1.09385	-0.14219	6.11984	8.12333	-57.0667
8.12375	89902.9	89902.9	-0.05498	-0.32643	-0.68851	-1.19552	-1.09258	-0.14094	6.14516	8.12375	-57.0581
8.12417	89902.9	89902.9	-0.1015	-0.34961	-0.70278	-1.21891	-1.10189	-0.13859	6.18734	8.12417	-57.0496
8.12458	89902.9	89902.9	-0.18204	-0.38494	-0.736	-1.24544	-1.12937	-0.13689	6.18734	8.12458	-57.0453
6.125	89902.9	89902.9	-0.22077	-0.36042	-0.77145	-1.25041	-1.14733	-0.13578	6.20489	6.125	-57.0539
8.12542	89902.9	89902.9	-0.28548	-0.33457	-0.78925	-1.25471	-1.14865	-0.13625	6.2225	8.12542	-57.0539
8.12583	89902.9	89902.9	-0.2972	-0.29818	-0.81732	-1.24034	-1.14995	-0.13711	6.24494	8.12583	-57.0496
8.12625	89902.9	89902.9	-0.31641	-0.25671	-0.83018	-1.21719	-1.1471	-0.13672	6.27672	8.12625	-57.0453
6.12667	89902.9	89902.9	-0.33424	-0.20892	-0.83759	-1.18254	-1.13528	-0.135	6.31062	6.12667	-57.0453
8.12708	89902.9	89902.9	-0.35397	-0.17233	-0.8382	-1.1378	-1.11316	-0.13352	6.33406	8.12708	-57.0453
6.1275	89902.9	89902.9	-0.36582	-0.15824	-0.82207	-1.08571	-1.08072	-0.13281	6.34734	6.1275	-57.0411
8.12792	89902.9	89902.9	-0.37595	-0.15938	-0.78971	-1.02524	-1.02234	-0.13156	6.36812	8.12792	-57.0388
8.12833	89902.9	89902.9	-0.39499	-0.15573	-0.75211	-0.97381	-0.95481	-0.13086	6.385	8.12833	-57.0411
8.12875	89902.9	89902.9	-0.41689	-0.14434	-0.7526	-0.97891	-0.94717	-0.12867	6.36719	8.12875	-57.0496
8.12917	89902.9	89902.9	-0.43125	-0.12721	-0.75013	-0.92316	-0.9752	-0.12602	6.36841	8.12917	-57.0624
8.12959	89902.9	89902.9	-0.42533	-0.11029	-0.72636	-0.86659	-0.89933	-0.12242	6.36453	8.12959	-57.0667
6.13	89902.9	89902.9	-0.40716	-0.10625	-0.67959	-0.10749	-0.89582	-0.11758	6.36422	6.13	-57.0581
8.13042	89902.9	89902.9	-0.38115	-0.11667	-0.64311	-1.15395	-1.01134	-0.11227	6.35906	8.13042	-57.0325
8.13083	89902.9	89902.9	-0.3832	-0.13223	-0.63488	-1.21185	-1.03173	-0.10828	6.34612	8.13083	-57.0195
8.13125	89902.9	89902.9	-0.38314	-0.14848	-0.64878	-1.27428	-1.0454	-0.10672	6.33841	8.13125	-57.0155
8.13167	89902.9	89902.9	-0.38802	-0.15768	-0.6723	-1.3249	-1.05802	-0.10555	6.32234	8.13167	-57.0283
8.13208	89902.9	89902.9	-0.3875	-0.15872	-0.6972	-1.34011	-1.06057	-0.10482	6.30841	8.13208	-57.0411
8.1325	89902.9	89902.9	-0.37357	-0.14038	-0.71979	-1.33558	-1.04887	-0.10453	6.29126	8.1325	-57.0453
8.13292	89902.9	89902.9	-0.33208	-0.09967	-0.73486	-1.28685	-1.03694	-0.10445	6.27381	8.13292	-57.0388
8.13333	89902.9	89902.9	-0.25938	-0.04492	-0.73994	-1.22772	-1.02431	-0.10841	6.25268	8.13333	-57.0388
8.13375	89902.9	89902.9</									

Appendix D Data from Dynamic Test Panel SCI2

6.14042	69902.9	69902.9	0.2194	-0.21868	-0.98698	-1.30034	-1.01053	-0.14953	5.88891	6.14042	-57.0539
6.14083	69902.9	69902.9	0.2832	-0.22669	-0.93651	-1.24718	-0.96952	-0.15297	5.88219	6.14083	-57.0411
6.14125	69902.9	69902.9	0.32096	-0.22843	-0.90628	-1.20223	-0.92539	-0.15758	5.875	6.14125	-57.0325
6.14167	69902.9	69902.9	0.31953	-0.2321	-0.91893	-1.20540	-0.9378	-0.16086	5.86531	6.14167	-57.0411
6.14208	69902.9	69902.9	0.28928	-0.23457	-0.94474	-1.23212	-0.96779	-0.16289	5.85703	6.14208	-57.0498
6.1425	69902.9	69902.9	0.27786	-0.23822	-0.95609	-1.25146	-0.97173	-0.1658	5.85172	6.1425	-57.0498
6.14292	69902.9	69902.9	0.26393	-0.2513	-0.95574	-1.28291	-0.97161	-0.1725	5.85047	6.14292	-57.0411
6.14333	69902.9	69902.9	0.25625	-0.27715	-0.95261	-1.27718	-0.98968	-0.175	5.84875	6.14333	-57.0325
6.14375	69902.9	69902.9	0.24499	-0.30438	-0.94867	-1.29409	-1.01412	-0.17489	5.84203	6.14375	-57.0368
6.14417	69902.9	69902.9	0.22939	-0.32161	-0.94395	-1.3044	-1.03936	-0.17983	5.83281	6.14417	-57.0411
6.14458	69902.9	69902.9	0.21491	-0.32402	-0.93755	-1.30706	-1.05925	-0.17422	5.82844	6.14458	-57.0325
6.145	69902.9	69902.9	0.20475	-0.3084	-0.93431	-1.30278	-1.07181	-0.17582	5.83672	6.145	-57.0325
6.14542	69902.9	69902.9	0.19082	-0.28444	-0.93083	-1.29791	-1.07586	-0.17687	5.85797	6.14542	-57.0411
6.14583	69902.9	69902.9	0.18986	-0.26992	-0.94586	-1.29258	-1.09455	-0.17773	5.87889	6.14583	-57.0501
6.14625	69902.9	69902.9	0.14271	-0.2765	-0.94763	-1.28019	-1.09671	-0.17631	5.8875	6.14625	-57.0624
6.14667	69902.9	69902.9	0.18462	-0.29949	-0.93327	-1.25447	-1.09069	-0.17227	5.91266	6.14667	-57.0624
6.14708	69902.9	69902.9	0.0625	-0.3308	-0.8918	-1.2088	-1.06428	-0.17078	5.92828	6.14708	-57.0539
6.1475	69902.9	69902.9	0.03359	-0.36185	-0.83261	-1.15497	-1.04929	-0.16836	5.94594	6.1475	-57.0368
6.14792	69902.9	69902.9	0.02201	-0.38021	-0.78581	-1.13169	-1.09405	-0.16641	5.96547	6.14792	-57.0197
6.14833	69902.9	69902.9	0.01204	-0.38418	-0.73276	-1.11988	-1.15022	-0.16523	5.98734	6.14833	-57.024
6.14875	69902.9	69902.9	-0.01867	-0.38268	-0.68203	-1.11374	-1.14339	-0.16484	6.00781	6.14875	-57.0411
6.14917	69902.9	69902.9	-0.0737	-0.37337	-0.67021	-1.13651	-1.09022	-0.16367	6.02391	6.14917	-57.0498
6.14958	69902.9	69902.9	-0.1459	-0.34661	-0.70466	-1.18949	-1.03871	-0.16109	6.03612	6.14958	-57.0453
6.15	69902.9	69902.9	-0.21139	-0.30247	-0.78068	-1.2554	-1.01702	-0.15719	6.05320	6.15	-57.0368
6.15042	69902.9	69902.9	-0.25458	-0.24557	-0.80863	-1.31031	-1.033	-0.15388	6.06687	6.15042	-57.0368
6.15083	69902.9	69902.9	-0.27084	-0.18047	-0.82543	-1.3366	-1.05919	-0.15291	6.09	6.15083	-57.0539
6.15125	69902.9	69902.9	-0.26719	-0.12253	-0.81083	-1.33336	-1.07215	-0.15484	6.09578	6.15125	-57.0709
6.15167	69902.9	69902.9	-0.27083	-0.09427	-0.7867	-1.30822	-1.07204	-0.1575	6.11218	6.15167	-57.0709
6.15208	69902.9	69902.9	-0.2875	-0.10158	-0.77052	-1.27208	-1.06482	-0.15989	6.12659	6.15208	-57.0795
6.1525	69902.9	69902.9	-0.30586	-0.13089	-0.77157	-1.23652	-1.04922	-0.16094	6.13644	6.1525	-57.0752
6.15292	69902.9	69902.9	-0.31029	-0.17018	-0.76568	-1.20304	-1.02802	-0.16189	6.14391	6.15292	-57.0581
6.15333	69902.9	69902.9	-0.3097	-0.2041	-0.79635	-1.18644	-1.00624	-0.16141	6.14872	6.15333	-57.0368
6.15375	69902.9	69902.9	-0.31706	-0.21699	-0.7957	-1.1791	-0.98813	-0.16555	6.15266	6.15375	-57.0263
6.15417	69902.9	69902.9	-0.33372	-0.20306	-0.76431	-1.05791	-0.91531	-0.17156	6.16062	6.15417	-57.0283
6.15458	69902.9	69902.9	-0.33822	-0.17031	-0.74956	-1.03069	-0.90535	-0.17305	6.16344	6.15458	-57.0283
6.155	69902.9	69902.9	-0.3235	-0.12709	-0.77191	-1.04644	-0.9306	-0.17125	6.16359	6.155	-57.0325
6.15542	69902.9	69902.9	-0.29733	-0.07817	-0.78419	-1.0725	-0.93466	-0.17203	6.15968	6.15542	-57.0368
6.15583	69902.9	69902.9	-0.27454	-0.03419	-0.78512	-1.09764	-0.92562	-0.17492	6.15109	6.15583	-57.0411
6.15625	69902.9	69902.9	-0.26523	0.01308	-0.78787	-1.12578	-0.9357	-0.17566	6.14406	6.15625	-57.0368
6.15667	69902.9	69902.9	-0.26602	0.05598	-0.80006	-1.15914	-0.90118	-0.17582	6.14031	6.15667	-57.0325
6.15708	69902.9	69902.9	-0.26882	0.02715	-0.81199	-1.19111	-0.90362	-0.17686	6.13531	6.15708	-57.0283
6.1575	69902.9	69902.9	-0.25723	-0.14468	-0.80446	-1.21196	-1.03068	-0.17562	6.12375	6.1575	-57.0368
6.15792	69902.9	69902.9	-0.2474	-0.14276	-0.77029	-1.21625	-1.04933	-0.17578	6.10625	6.15792	-57.0368
6.15833	69902.9	69902.9	-0.17012	-0.81892	-0.725	-1.20907	-1.04076	-0.17484	6.09126	6.15833	-57.0453
6.15875	69902.9	69902.9	-0.11263	-0.69931	-0.68701	-1.19494	-1.02466	-0.17171	6.07859	6.15875	-57.0539
6.15917	69902.9	69902.9	-0.07295	-0.33945	-0.67289	-1.17976	-1.01122	-0.16617	6.08969	6.15917	-57.0539
6.15958	69902.9	69902.9	-0.05229	-0.08985	-0.68823	-1.16297	-0.98952	-0.16392	6.08375	6.15958	-57.0498
6.16	69902.9	69902.9	-0.03952	0.40469	-0.69847	-1.14003	-0.95493	-0.15422	6.055	6.16	-57.0368
6.16042	69902.9	69902.9	-0.02324	0.51419	-0.70959	-1.10899	-0.91103	-0.14922	6.04078	6.16042	-57.0197
6.16083	69902.9	69902.9	-0.00566	0.3916	-0.74226	-1.10042	-0.89508	-0.14539	6.02516	6.16083	-57.0069
6.16125	69902.9	69902.9	0.00495	0.13203	-0.80188	-1.11779	-0.88775	-0.14172	6.01047	6.16125	-57.0027
6.16167	69902.9	69902.9	0.01667	-0.1278	-0.84211	-1.11652	-0.87744	-0.1407	5.99781	6.16167	-57.0197
6.16208	69902.9	69902.9	0.04753	-0.27689	-0.85346	-1.0952	-0.84246	-0.13869	5.98516	6.16208	-57.0368
6.1625	69902.9	69902.9	0.09398	-0.28503	-0.85683	-1.08119	-0.81113	-0.13695	5.96929	6.1625	-57.0411
6.16292	69902.9	69902.9	0.14005	-0.20944	-0.86273	-1.06617	-0.81234	-0.13149	5.95234	6.16292	-57.0325
6.16333	69902.9	69902.9	0.1868	-0.1188	-0.87897	-1.0771	-0.84164	-0.12609	5.93766	6.16333	-57.024
6.16375	69902.9	69902.9	0.16699	-0.03711	-0.89643	-1.13876	-0.87315	-0.12266	5.92562	6.16375	-57.0325
6.16417	69902.9	69902.9	0.16797	0.02357	-0.91033	-1.16633	-0.90894	-0.12078	5.91812	6.16417	-57.0325
6.16458	69902.9	69902.9	0.17969	0.04434	-0.90396	-1.18208	-0.9613	-0.12031	5.91437	6.16458	-57.0197
6.165	69902.9	69902.9	0.19655	-0.01899	-0.97176	-1.19764	-1.00763	-0.12094	5.90894	6.165	-57.0027
6.16542	69902.9	69902.9	0.21172	-0.1765	-0.82088	-1.18648	-1.02038	-0.12088	5.905	6.16542	-56.9984
6.16583	69902.9	69902.9	0.21445	-0.35838	-0.76774	-1.17907	-1.01007	-0.11981	5.90406	6.16583	-57.0155
6.16625	69902.9	69902.9	0.21536	-0.43379	-0.72364	-1.16297	-0.9891	-0.11844	5.90203	6.16625	-57.0453
6.16667	69902.9	69902.9	0.2188	-0.32604	-0.68944	-1.1376	-0.9445	-0.11981	5.90047	6.16667	-57.0581
6.16708	69902.9	69902.9	0.2054	-0.08652	-0.66523	-1.11293	-0.89659	-0.1232	5.90344	6.16708	-57.0539
6.1675	69902.9	69902.9	0.17467	0.10755	-0.68724	-1.12693	-0.97559	-0.12484	5.90719	6.1675	-57.0498
6.16792	69902.9	69902.9	0.14017	0.1043	-0.73404	-1.15995	-0.98989	-0.12482	5.91203	6.16792	-57.0411
6.16833	69902.9	69902.9	0.11908	-0.10052	-0.74898	-1.15636	-0.90211	-0.12711	5.9175	6.16833	-57.0283
6.16875	69902.9	69902.9	0.11784	-0.36629	-0.73276	-1.11304	-0.91045	-0.13125	5.92109	6.16875	-57.0155
6.16917	69902.9	69902.9	0.1293	-0.53008	-0.71203	-1.06912	-0.93992	-0.13469	5.92609	6.16917	-57.0283
6.16958	69902.9	69902.9	0.12958	-0.52378	-0.70091	-1.03439	-0.96805	-0.13625	5.93768	6.16958	-57.0411
6.17	69902.9	69902.9	0.13639	-0.38468	-0.69047	-1.0264	-0.9215	-0.13617	5.95031	6.17	-57.0368
6.17042	69902.9	69902.9	0.14089	-0.23418	-0.70241	-1.02234	-0.99478	-0.13609	5.96437	6.17042	-57.0368
6.17083	69902.9	69902.9	0.12708	-0.09782	-0.70883	-1.01424	-0.99732	-0.13734	5.97781	6.17083	-57.0411
6.17125	69902.9	69902.9	0.09212	-0.00332	-0.71782	-1.00439	-0.99583	-0.14117	5.99109	6.17125	-57.0325
6.17167	69902.9	69902.9	0.05098	0.04208	-0.71956	-0.99512	-0.97972	-0.14555	6.00787	6.17167	-57.024
6.17208	69902.9	69902.9	0.01777	0.01354	-0.7089	-0.99261	-0.98748	-0.15008	6.02612	6.17208	-57.0197
6.1725	69902.9	69902.9	0.00545	-0.11029	-0.67751	-0.96153	-0.984	-0.15398	6.04703	6.1725	-57.024
6.17292	69902.9	69902.9	-0.00287	-0.28915	-0.62411	-0.92435	-0.95771	-0.15648	6.0576	6.17292	-57.024
6.17333	69902.9	69902.9	-0.01934	-0.44941	-0.55693	-0.87026	-0.92586	-0.15867	6.06422	6.17333	-57.0197
6.17375	69902.9	69902.9	-0.04922	-0.47044	-0.52438	-0.83585	-0.93386	-0.16008	6.07437	6.17375	-57.0283
6.17417	69902.9	69902.9	-0.08605	-0.36536	-0.53133	-0.83076	-0.96906	-0.16008	6.08594	6.17417	-57.0453
6.17458	69902.9	69902.9	-0.1274	-0.21739	-0.5282	-0.81327	-0.97888	-0.16148	6.10109	6.17458	-57.0498
6.175	69902.9	69902.9	-0.15</								

Appendix D

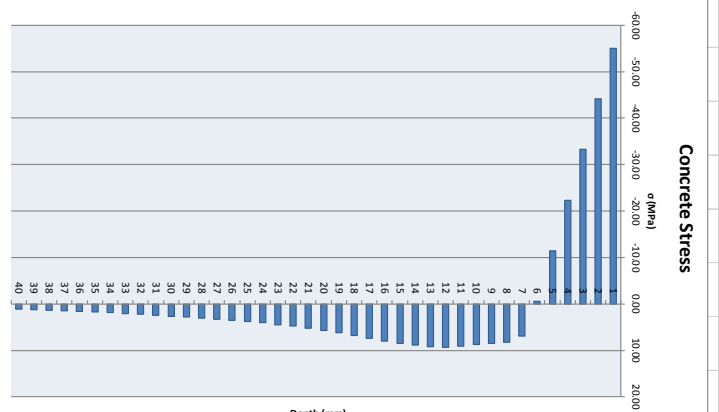
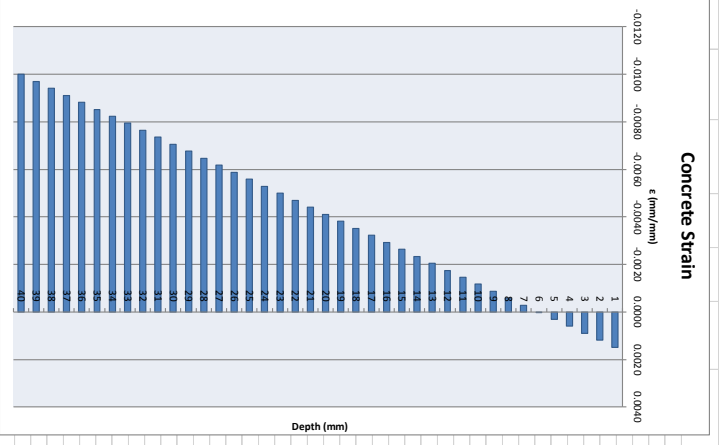
Data from Dynamic Test Panel SCI2

6.18167	69902.9	69902.9	-0.13353	-0.24473	-0.50341	-0.80133	-0.92748	-0.12719	6.19406	6.18187	-57.0112
6.18208	69902.9	69902.9	-0.11855	-0.21808	-0.53272	-0.80539	-0.93003	-0.12786	6.19297	6.18208	-57.0197
6.18225	69902.9	69902.9	-0.09609	-0.12546	-0.56596	-0.82543	-0.93165	-0.12888	6.19406	6.18225	-57.0204
6.18282	69902.9	69902.9	-0.07715	-0.02435	-0.60268	-0.85902	-0.92771	-0.12305	6.19453	6.18282	-57.0197
6.18333	69902.9	69902.9	-0.0582	0.03815	-0.63002	-0.89679	-0.92713	-0.12031	6.18806	6.18333	-57.0089
6.18375	69902.9	69902.9	-0.03203	0.04349	-0.63591	-0.92999	-0.92921	-0.12125	6.17812	6.18375	-56.9994
6.18417	69902.9	69902.9	-6.5E-05	0.01328	-0.61913	-0.95447	-0.93269	-0.12414	6.16891	6.18417	-57.0027
6.18458	69902.9	69902.9	0.02259	-0.0207	-0.58489	-0.9759	-0.94508	-0.12711	6.15891	6.18458	-57.0112
6.185	69902.9	69902.9	0.01485	-0.04069	-0.58148	-0.99142	-0.95505	-0.12681	6.14141	6.185	-57.0165
6.18542	69902.9	69902.9	-0.00475	-0.04876	-0.58079	-1.00242	-0.94908	-0.13062	6.12125	6.18542	-57.0155
6.18583	69902.9	69902.9	-0.0099	-0.08517	-0.58195	-1.00613	-0.9057	-0.13281	6.10562	6.18583	-57.0112
6.18625	69902.9	69902.9	0.00033	-0.1	-0.57245	-0.98864	-0.85485	-0.13656	6.09891	6.18625	-57.0112
6.18667	69902.9	69902.9	0.0184	-0.14212	-0.56724	-0.96767	-0.80886	-0.14047	6.09406	6.18667	-57.0112
6.18708	69902.9	69902.9	0.04089	-0.17617	-0.60106	-0.98667	-0.81002	-0.14109	6.08344	6.18708	-57.0027
6.1875	69902.9	69902.9	0.05697	-0.19648	-0.63558	-1.00694	-0.82985	-0.14125	6.06837	6.1875	-57.0069
6.18792	69902.9	69902.9	0.07539	-0.19837	-0.65145	-0.99373	-0.84095	-0.14477	6.05207	6.18792	-57.0325
6.18833	69902.9	69902.9	0.08349	-0.18724	-0.67137	-0.96871	-0.84419	-0.14859	6.03375	6.18833	-57.0411
6.18875	69902.9	69902.9	0.09681	-0.17715	-0.71017	-0.96061	-0.85867	-0.15133	6.01662	6.18875	-57.0283
6.18917	69902.9	69902.9	0.08919	-0.17591	-0.76207	-0.97219	-0.89539	-0.15242	6.00672	6.18917	-57.0112
6.18958	69902.9	69902.9	0.08171	-0.17467	-0.80585	-0.99049	-0.93373	-0.15133	6.00391	6.18958	-57.0027
6.19	69902.9	69902.9	0.07982	-0.1638	-0.82985	-1.00358	-0.95331	-0.15102	6.00094	6.19	-57.0027
6.19042	69902.9	69902.9	0.09277	-0.14316	-0.83354	-1.01273	-0.96061	-0.15242	5.99203	6.19042	-57.0027
6.19083	69902.9	69902.9	0.11367	-0.12422	-0.8223	-1.02177	-0.95794	-0.15461	5.98109	6.19083	-57.0027
6.19125	69902.9	69902.9	0.1293	-0.12461	-0.80585	-1.02698	-0.83683	-0.15802	5.97158	6.19125	-57.0155
6.19167	69902.9	69902.9	0.13757	-0.15578	-0.78906	-1.02338	-0.80732	-0.15664	5.96856	6.19167	-57.0155
6.19208	69902.9	69902.9	0.13678	-0.21595	-0.77019	-1.00902	-0.89909	-0.15649	5.97141	6.19208	-57.0112
6.1925	69902.9	69902.9	0.12904	-0.28073	-0.74701	-0.98331	-0.845	-0.15766	5.98344	6.1925	-57.0027
6.19292	69902.9	69902.9	0.11836	-0.32077	-0.71504	-0.9481	-0.79253	-0.15844	5.98719	6.19292	-56.9984
6.19333	69902.9	69902.9	0.10423	-0.31823	-0.68708	-0.93176	-0.76486	-0.15687	6.00369	6.19333	-56.9984
6.19375	69902.9	69902.9	0.09245	-0.27174	-0.71041	-0.94679	-0.79338	-0.15289	6.00016	6.19375	-56.9956
6.19417	69902.9	69902.9	0.09108	-0.20072	-0.71944	-0.96501	-0.79207	-0.15031	5.99594	6.19417	-56.9913
6.19458	69902.9	69902.9	0.08919	-0.14038	-0.7165	-0.98339	-0.79839	-0.14797	5.99653	6.19458	-56.9813
6.195	69902.9	69902.9	0.07695	-0.12188	-0.71889	-0.96305	-0.78825	-0.14312	6.00856	6.195	-56.9899
6.19542	69902.9	69902.9	0.05189	-0.14874	-0.73183	-0.98053	-0.7874	-0.13758	6.00703	6.19542	-56.9941
6.19583	69902.9	69902.9	0.0139	-0.20749	-0.75936	-1.01111	-0.81025	-0.13494	6.00297	6.19583	-56.9984
6.19625	69902.9	69902.9	-0.02393	-0.27305	-0.78465	-1.04399	-0.83239	-0.13125	6.00281	6.19625	-57.0027
6.19667	69902.9	69902.9	-0.05378	-0.32528	-0.78705	-1.06729	-0.85323	-0.12516	6.01094	6.19667	-57.0069
6.19708	69902.9	69902.9	-0.08229	-0.34551	-0.78778	-1.07459	-0.85462	-0.12	6.02125	6.19708	-57.0197
6.1975	69902.9	69902.9	-0.10378	-0.33314	-0.76137	-1.08937	-0.84929	-0.11652	6.03125	6.1975	-57.0112
6.19792	69902.9	69902.9	-0.11296	-0.29802	-0.73056	-1.05652	-0.84628	-0.11742	6.045	6.19792	-56.9984
6.19833	69902.9	69902.9	-0.11458	-0.25671	-0.70183	-1.0403	-0.83076	-0.11602	6.05869	6.19833	-56.9956
6.19875	69902.9	69902.9	-0.12038	-0.22135	-0.67751	-1.01968	-0.79847	-0.11539	6.07641	6.19875	-56.9771
6.19917	69902.9	69902.9	-0.13971	-0.2002	-0.65376	-0.99072	-0.7506	-0.11516	6.09062	6.19917	-56.9728
6.19958	69902.9	69902.9	-0.17174	-0.18229	-0.65098	-0.98919	-0.71863	-0.11414	6.09672	6.19958	-56.9728
6.2	69902.9	69902.9	-0.19505	-0.15475	-0.68662	-0.99331	-0.72913	-0.11039	6.09578	6.2	-56.9813

Appendix E Moment-Curvature Model

Concrete Section Model

Concrete			Section			Properties			Layers			Forces/Loading		
$F_c =$	124 MPa	Type:	Rectangular	$f_{y,avg} =$	0.918 mm	$X_F =$	0.00 kN							
$V_c =$	2450 kg/m ²	$h =$	38 mm	# of layers =	40	$ZM =$	1287.19 kNmm							
$E_c =$	37000 MPa	$b =$	534 mm	$\epsilon_c =$	0.0018	$a =$	457.5 mm							
$\epsilon_{c1} =$	0.004	$L =$	915 mm	$\epsilon_{c2} =$	-0.0100	$P =$	5.63 kN							
$n =$	8.15	$A_s =$	2022 mm ²											
$k =$	2.69	$I =$	2.44E+06 mm ⁴											
$f_c =$	8.00 MPa	$c =$	5.75 mm											
Layer	b (mm)	b_{layer} (mm)	d (mm)	Average (mm ²)	Elastic (MPa)	Concrete (MPa)	Force (kN)	Y (mm)	M_y (kNmm)					
TOP														
1	534	0.95	0	507.3	0.0018	-65.94	-65.94	0.00	0.00					
2	534	0.95	1.9	507.3	0.0012	-55.04	-72.92	0.95	-26.52					
3	534	0.95	2.85	507.3	0.0006	-44.14	-82.39	1.90	-42.54					
4	534	0.95	3.8	507.3	0.0006	-33.24	-88.86	2.85	-48.06					
5	534	0.95	4.75	507.3	0.0003	-22.34	-11.33	3.80	-43.07					
6	534	0.95	5.7	507.3	0.0003	-11.44	-5.81	4.75	-27.58					
7	534	0.95	6.65	507.3	-0.0003	-0.55	-0.28	5.70	-1.58					
8	534	0.95	7.6	507.3	-0.0006	8.25	4.19	6.65	23.30					
9	534	0.95	8.55	507.3	-0.0009	8.25	4.34	7.60	31.82					
10	534	0.95	9.5	507.3	-0.0012	8.76	4.45	8.55	37.07					
11	534	0.95	10.45	507.3	-0.0015	9.05	4.59	9.50	42.24					
12	534	0.95	11.4	507.3	-0.0018	9.32	4.73	10.45	47.98					
13	534	0.95	12.35	507.3	-0.0020	9.21	4.67	11.40	53.89					
14	534	0.95	13.3	507.3	-0.0023	8.86	4.50	12.35	57.70					
15	534	0.95	14.25	507.3	-0.0026	8.48	4.30	13.30	59.81					
16	534	0.95	15.2	507.3	-0.0029	8.06	4.09	14.25	61.28					
17	534	0.95	16.15	507.3	-0.0032	7.39	3.75	15.20	62.14					
18	534	0.95	17.1	507.3	-0.0035	6.77	3.43	16.15	60.55					
19	534	0.95	18.05	507.3	-0.0038	6.20	3.15	17.10	58.72					
20	534	0.95	19	507.3	-0.0041	5.68	2.88	18.05	56.80					
21	534	0.95	19.95	507.3	-0.0044	5.24	2.66	19.05	54.80					
22	534	0.95	20.9	507.3	-0.0047	4.80	2.44	20.90	52.92					
23	534	0.95	21.85	507.3	-0.0050	4.51	2.29	21.85	50.00					
24	534	0.95	22.8	507.3	-0.0053	4.05	2.06	22.80	46.87					
25	534	0.95	23.75	507.3	-0.0056	3.84	1.95	23.75	44.87					
26	534	0.95	24.7	507.3	-0.0059	3.58	1.82	24.70	43.87					
27	534	0.95	25.65	507.3	-0.0062	3.32	1.68	25.65	43.18					
28	534	0.95	26.6	507.3	-0.0065	3.04	1.54	26.60	41.04					
29	534	0.95	27.55	507.3	-0.0068	2.81	1.42	27.55	39.22					
30	534	0.95	28.5	507.3	-0.0071	2.65	1.34	28.50	38.29					
31	534	0.95	29.45	507.3	-0.0073	2.45	1.24	29.45	36.59					
32	534	0.95	30.4	507.3	-0.0076	2.25	1.14	30.40	34.69					
33	534	0.95	31.35	507.3	-0.0079	2.08	1.06	31.35	33.11					
34	534	0.95	32.3	507.3	-0.0082	1.88	0.96	32.30	30.87					
35	534	0.95	33.25	507.3	-0.0085	1.77	0.90	33.25	29.79					
36	534	0.95	34.2	507.3	-0.0088	1.65	0.84	34.20	28.59					
37	534	0.95	35.15	507.3	-0.0091	1.54	0.78	35.15	27.45					
38	534	0.95	36.1	507.3	-0.0094	1.39	0.71	36.10	26.65					
39	534	0.95	37.05	507.3	-0.0097	1.26	0.64	37.05	25.65					
40	534	0.95	38	507.3	-0.0100	1.14	0.58	38.00	24.96					
Bottom	534	0.95	38.95	507.3	-0.0100	1.14	0.58	38.95	22.51					

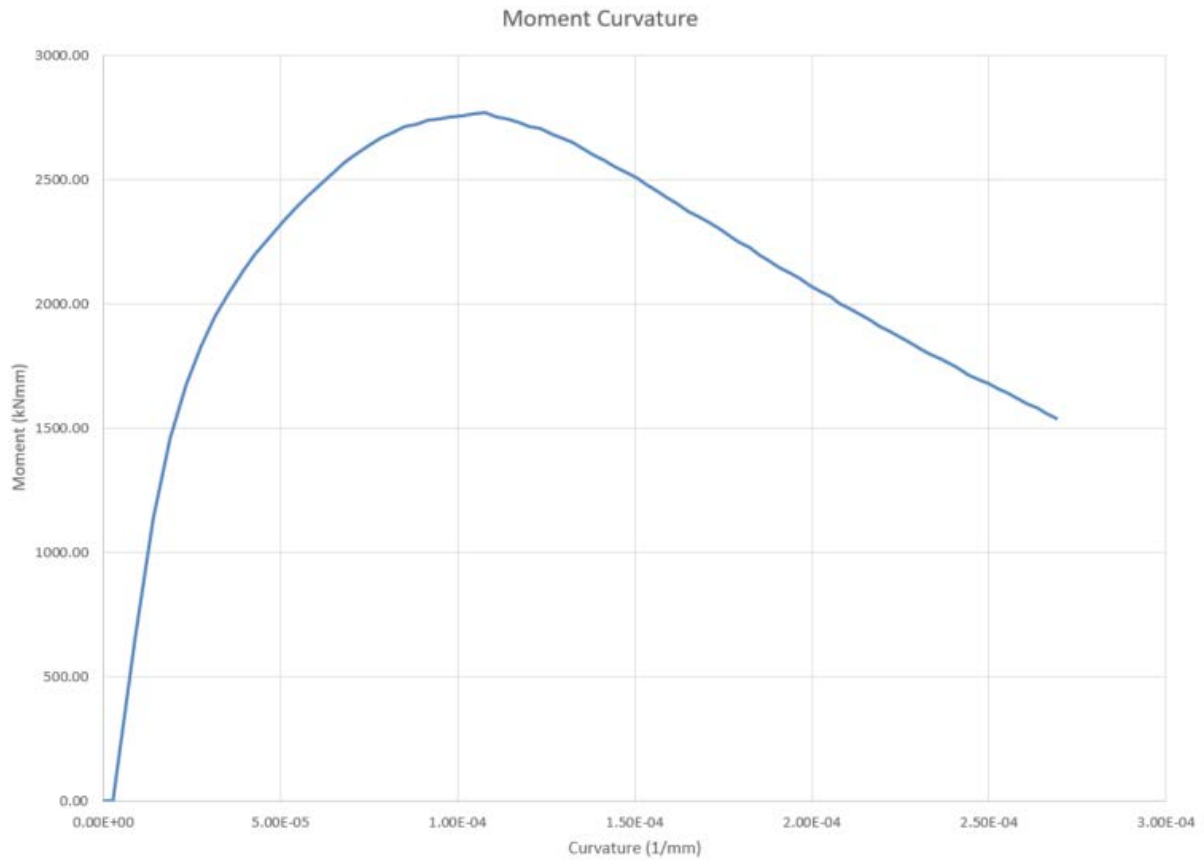


Appendix E Moment-Curvature Model

Tab 2: 'Stress-Strain'

Step	ϵ_x	ϵ_y	M (kNm)	P (kN)	ϕ (1/mm)
0	0.0000	0.0000	0.00	0.00	0.00E+00
1	-0.0001	0.0000	0.00	0.00	2.63E-06
2	-0.0002	0.0001	657.62	2.87	8.88E-06
3	-0.0003	0.0002	1135.81	4.97	1.41E-05
4	-0.0004	0.0003	1461.47	6.39	1.89E-05
5	-0.0005	0.0004	1672.01	7.31	2.33E-05
6	-0.0006	0.0004	1826.03	7.98	2.75E-05
7	-0.0007	0.0005	1945.83	8.51	3.15E-05
8	-0.0008	0.0005	2042.34	8.93	3.54E-05
9	-0.0009	0.0006	2125.80	9.29	3.92E-05
10	-0.0010	0.0006	2201.50	9.62	4.29E-05
11	-0.0011	0.0007	2264.49	9.90	4.66E-05
12	-0.0012	0.0007	2324.35	10.16	5.03E-05
13	-0.0013	0.0007	2377.52	10.39	5.38E-05
14	-0.0014	0.0008	2428.53	10.62	5.74E-05
15	-0.0015	0.0008	2478.16	10.83	6.09E-05
16	-0.0016	0.0008	2521.19	11.02	6.44E-05
17	-0.0017	0.0009	2564.73	11.21	6.79E-05
18	-0.0018	0.0009	2601.95	11.37	7.14E-05
19	-0.0019	0.0009	2636.26	11.52	7.48E-05
20	-0.0020	0.0010	2666.34	11.66	7.82E-05
21	-0.0021	0.0010	2684.29	11.73	8.15E-05
22	-0.0022	0.0010	2710.00	11.85	8.49E-05
23	-0.0023	0.0011	2719.17	11.89	8.82E-05
24	-0.0024	0.0011	2735.74	11.96	9.15E-05
25	-0.0025	0.0011	2741.81	11.99	9.48E-05
26	-0.0026	0.0011	2749.56	12.02	9.80E-05
27	-0.0027	0.0011	2755.37	12.05	1.01E-04
28	-0.0028	0.0012	2764.79	12.09	1.05E-04
29	-0.0029	0.0012	2765.89	12.09	1.08E-04
30	-0.0030	0.0012	2751.03	12.03	1.11E-04
31	-0.0031	0.0012	2741.75	11.99	1.14E-04
32	-0.0032	0.0012	2731.04	11.94	1.17E-04
33	-0.0033	0.0013	2713.90	11.86	1.20E-04
34	-0.0034	0.0013	2702.70	11.82	1.23E-04
35	-0.0035	0.0013	2683.74	11.73	1.26E-04
36	-0.0036	0.0013	2665.17	11.65	1.29E-04
37	-0.0037	0.0013	2647.77	11.57	1.32E-04
38	-0.0038	0.0013	2622.01	11.46	1.35E-04
39	-0.0039	0.0014	2596.23	11.35	1.38E-04
40	-0.0040	0.0014	2576.05	11.26	1.41E-04
41	-0.0041	0.0014	2550.36	11.15	1.44E-04
42	-0.0042	0.0014	2527.23	11.05	1.47E-04
43	-0.0043	0.0014	2505.07	10.95	1.50E-04
44	-0.0044	0.0014	2476.98	10.83	1.53E-04
45	-0.0045	0.0014	2453.40	10.73	1.56E-04
46	-0.0046	0.0014	2424.29	10.60	1.59E-04
47	-0.0047	0.0015	2400.33	10.49	1.62E-04
48	-0.0048	0.0015	2371.23	10.37	1.65E-04
49	-0.0049	0.0015	2349.50	10.27	1.68E-04
50	-0.0050	0.0015	2325.60	10.17	1.71E-04
51	-0.0051	0.0015	2300.56	10.06	1.74E-04
52	-0.0052	0.0015	2271.83	9.93	1.77E-04
53	-0.0053	0.0015	2247.84	9.83	1.80E-04
54	-0.0054	0.0015	2223.19	9.72	1.82E-04
55	-0.0055	0.0015	2195.58	9.60	1.85E-04
56	-0.0056	0.0015	2168.73	9.48	1.88E-04
57	-0.0057	0.0016	2144.00	9.37	1.91E-04
58	-0.0058	0.0016	2120.96	9.27	1.94E-04
59	-0.0059	0.0016	2099.07	9.18	1.97E-04
60	-0.0060	0.0016	2073.11	9.06	1.99E-04
61	-0.0061	0.0016	2050.96	8.97	2.02E-04
62	-0.0062	0.0016	2027.77	8.86	2.05E-04
63	-0.0063	0.0016	2000.29	8.74	2.08E-04
64	-0.0064	0.0016	1978.61	8.65	2.11E-04
65	-0.0065	0.0016	1955.41	8.55	2.14E-04
66	-0.0066	0.0016	1932.62	8.45	2.16E-04
67	-0.0067	0.0016	1910.26	8.35	2.19E-04
68	-0.0068	0.0016	1886.87	8.25	2.22E-04
69	-0.0069	0.0016	1865.30	8.15	2.25E-04
70	-0.0070	0.0016	1846.53	8.07	2.27E-04
71	-0.0071	0.0016	1820.96	7.96	2.30E-04
72	-0.0072	0.0017	1797.11	7.86	2.33E-04
73	-0.0073	0.0017	1779.44	7.78	2.36E-04
74	-0.0074	0.0017	1758.60	7.69	2.39E-04
75	-0.0075	0.0017	1737.18	7.59	2.41E-04
76	-0.0076	0.0017	1714.07	7.49	2.44E-04
77	-0.0077	0.0017	1695.71	7.41	2.47E-04
78	-0.0078	0.0017	1679.84	7.34	2.50E-04
79	-0.0079	0.0017	1656.87	7.24	2.53E-04
80	-0.0080	0.0017	1638.43	7.16	2.55E-04
81	-0.0081	0.0017	1618.13	7.07	2.58E-04
82	-0.0082	0.0017	1597.95	6.99	2.61E-04
83	-0.0083	0.0017	1578.49	6.90	2.63E-04
84	-0.0084	0.0017	1557.71	6.81	2.66E-04
85	-0.0085	0.0017	1539.46	6.73	2.69E-04
86	-0.0086	0.0017	1520.31	6.65	2.72E-04
87	-0.0087	0.0017	1501.43	6.56	2.74E-04
88	-0.0088	0.0017	1483.37	6.48	2.77E-04
89	-0.0089	0.0017	1468.56	6.42	2.80E-04
90	-0.0090	0.0017	1450.90	6.34	2.83E-04
91	-0.0091	0.0017	1435.18	6.27	2.85E-04
92	-0.0092	0.0018	1419.79	6.21	2.88E-04
93	-0.0093	0.0018	1400.64	6.12	2.91E-04
94	-0.0094	0.0018	1382.72	6.04	2.94E-04
95	-0.0095	0.0018	1366.12	5.97	2.96E-04
96	-0.0096	0.0018	1349.94	5.90	2.99E-04
97	-0.0097	0.0018	1334.88	5.84	3.02E-04
98	-0.0098	0.0018	1317.77	5.76	3.05E-04
99	-0.0099	0.0018	1303.39	5.70	3.07E-04
100	-0.0100	0.0018	1287.19	5.63	3.10E-04

Appendix E Moment-Curvature Model



Appendix E Moment-Curvature Model

Sub Macro1()

```
Application.ScreenUpdating = False
Sheets("Data").Select
Range("H7").Select
ActiveCell.FormulaR1C1 = "0"
Range("H8").Select
ActiveCell.FormulaR1C1 = "0"
Sheets("Stress-Strain").Select
    Dim counter As Integer
    For counter = 0 To 100
        Cells(counter + 5, 1).Value = counter
        Cells(counter + 5, 2).Value = Cells(couter + 1, 2) - ((0.01 / 100) * counter)
        Cells(counter + 5, 2).Select
            Selection.Copy
    Sheets("Data").Select
        Range("H8").Select
            Selection.PasteSpecial Paste:=xlPasteValues, Operation:=xlNone, SkipBlanks _
                :=False, Transpose:=False
        Range("K5").Select
            Selection.GoalSeek Goal:=0, ChangingCell:=Range("H7")
            Range("H7").Copy
    Sheets("Stress-Strain").Select
        Cells(counter + 5, 3).Select
            Selection.PasteSpecial Paste:=xlPasteValues, Operation:=xlNone, SkipBlanks _
                :=False, Transpose:=False
    Sheets("Data").Select
        Range("K6").Select
            Selection.Copy
    Sheets("Stress-Strain").Select
        Cells(counter + 5, 4).Select
            Selection.PasteSpecial Paste:=xlPasteValues, Operation:=xlNone, SkipBlanks _
                :=False, Transpose:=False
    Sheets("Data").Select
        Range("K8").Select
            Selection.Copy
    Sheets("Stress-Strain").Select
        Cells(counter + 5, 5).Select
            Selection.PasteSpecial Paste:=xlPasteValues, Operation:=xlNone, SkipBlanks _
                :=False, Transpose:=False
    Next counter
Application.ScreenUpdating = True
```

End

Sub

Appendix F SDOF Model

Single Degree of Freedom Model

Predictor Method Model		Forcing Function	
Resistance function		$F_0 = 101788.657 \text{ N}$	
$F_0 =$	8903 N	$\Delta t = 0.00041667 \text{ s}$	
$x_0 =$	2.316 mm		
$x_{max} =$	36.397 mm		
$\Delta x =$	1 mm		

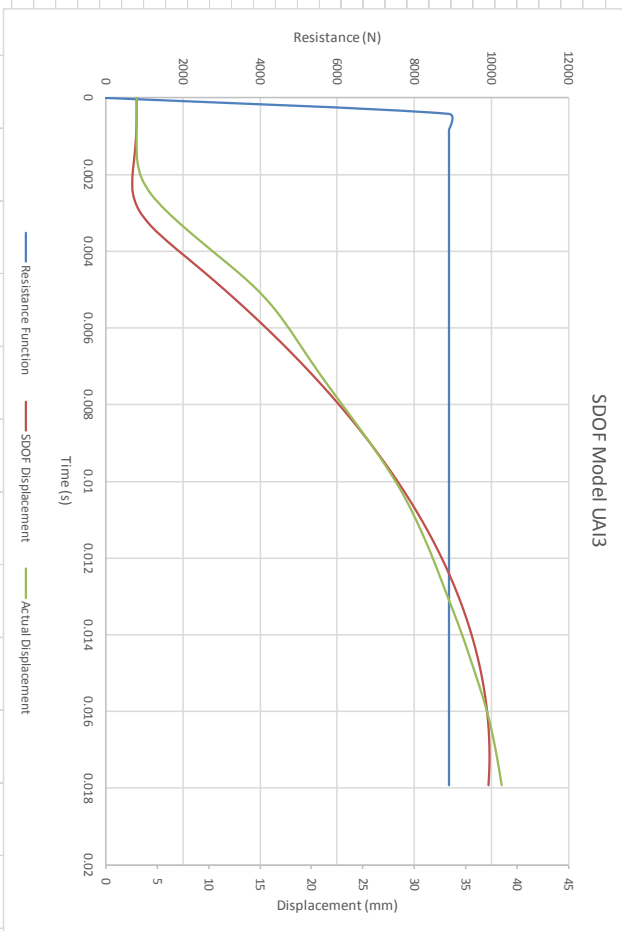
Note: Once parameters for resistance function and forcing function are inputted, functions will be plotted. If there is an issue with the plot, troubleshooting using the respective sheet.

Input	Output
Calculation	

Outputs		Actual	
$x_{max} =$	37.30407 mm	$x_{max} =$	36.85312 mm
$\dot{x}_{max} =$	4.528831 m/s		
$\ddot{x}_{max} =$	3637.012 m/s ²		

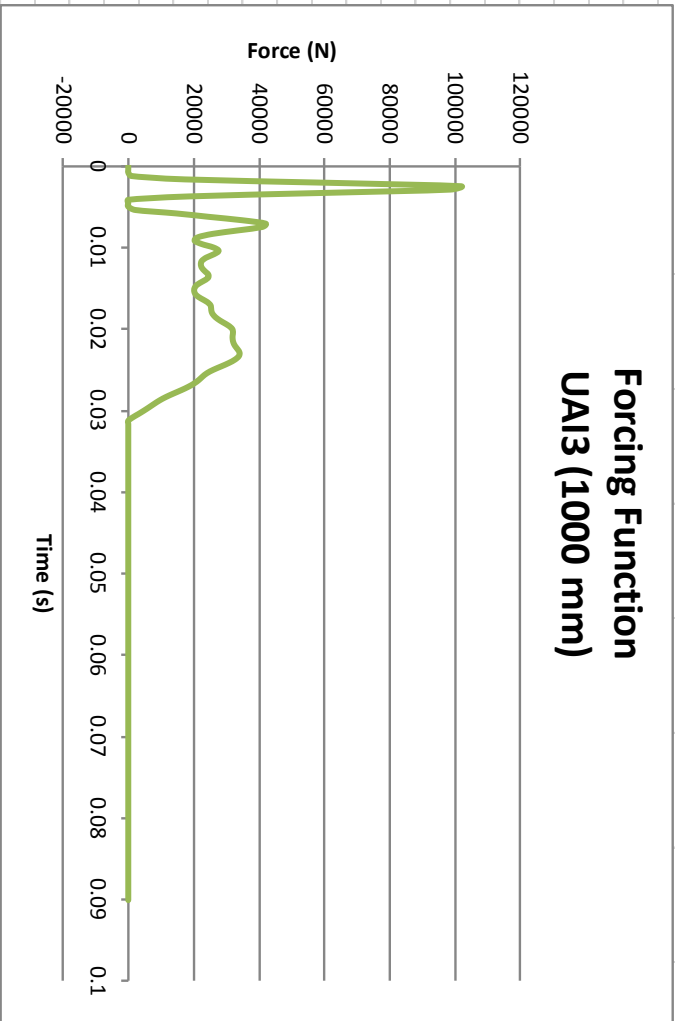
Predictor Method		Equations	
Initial Conditions			
$t =$	0 s	$x_1 = x_0 + \dot{x}_0 \Delta t + \frac{1}{2} \ddot{x}_0 \Delta t^2$	
$x_0 =$	3 mm	$\dot{x}_1 = \dot{x}_0 + \ddot{x}_0 \Delta t$	
$\dot{x}_0 =$	0 m/s	$F(t) = R(x_0)$	
$\ddot{x}_0 =$	3985.616 m/s ²	$\ddot{x}_1 = \frac{M}$	
$\Delta t =$	0.000417 s		
$M =$	25.539 kg		

n	t(s)	R _n (N)	P _n (N)	x _n (m/s ²)	\dot{x}_n (m/s)	x _n (mm)	x _{actual} (mm)
0	0	0	0	0	0	3	3.000625
1	0	0	0	0	0	3	3.0034375
2	0.000417	8903	0	-348.604096	0	3	3.0034375
3	0.000833	8903	18.30167	-347.887479	-0.145252	2.96973922	3.00296875
4	0.00125	8903	974.39	-310.451075	-0.290205	2.87901911	3.00578125
5	0.001667	8903	17402.68	-332.811936	-0.419559	2.73115154	3.0846875
6	0.002083	8903	6162.451	2064.35675	-0.280888	2.58522502	3.47765624
7	0.0025	8903	101788.7	3637.01229	0.579261	2.64738607	4.38968747
8	0.002917	8903	98517.41	3508.92391	2.094683	3.20445769	5.78203119
9	0.003333	8903	58766.88	1952.46027	3.556734	4.38183632	7.4649999
10	0.00375	8903	18622.41	380.571245	4.37026	6.03329348	9.28437486
11	0.004167	8903	0	-348.604096	4.528831	7.88727077	11.1651561
12	0.004583	8903	0	-348.604096	4.383579	9.74402297	13.027656
13	0.005	8903	0	-348.604096	4.238328	11.5402336	14.7262497
14	0.005417	8903	0	-348.604096	4.093076	13.2759627	16.1556247
15	0.005833	8903	0	-348.604096	3.947824	14.9511503	17.3542184
16	0.00625	8903	0	-348.604096	3.802572	16.5658163	18.4292184
17	0.006667	8903	0	-348.604096	3.657321	18.1199608	19.4664059
18	0.007083	8903	0	-348.604096	3.512069	19.6135837	20.5240621
19	0.0075	8903	0	-348.604096	3.366817	21.046685	21.6299966
20	0.007917	8903	0	-348.604096	3.221566	22.4192648	22.7717183
21	0.008333	8903	0	-348.604096	3.076314	23.7313231	23.9154883
22	0.00875	8903	0	-348.604096	2.931062	24.9828998	25.0464058
23	0.009167	8903	0	-348.604096	2.78581	26.173875	26.1485932
24	0.009583	8903	0	-348.604096	2.640559	27.3043686	27.2018745
25	0.01	8903	0	-348.604096	2.495307	28.3743406	28.1873432
26	0.010417	8903	0	-348.604096	2.350055	29.3837911	29.0803119
27	0.010833	8903	0	-348.604096	2.204804	30.3327201	29.8745306
28	0.01125	8903	0	-348.604096	2.059552	31.2211275	30.6029681



Appendix F SDOF Model

Time MGCplus_1 (Sampl		Force Hammer	
s	s	kN	N
4.520834		0	-0.06394
4.52125		0.000416667	-0.03255
4.521667		0.000833333	0.018302
4.522084		0.00125	0.97439
4.5225		0.001666667	17.40268
4.522917		0.002083333	61.62461
4.523334		0.0025	101.7887
4.52375		0.002916667	98.51741
4.524167		0.003333333	58.76688
4.524584		0.00375	18.62241
4.525		0.004166667	-4.79052
4.525417		0.004583334	-13.8555
4.525834		0.005	-10.2247
4.52625		0.005416667	2.166083
4.526667		0.005833334	14.61423
4.527084		0.00625	24.54578
4.5275		0.006666667	34.76471
4.527917		0.007083334	42.03638
4.528334		0.0075	40.98102
4.52875		0.007916667	33.59236
4.529167		0.008333334	25.95142
4.529584		0.00875	21.37878
4.53		0.009166667	20.29504
4.530417		0.009583334	22.44167
4.530834		0.01	26.00632
4.53125		0.010416667	27.65973
4.531667		0.010833334	26.24517
4.532084		0.011250001	23.86977
4.5325		0.011666667	22.49935
4.532917		0.012083334	22.21695
4.533334		0.012500001	22.52194
4.53375		0.012916667	23.44108



Appendix F SDOF Model

Time MGcplus_1 (Sa Laser		s		mm	
4.520834	0	0.000625	3.000625		
4.52125	0.000417	0.003437	3.003437		
4.521667	0.000833	0.003437	3.003437		
4.522084	0.00125	0.002969	3.002969		
4.5225	0.001667	0.005781	3.005781		
4.522917	0.002083	0.084687	3.084687		
4.523334	0.0025	0.477656	3.477656		
4.52375	0.002917	1.389687	4.389687		
4.524167	0.003333	2.782031	5.782031		
4.524584	0.00375	4.465	7.465		
4.525	0.004167	6.284375	9.284375		
4.525417	0.004583	8.165156	11.165156		
4.525834	0.005	10.02766	13.02766		
4.52625	0.005417	11.72625	14.72625		
4.526667	0.005833	13.15562	16.15562		
4.527084	0.00625	14.35422	17.35422		
4.5275	0.006667	15.42922	18.42922		
4.527917	0.007083	16.46641	19.46641		
4.528334	0.0075	17.52406	20.52406		
4.52875	0.007917	18.63	21.63		
4.529167	0.008333	19.77172	22.77172		
4.529584	0.00875	20.91547	23.91547		
4.530417	0.009167	22.04641	25.04641		
4.530834	0.01	24.20187	27.20187		
4.53125	0.010417	25.18734	28.18734		
4.531667	0.010833	26.08031	29.08031		
4.532084	0.01125	26.87453	29.87453		
4.5325	0.011667	27.60297	30.60297		
4.532917	0.012083	28.28906	31.28906		
4.533334	0.0125	28.92891	31.92891		
4.53375	0.012917	29.52875	32.52875		

Appendix G Energy Conservation Calculations

Data Sourced from Static Bending and Impact Tests									
Static Bending data from UHPC Panels spreadsheet					Impact data from UAI3 (1000mm drop) Spreadsheet rows 10858-11266				
Panel:	UAS1								
Load kN	Stroke mm	LVDT Bottom mm	Time MGC s	Force Nor kN	Force Sou kN	Force Han kN	Laser mm	Reactions kN	
0	0	0	4.5225	0.041121	-0.05039	101.7887	36.85312	40.2815	
0.003125	-0.00482	0.006562	4.522917	-0.39291	-0.43542	17.40268	0.005781	-0.01853	
0.003125	-0.00472	0.006406	4.523334	-1.73287	-1.31969	101.7887	0.477656	-6.10511	
0.003125	-0.00459	0.00625	4.52375	-3.62408	-2.1399	98.51741	1.389687	-11.528	
0.003125	-0.00439	0.005937	4.524167	-4.20741	-1.98144	58.76688	2.782031	-12.3777	
0.002865	-0.0042	0.005703	4.524584	-2.91842	0.00417	18.62241	4.465	-5.8285	
0.002604	-0.00397	0.005469	4.525	-0.80133	1.839897	-4.79052	6.284375	2.077123	
0.002604	-0.00371	0.005156	4.525417	1.651204	2.257244	-13.8555	8.165156	7.816897	
0.002604	-0.00355	0.004844	4.525834	4.488889	2.003106	-10.2247	10.02766	12.98399	
0.002083	-0.00329	0.004531	4.52625	7.783189	2.105734	2.166083	11.72625	19.77785	
0.002083	-0.00306	0.004297	4.526667	10.33697	3.073869	14.61423	13.15562	26.82167	
0.002083	-0.00286	0.003984	4.527084	11.18962	4.734572	24.54578	14.35422	31.84837	
0.001693	-0.00264	0.003672	4.5275	10.20457	6.877257	34.76471	15.42922	34.16365	
0.001563	-0.00241	0.003437	4.527917	8.559041	9.277323	42.03638	16.46641	35.67273	
0.001563	-0.00225	0.003203	4.528334	7.399317	11.32815	40.98102	17.52406	37.45494	
0.001302	-0.00202	0.002969	4.52875	7.400823	12.28331	33.59236	18.63	39.36827	
0.001042	-0.00186	0.002734	4.529167	8.209572	11.93118	25.95142	19.77172	40.2815	
0.001042	-0.00169	0.0025	4.529584	8.961793	10.58983	21.37878	20.91547	39.10325	
0.001042	-0.00153	0.002344	4.53	9.04612	9.140408	20.29504	22.04641	36.37306	
0.000651	-0.0013	0.002187	4.530417	8.372665	8.549774	22.44167	23.14859	33.84488	
0.000521	-0.00107	0.001875	4.530834	7.084714	8.647306	26.00632	24.20187	31.46404	
0.000521	-0.00068	0.001719	4.53125	5.683826	8.638502	27.65973	25.18734	28.64466	
0.001042	-0.0002	0.001562	4.531667	4.904036	8.092348	26.24517	26.08031	25.99277	
0.001563	0.000391	0.001328	4.532084	5.27366	7.206107	23.86977	26.87453	24.95953	
0.002474	0.001172	0.001094	4.5325	6.736056	6.510297	22.49935	27.60297	26.4927	
0.003776	0.002116	0.000937	4.532917	8.680202	6.160596	22.21695	28.28906	29.6816	
0.005729	0.00319	0.000625	4.533334	10.25762	5.884449	22.52194	28.92891	32.28414	
0.008203	0.004395	0.000391	4.53375	10.71354	5.360419	23.44108	29.52875	32.14792	
0.011328	0.005827	0.000312	4.534167	9.886491	4.480665	24.50419	30.12281	28.73431	
0.014844	0.007324	0.000312	4.534584	8.069761	3.316192	24.38211	30.72547	22.77191	
0.019531	0.009017	0.000312	4.535	5.771164	1.984225	22.7704	31.31797	15.51078	
0.024349	0.010905	0.000312	4.535417	3.56535	0.629322	21.05514	31.87625	8.389345	
0.030078	0.012826	0.000469	4.535834	1.95712	-0.49496	20.27535	32.40422	2.924328	
0.036458	0.014909	0.000859	4.53625	1.176635	-1.16853	20.20608	32.92047	0.016217	
0.04349	0.017155	0.001328	4.536667	1.202002	-1.24231	20.75235	33.42828	-0.08062	
0.050911	0.019499	0.002031	4.537084	1.776072	-0.64369	22.21417	33.9	2.264773	
0.058984	0.02194	0.002969	4.5375	2.527252	0.516153	24.05372	34.30984	6.08681	
0.067448	0.024414	0.003906	4.537917	3.159007	2.016195	25.15784	34.66	10.3504	
0.076563	0.027018	0.005078	4.538334	3.55423	3.549481	25.36889	34.96859	14.20742	
0.086068	0.029753	0.006406	4.53875	3.700296	4.790519	25.5248	35.24578	16.98163	
0.096094	0.03252	0.007812	4.539167	3.691261	5.528493	26.14995	35.49641	18.43951	
0.10651	0.035384	0.009375	4.539584	3.566161	5.757496	27.29022	35.72297	18.64731	
0.117318	0.038346	0.011016	4.54	3.465154	5.630542	28.91432	35.92781	18.19139	
0.128646	0.041276	0.012734	4.540417	3.530484	5.339917	30.66965	36.11172	17.7408	
0.140234	0.044303	0.014687	4.540834	3.742343	5.101647	31.81629	36.27109	17.68798	
0.151953	0.047331	0.016641	4.54125	3.961384	5.074195	32.0556	36.41172	18.07116	
0.164193	0.050521	0.018672	4.541667	4.088453	5.255937	31.93664	36.53781	18.68878	
0.176563	0.053613	0.020781	4.542084	4.095287	5.442197	31.95239	36.645	19.07497	
0.189063	0.056803	0.022969	4.5425	3.957909	5.379995	32.1763	36.73266	18.67581	
0.201953	0.059993	0.025312	4.542917	3.793426	4.979907	32.69245	36.80094	17.54666	

Appendix G Energy Conservation Calculations

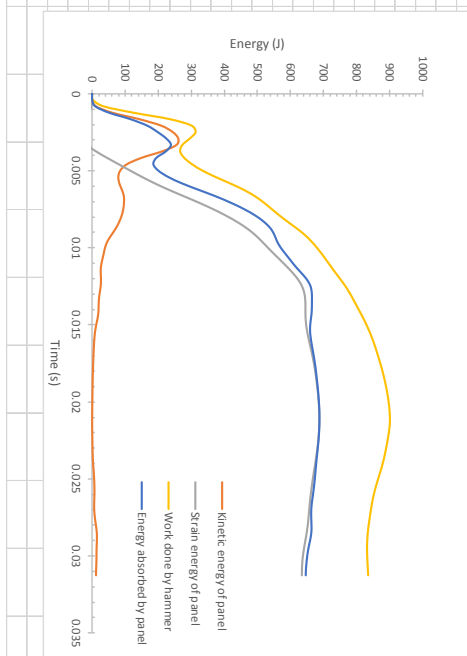
Energy Calculations Panel: UA13

		Variables				Formulas			
t = Time		$a_h =$	9.81 m/s^2	$P =$	Hammer Impact load	$v(t) =$	$u(t) - u(t-1)$	$K_p(t) =$	$\frac{M_p \cdot v(t)^2}{2}$
$a_h =$ Acceleration of hammer		$M_h =$	137 kg	$I =$	Panel bending load (from reactions)	$I(t) = \int P(t) \cdot dt = I(t-1) + \frac{P(t) - P(t-1)}{2} \cdot (t - t-1)$	$U_p(t) =$	$U_p(t-1) + \frac{P_0(t-1) + P_0(t)}{2} \cdot (t - t-1) - u(t) - u(t-1)$	
$M_h =$ Mass of hammer		$h_h =$	1 m	$K_k =$	Kinetic energy of hammer	$K_h(t) = \frac{1}{2} \cdot M_h \cdot \left[2 \cdot a_h \cdot h_h - \left(\sqrt{2} \cdot M_h \cdot h_h - \frac{1}{M_h} \cdot I(t) \right)^2 \right]$	$W(t) =$	$W(t-1) + \frac{P_k(t-1) + P_k(t)}{2} \cdot (t - t-1) - u(t) - u(t-1)$	
$h_h =$ Drop height of hammer		$U_p =$	Strain energy of panel	$W =$	Work done by hammer				
$x =$ Panel displacement @ midspan		$M_p =$	25.539 kg	$E_p =$	Energy absorbed by panel				
$v_p =$ Panel velocity @ midspan									
$M_p =$ Equivalent panel mass									

t (s)	P _i (N)	P ₀ (N)	x (m)	v (m/s)	I (N·s)	K _i (J)	K _p (J)	U _p (J)	W (J)	E _p (J)
0	17402.68	-18.5333	5.78125E-06	0	0	0	0	-0.00011	0.100609	-0.00011
0.000417	61624.61	-1656.65	8.46875E-05	0.189375	16.46402	71.93722	0.457951	-0.0662	3.218483	0.391753
0.000833	101788.7	-6105.11	0.00047656	0.943125	50.50845	214.4139	11.35827	-1.59126	35.32664	9.767011
0.00125	98517.41	-11528	0.001389687	2.188875	92.23888	377.5161	61.18088	-9.63222	126.6693	51.54866
0.001667	58766.88	-12377.7	0.002782031	3.341625	125.0064	496.678	142.5901	-26.2747	236.1662	116.3154
0.002083	18622.41	-5828.5	0.004465	4.039125	141.1292	552.4329	208.3284	-41.5949	301.2881	166.7334
0.0025	-4790.52	2077.123	0.006284375	4.3665	144.0109	562.1982	243.4674	-45.0075	313.8708	198.4599
0.002917	-13855.5	7816.897	0.008165156	4.513875	140.1263	549.0199	260.1794	-35.7033	296.3362	224.4761
0.003333	-10224.7	12983.99	0.010027656	4.47	135.1095	531.838	255.1461	-16.3324	273.9115	238.8136
0.00375	2166.083	19777.85	0.01172625	4.076625	133.4307	526.0469	212.2146	11.49208	267.0673	223.7067
0.004167	14614.23	26821.67	0.01315625	3.4305	136.9286	538.0824	150.2757	44.79617	279.06	195.0718
0.004583	24545.78	31848.37	0.014354218	2.876625	145.0849	565.8224	105.6672	79.95694	302.5285	185.6242
0.005	34764.71	34163.65	0.015429218	2.58	157.4413	606.9114	84.99889	115.4384	334.4079	200.4373
0.005417	42036.38	35672.73	0.01646406	2.48925	173.4415	658.4617	79.12448	151.6551	374.2364	230.7796
0.005833	40981.02	37454.94	0.017524062	2.538375	190.7368	712.0828	82.27832	190.3271	418.1384	272.6054
0.00625	33592.36	39368.27	0.01863	2.65425	206.2729	758.3883	89.96166	232.8079	459.3751	322.7696
0.006667	25951.42	40281.5	0.019771718	2.740125	218.6778	794.0964	95.87703	278.2767	493.3662	374.1538
0.007083	21378.78	39103.25	0.020915468	2.745	228.5383	821.6787	96.21849	323.6749	520.4332	419.8934
0.0075	20295.04	36373.06	0.022046406	2.71425	237.2204	845.5772	94.07485	366.3544	543.9984	460.4292
0.007917	22441.67	33844.88	0.023148593	2.64525	246.1238	869.1087	89.35262	405.0511	567.5504	494.4037
0.008333	26006.32	31464.04	0.024201874	2.527875	256.2172	895.3119	81.59903	439.4454	593.0651	521.0444
0.00875	27659.73	28644.66	0.025187343	2.365125	267.3976	923.4692	71.43023	469.063	619.5082	540.4932
0.009167	26245.17	25992.77	0.026080312	2.143125	278.6278	950.6332	58.65011	493.4578	643.5758	552.1079
0.009583	23869.77	24959.53	0.02674531	1.906125	289.0684	975.4476	46.33964	513.6914	663.477	560.087
0.01	22492.35	26492.7	0.027602968	1.74825	298.7286	997.5136	39.02841	532.4313	680.3053	565.5246
0.010417	22216.95	29681.6	0.028289062	1.666625	308.0445	1018.148	34.62288	551.7017	695.7655	586.3246
0.010833	22521.94	32284.14	0.028928906	1.553625	317.3651	1038.158	30.11232	571.5259	710.0182	601.6382

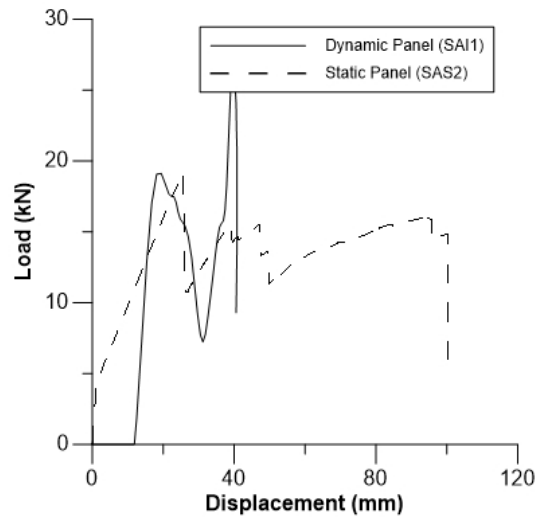
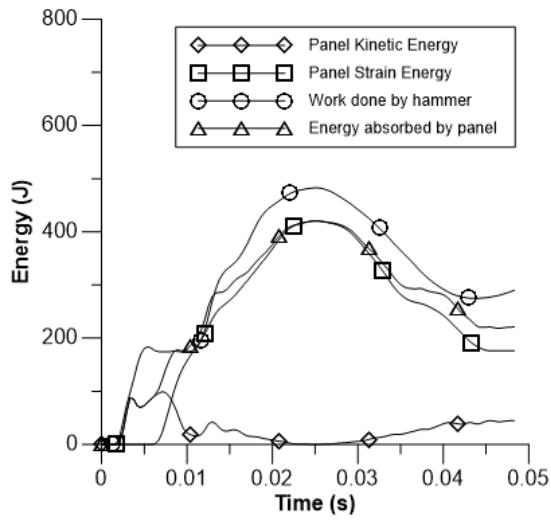
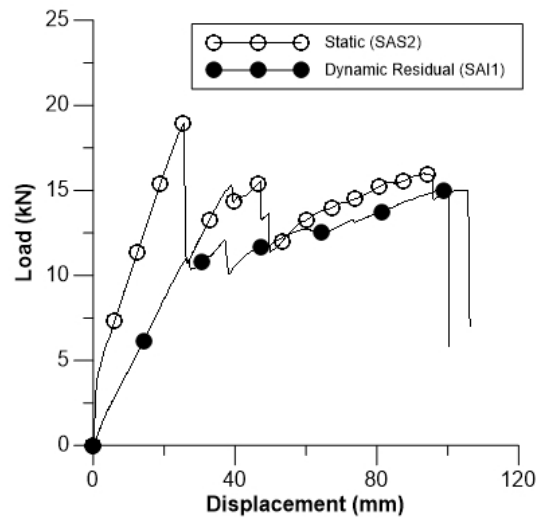
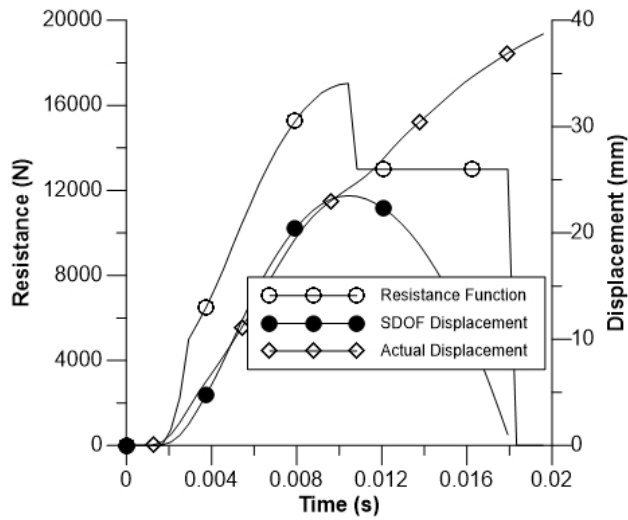
Outputs	
$x_{max} =$	36.85312 mm
$K_p =$	1343.9 J
$K_h =$	260.2 J
$U_p =$	688.6 J
$W =$	901.3 J

Check: $E_p = U_p + K_p$
 $E_p = 948.8 \text{ J}$
 $W_{actual} = 901.3 \text{ J}$
 Off by -5.3 %



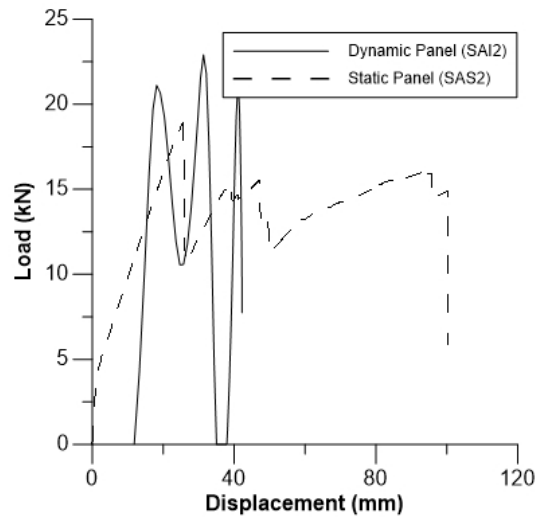
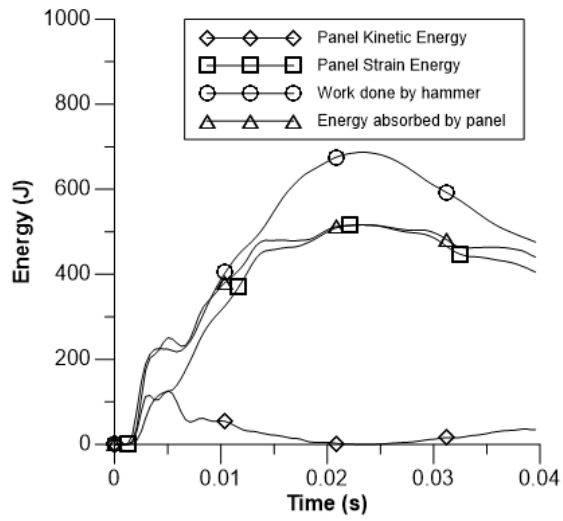
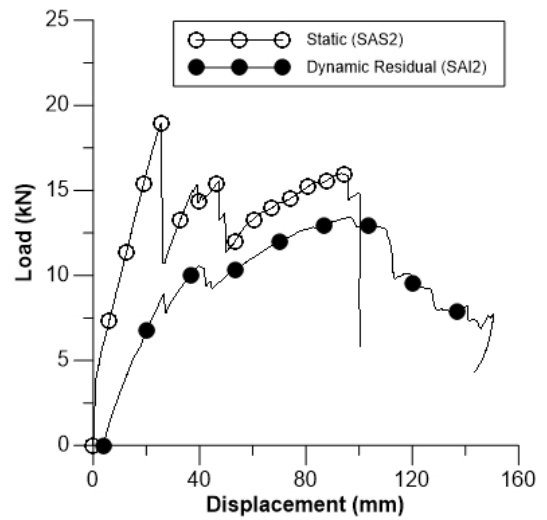
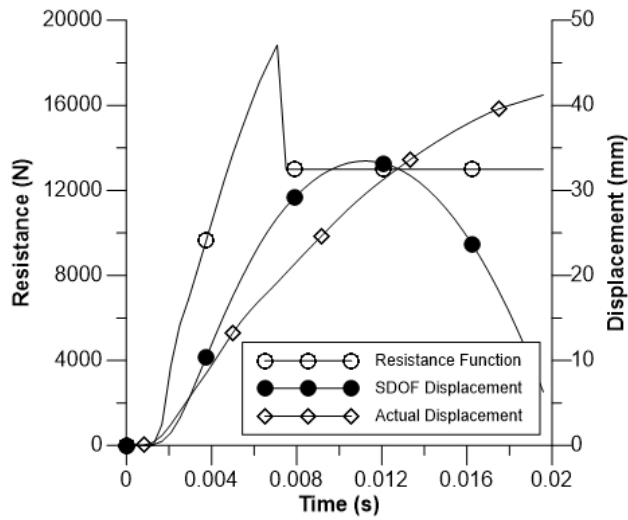
Appendix H SFRC Panel Graphs

PANEL SAI1



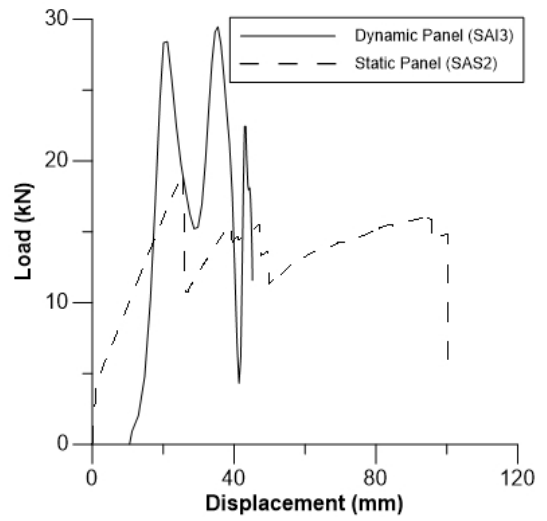
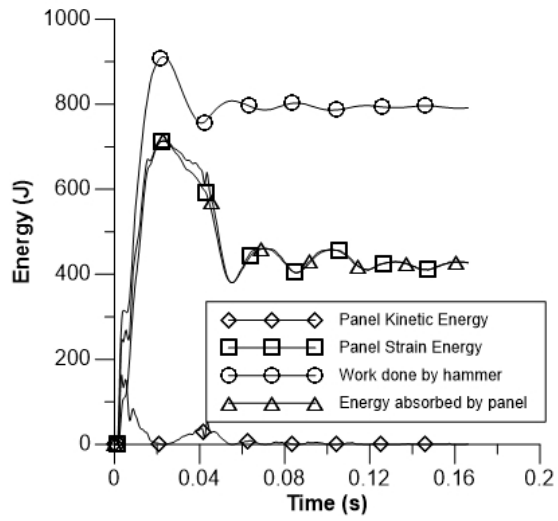
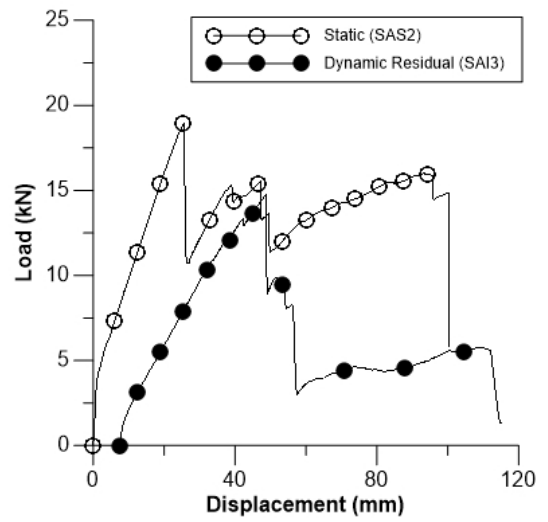
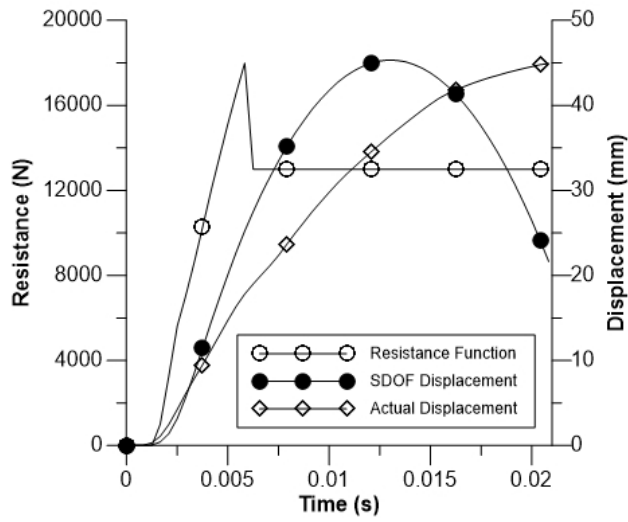
Appendix H SFRC Panel Graphs

PANEL SAI2



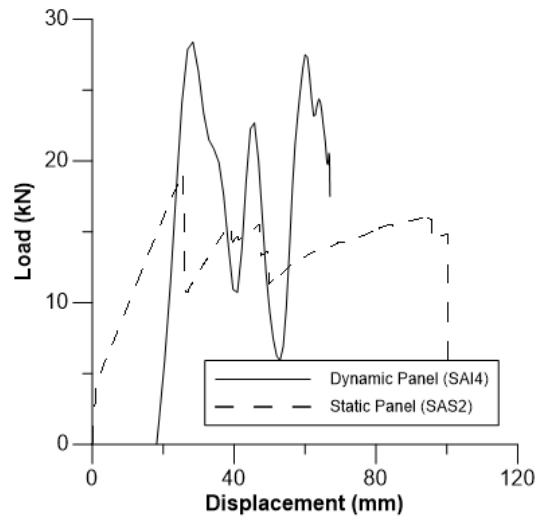
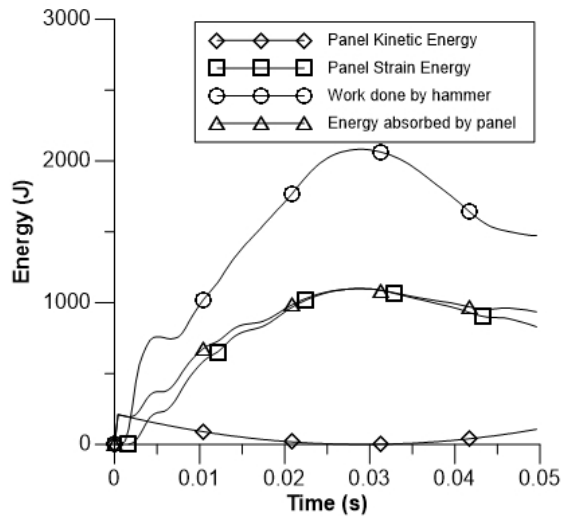
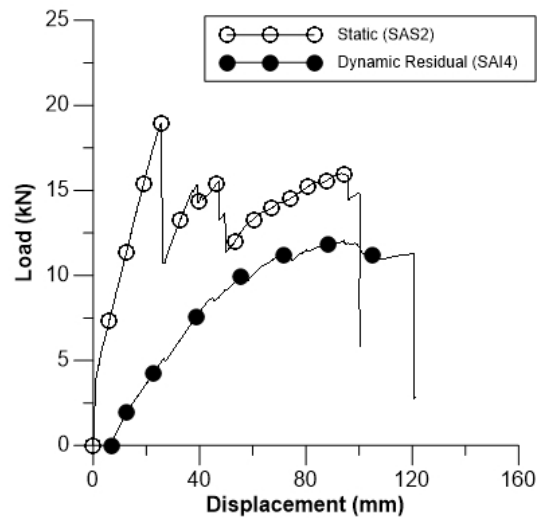
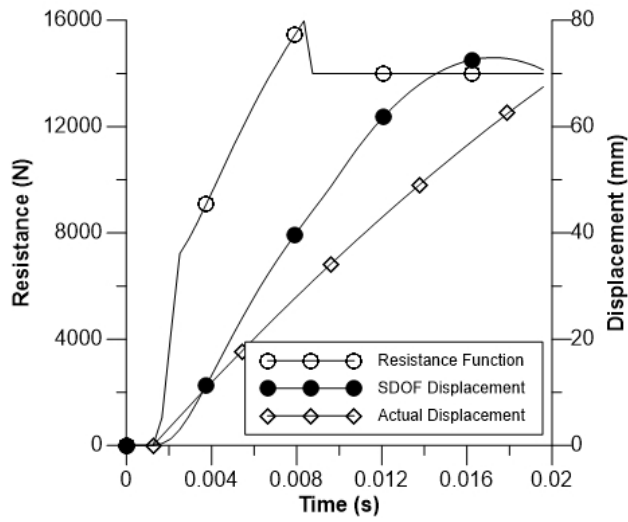
Appendix H SFRC Panel Graphs

PANEL SAI3



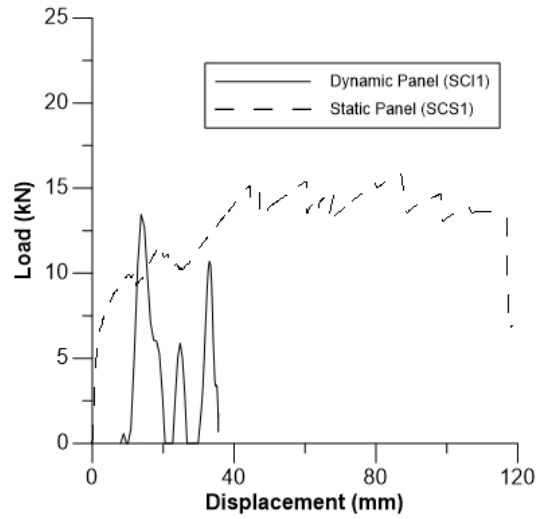
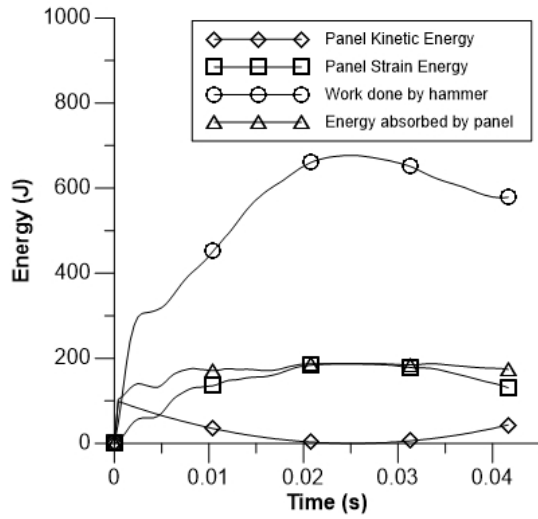
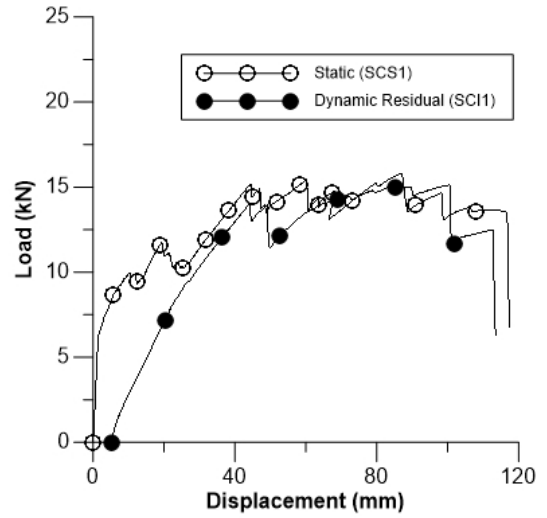
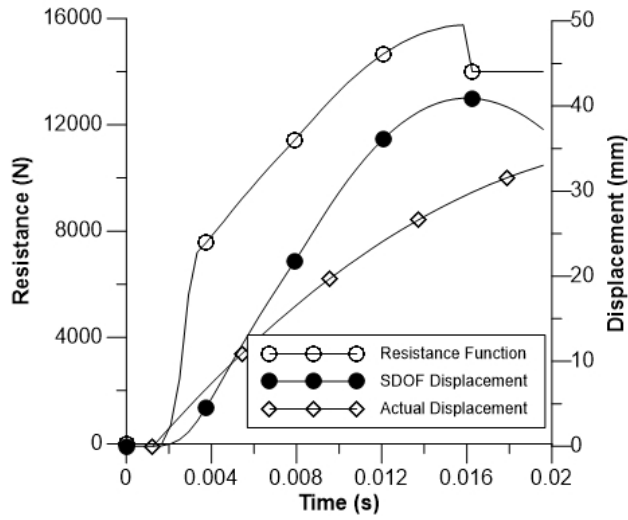
Appendix H SFRC Panel Graphs

PANEL SAI4



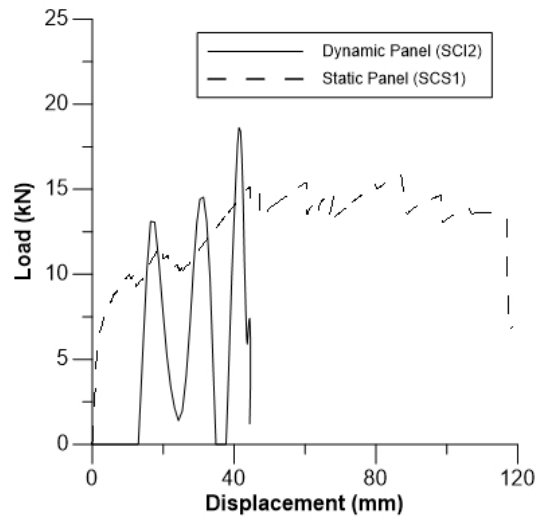
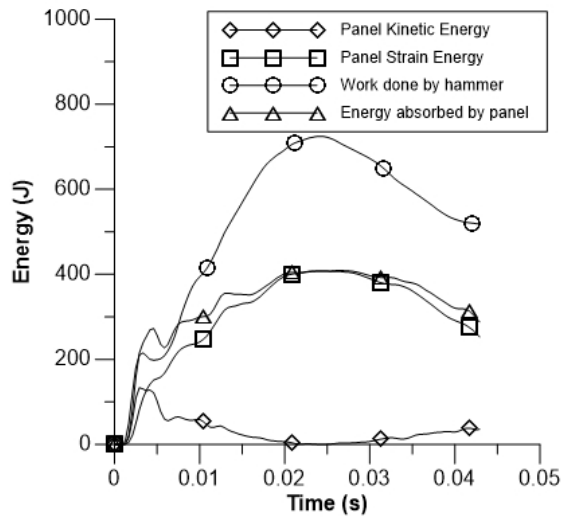
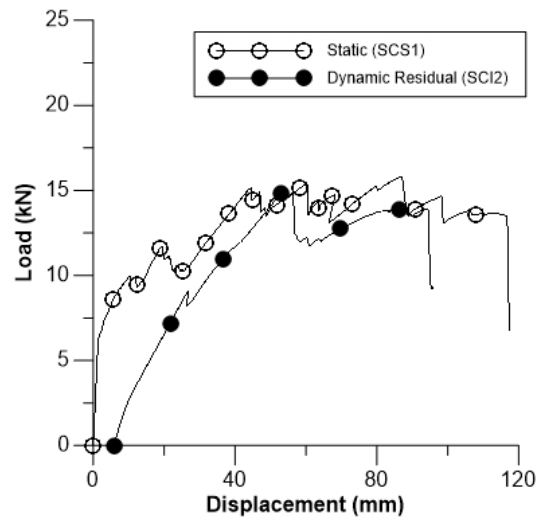
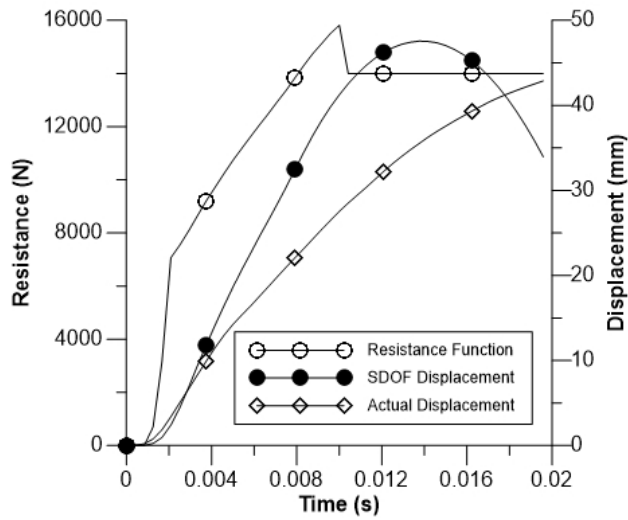
Appendix H SFRC Panel Graphs

PANEL SCI1



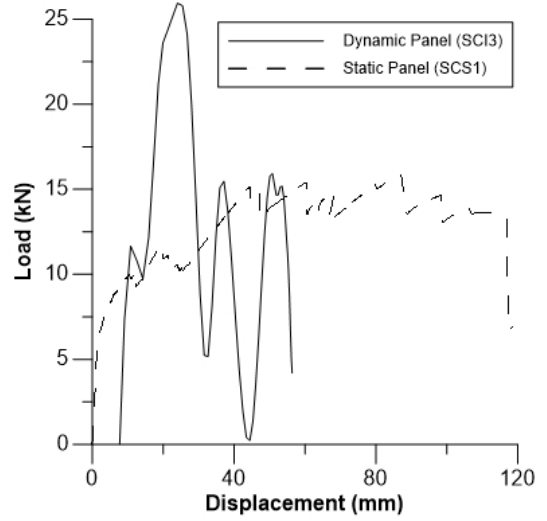
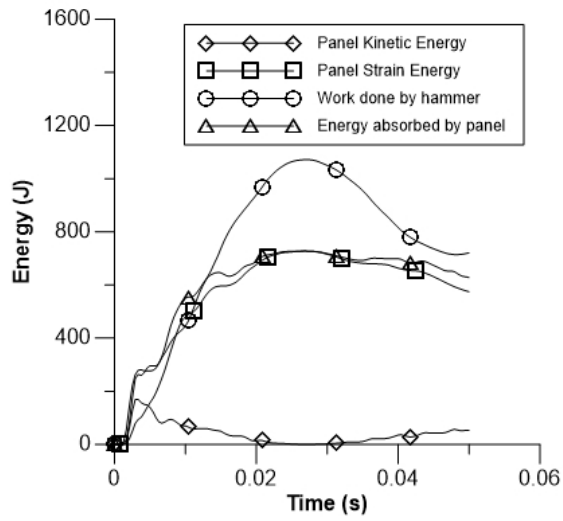
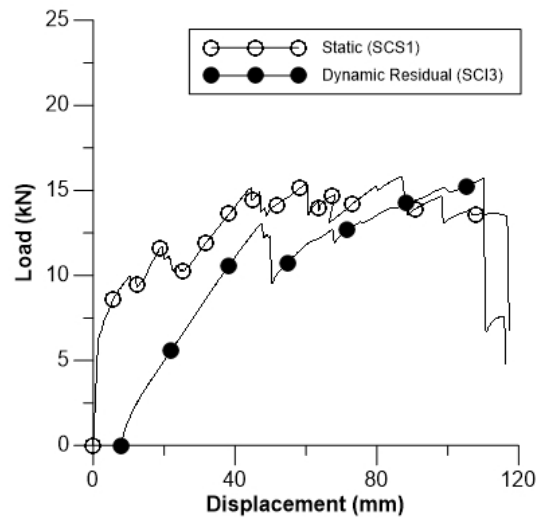
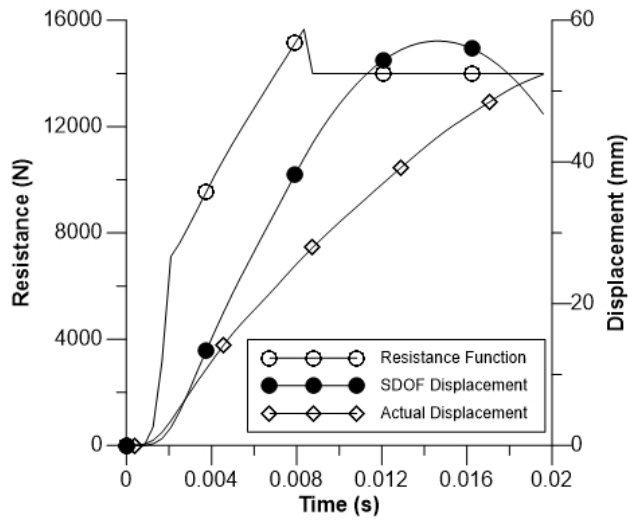
Appendix H SFRC Panel Graphs

PANEL SCI2



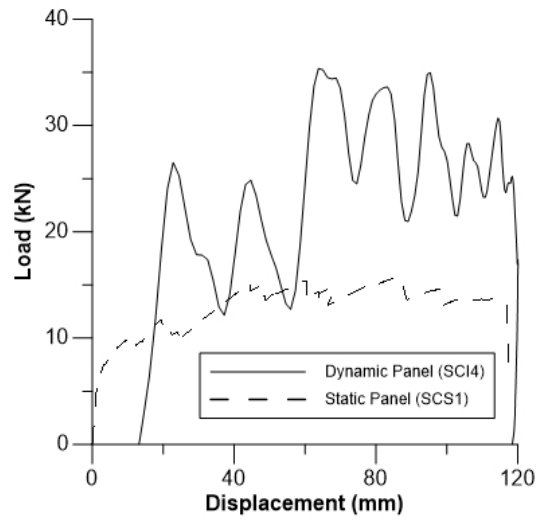
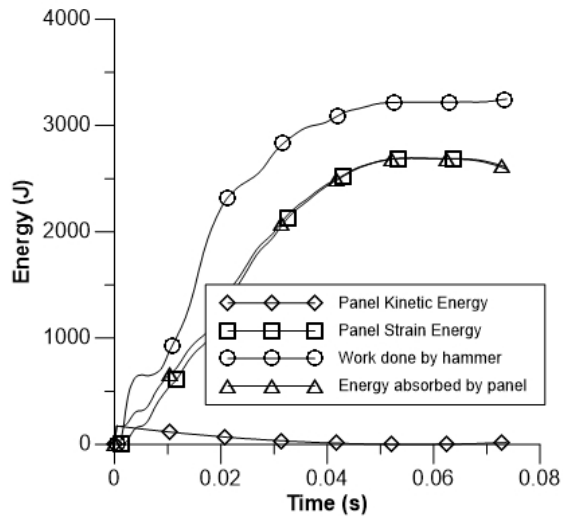
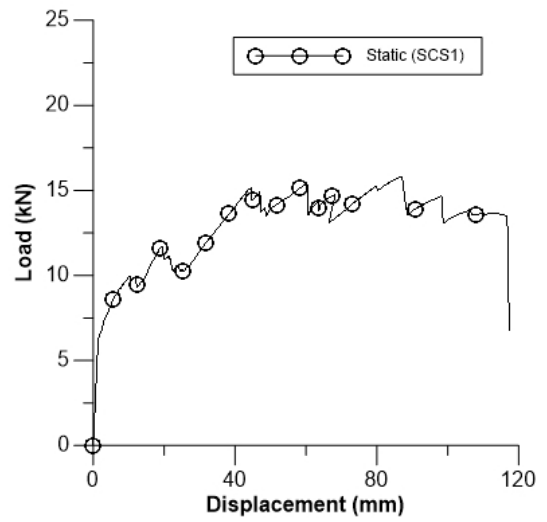
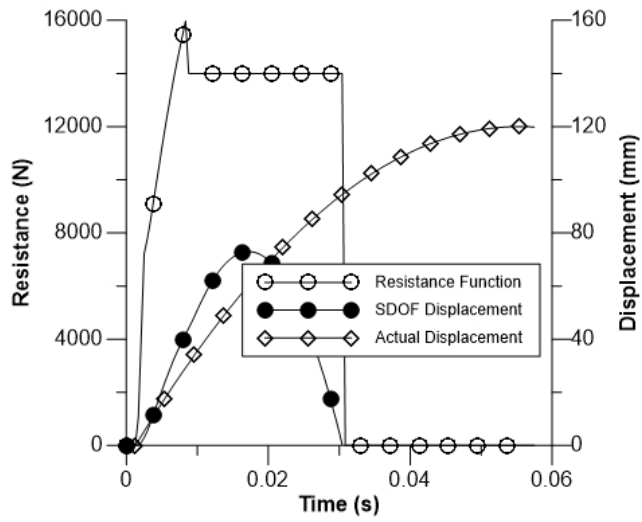
Appendix H SFRC Panel Graphs

PANEL SCI3



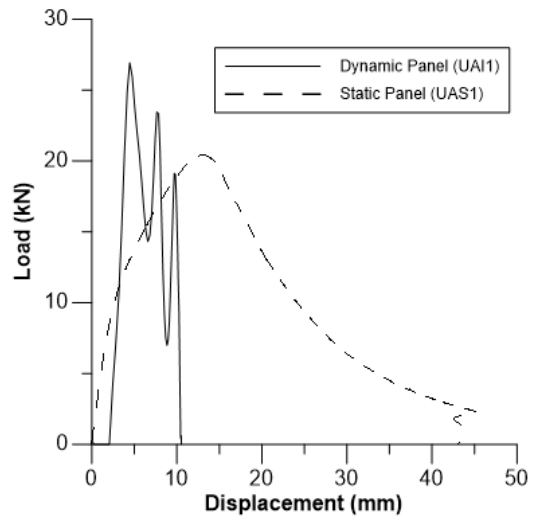
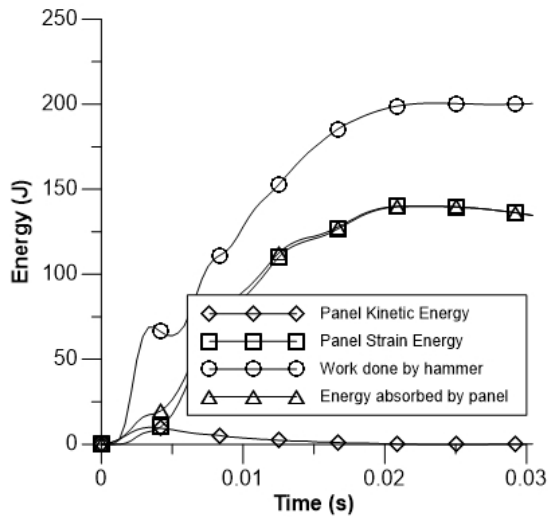
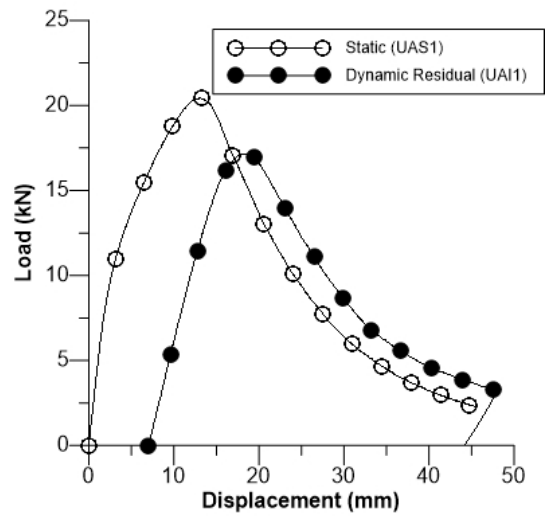
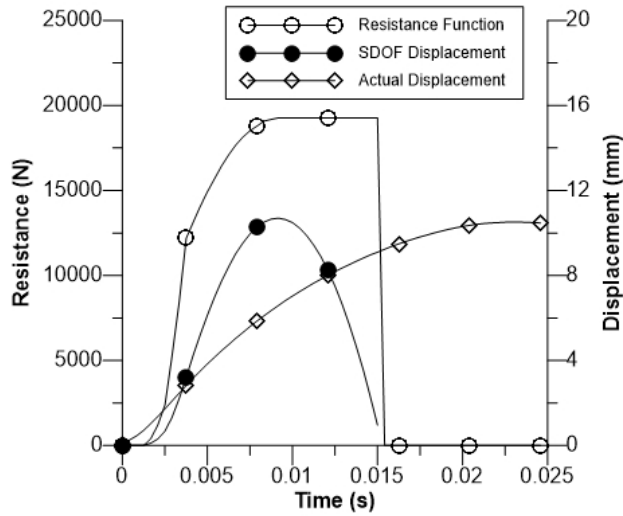
Appendix H SFRC Panel Graphs

PANEL SCI4



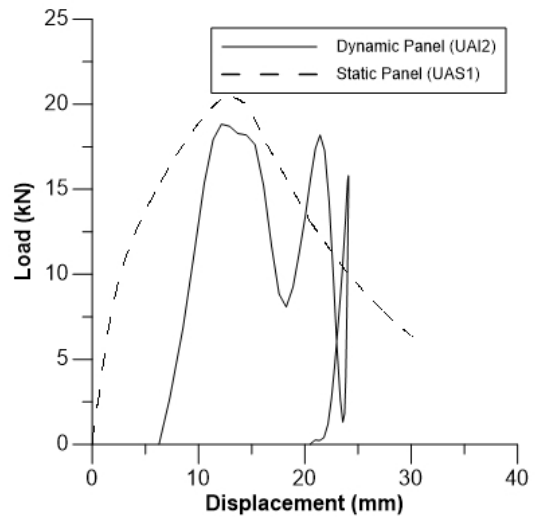
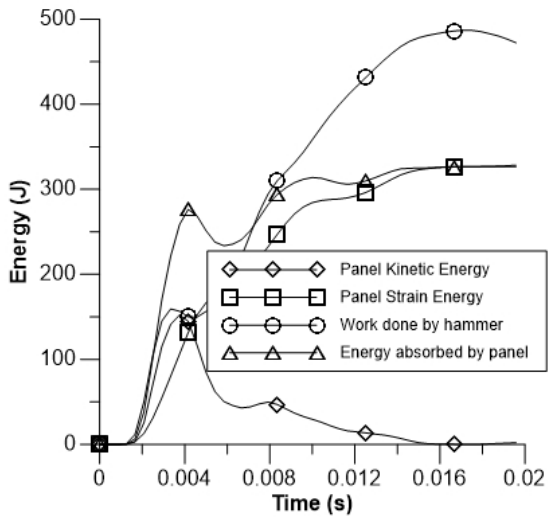
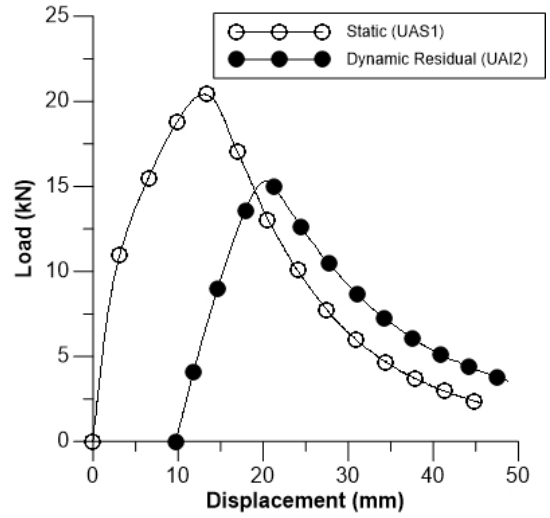
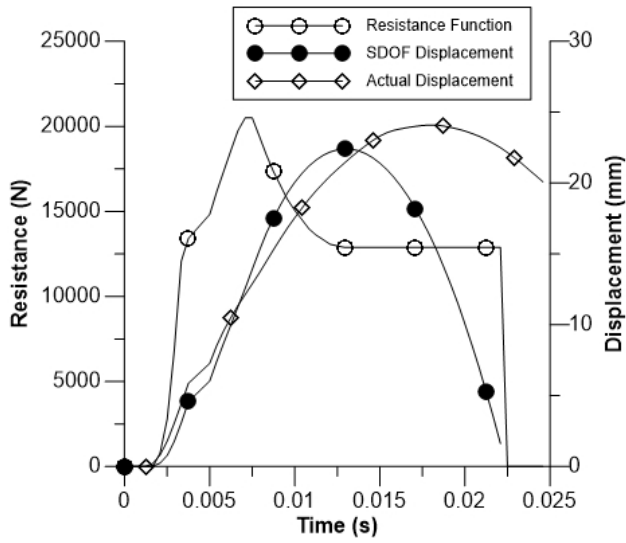
Appendix I UHPFRC Panel Graphs

PANEL UAI1



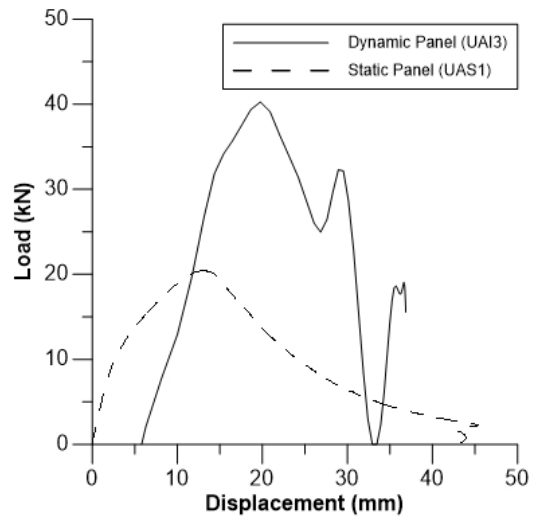
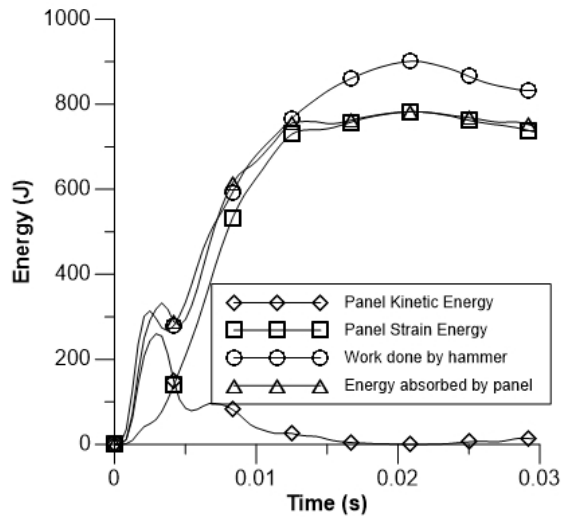
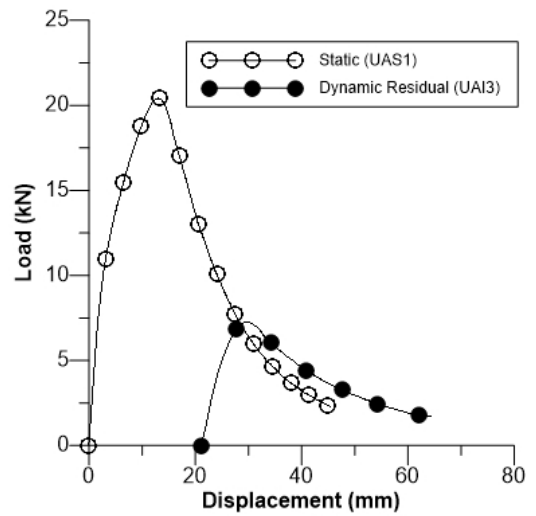
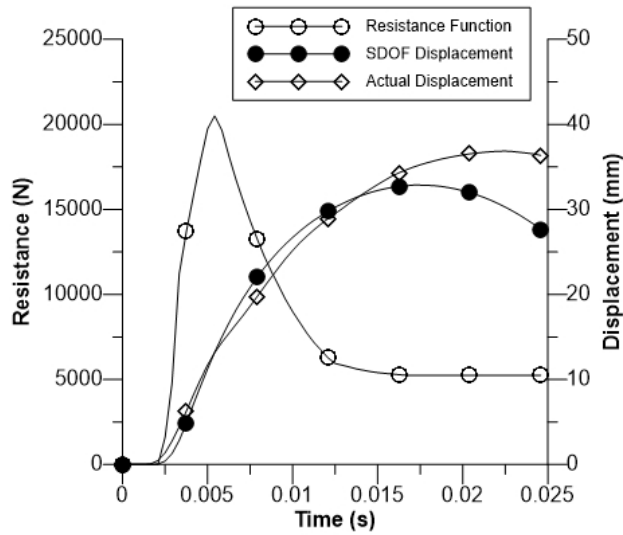
Appendix I UHPFRC Panel Graphs

PANEL UAI2



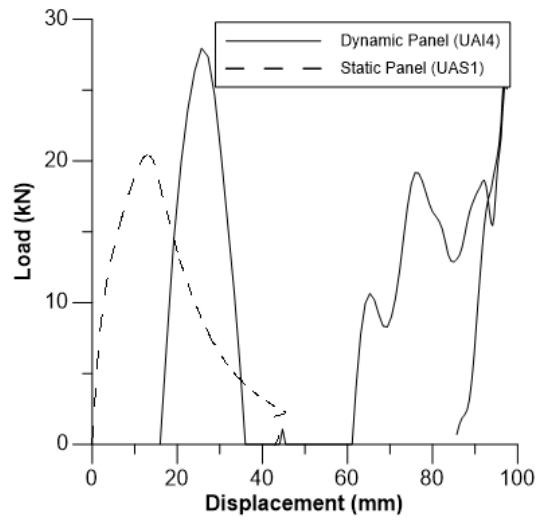
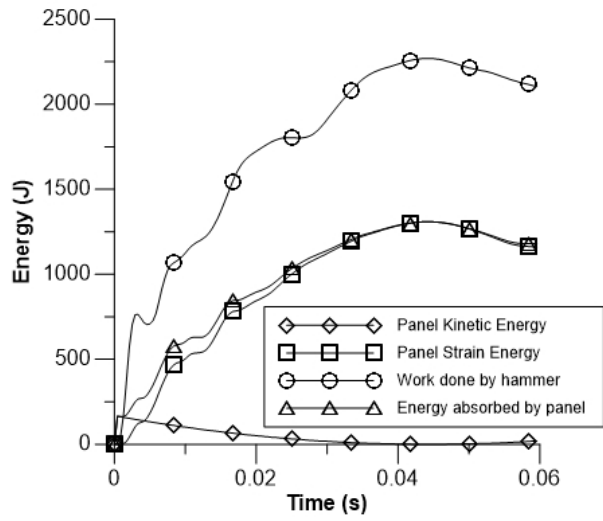
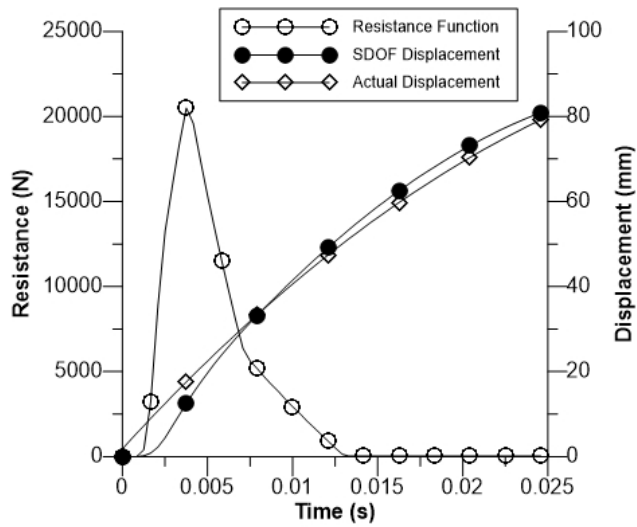
Appendix I UHPFRC Panel Graphs

PANEL UAI3



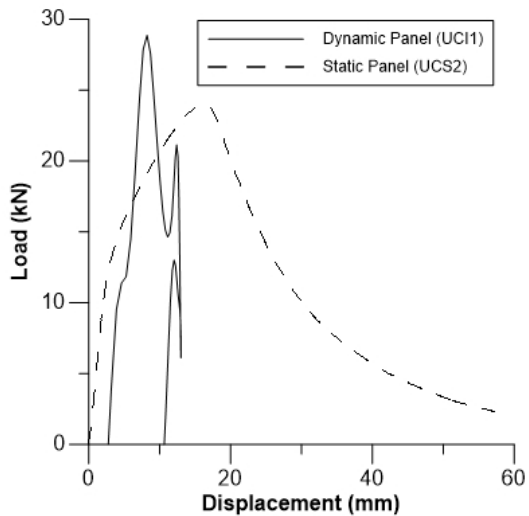
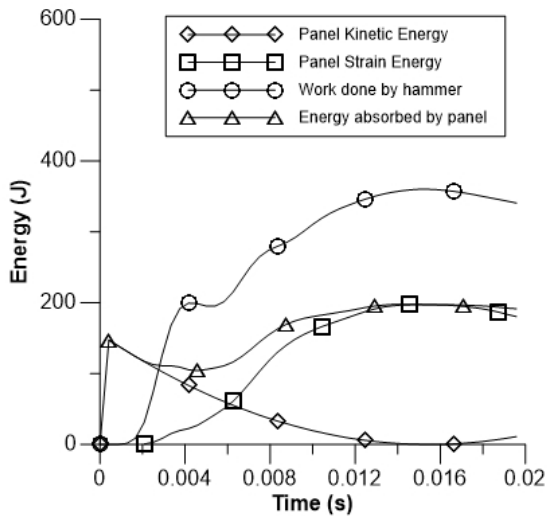
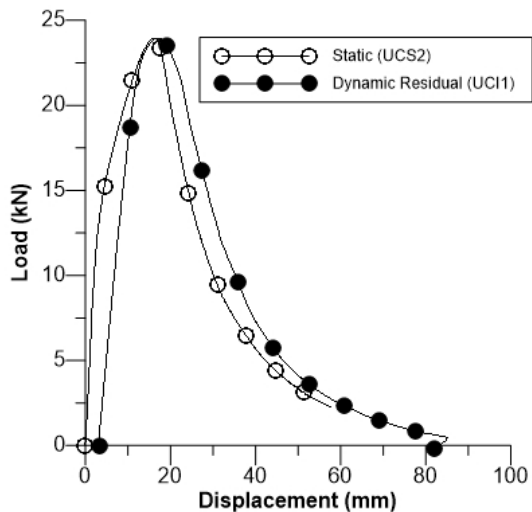
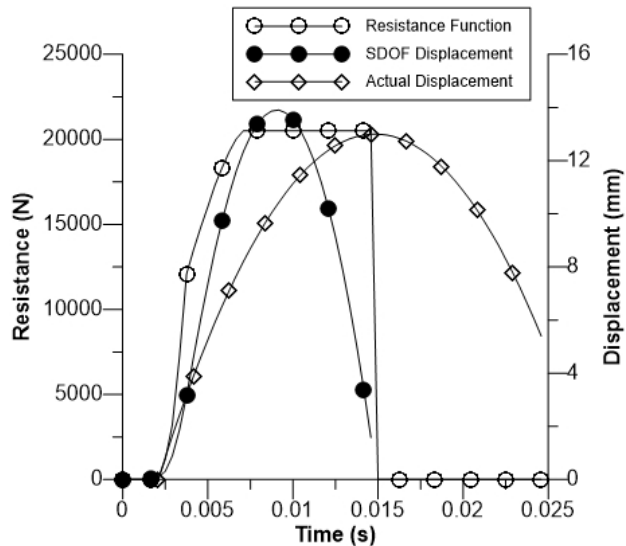
Appendix I UHPFRC Panel Graphs

PANEL UA14



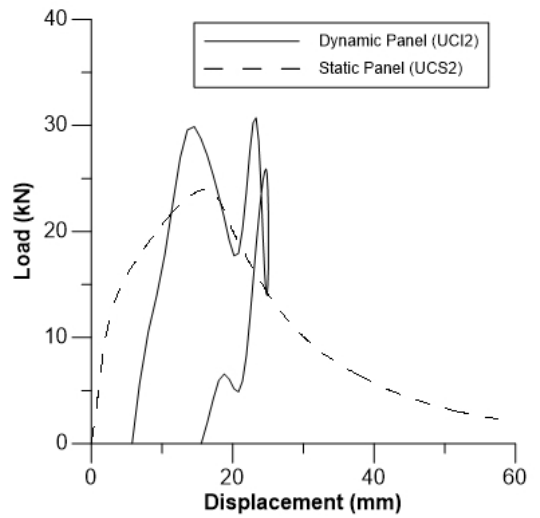
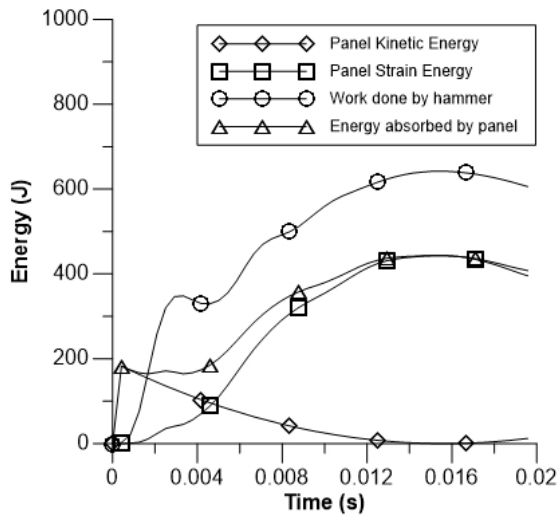
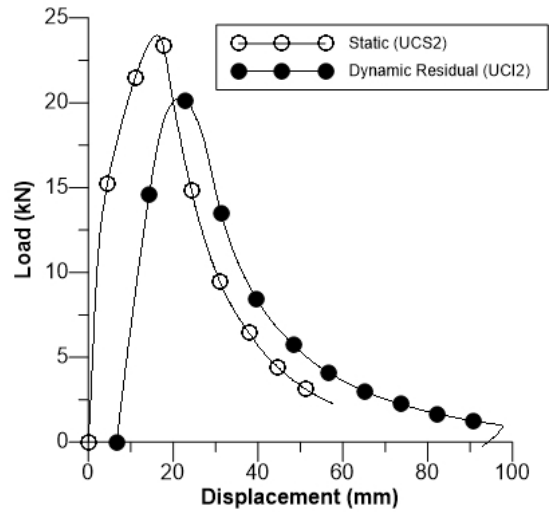
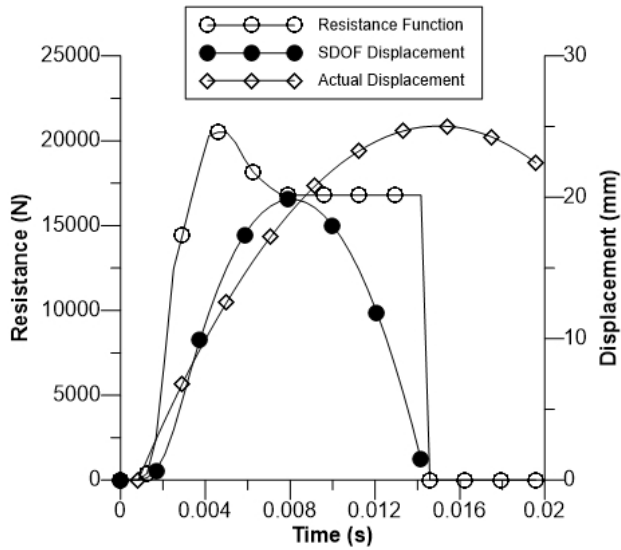
Appendix I UHPFRC Panel Graphs

PANEL UC11



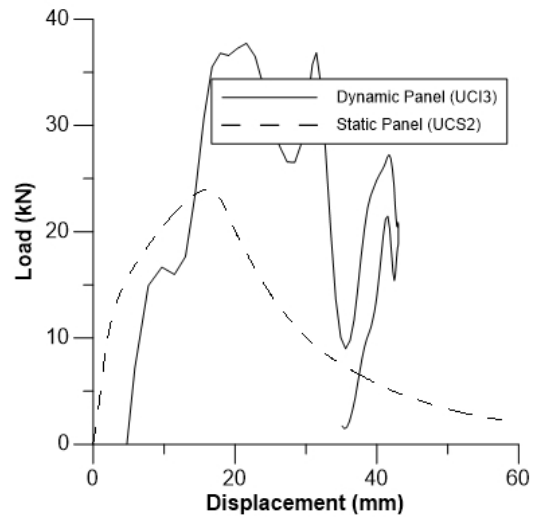
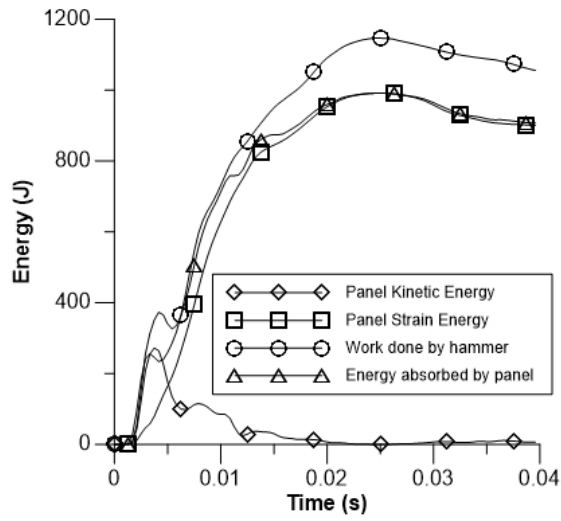
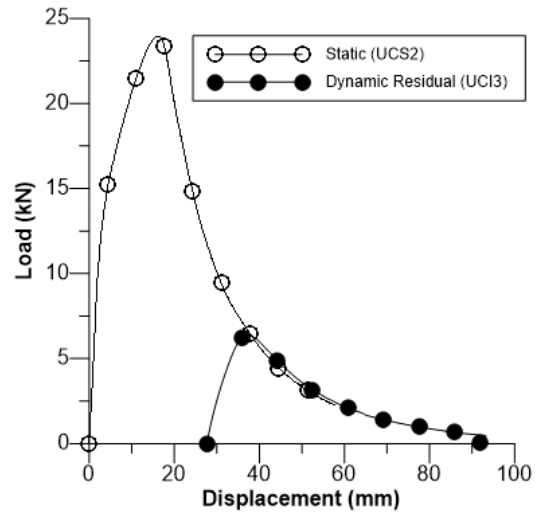
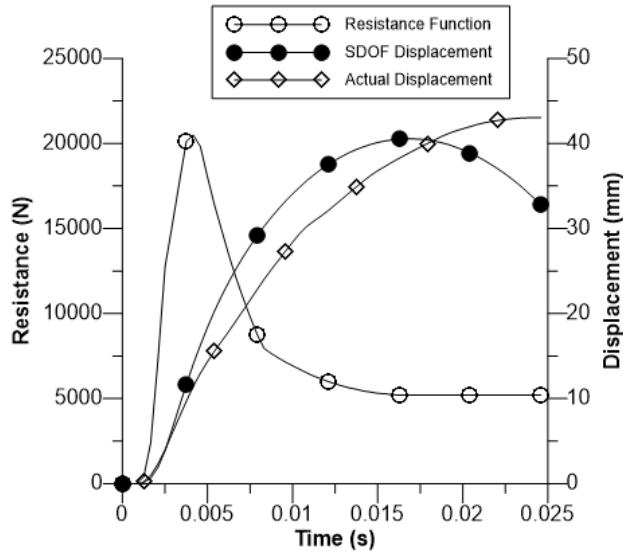
Appendix I UHPFRC Panel Graphs

PANEL UCI2



Appendix I UHPFRC Panel Graphs

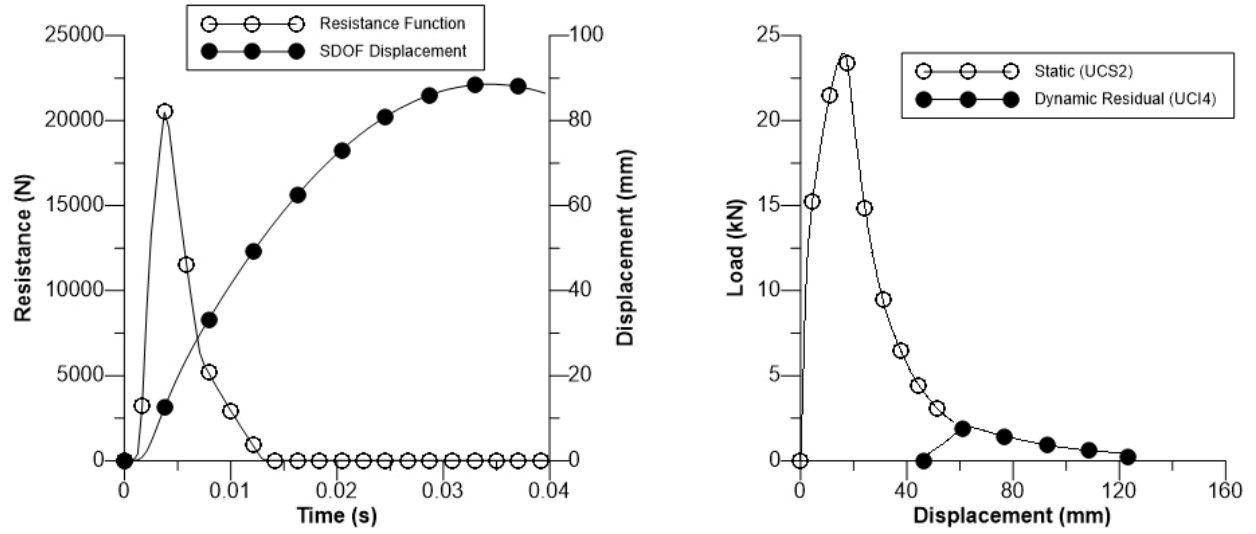
PANEL UC13



Appendix I UHPFRC Panel Graphs

0.85-

PANEL UC14



CURRICULUM VITA

Name: Matthew Jordan Beirnes

Place and date of birth: Richmond Hill, Ontario
07 July 1989

Education: Royal Military College of Canada (2008-2012)
Kingston, Ontario
BEng in Civil Engineering, 2012

Experience: 2 Combat Engineer Regiment
Squadron Operations Officer
CFB Petawawa
July 2014 – June 2015

2 Combat Engineer Regiment
Airborne Engineer Troop Commander
CFB Petawawa
April 2013 – June 2015